University of Central Florida

STARS

Electronic Theses and Dissertations

2017

Continuous Oscillation: Vibrational Effects and Acceptable Frequency Ranges of Small Bore Piping in Field Applications

Marie Kasprzyk
University of Central Florida

Part of the Mechanical Engineering Commons

Find similar works at: https://stars.library.ucf.edu/etd

University of Central Florida Libraries http://library.ucf.edu

CONTINUOUS OSCILLATION: VIBRATIONAL EFFECTS AND
ACCEPTABLE FRQUENCY RANGES
OF SMALL BORE PIPING IN FIELD APPLICATIONS

by

MARIE KASPRZYK
B.S. University of Central Florida, 2013

A thesis submitted in partial fulfillment of the requirements
for the degree of Master of Science
in the Department of Mechanical and Aerospace Engineering
in the College of Engineering and Computer Science
at the University of Central Florida
Orlando, Florida

Summer Term
2017

ABSTRACT

In turbomachinery, a common failure mode is cracking of welds at the equipment and piping connection point. Each incidence of these cracks causes a forced shutdown to perform repairs that cost millions of dollars. This type of failure is predominately seen in small bore piping, which has a nominal diameter of 2 inches and smaller. This thesis addresses the failure prediction analysis of small bore piping, specifically in turbomachinery applications. Performing failure analysis to predict the potential cracking of welds will allow for replacement of the piping during a planned shutdown which in the long term saves money due to costs such as expediting materials, overtime pay, and extended downtime.

This analysis uses real-world applications of a chemical plant in Louisiana. The piping analyzed was connected to centrifugal compressors. The data used from these pieces of equipment included the material of construction, the piping schedule, lengths, nominal diameter, and running speeds. Based on research that shows welding the connection point with a full penetration weld greatly increases the life expectancy of the connection, this thesis uses full penetration welds in the analysis. The piping was analyzed using the software ANSYS to perform a finite element analysis, specifically examining the stress due to the induced harmonic forces.

It is a common fact that having fewer supports on a vibrating pipe induces greater stresses and strains on the weld connections. Supports installed 12" from the equipment only show one to two ranges of frequencies to avoid compared to the longer piping which has four to five ranges of unacceptable frequencies. Tables are developed to relay acceptable frequencies based on observed stresses of the welds in the model.

This thesis is dedicated to Dr. Suhada Jayasuriya who first encouraged me to write an undergraduate thesis and also inspired me to pursue my Ph.D. This master's thesis is my first step in fulfilling this goal.

I would also like to dedicate this thesis to my Mother and Brother who have been a huge encouragement throughout the writing of this thesis.

I would also like thank Cliff Hebert, currently the Plastics Business Reliability Improvement Director at the Dow Chemical Company who proposed the topic of this thesis. This thesis is written in the hopes of assisting him and other engineers at Dow with troubleshooting vibration issues.

TABLE OF CONTENTS

LIST OF FIGURES

LIST OF TABLES

NOMENCLATURE

A_5 Cross-Sectional Area of Concrete Foundation

c_1 Dampening Constant of Bearing Oil

c_5 Dampening Constant of the Concrete

C_{eq} Equivalent Dampening Constant

CS   Carbon Steel

d Oil Thickness Between Shaft and Bearing

e Eccentricity

E Modulus of Elasticity

FBD   Free Body Diagram

FPA   Flanged Piping Assembly

J Mass Moment of Inertia of the Rotor

k_2 Spring Constant of the Bearing

k_3 Spring Constant of the Bearing Housing

k_4 Spring Constant of the Compressor

k_5 Spring Constant of the Concrete

K_{eq} Equivalent Spring Constant

l Length of the Bearing

L Length of the Bearing Housing

L_5 Thickness of the Concrete Base

m_d Mass of the Rotor Impeller (Disk)

m_e Mass of Unbalance

m_s Mass of the Rotor Shaft

M Mass of Rotor

r_d Radius of the Rotor Impeller (Disk)

r_e Location of Eccentricity from the Center of Mass

r_s Radius of the Rotor Shaft

R Radius of Shaft

SS Stainless Steel

$SWFA$ Socket Weld Flanged Assembly

U Unbalance

x Distance

$\dot{x}$ Velocity

$\ddot{x}$ Acceleration

X Amplitude

ξ Dampening Ratio

μ Viscosity of the oil

ω Speed of Rotor (RPM)

$\dot{\omega}$ Angular Velocity

ωc Frequency Converged

Φ Phase Angle

CHAPTER ONE: INTRODUCTION

This study will determine what amplitudes and frequencies of vibration are acceptable for small bore piping and which do not exceed the endurance limit stress at the connection point. Small bore piping has a diameter of 2 inches or smaller, of which does not include tubing (Yoon, 2013). Small bore piping is of particular interest due to its greater susceptibility of failure due to vibrations compared to piping with a larger cross sectional area.

In large production units, the use of small bore piping is very common. Vibrations are induced on the piping due to its attachment to rotating equipment such as a pumps, turbo machinery, or compressors. Vibrations are induced by the movement of the rotating equipment, flow induced (Xiu, 2013), or by the frequency of the vibrations coinciding with the natural frequency of the pipe itself.

First, equations will be derived, based on multiple boundary conditions to describe the response of multiple small bore piping configurations. Second testing will be completed via ANSYS to see how the piping responds. Specific frequencies will be applied to the different piping configurations. The force of vibration which is calculated will be used to determine the stresses seen at the connection point(s).

The goal, is to be able to determine, if piping that is vibrating in the field is experiencing acceptable or detrimental vibrations. If the folks in the field are able to measure the frequencies, they will be able to see what stress levels the connection point is experiencing. The best method to relay the displacement and boundary conditions to stress or expected failure would be by a table, see table 1 for an example.

Table 1 Example of a Table to Interpret the Results Measured

Displacement	Connection (weld)	Pipe Length	Stress at Connection	Acceptable	Unacceptable
0.0001	Full Pen weld	12 inches		x	
.01	Fillet Weld	3 inches			x

Statement of the Problem

Much research has been applied to small bore piping in the turbo machinery scenery, such as power plants. Small bore piping is very prominent in the turbomachinery industry. The goal of this research is to allow vibration technicians to go into the field and take a few simple measurements and field observations to determine if piping vibrating in the field will experience failure in the near future. Currently, vibration is only used as preventative measure to detect oncoming failures for components in rotating machinery such as bearings, rotors, and also misalignment of a piece of equipment.

The main goal for chemical plants is production. Vibrations can ultimately cause production losses if they are not controlled or eliminated. Ultimately, vibration can cause a company to lose hundreds of thousands to millions of dollars. If reasonably accurate analysis of vibrations in the field can be calculated, it will greatly assist in the in the reduction of failures and increase the amount of production.

LOPC's is another event that proper evaluation of vibrations can prevent. LOPC is the Loss of Primary Containment of a liquid. This type of scenario can cause not only production losses, if production unit is shut down because of a required repair, but there is also the high potential of personnel being in the line of fire of the containment. The risk is the possibility of a life critical injury which can become a federal agency reportable (Xue, 2013). Safety has become one of the top goals for many companies. It has been proven that the safer the employees are, the

higher the reliability of the plant is. This is not only due to the increased reliability of the equipment, but also keeping the folks safe that have invaluable experience and knowledge. The safer our production units are, the more reliable they are, which results in higher production.

Background of the Study

Traditionally small bore piping has been studied to determine the fatigue and failure of a fixed connection point. Acceptable piping vibration can be determined by simple means of observation, or by more complicated means which include compacted instrument measurement or numerical analysis techniques (Fei, 2013). The vibration in the other research has been measured by mounting accelerometers in the direction of all three axes on a piece of piping. Data was collected at the elbow and fixed connection of the pipe. The dynamic stresses of the welded connection (fixed connection) were also modeled using FEA. This method was also used to calculate the natural frequency for multiple mode shapes. Fei was able to measure the velocity of the small bore piping and compare it to the allowable value to determine of any of the boundary condition of the piping needed to be changed, such as adding a support to the system.

There are two ways that small bore piping fatigue failures occur; most often by mechanical vibration induced fatigue, and second by thermal fluctuation (Fei, 2013). When applying calculations and fatigue strengths, the following factors must be included. These include weld quality, material, possibility of corrosion fatigue, static stress level, misuse in service, history of previous failures, and variability of operating conditions (Hablin, 2003). The fixed connection of the piping studied has been mostly on socket welds, Figure 1.
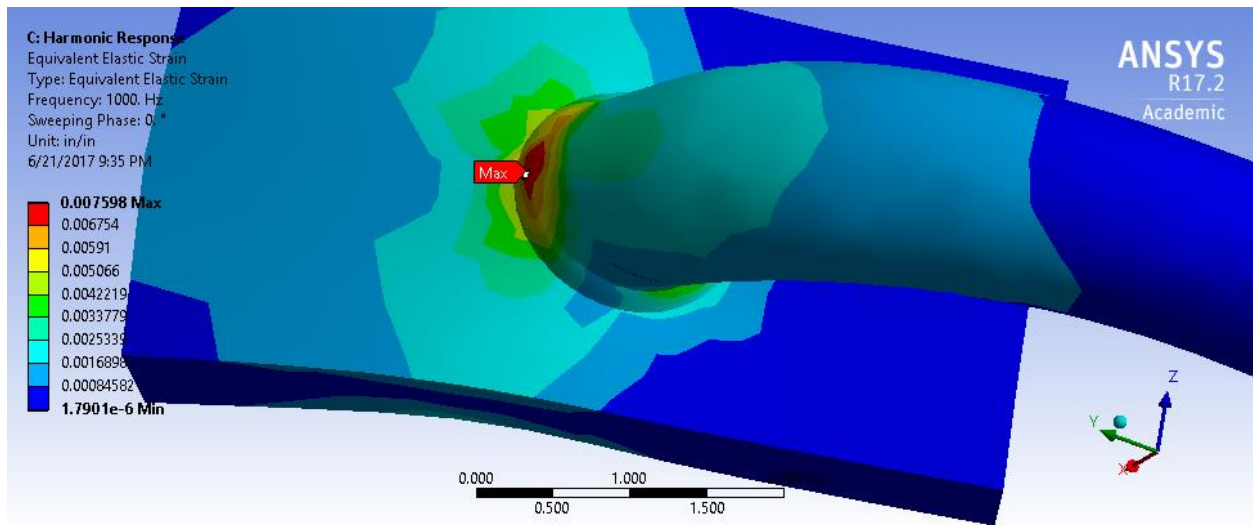
Figure 1 Analyzing the Strain at the Weld Connection

<div align="center">Hypothesis</div>

It is expected that models induced to high frequency vibrations, will be considered to experience a high likely hood of failure. It is also anticipated that piping that is supported further apart will likely have a greater likelihood of failure due to experiencing more stress. In the real word, when a pipe fails, it is often due "lack" of support or supports mounted too far away from each other. It is likely that the 12" long supported piping will experience stresses that are not likely to cause a failure. It is also assumed that the modes shapes of the shorter sections of piping will experience smaller deflections at the mode shape compared to the longer lengths of piping.

<div align="center">Methods and Procedures</div>

Models will be built using the two most commonly used materials in industry for turbomachinery. These include carbon steel and stainless steel which are used for specific applications on the turbomachinery. Carbon steel is used usually on the process side there the

cleanliness is not as critical. Components on the compressor such as the mechanical seal use

stainless steel piping to ensure that no foreign objects enter the seal due to corrosion etc.

Limitation

Due to utilizing a student version of ANSYS, the accuracy of the stress and strains of the

entire piping assemblies are not as accurate for some of the models. There was only a limited

allowable number of nodes and size of mesh. Therefore a refined mesh was applied to the welds

to increase the validity of the results. As the length of the piping assemblies was increased, the

more nodes and meshes were utilized, therefore for a few of 48" long piping assemblies, the

refinement of the mesh was not able to be utilized, and therefore the required mesh convergence

was not reaches. The analysis was also only conducted up to 350 Hz due to the size limitations in

the student version of ANSYS.

CHAPTER TWO: EXPERIMENTAL SETUP

ANSYS R17.2 was used during this study to model and analyze small bore piping. The analysis techniques utilized are mode shapes and harmonic response, to determine how the system will respond. For the majority of the models the mesh size was set to be a min of 0.2 to a max of 5 inches. There were two main types of experimental setups utilized which include flanged piping and socket weld piping. The connections at the compressor vary for each of the scenarios. The flanged assembly had a long 90 degree bend piping coming directly off the compressor. The socket welded assembly had a straight run of pipe coming off the compressor, with a length of 12 inches. To provide an organized representation of how the models and sizes were created, see Table 2 below.

Table 2 Piping Assembly Configurations

Piping Configuration	Compressor End Connections	Pipe lengths (in)	Pipe Diameters (in)	Materials
Flanged Assembly	90deg bend	12, 24, 36, & 48	1, & 2	Carbon Steel
				Stainless Steel
Socket Weld Assembly	12 inch long straight pipe	12, 24, 36, & 48	1, & 2	Carbon Steel
				Stainless Steel

A rectangular shaped block represents a small portion of the compressor. The body of the compressor utilized in the analysis is 1" thick to minimize the effect of the mass of the "compressor body" yet allow enough surface area for the weld connection. In reality the body of the turbine/compressor is very thick and has a series of passages machined throughout. Therefore the block is a very simplistic representation of an actual compressor body.

There are thirty-two different piping assemblies studied, which were in direct association with the different piping lengths, diameters and materials utilized. For each of the diameter pipe sizes, the only change to the models is the length of the pipe between the compressor and end of

pipe and the material of construction. The parts include the compressor block, the compressor end connection, the long run of piping, and flanges. Each were drawn up separately in ANSYS separately and then assembled using alignment and tangent conditions. The locations where the piping meets up were then swept with a weld profile. The main interest of this study is the weld connections at the compressor to compressor end connection which is where a majority of the failures occur (Xiu, 2012). The mesh size was refined at the weld connection to the compressor to provide more accurate results of the FEA.

There are three main connections for the Socket Weld Piping Assembly (SWPA) where the weld is drawn, modeled, and analyzed. These connections include the 1) compressor to compressor end connection, 2) the long run of straight pipe to the flange, and 3) the long run of straight piping to the socket weld 90. There were two main connections for the Flanged Piping Assembly (FPA) where the weld is drawn which include at the compressor and at the flange. These are drawn as a full penetration welds in the model. This type of weld was utilized which is the recommended weld for turbomachinery applications (Xu, 2012). Each of the compressor end connections are directly welded to the compressor body using a full penetration weld of the same material as that of the piping. It is very important that the weld material is the same as that of the piping. A Dissimilar Metal Weld (DMW) has a greater likelihood of crack initiation (Zeng, 2015). The welds will be analyzed throughout the entirety of this thesis.
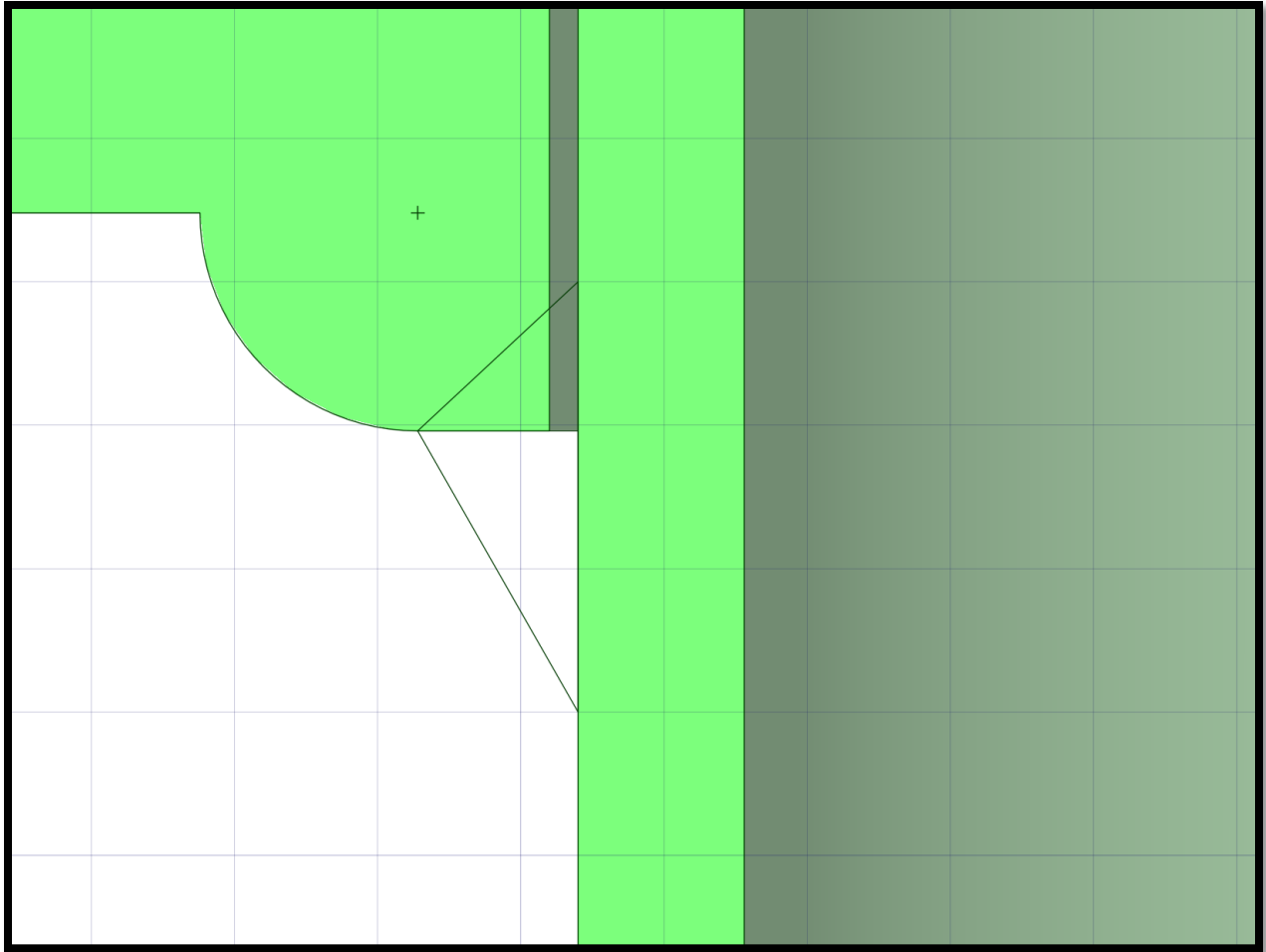
Figure 2 Example of Full Penetration Weld Created for Each Assembly

Full penetration welds are utilized instead of a filet weld due to its proven increased

expectancy of the life of the weld (Xu, 2012). During a study it was shown that no weld failed

when using a weld penetration of 0.7mm (.0276in) (Xu, 2012). If the ASME standard does not

already require a certain depth of weld penetration, I am sure that it will be implemented.

Considering this, the welds in the piping models were welded as a full pen weld to increase their

validity and the overall life expectancy.
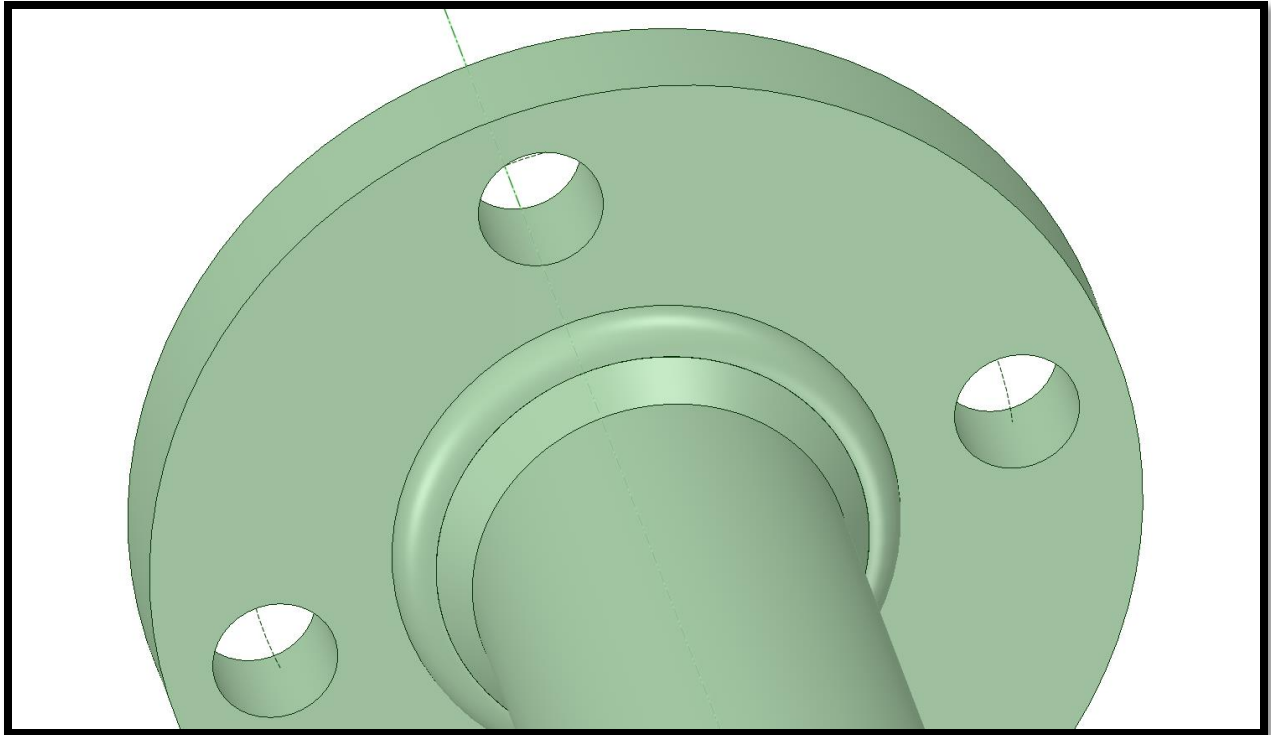
Figure 3 Full Penetration Weld Swept Around the Pipe

To increase the validity of the solution, the mesh at the weld connections were refined. The results of the stress, strain, and displacement were performed at the welds themselves. For the FPA, the results were recorded for both the weld at the compressor connection and at the flange connection. For the SWPA, only the weld at the compressor connection was analyzed.
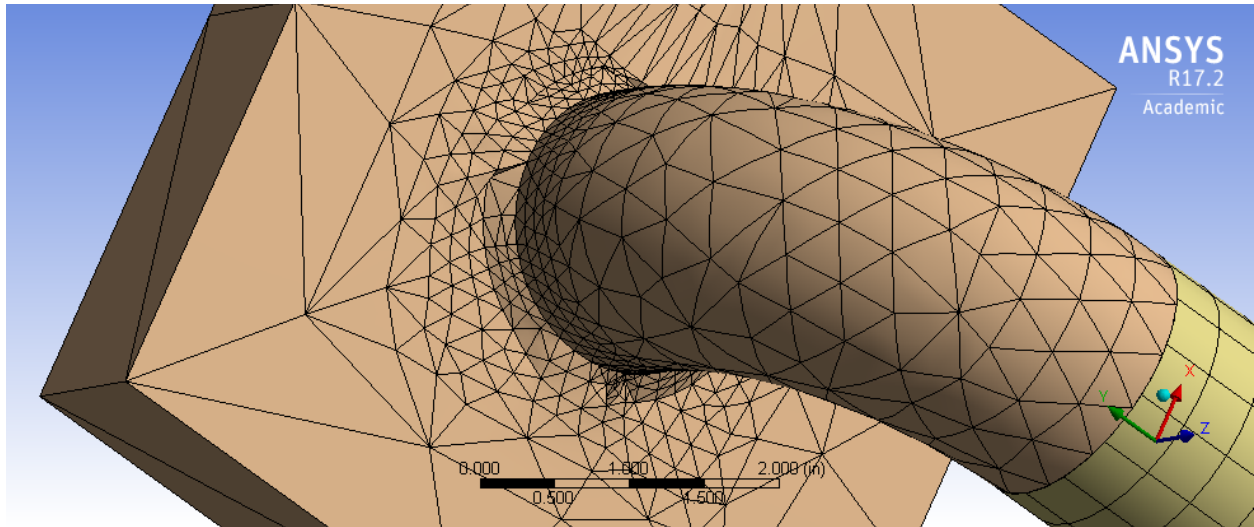
Figure 4 Mesh Refinement Mesh of the Weld at Compressor
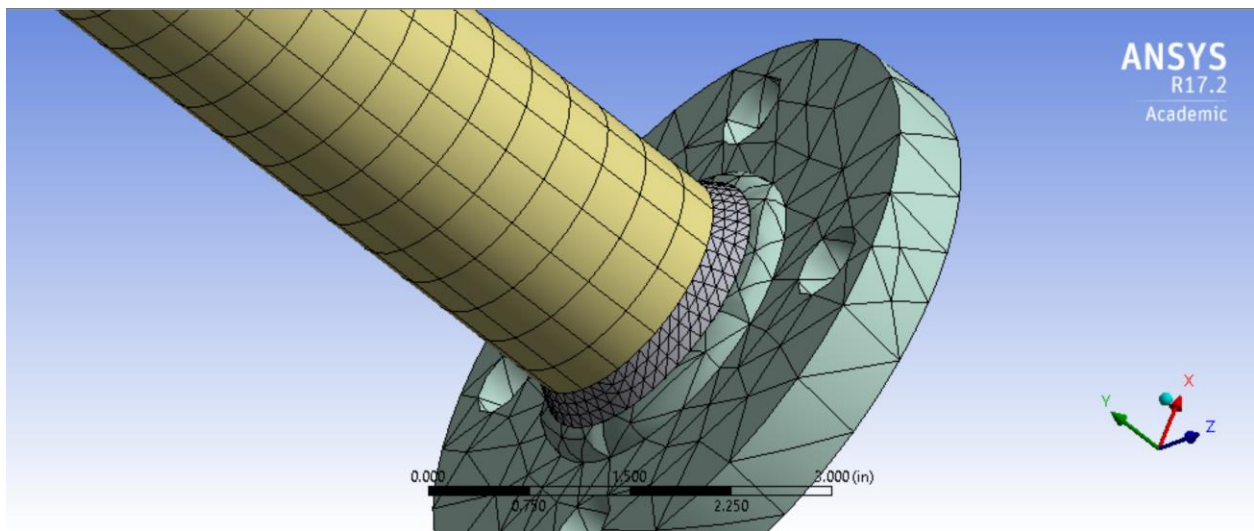
Figure 5 Mesh Refinement of the Weld at Flange

The mesh convergence of the SWPA and FPA were analyzed to ensure that the results reviewed were accurate. The mesh convergence of the FPA occurred at a frequency of 54.2 Hz with about 32,000 nodes and for the SWPA at a frequency of 71.5 Hz with about 19,000 nodes. The plots of the mesh convergence can be seen in Figure 6 and Figure 7.
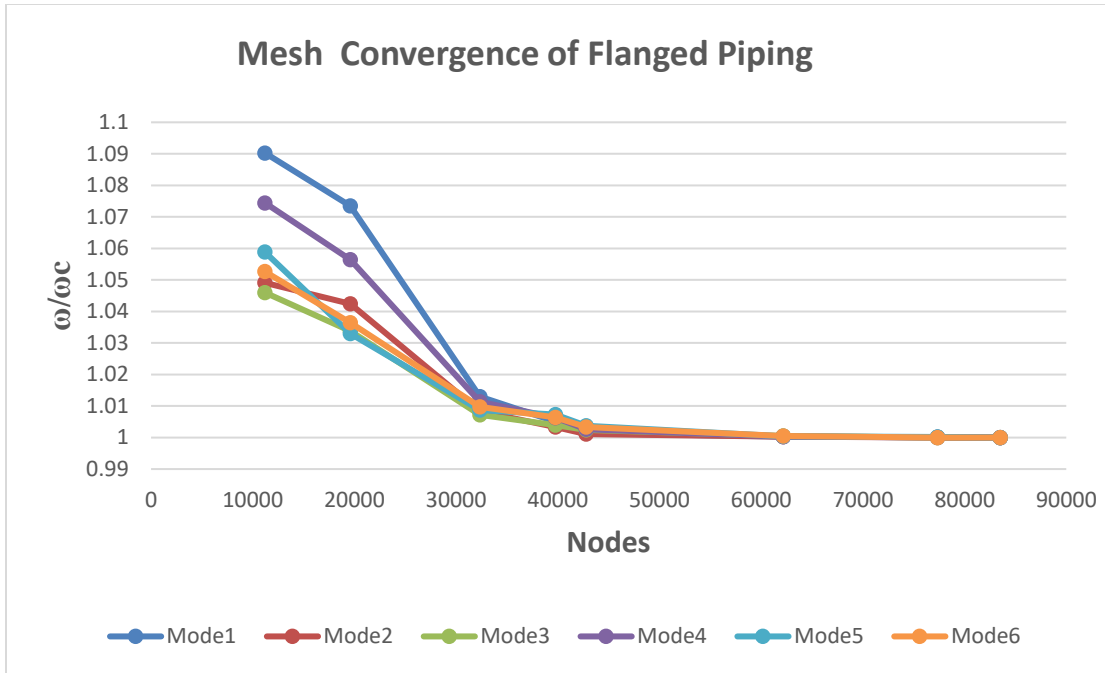
Figure 6 Mesh Convergence of FPA
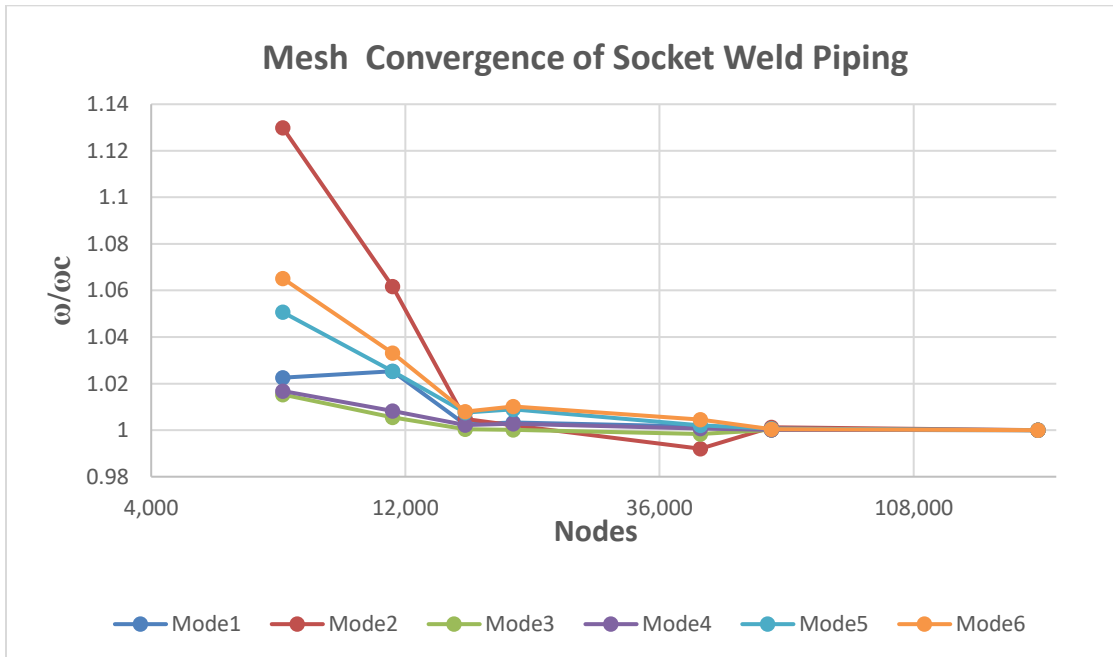
Figure 7 Mesh Convergence of SWPA

The two materials utilized in the ANSYS analysis are a stainless steel and carbon steel, the material properties can be seen below in Table 3 and Table 4**.** In the ANSYS program, the

11

materials are only referred to as stainless steel or structural steel, see properties of the materials

listed in Table 3 and Table 4. Carbon steel is the most commonly utilized material in

turbomachinery applications, the 2nd most utilized material in piping for turbomachinery

applications is stainless steel. To give a quick comparison, 304 SS has a yield stress of 215 MPa,

which is 35 MPa lower than that of A36 carbon steel which has a yield strength of 250 MPa.

Stainless steel is often used in turbomachinery for applications that are required to ensure no

contamination is carried to the component. This contamination is usually caused by corrosion of

the internals of the piping. For example, when tubing up a mechanical seal, stainless steel is

always used because any rust that enters the seal will cause the seal to fail, this would initiate a

shutdown of the compressor.

Table 3 Properties of Stainless Steel Used by ANSYS

Stainless Steel		
Property	**Value**	**Unit**
Density	**7750**	**kg/m^3**
Coefficient of Thermal Expansion	**1.7x10^-5**	**1/C**
Zero-thermal-Strain Reference Temperature	**22**	**C**
Young's Modulus	**1.93x10^11**	**Pa**
Poisson's Ratio	**0.31**	
Bulk Modulus	**1.693X10^11**	**Pa**
Shear Modulus	**7.3664X10^10**	**Pa**

Table 4 Properities of Carbon Steel Used by ANSYS

Structural Steel		
Property	Value	Unit
Density	7850	kg/m^3
Coefficient of Thermal Expansion	1.2x10^-5	1/C
Zero-thermal-Strain Reference Temperature	22	C
Young's Modulus	2.0 x 10^11	Pa
Poisson's Ratio	0.3	
Bulk Modulus	1.666 X 10^11	Pa
Shear Modulus	7.6923 X 10^10	Pa

To determine which stresses experienced by the piping were unacceptable, the results were compared to the endurance limit of the material. For carbon steel, the minimum endurance limit is 27 ksi and stainless steel 37 ksi (Hibbeler, 2011). All the stresses experienced below the limit would not causes the weldment of the specimen to fail.

Flanged Assembly

One of the most common and utilized piping connections is flanged, it allows the user to easily perform maintenance in the field. When welded piping needs maintenance it will require performing hot work in the field which requires extensive safety initiatives to ensure that a fire does not occur. With flanged connections it only requires a cleared line and a couple of wrenches. In this study, socket weld flanges are utilized in the piping assembly. It is important that when socket weld flanges are installed on piping, a gap of 1/16" (0.16 mm) is left between the pipe and the end of the flange, per ASME B&PV code, section III (Choi, 2007). This gap

accounts for heating of the piping during welding, which if not utilized, and the pipe is flush against the flange, it will result in applied residual stresses on the weld resulting in a decreased life of the weld (Xu, 2012). As the gap is decreased, the change in the stress intensity factor (ΔK) increases (Choi, 2007). It is also important that there is a radial gap between the pipe and the flange. Larger radial gaps can improve the fatigue resistance of the weld and it is recommend that this gap be 0.1mm to .04 mm (1/256" – 1/70") (Xu, 2012). Schedule 40, 150 lb flanges were utilized in the analysis which is the typical pipe specifications for turbomachinery applications.

Boundary Conditions

There are three boundary conditions applied to the assemblies. The first is a thermal condition of 100 deg F, the second is a fixed support, and the third is a displacement support which was fixed on along the axis of the rotor and free in the radial direction of the rotor. Connection point "A" is where the piping is directly welded to the compressor, see Figure 8. For simplification, the compressor was not modeled, but just a very small portion of the compressor body. Connection point "B" is the location where the pipe is welded to a 150lb flange. Point "B" is modeled as fixed connections. At "B" I am considering this connection to be secured via u-bolts or some other device. Point "A" represents the compressor which is rigidly fixed to a concrete support. Point "A" is fixed in the "y" and "z" planes and free in the "x" plan as seen in Figure 8.
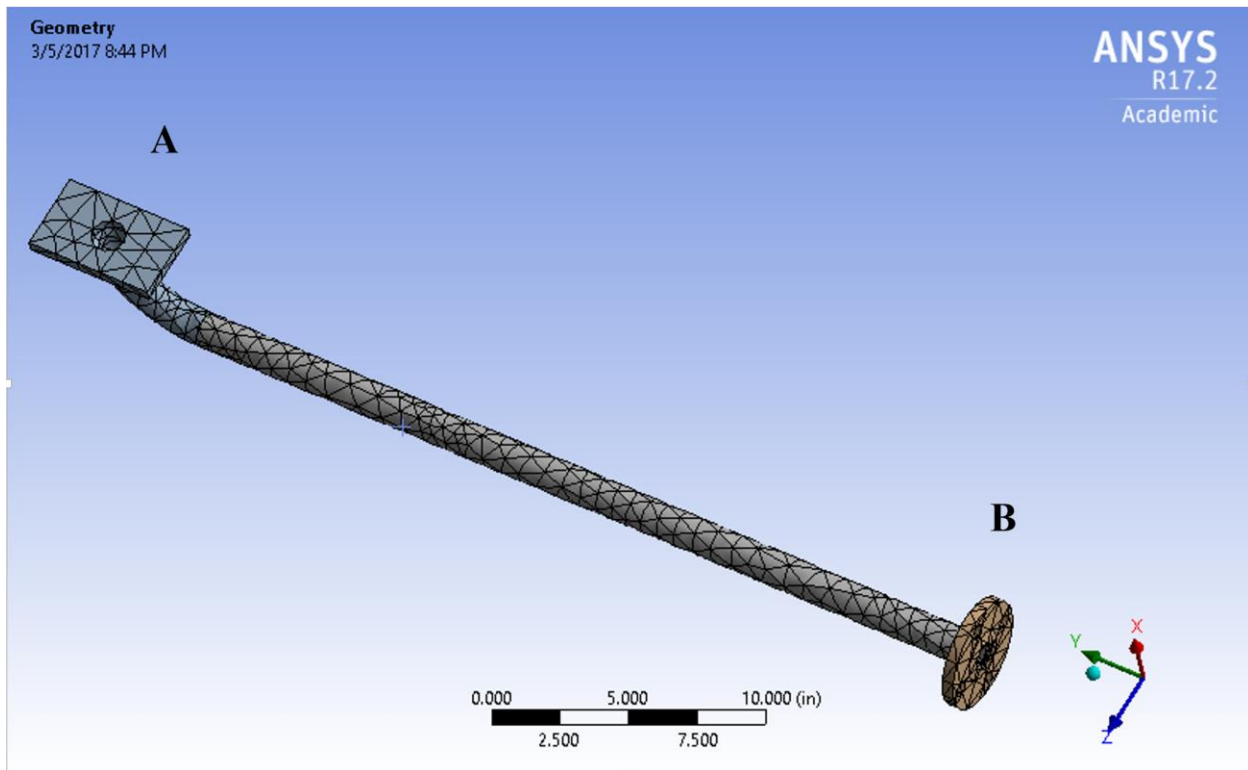
Figure 8 Flange Piping to Multi-Stage Centrifugal Compressor

Results

The main results reported throughout, of the 32 different models, include the mode shapes, stress, and allowable frequencies. The overall results of the paper include tables at which frequencies will be acceptable to allow the piping to vibrate based on the length, piping diameter, and material of construction. These allowable frequencies were determined by studying how the stress changed at the weld connections. When the stress became above a specific threshold, it was considered a frequency that was not recommended for the piping to be succumbed to. It is also important that, not only the tables of recommended frequencies are studied, but also understanding the modes shape response. There are some locations where the stress is very minimal and yet it is at a location of a point of natural frequencies. Therefore the technician

should not only use the tables of acceptable vibration but also the tables of the mode shapes when determining what frequencies to avoid.

Mode Shapes

There are two different sets of mode shapes determined for each piping assembly, the modes shapes of the material are comprised of carbon steel and stainless steel. Each were determined with an applied thermal load of 100 degrees F. Only the first 6 modes were recorded for each assembly. Below is the pictorial representation of each of the mode shapes captured for each FPA, Figure 9- Figure 14. All Figures are 1 inch in diameter.
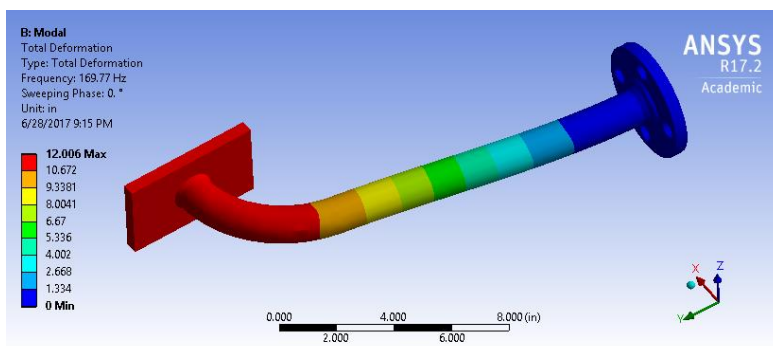
Figure 9 The 1st Mode for CS 24 Inch Pipe, at 169.77 Hz
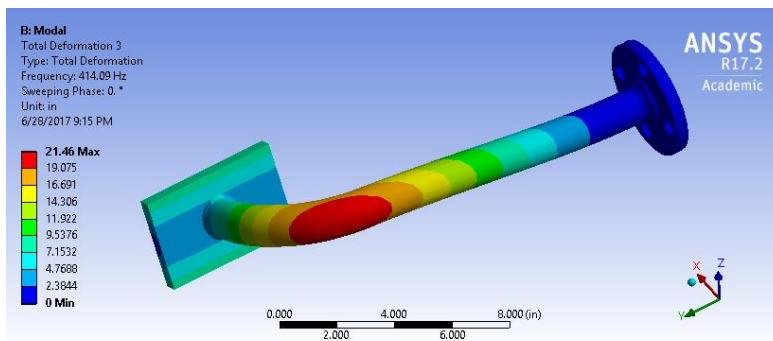
Figure 10 The 2nd Mode for CS 24 Inch Pipe, at 414.09Hz
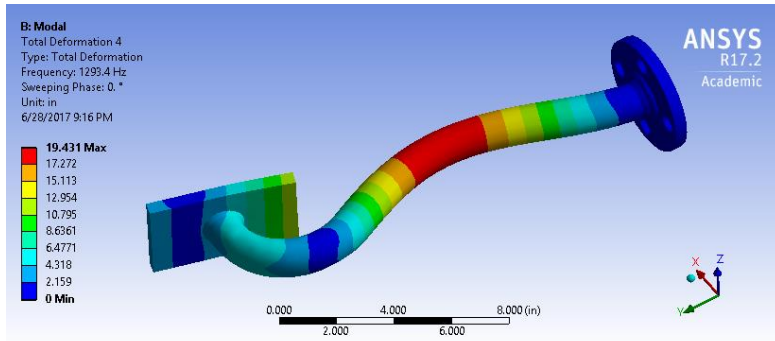
Figure 11 The 3rd Mode for CS 24 Inch Pipe, at 1293.4 Hz
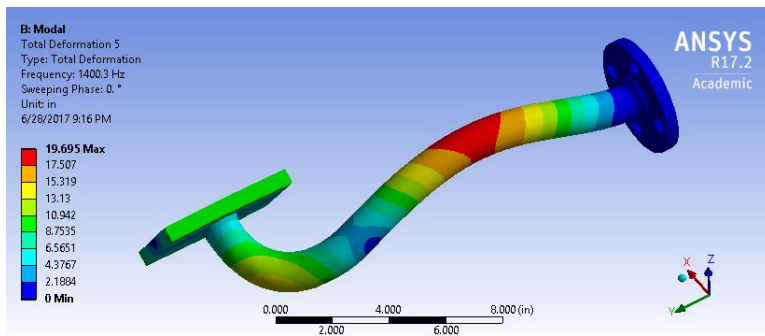
Figure 12 The 4th Mode for CS 24 Inch Pipe, at 1400 Hz
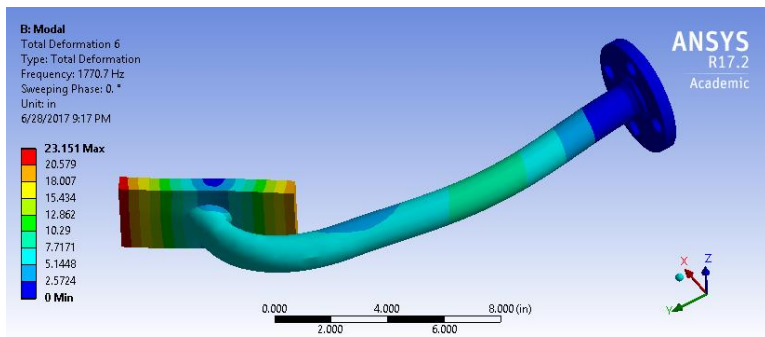
Figure 13 The 5th Mode for CS 24 Inch Pipe, at 1770.7 Hz
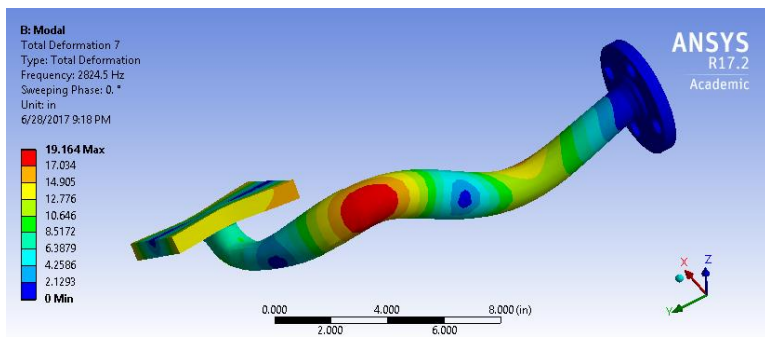
Figure 14 The 6th Mode for CS 24 Inch Pipe, at 2824.5 Hz

17

Stress and Strain

The stress and strain were also studied at the welds. Looking at all the models, the largest stresses and strains were seen at the welds. When studying the FPA, the maximum stress was seen alternating between the compressor connection and flange connection welds. Therefore confining the maximum stress and strain to be at the compressor weld is not probable. The total elastic strain and stress of the piping was determined at a frequency of 350 HZ. See Figure 15and Figure 16 for an example of the location of the maximum stress and strain at the welded flanged connections for a FPA.
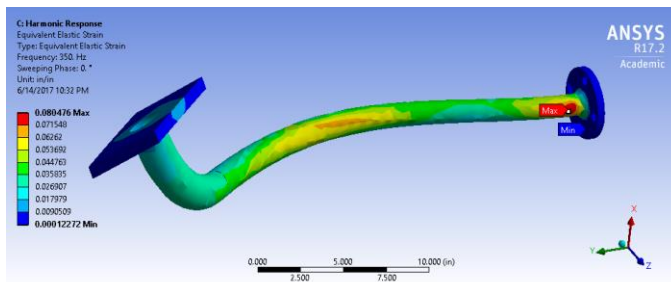
Figure 15 Strain of the Straight Length 24"of Piping
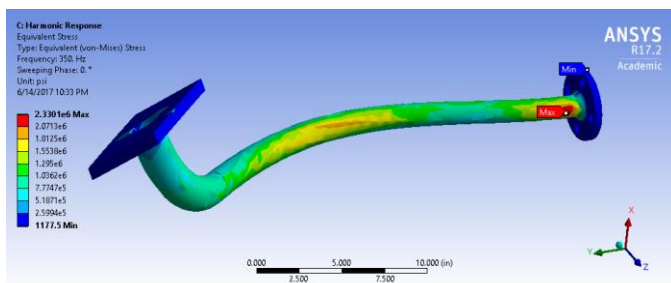
Figure 16 Stress of the Straight Length 24"of Piping

Deformation

As utilized for the stresses and strains, the total deformation of the piping was determined at a frequency of 350 HZ. The deformation was specifically studied and recorded at the weld locations. For the FPA, the welds were studied at the flange and compressor while for the SWPA

only the weld at the compressor was studied. Oftentimes the exact location of the stresses and strains was where the maximum displacement of the weld occurred. See Figure 17 for a visual representation of what the piping assemblies looked like when modeled for deformation.
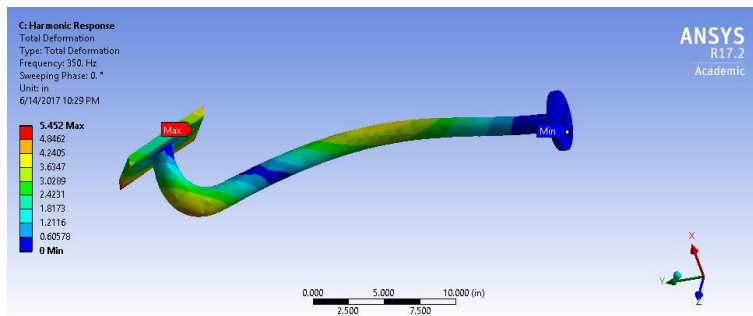
Figure 17 Total Deformation of the 24" FPA, CS

<u>Socket Weld Assembly</u>

Socket Weld piping is also a very popular type of connection in turbomachinery. Many applications require the piping to be welded due to the material that is being transported. This is especially true if the piping is transporting hydrocarbons. This is accomplished by avoiding flanged connections which have gaskets and bolts where corrosion, improper maintenance or incorrect torque could result in a leak. If the piping is connected via welds, the potential for a leakage drops dramatically. The failures that could occur if the weld fails include incorrect welding techniques, cracking due to vibrations, or corrosion. Therefore the potential for the welds to crack due to vibrations is very important study and eliminate and mitigate the potential if possible.
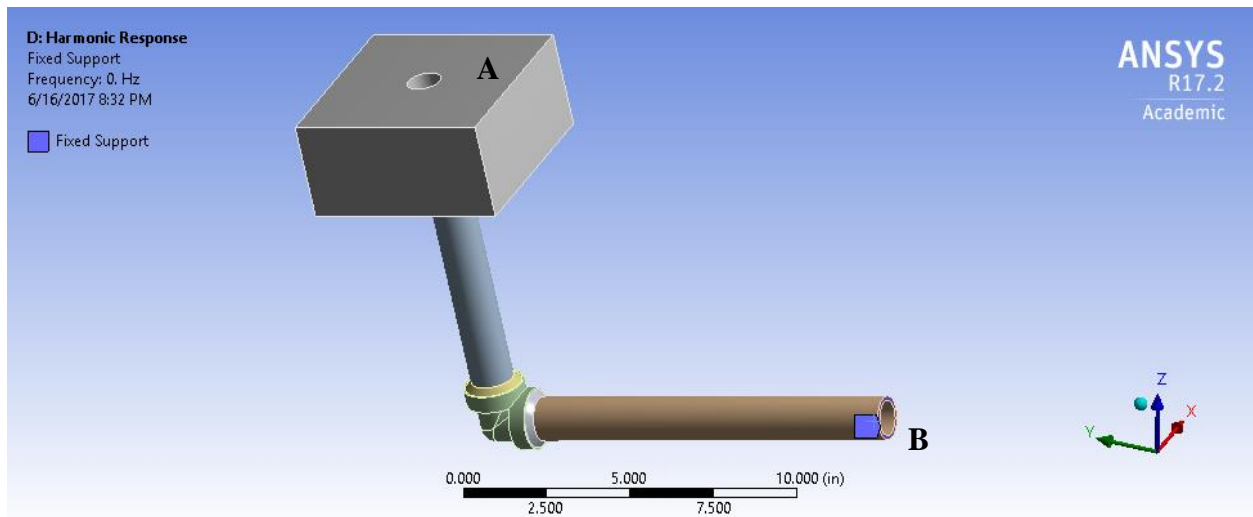
Figure 18 Socket Welded Piping to Multi-Stage Centrifugal Compressor

Just as in the flanged piping connections, there are three boundary conditions applied to the assemblies. The first is a thermal condition of 100 deg F, the second is a fixed support, and the third is a displacement support. Connection point "A" is where the piping is directly welded to the compressor. For simplification, the compressor was not modeled, but just a very small portion of the compressor body to allow the weld connection to be modeled. Connection point "B" is the location where the pipe is fixed. At "B" I am considering this connection to be secured via u-bolts or some other device. At "A" the block is fixed in the "x" and "y" plane while free in the "z" plane, Figure 18.

Results

Mode Shapes

Just as in the flanged connections, there are six mode shapes determined recorded for each piping assembly. The mode shapes are determined with only a thermal load of 100 degrees

F applied. A comparison of the mode shapes of the SWPA vs the FPA, are much different for the

shorter lengths of piping. As the length is increased, the mode shape frequencies become very

similar.
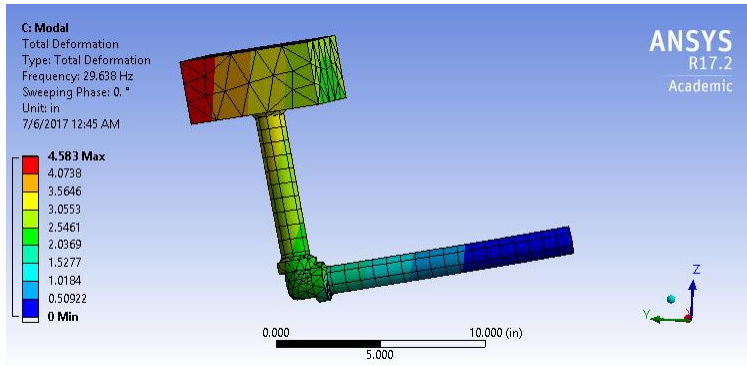
Figure 19 The 1st Mode for CS 12 Inch Pipe, at 129.638 Hz
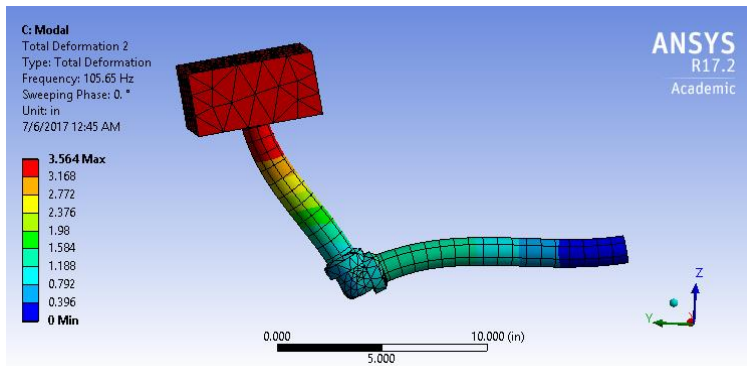
Figure 20 The 2nd Mode for CS 12 Inch Pipe, at 105.65 Hz
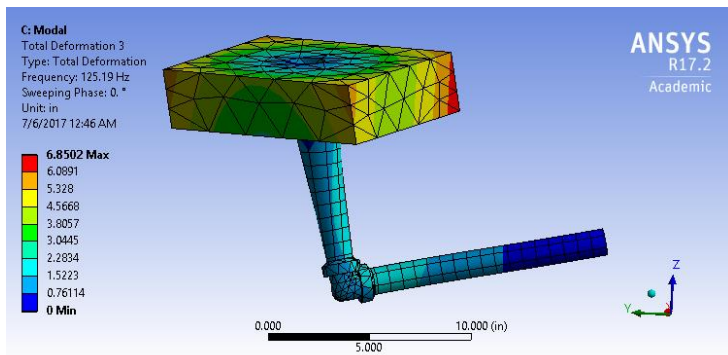
Figure 21 The 3rd Mode for CS 12 Inch Pipe, at 125.19 Hz
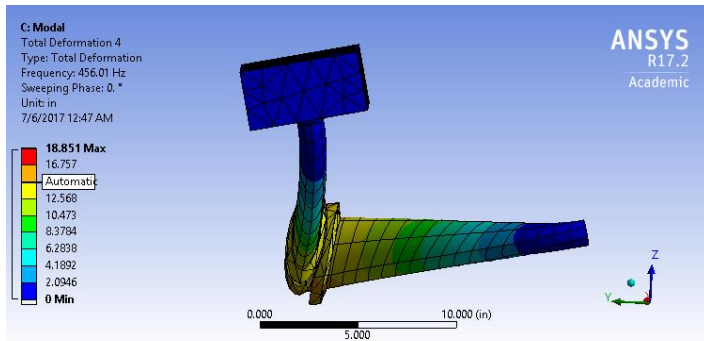
Figure 22 The 4th Mode for CS 12 Inch Pipe, at 456.01 Hz
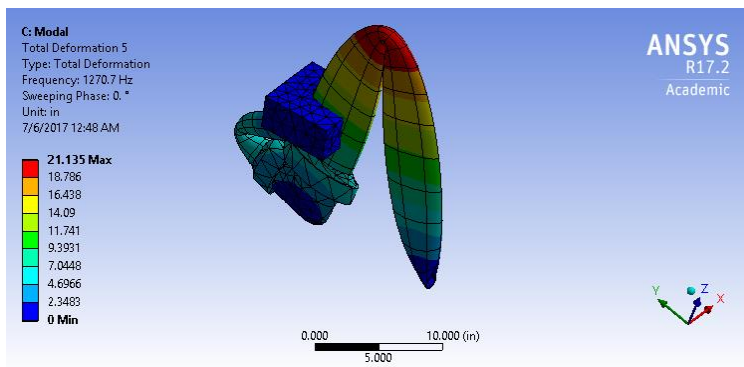
Figure 23 The 5th Mode for CS 12 Inch Pipe, at 1270.7 Hz
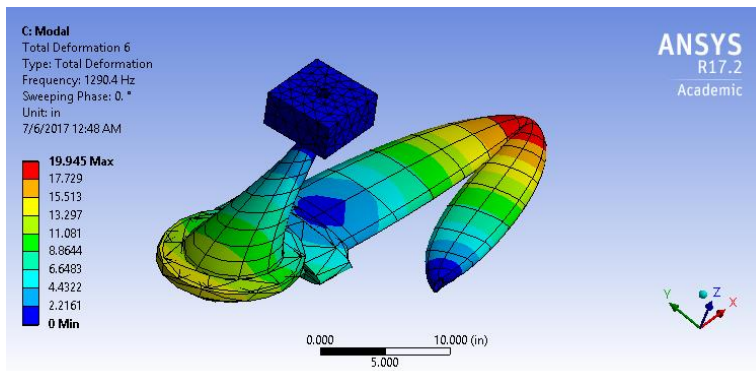
Figure 24 The 6th Mode for CS 12 Inch Pipe, at 1290.4 Hz

Stress and Strain

The total elastic strain and stress of the piping was determined at a frequency of 350 Hz

which is the maximum frequency that the small bore piping was evaluated. The stress was the

only variable at which was seen a valuable change when comparing between the different piping

lengths. The strain throughout was very low, in the range of 10^{-5} to 10^{-7}. The results therefore of the strain did not relay any insightful information.
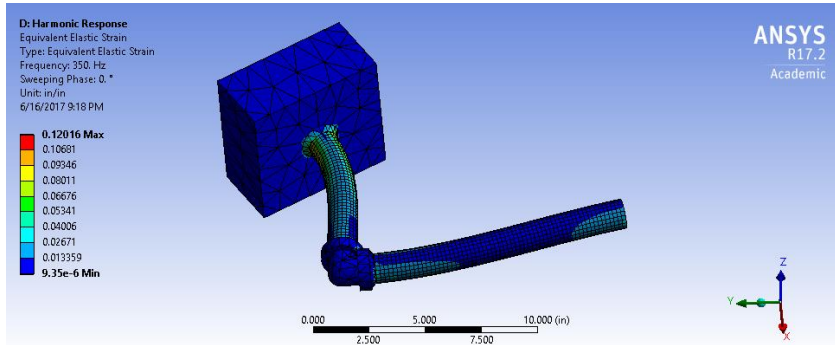
Figure 25 Strain of the 12", SWPA, CS

Deformation

The total deformation of the piping is determined at a frequency of 350 HZ. When evaluating the total deformation at the six modes of vibration, there was a definite observation of the displacement decreasing as at the length of the piping was increased.
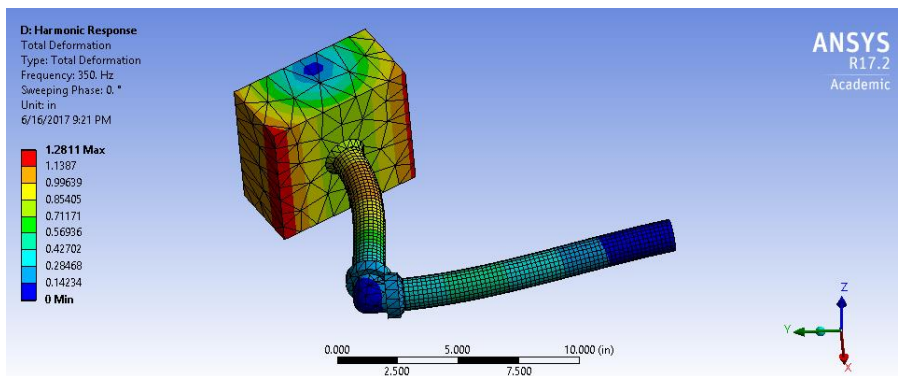
Figure 26 Total Deformation of the 12", SWPA, CS

Harmonic Response

To model the vibration that the piping would be experiencing, a harmonic response was applied to the piping at a range of 0 -350 HZ, as a rotational force. The solutions were derived at

intervals of 350 Hz. The maximum of 350 Hz was chosen as the maximum due to the prevalence

of turbomachinery that runs up to 20,000 rpm (~ 333 Hz). To verify the forces applied to the

piping assembly in ANSYS were accurate, the force transmitted to the base was calculated. This

included the use of a simple FBD, which accounted for the spring factor of the compressor

bearings and foundation, the dampening factors of the bearing oil and of the concrete. The

calculations reviled a force of 10 lbf impacting the concrete foundation.

Eccentricity

All the dynamic forces originate from the Rotor, which in a perfect world, would be

perfectly balanced, but since this is not the case, any connections to the turbomachinery

experience force or vibration due to this unbalance (U). The total mass of the rotor multiplied by

the eccentricity is known as the unbalance (Norfield, 2016). Eccentricity is the how much the

mass center is displaced from the bearing center (Norfield, 2006). Throughout this paper, it is

assumed that the rotor has a diameter of 12 inches. The max allowable unbalance of a 500lb and

1000lb rotor is shown in Table 5 and

Table 6. These values were calculated using equation (1) which uses a Gnumber 2.5

mm/s from the ISO 1940 for steam or gas turbines, and an RPM of 0 to 20,000 rpm.

Table 5 Allowable Unbalance of a 500 lb Rotor from 0-20,000 rpm

Itteration	Allowable Unbalance (in*lb)	RPM
0	0	0
1	0.235	2000
2	0.117	4000
3	0.078	6000
4	0.059	8000
5	0.047	10000
6	0.039	12000
7	0.034	14000
8	0.029	16000
9	0.026	18000
10	0.023	20000

Table 6 Allowable Unbalance of a 1000 lb Rotor from 0-20,000 rpm

Itteration	Allowable Unbalance (in*lb)	RPM
0	0	0
1	0.469	2000
2	0.235	4000
3	0.156	6000
4	0.117	8000
5	0.094	10000
6	0.078	12000
7	0.067	14000
8	0.059	16000
9	0.052	18000
10	0.047	20000

$$U = \frac{9.54 \; x \; G2.5 \; x \; mass(g)}{rpm} \tag{13}$$

The rotor in the model was assumed to be 1000lbs, therefore the maximum allowable

unbalance is 0.047 lb*in. We will assume that the distance from the center of the rotor to have an

unbalance mass located 5.5 in (r_e) from the center of gravity, this is the "rotating radius" in

ANSYS. Equation 2 and an unbalance of 0.040 was used to calculate the unbalanced mass(m_e)

of 0.000001755 lb. Allowable eccentricity is about .00008in using the G2.5 standard for a rotor traveling at 20,000 rpm. (ISO 1940, 2003).These values were plugged into ANSYS under the definition of the rotating force.

$$U = \ r_e m_e = eM \tag{14}$$

To represent this in the ANSYS model, a rotating force was applied to the "block" end of the piping assembly, point "A", which represents the compressor/turbine body, Figure 27. The rotating force was applied in counterclockwise direction which is represented by the rotational arrow symbol (b). The location of the center of the rotor (a) was applied approximately 5 inches from the edge of the compressor body. There were two supports applied for the harmonic response simulation at point "A" and "B" in Figure 18, as previously discussed.
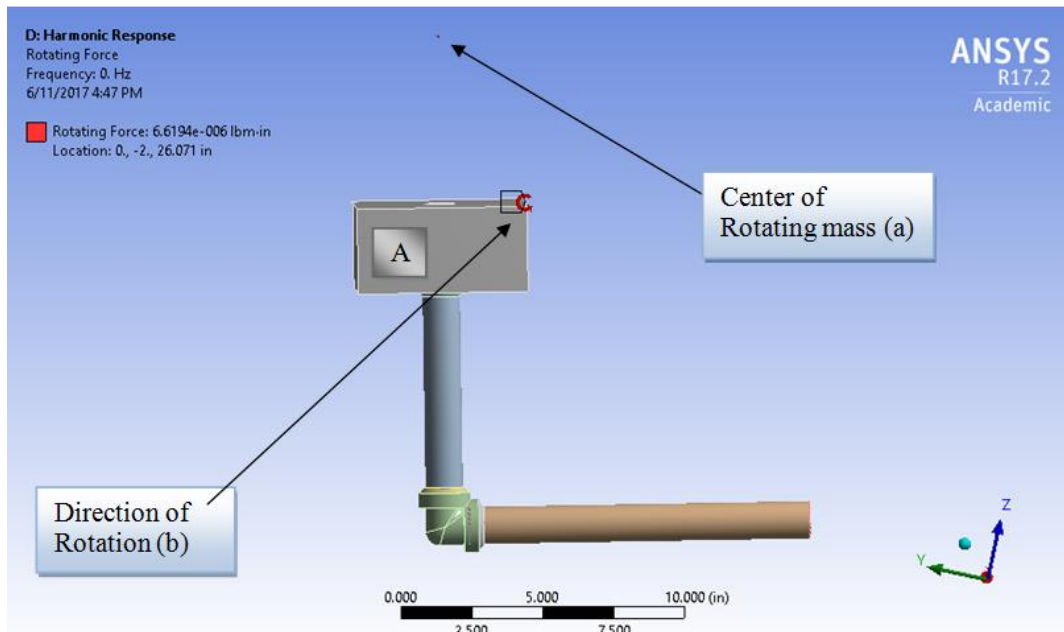
Figure 27 Rotating Force Conditions Applied to the Piping Assembly

Compressor FBD and Calculation Derivation

Looking at the compressor as a whole, it was determined how to draw the free body diagram (FBD) of the force transmitted from the mass unbalanced shaft to the compressor concrete foundation. Beginning from the shaft and working down the compressor to the foundation, the diagram was derived. Thinking about the problem, first beginning at the shaft where there is a whirling motion due to the imbalance in the rotor (Volokhovskaya, 2016). This unbalance will create a force between the shaft and the bearing. This equal balance exerts a force on the oil, which exerts a force on the bearing to the bearing housing and ultimately to the compressor supports and piping connected to the body. This Force is interpreted as a vibration or frequency. So exactly what force is being transmitted to the piping. The force depends on the unbalance that the rotor experiences. The force is transmitted from the shaft to the bearing to the compressor body to the concrete supports and piping. The damping force of the oil was determined using equation

$$c_1 = \frac{2\pi\mu R l}{d} \tag{1}$$

where μ is the absolute viscosity of the bearing oil, R is the radius of the shaft, l is the total length along that shaft that the oil is contacting, and d is the oil thickness between the shaft and the bearing. The normal thickness of oil between the shaft and bearing is 1.5 mils per inch of shaft diameter (Leader). There is also a dampening force between the compressor foot and the concrete foundation. This was calculated using the following equation.

$$\xi = \frac{c_5}{2\sqrt{k_5 m_5}} \tag{2}$$

where ξ is the dampening ratio, c_5 is the dampening constant to be solved, k_5 is the spring constant, and m_5 is the mass of the concrete base. The typical dampening ratio for concrete is from 0.04 – 0.07 (Sing, 2014; Consuegra, 2012). Based on this, a dampening ratio of 0.055 was utilized to calculate the dampening constant of the concrete foundation.

Between the shaft and bearing there is not a spring coefficient, only damping (Rao, 2011). Between the bearing (k_2), the bearing housing (k_3), the compressor (k_4), and the concrete foundation (k_5) there are spring constants. The constants for the bearing and housing were calculated using the deflection equation (3). The bearing housing is situated on the outer body of the compressor causing the housing to deflect in a radial manner. This force is in turn applying a shear force on the bolts that connect the bearing housing to the compressor. This shear force in turn translates a downward, radial force to the compressor body. The dampening of the bolts will be considered negligible and will not be modeled.

$$k = \frac{3EI}{L^3} \tag{3}$$

There are four feet that connect the compressor to the concrete foundation. These feet experience an axial force and therefore were calculated with the stiffness compression equation (4). The dimensions of the concrete are assumed from field experience with working on compressors. The dimension A is the cross sectional area of the concrete face contacting the compressor foot, E is the concrete Modulus of Elasticity with a value of 210 GPa (Zhang, 2015), and L is the thickness of the concrete base.

$$k_5 = \frac{A_5 E}{L_5} \tag{4}$$

After determining the dampening and spring constants, the Equation of Motion was derived. The equation is developed based on linear system components dealing with a mass eccentricity (Rao, 2011)

$$M\ddot{x} + C_{eq}\dot{x} + K_{eq}x = m_e e \omega^2 \sin \omega t \tag{5}$$

The unbalance force applied from the rotor to the compressor is

$$F_R = m_e e \omega^2 = U\omega \tag{6}$$

Combining these two equations the final equation of motion is

$$M\ddot{x} + C_{eq}\dot{x} + K_{eq}x = F_R \sin \omega t \tag{7}$$

The solve the differential equation, the solution $x(t) = X \sin(\omega t - \phi)$ was plugged into equation (7) to obtain the amplitude and phase angle

$$X = \frac{F_R}{\sqrt{\left[(K_{eq} - M\omega^2)^2 + (C_{eq}\omega)^2\right]}} \tag{8}$$

$$\phi = \tan^{-1}\left(\frac{C_{eq}\omega}{K_{eq} - M\omega^2}\right) \tag{9}$$

Therefore the force transmitted to the concrete foundation is

$$F_T = F_R \sqrt{\frac{K_{eq}^2 + (C_{eq}\omega)^2}{(K_{eq} - M\omega^2)^2 + (C_{eq}\omega)^2}} \tag{10}$$

Table 7 The Force Transmitted to the Compressor Foundation

Speed (RPM)	Force (N)	Force (lbf)
2000	45.564	10.243
4000	44.734	10.057
6000	44.584	10.023
8000	44.532	10.011
10000	44.508	10.006
12000	44.494	10.003
14000	44.486	10.001
16000	44.481	10
18000	44.478	9.999
20000	44.475	9.998

The force transmitted to the piping needed to be converted to the unbalance mass exerted to the piping. Ansys applied the rotating unbalance force via the unbalance mass and the location on the rotor that the unbalance mass was located. The unbalance transmitted to the foundation/piping is

$$U_T = \frac{F_T}{\omega} \tag{11}$$

The mass unbalance was then determined by dividing by the distance that the unbalance was from the rotor, 5.5 inches was utilized

$$m_{eT} = \frac{U_T}{r_e} \tag{12}$$

Table 8 The Unbalance and Mass Eccentricity Transmitted to the Compressor Foundation

Speed (RPM)	Unbalance (m*kg)	Mass (kg)	Mass (lb)
2000	**1.139e-5**	**8.154e-5**	**1.798e-4**
4000	**2.796e-6**	**2.001e-5**	**4.412e-5**
6000	**1.238e-6**	**8.865e-6**	**1.954e-5**
8000	**6.958e-7**	**4.981e-6**	**1.098e-5**
10000	**4.451e-7**	**3.186e-6**	**7.024e-6**
12000	**3.09e-7**	**2.212e-6**	**4.876e-6**
14000	**2.27e-7**	**1.625e-6**	**3.582e-6**
16000	**1.738e-7**	**1.244e-6**	**2.742e-6**
18000	**1.373e-7**	**9.827e-7**	**2.166e-6**
20000	**1.112e-7**	**7.959e-7**	**1.755e-6**

Full Compressor Analysis

An optional method to analyze the stress placed on the weld is to take the compressor body and model it using FEA. This will include modeling the bearing and bearing housing. This model will be ran with an unbalance force, based on the maximum allowable unbalance of the rotor, applied to the bearing. It will be evaluated to see how much the compressor body displaces due to the mass eccentricity. The location of the compressor body at which the displacement will be recorded is where the piping will be connected to the compressor.

The displacement will be gathered from the compressor model and applied to a separately modeled piping assembly. The displacement will be applied to the compressor end of the assembly, this is 'A' in Figure 18. The stresses at the welds will be gathered at the weld for the specified frequency range and evaluated which frequency ranges should be avoided.

31

CHAPTER THREE: FLANGED CONNECTIONS

This chapter will cover the results from the Finite Element Analysis (FEA) specifically interested in the weld connections at the compressor or turbine. We will be looking at the Mode shapes of the piping, the stresses at the weld, and how each change as the piping supports are spread further apart. The stress will be a key factor in the evaluation because we will use this variable to determine what vibration amplitudes that are considered acceptable or unacceptable. The frequency will be the targeted data which can be gathered in the field by the technicians.
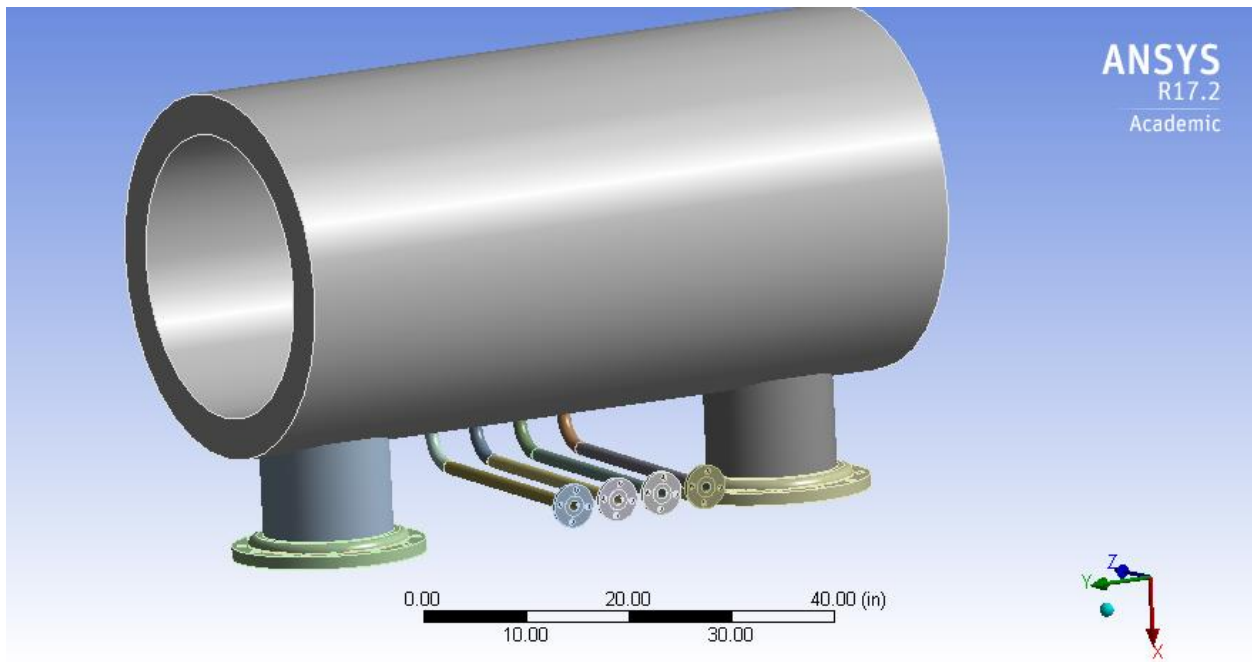
Figure 28 Compressor Body with the Flanged Piping Assembly

Above is a representation of how and where the FPA's are connected to the turbomachinery. The process side inlet and outlet are the 12" flanged connections, the large cylinder is the body of the compressor (thickness not to scale) and the hollow section is where the rotor would be located. This is a very basic representation and should not be utilized as a fact.

<u>Mode Shapes</u>

The mode shapes for each the FPA were gathered for each length of piping and recorded in tables below. The comparison of the Carbon Steel (CS) vs Stainless Steel (SS) Mode shapes revealed that the each were within 4% of each other, Table 11, and Table 14. Therefore the technician performing an analysis in the field does not need to be concerned with the material of construction when determining the mode shapes of the piping.

1" Diameter Piping

Table 9 Mode Shapes of the FPA, CS, 1" Diameter Piping

	Frequency and Displacement at Pipe Length							
	12"		24"		36"		48"	
Mode	HZ	in	HZ	in	HZ	in	HZ	in
1	169.77	12.01	59.66	10.48	33.52	9.65	21.56	8.92
2	414.09	21.46	179.17	15.75	113.78	12.41	79.69	10.66
3	1293.40	19.43	404.52	15.06	212.88	12.64	131.69	10.85
4	1400.30	19.70	473.05	15.33	264.38	14.86	174.83	13.86
5	1770.70	23.151	1027.90	14.71	542.06	12.48	333.39	10.59
6	2824.5	19.164	1092.5	15.28	588.83	12.966	367.65	11.93

Table 10 Mode Shapes of the FPA, SS, 1" Diameter Piping

	Frequency and Displacement at Pipe Length							
	12"		25"		36"		48"	
Mode	HZ	in	HZ	in	HZ	in	HZ	in
1	162.50	12.06	58.30	10.52	33.51	9.73	21.23	8.96
2	400.08	21.50	175.12	15.77	113.26	12.55	77.74	10.74
3	1242.07	19.64	394.58	15.10	213.08	12.77	129.17	11.05
4	1344.60	19.77	461.56	15.42	264.03	14.97	170.68	13.90
5	1730.00	23.624	1002.60	14.75	542.63	12.60	325.85	10.76
6	2736.2	19.061	1065.6	15.334	589.04	13.10	360.08	11.83

Table 11 % Difference of the FPA, CS vs SS, 1" Diameter Piping

	% Difference Between Mode Shapes							
	12"		**24"**		**36"**		**48"**	
Mode	HZ	in	HZ	in	HZ	in	HZ	in
1	4.282	0.431	2.281	0.456	0.021	0.827	1.517	0.410
2	3.383	0.205	2.260	0.165	0.457	1.108	2.445	0.717
3	3.969	1.079	2.457	0.271	0.094	0.979	1.914	1.873
4	3.978	0.384	2.429	0.590	0.132	0.755	2.374	0.273
5	2.299	2.002	2.461	0.312	0.105	0.984	2.262	1.580
6	3.126	0.537	2.462	0.352	0.036	1.046	2.059	0.872

Figures of the six mode shapes, unmodified, were also included in Appendix C. The

figures in this chapter were scaled to create a realistic shape of the piping deformation. When

studying the stainless steel configuration, just as the table comparing the difference in frequency

and displacements between the materials of construction, the same can be said of the physical

deformation. When comparing the mode and length of the SS to the CS models, both look to be

almost identical. This further confirms that when preparing piping in the field for adequate

support due to frequency it will be induced to, the carbon steel and stainless steel mode shapes

that the two different materials experience are very similar. For the piping 12 inches in length,

when the amplitude of displacement reaches above 15 inches, the piping, is construed into very

deformed configurations in which the piping itself would fail.

Figure 29 The 1st Mode for FPA, 1 Inch Diameter, CS, 12 Inches

Figure 30 The 1st Mode for FPA, 1 Inch Diameter, SS, 12 Inches Long
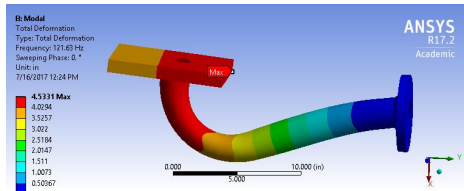
Figure 31 The 1st Mode for FPA, 2 Inch Diameter, CS, 12 Inches Long

The first mode of the 12" piping, Figure 29 and Figure 30, shows that the maximum

deformation occurs at the compressor to piping connection. The first mode the piping bends in

the downward direction away from the compressor body. The mode shape looks exactly the

same for the 1" CS and SS, the 2" diameter, Figure 31, is very similar in shape but is instead bent

toward the piping at about a 30 degree angle instead of about 60 degrees.

Figure 32 The 5th Mode for FPA, 1 Inch Diameter, CS, 48 Inches Long

Figure 33 The 5th Mode for FPA, 1 Inch Diameter, SS, 48 Inches Long
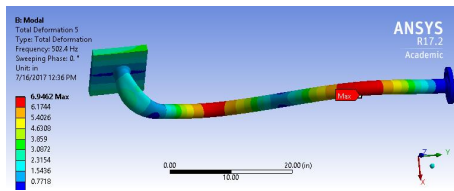
Figure 34 The 5th Mode for FPA, 2 Inch Diameter, CS, 48 Inches Long

The fifth mode of the 1" and 2", 48" long piping comparison shows that the 2" diameter

piping, Figure 34, has a displacement of about half the 1" diameter piping, Figure 32and Figure

33, 6.8 vs. 10.8 inches. The one difference between the CS and SS piping is that the amplitude

direction is opposite with the upward being first for the SS, when coming from the compressor, and being second for the CS.

Studying the 24 inch long, 1" diameter piping, for modes 3 – 6, the bends are extreme and at a sharp points and the piping itself is flattened. This sharp degree at the bends decreases as the length in the piping is increased. When the length reaches 48 inches, the modes shapes look to be what is typically seen in a college textbook when explaining the appearance of the first six modes of vibration. In Figure 35, Figure 36, and Figure 37 the scaling of the displacement has been decreased to 0.21 the actual. It is interesting to note that in Figure 37, mode 6, the displacement is not only in the vertical direction but also in the horizontal.
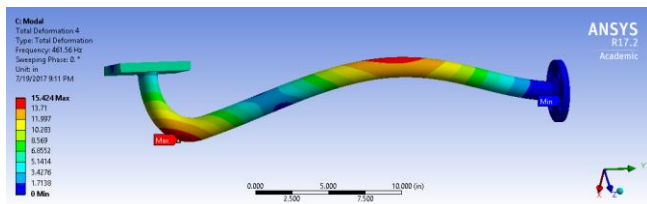
Figure 35 The 4th Mode for FPA, 1 Inch Diameter, SS, 24 Inches Long

Figure 36 The 5th Mode for FPA, 1 Inch Diameter, SS, 24 Inches Long
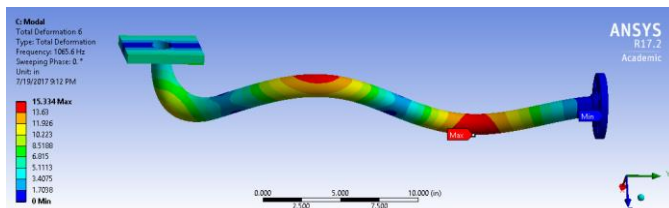
Figure 37 The 6th Mode for FPA, 1 Inch Diameter, SS, 24 Inches Long

When looking at the first mode vs. the third mode of the 1" diameter, 12" long CS piping, Figure 38 and Figure 39, it can be distinctively seen that the connection to the

compressor, the piping is displaced in opposite directions with respect to the compressor body. In Figure 38 the compressor body looks to be turned inward toward the piping and flange. For the third mode 90 degree pipe bend is now almost 180 degrees in direction from the compressor body. This may be the compressor body moving in the upward direction away from the piping assembly. The figures were scale to about 0.25 from the actual displacement.
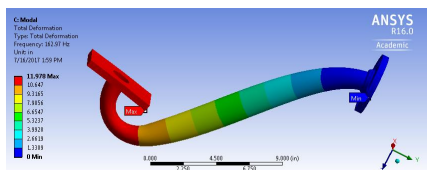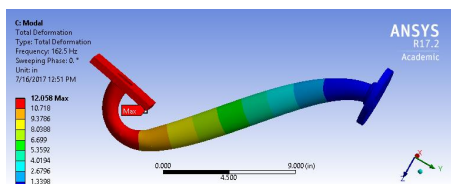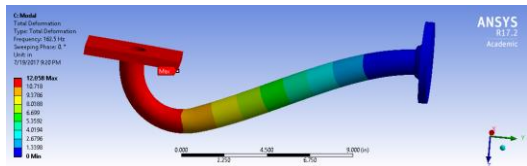

Figure 38 The 1st Mode for FPA, 1 Inch Diameter, CS, 12 Inches Long
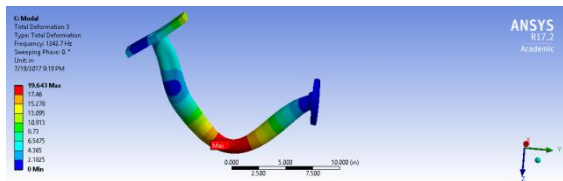
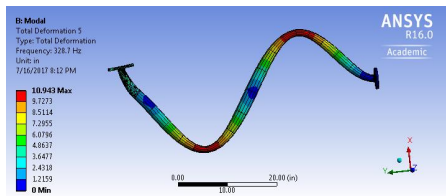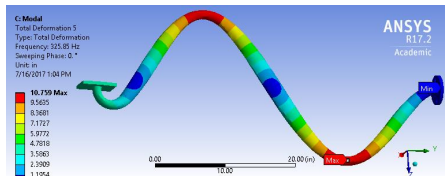**Figure 39 The 3rd Mode for FPA, 1 Inch Diameter, SS, 12 Inches Long**

2" Diameter Piping

The maximum displacement at the each of the mode shapes is much smaller for the 2" piping vs. the previous, almost half the amplitude. The comparison between the SS and CS was similar where the frequency and amplitude displacement were within 2% almost for the entire board.

Table 12 Mode Shapes of the FPA, CS, 2" Diameter Piping,

	Frequency and Displacement at Pipe Length, Fixed Displacement BC							
	12"		24"		36"		48"	
Mode	HZ	in	HZ	in	HZ	in	HZ	in
1	121.63	4.53	55.13	4.16	20.10	2.51	21.91	3.86
2	279.32	8.04	160.80	8.43	74.59	6.16	83.60	7.18
3	681.45	7.75	560.89	8.96	291.20	8.16	191.22	7.50
4	1067.00	11.80	567.89	8.28	292.04	7.96	212.60	7.10
5	1605.80	13.025	692.42	6.72	437.01	4.07	502.40	6.95
6	2190.8	12.203	1147.00	10.69	695.86	8.6946	505.49	7.18

Table 13 Mode Shapes of the FPA, SS, 2" Diameter Piping,

	Frequency and Displacement at Pipe Length, Fixed Displacement BC							
	12"		24"		36"		48"	
Mode	HZ	in	HZ	in	HZ	in	HZ	in
1	120.36	4.56	54.54	4.19	19.88	2.52	21.62	3.88
2	276.11	8.09	158.75	8.49	73.62	6.21	82.39	7.23
3	674.16	7.80	554.52	9.01	288.03	8.21	188.75	7.55
4	1055.10	11.88	561.76	8.34	288.71	8.01	209.68	7.14
5	1587.90	13.115	684.79	6.77	432.20	4.10	495.80	6.99
6	2164.9	13.302	1133.90	10.76	687.97	8.7414	498.91	7.33

Table 14 % Difference of the FPA, CS vs SS, 2" Diameter Piping

	% Difference Between Displacements and Mode							
	12"		24"		36"		48"	
Mode	HZ	in	HZ	in	HZ	in	HZ	in
1	1.044	0.620	1.070	0.630	1.075	0.635	1.314	0.644
2	1.149	0.707	1.275	0.686	1.301	0.677	1.458	0.664
3	1.070	0.623	1.136	0.638	1.089	0.667	1.292	0.604
4	1.115	0.682	1.079	0.741	1.140	0.630	1.373	0.612
5	1.115	0.686	1.102	0.682	1.101	0.644	1.314	0.597
6	1.182	8.262	1.142	0.688	1.134	0.535	1.302	2.060

The figures of the modes shapes were recorded in Appendix C, the 2" diameter piping mode shape configurations were not the same as that of the 1", they were less deformed which is to be expected due to the larger cross-sectional area and greater thickness of the piping. The 12" lengths experienced major deformation like the 1" piping diameter, especially for modes 4 - 6. The 24 inch long piping has a few obscure deformities for the last four modes but the shapes have improved dramatically compared to the previous. The two longest lengths of piping, the amplitudes exhibit the classical shapes of the first six modes of vibration.

The fifth mode of the 24" long, 2" diameter piping looks very similar to the third mode of the 1" diameter, Figure 40 and Figure 41. The flange for the 5th mode, 2" diameter, Figure 40, it

is observed that the piping at the compressor is straightened out at the compressor, but instead of

the piping displacing downward, like in Figure 41, it is displaced upward.

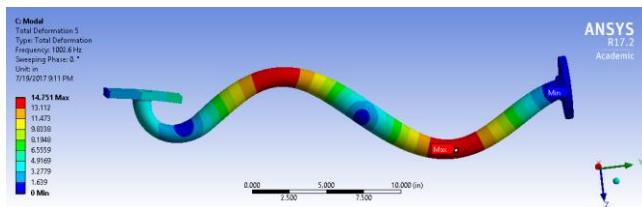**Figure 40 The 5th Mode for FPA, 2 Inch Diameter, CS, 24 Inches Long**
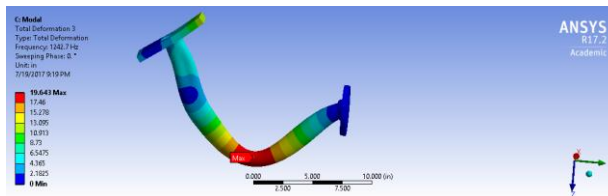
Figure 41 The 3rd Mode for FPA, 1 Inch Diameter, SS, 12 Inches Long

The stainless steel piping, when compared to the carbon steel exhibits almost the same

mode shape deformations. The same comparison is observed that the SS and CS piping

assemblies are very similar in their response. See the 24" long CS and SS flange piping

assembly in Figure 42 and Figure 43, to see the similarity in the shape deformation. The actual

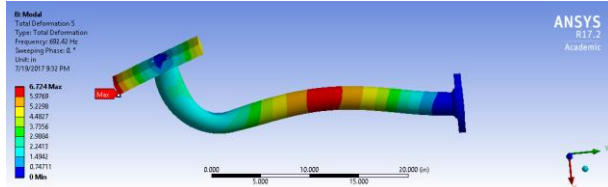maximum displacement of each is almost the same with the CS at 8.43" and the SS at 8.46".

Figure 42 The 2nd Mode for FPA, 2 Inch Diameter, CS, 24 Inches Long

Figure 43 The 2nd Mode for FPA, 2 Inch Diameter, SS, 24 Inches Long

Acceptable Vibration Range

It is known that it is not ideal to induce a body to its natural frequency. Therefore it should be common knowledge that the 6 modes reported earlier would indicate values at which would be unacceptable frequencies to induce upon the piping. The question then lies, at what range of frequencies about the natural frequency ar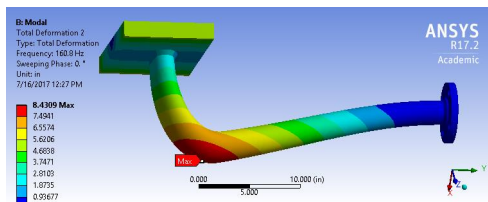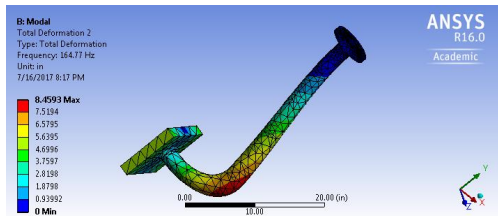e allowed. Each of the piping assemblies were studied at 5 Hz intervals from 0 -350 Hz to see what stresses were induced to the piping welds. The tables begin with the mode shape frequencies, all within 350 Hz, and the stress at those frequencies. The frequencies are then studied between the modes to determine if there are other large peaks in stress besides at the mode shape, these are labeled as "before and "after".

1" Diameter Piping

The desired stress at the welds was determined to be less than the endurance limit. Unfortunately the model did not relay any stresses above the endurance limit. It is clear that the method utilized to determine the unacceptable frequencies was not adequate. The models are linear and are expected, when modeled correctly, that there will be unacceptable frequencies that correspond to the tables below. In the table, the acceptable frequencies were recorded as follows, less than 1 psi before the first mode, less than 2psi before the second mode, and subsequently. The exception to the rule includes that when the stress in the welds are much smaller than the peaks and less than 6 psi. The list of allowable frequencies were determined from the peak in stress at the welds and the maximum allowable stress per mode shape. These are the recommended frequencies that the pipe is allowed to experience. The last column in the tables is the unacceptable frequency range at which it is not recommend to allow the pipe to

vibrate at. It is expected that the likelihood of failure of the weld will be greatly increased at these frequencies. It is recommended that the piping be either supported differently or a mass added to the pipe to decrease its natural frequency if it experiences any frequencies to avoid.

Table 15 Frequencies to Avoid, FPA 1" Diameter, CS, 12" Long

Mode	Mode Location	Peak Frequency (Hz)	Peak Stress (psi)	Frequency Allowable (Hz)	Stress Allowable (psi)	Frequency Avoid (Hz)
				12" Long Piping, CS, 1"		
1	Before	N/A	N/A	0-100	<1	120-230
	During	169	198.29	100 -120	<2	
	After	N/A	N/A	230 - 350	<4	N/A

Table 16 Frequencies to Avoid, FPA 1" Diameter, SS, 12" Long

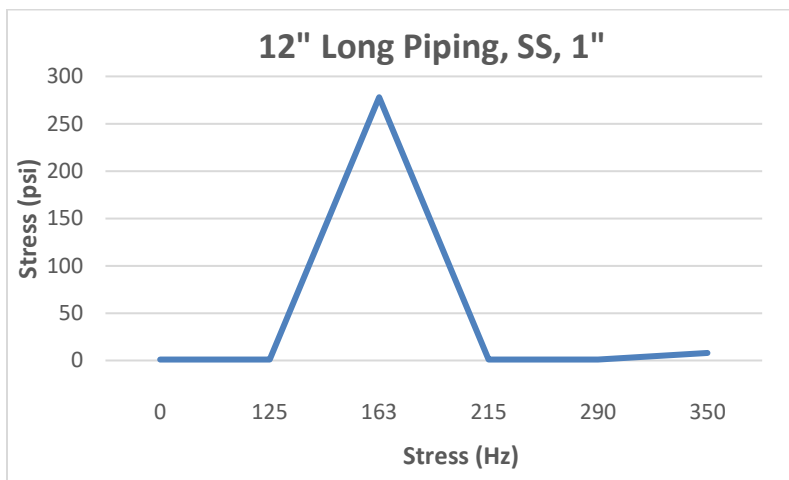| Mode	Mode Location	Peak Frequency (Hz)	Peak Stress (psi)	Frequency Allowable (Hz)	Stress Allowable (psi)	Frequency Avoid (Hz)
				12" Long Piping, SS, 1"		
1	Before	N/A	N/A	0-95	<1	N/A
	During	162.5	277.76	100 - 125	<2	125-215
	After	350	8.033	215 - 290	<4	290-350

Figure 44 Stress vs. Frequency of FPA 1" Diameter, SS, 12" Long

As previously stated about the mode shapes, the material of construction of the SS and CS does not greatly affect the acceptable range of frequencies. The acceptable and unacceptable

ranges for the same pipe length but different materials is so similar, there is not really a need for separate tables. This will simplify the job for the technician gathering and analyzing the results of the data, knowing that he has one less piece of information to gather, the material of construction. This is true for pipe lengths supported at the 24 and 36 inch range. When the piping supports become closer together, 12" span, or quite far apart, 48" span, the results begin to vary. It is highly recommended that at the 12" and 48" spans the material of construction be known and the table per the material of construction be utilized.

Table 17 Frequencies to Avoid, FPA 1" Diameter, CS, 24" Long

Mode	Mode Location	Peak Frequency (Hz)	Peak Stress (psi)	Frequency Allowable (Hz)	Stress Allowable (psi)	Frequency Avoid (Hz)
		24" Long Piping, CS, 1"				
1	During	59.66	51.631	0-40	<1	40-70
	After	110	18.629	70-100	<2	100-120
2	Before	110	18.629	120-160	<2	160-200
	During	179.17	1.702	200-250	<3	250-320
	After	300	27.096	320-350	<6	N/A

Table 18 Frequencies to Avoid, FPA 1" Diameter, SS, 24" Long

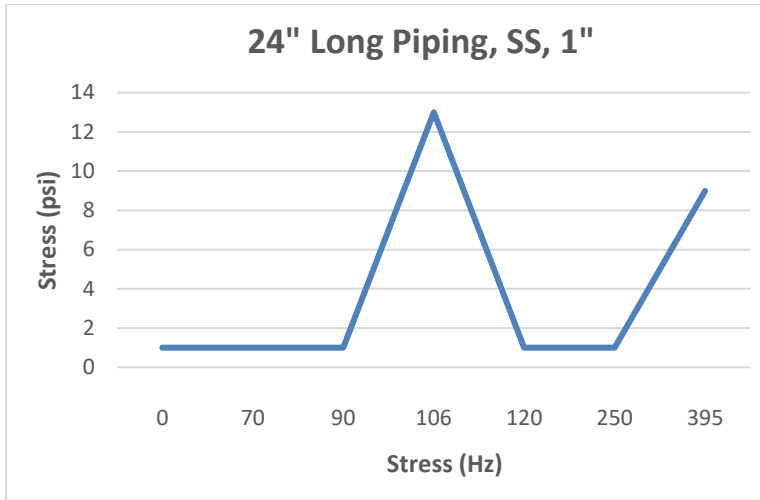| Mode	Mode Location	Peak Frequency (Hz)	Peak Stress (psi)	Frequency Allowable (Hz)	Stress Allowable (psi)	Frequency Avoid (Hz)
		24" Long Piping, SS, 1"				
1	During	58.3	0.844	0-50	<1	50-70
	After	106	13	70-90	<2	90-120
2	During	175.12	0.42212	120-170	<2	170-190
	After	395	9	190-250	<2	250-350

Figure 45 Stress vs. Frequency of FPA 1" Diameter, SS, 24" Long

Studying the table to see what ranges of frequency are to be avoided, for all stainless steel

lengths and carbon steel, for the 24" and 36" lengths, the 270-285 Hz range is to be avoided. The

second similarity comparison attains to the 24" and 36" lengths of SS and CS piping, at which

the 55-65 Hz range is to be avoided. Therefore 40% - 50% of the data for each table, can be

equally compared to another table with different material and length size having the same

undesirable frequency.

Table 19 Frequencies to Avoid, FPA 1" Diameter, CS, 36" Long

				36" Long Piping, CS, 1"		
Mode	**Mode Location**	**Peak Frequency (Hz)**	**Peak Stress (psi)**	**Frequency Allowable (Hz)**	**Stress Allowable (psi)**	**Frequency Avoid (Hz)**
1	**During**	33.52	7	0-28	<1	28-40
	After	60	7	40-55	<1	55-65
2	**During**	113.78	1	65- 135	<1	135-180
	After	165	6	180-190	<3	190-240
3	**During**	212.88	25	240-260	<4	260-310
4	**During**	264.38	0.253	310 - 350	< 5	N/A
	After	290	101	N/A	N/A	N/A

Table 20 Frequencies to Avoid, FPA 1" Diameter, SS, 36" Long

Mode	Mode Location	Peak Frequency (Hz)	Peak Stress (psi)	Frequency Allowable (Hz)	Stress Allowable (psi)	Frequency Avoid (Hz)
36" Long Piping, SS, 1"						
1	During	33.51	6	0-28	< .5	28-45
1	After	60	27	45- 55	< .5	55-65
2	During	113.26	0.5	65- 110	< 1	110 - 120
2	After	165	5.5	120 -140	< 1	140-175
3	Before	165	5.5	175 - 185	<3	185-240
3	During	213.08	969	240- 260	< 4	260-310
4	During	264.03	3.44	310 - 340	<5	340-350
4	After	290	2072	N/A	N/A	N/A
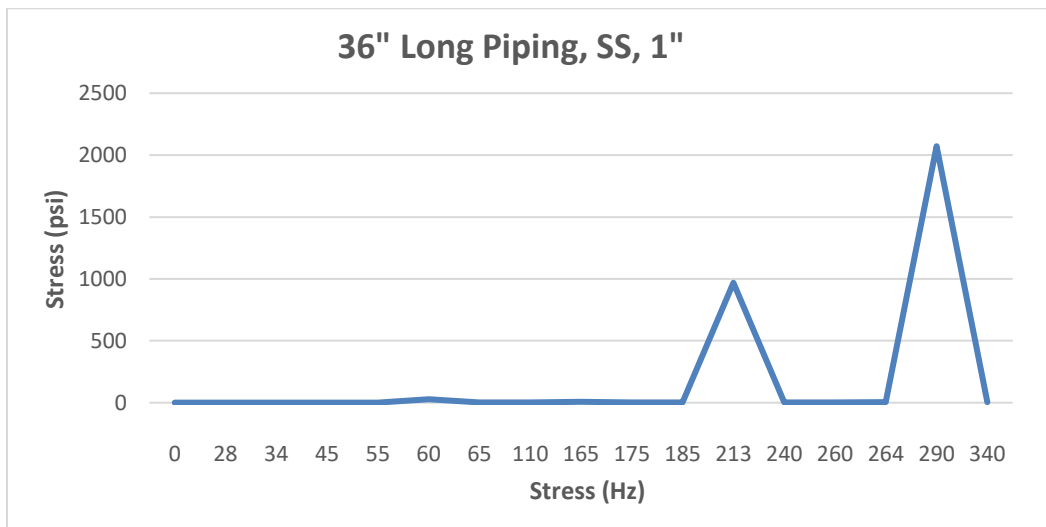
Figure 46 Stress vs. Frequency of FPA 1" Diameter, SS, 36" Long

Table 21 Frequencies to Avoid, FPA 1" Diameter, CS, 48" Long

Mode	Mode Location	Peak Frequency (Hz)	Peak Stress (psi)	Frequency Allowable (Hz)	Stress Allowable (psi)	Frequency Avoid (Hz)
48" Long Piping, CS, 1"						
1	Before	15	2.1	0-9	<1	9 - 25
1	During	21.56	1.268	25 -40	< 2	40 >

Table 22 Frequencies to Avoid, FPA 1" Diameter, CS, 48" Long

48" Long Piping, SS, 1"						
Mode	**Mode Location**	**Peak Frequency (Hz)**	**Peak Stress (psi)**	**Frequency Allowable (Hz)**	**Stress Allowable (psi)**	**Frequency Avoid (Hz)**
1	During	21.23	0.377	0 - 15	< 1	15 - 25
2	During	77.74	0.2748	25 - 70	< 1	70 -85
3	During	129.17	121	85 - 110	< 1	110- 140
4	During	170.68	1.2	140 - 165	< 2	165 - 175
	After	275	18	175 -225	< 2	255 - 285
5	During	325.85	107	285 -300	< 4	300 >
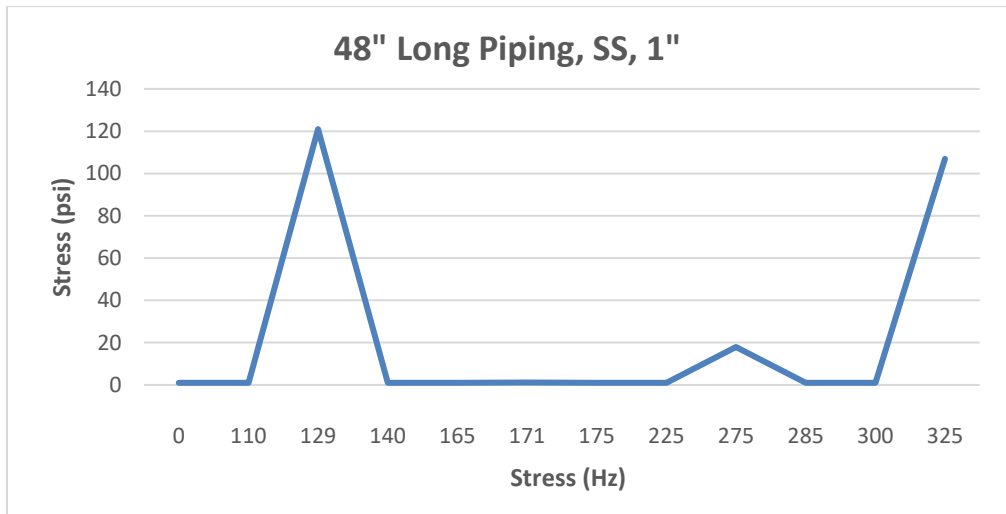
Figure 47 Stress vs. Frequency of FPA 1" Diameter, SS, 48" Long
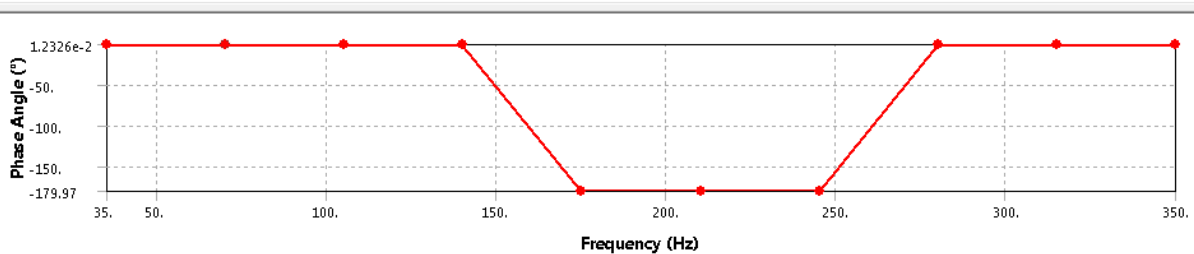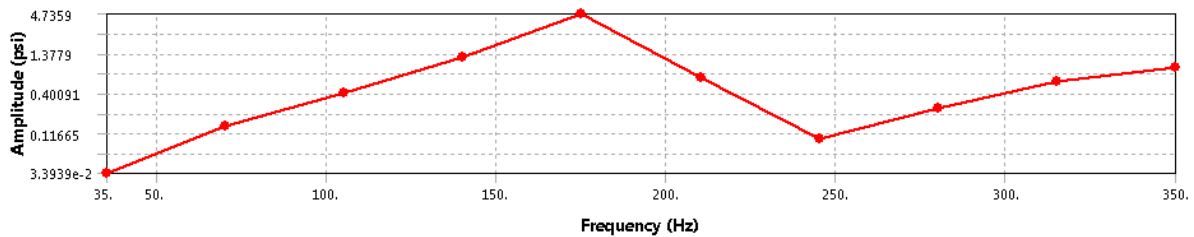
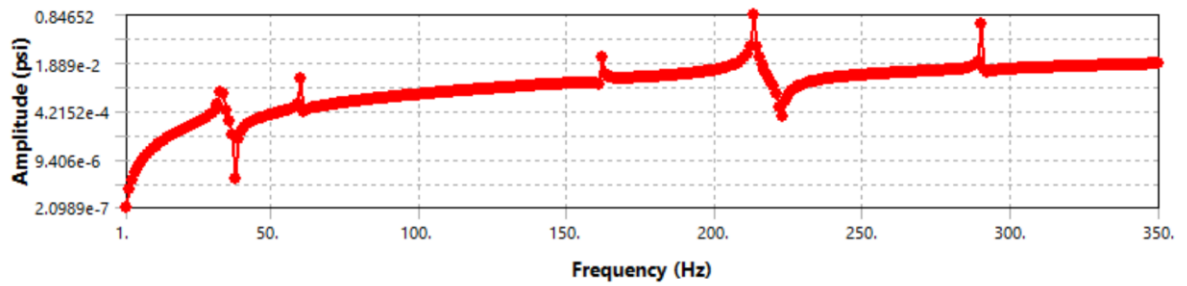**Figure 48 Phase Angle and Amplitude of FPA, CS, 1" Diameter, 12" Long**
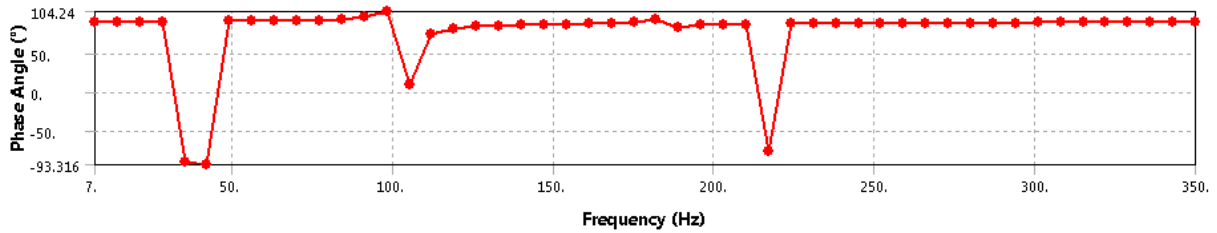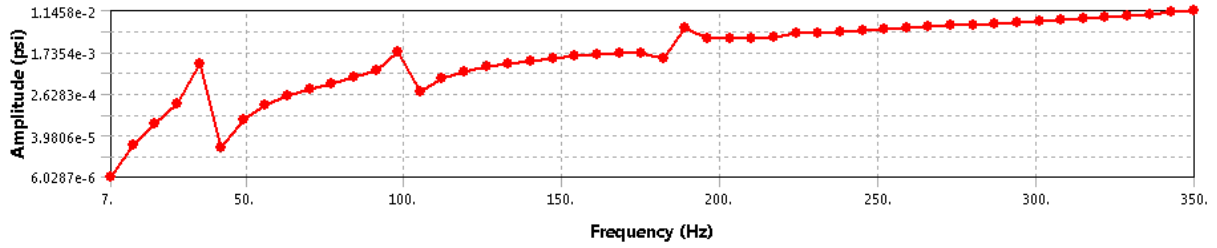
Figure 49 Phase Angle and Amplitude of FPA, CS, 1" Diameter, 36" Long
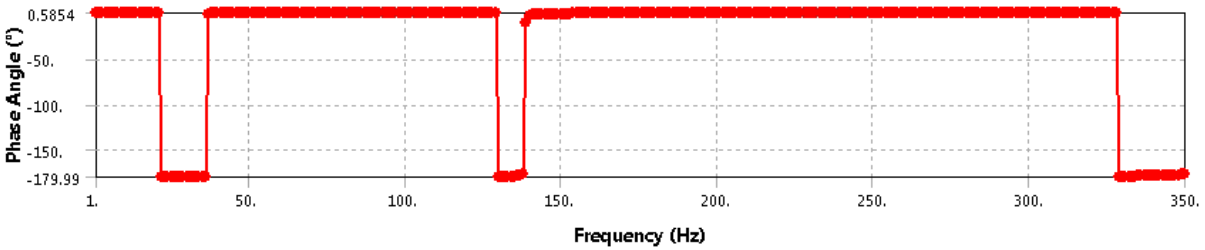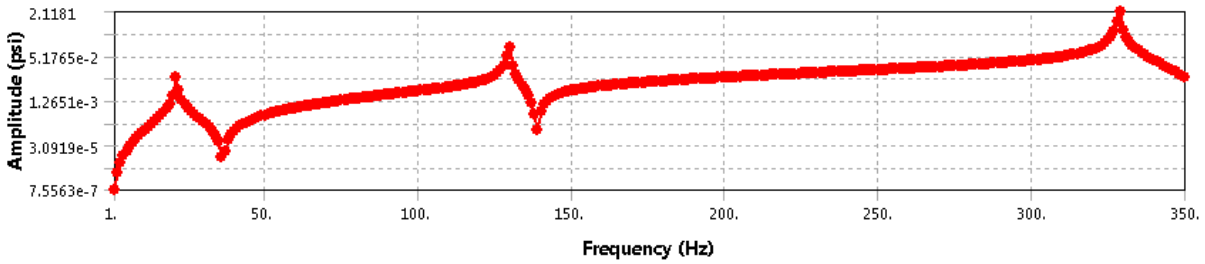
Figure 50 Phase Angle and Amplitude of FPA, CS, 1" Diameter, 48" Long
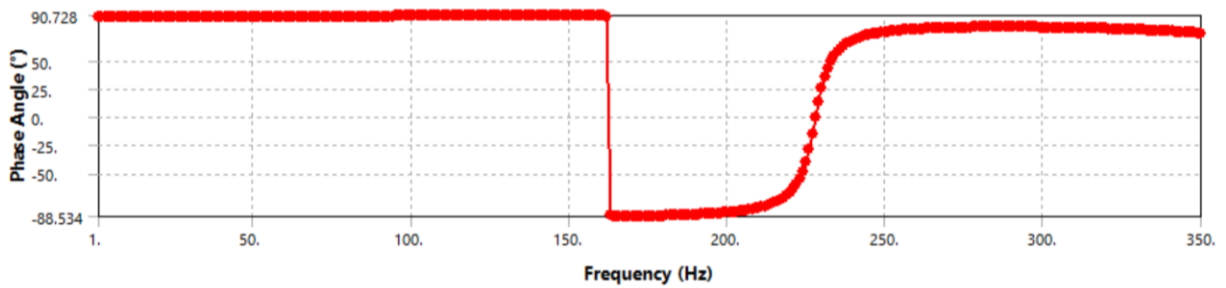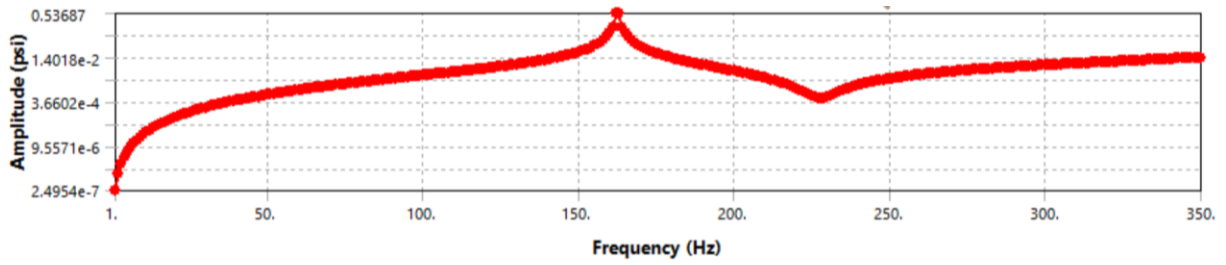
Figure 51 Phase Angle and Amplitude of FPA, SS, 1" Diameter, 12" Long
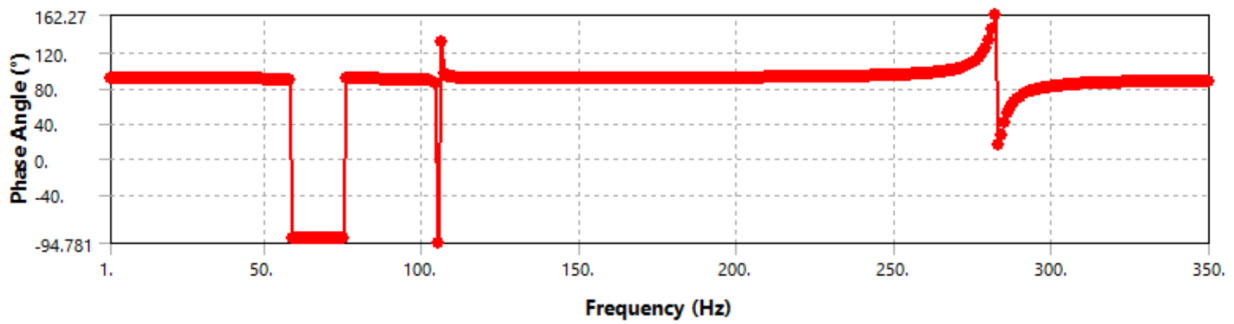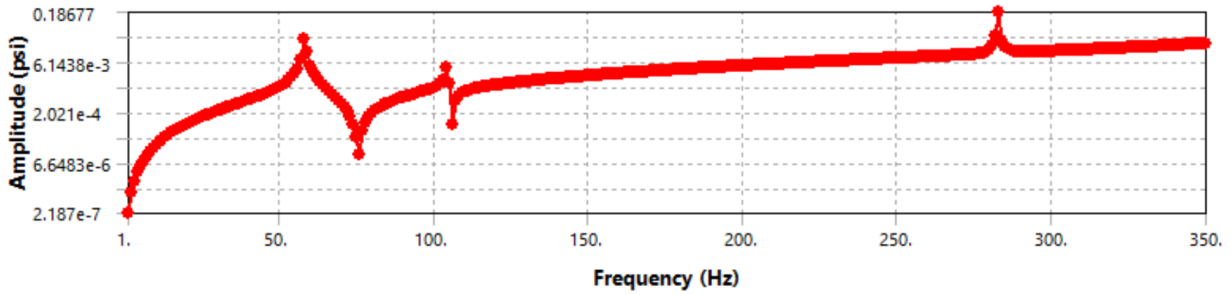
Figure 52 Phase Angle and Amplitude of FPA, SS, 1" Diameter, 24" Long
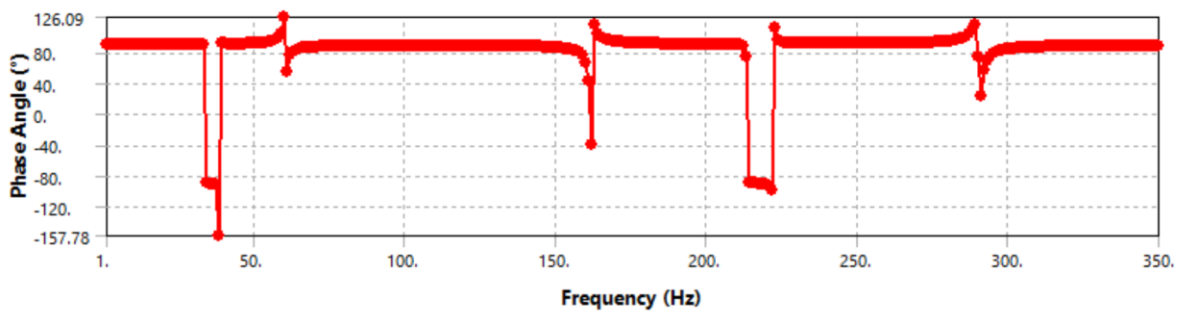
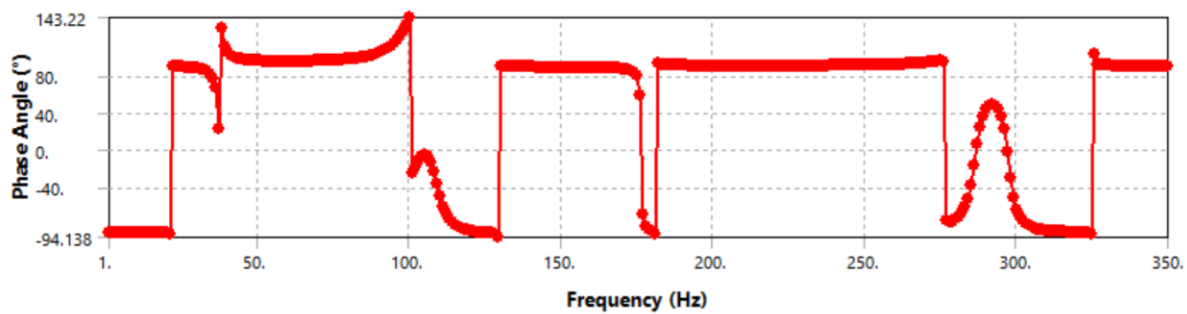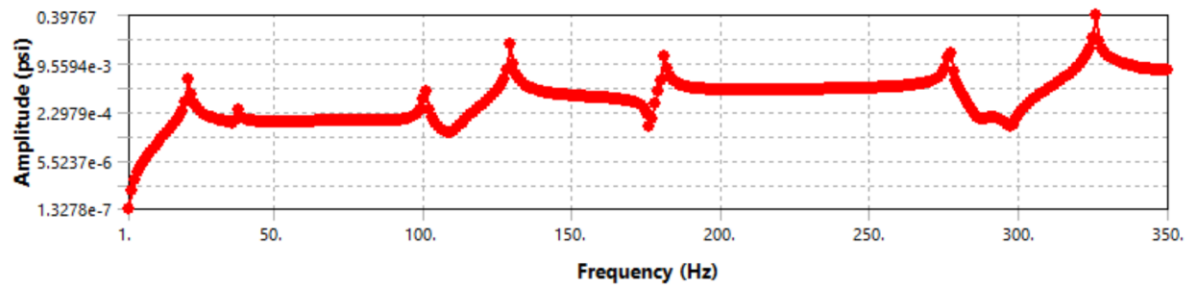**Figure 53 Phase Angle and Amplitude of FPA, SS, 1" Diameter, 36" Long**

Figure 54 Phase Angle and Amplitude of FPA, SS, 1" Diameter, 48" Long

2" Diameter Piping

The FPA had four corresponding frequencies across different piping lengths compared to the 2" SWPA which only had one. These included 15 – 30 Hz, 70-80 Hz, 100 – 155 Hz, and 120 – 180 Hz. The comparison of the same length of piping, CS vs SS, the frequencies to avoid corresponded almost exactly. There are discrepancies between the two, therefore it is necessary for the technician to utilize both material tables when analyzing the piping. The analysis provided below is exceedingly lower than the endurance limit of the materials and therefore would not experience failure and need to be determined via another method.

Table 23 Frequencies to Avoid, FPA 2" Diameter, CS, 12" Long

Mode	Mode Location	Peak Frequency (Hz)	Peak Stress (psi)	Frequency Allowable (Hz)	Stress Allowable (psi)	Frequency Avoid (Hz)
1	**Before**	N/A	N/A	0 - 55	<1	75>
	During	121.63	206.22	55-75	<2	

Table 24 Frequencies to Avoid, FPA 2" Diameter, SS, 12" Long

Mode	Mode Location	Peak Frequency (Hz)	Peak Stress (psi)	Frequency Allowable (Hz)	Stress Allowable (psi)	Frequency Avoid (Hz)
1	**During**	120.36	66.61	0 - 100	< 1	100-155
	After	250	598	155 - 210	<2	210 - 305
2	**During**	276.11	5.06	305 - 350	< 3	N/A

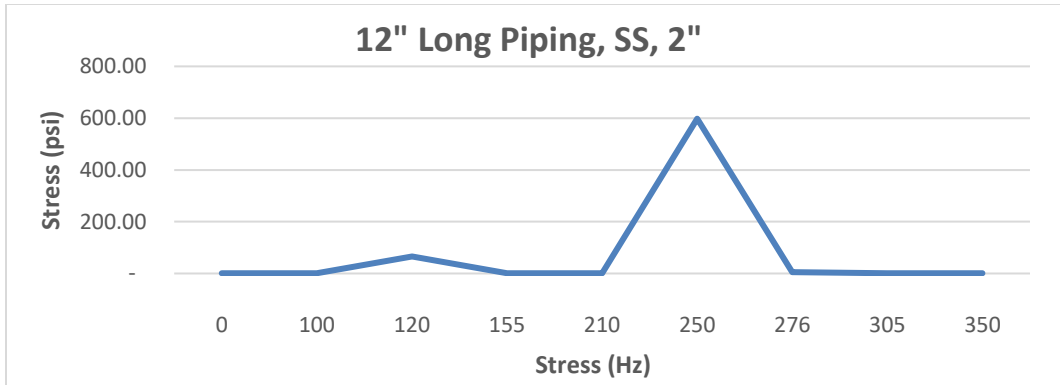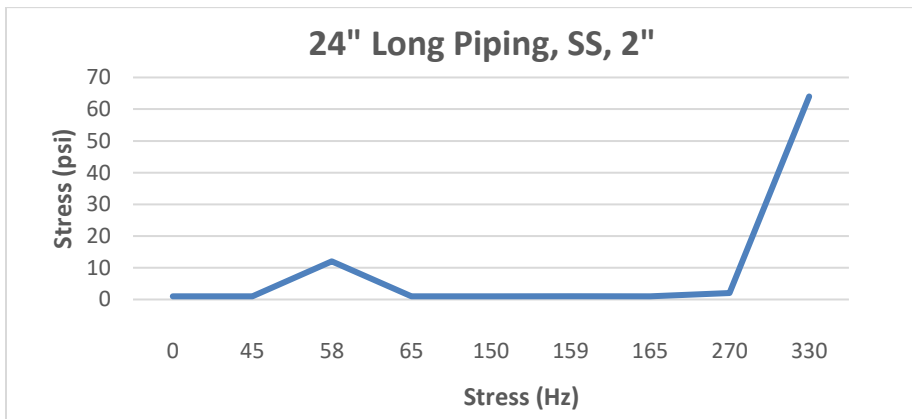**Figure 55 Stress vs. Frequency of FPA 2" Diameter, SS, 12" Long**

Table 25 Frequencies to Avoid, FPA 2" Diameter, CS, 24" Long

Mode	Mode Location	Peak Frequency (Hz)	Peak Stress (psi)	Frequency Allowable (Hz)	Stress Allowable (psi)	Frequency Avoid (Hz)
		24" Long Piping, CS, 2"				
1	During	55.13	40.997	0-55	< 1	55-65
	After	130	25	65 - 120	<1	120-170
2	During	160.8	1.11	170 - 240	<2	240 >
	After	330	22	N/A	N/A	N/A

Table 26 Frequencies to Avoid, FPA 2" Diameter, SS, 24" Long

Mode	Mode Location	Peak Frequency (Hz)	Peak Stress (psi)	Frequency Allowable (Hz)	Stress Allowable (psi)	Frequency Avoid (Hz)
		24" Long Piping, SS, 2"				
1	During	58.301	11.89	0 -45	<1	45 - 65
2	During	158.75	1.0648	65 - 150	< 2	150 - 165
	After	330	64	165-270	<3	270 >

Figure 56 Stress vs. Frequency of FPA 2" Diameter, SS, 24" Long

50

Table 27 Frequencies to Avoid, FPA 2" Diameter, CS, 36" Long

Mode	Mode Location	Peak Frequency (Hz)	Peak Stress (psi)	Frequency Allowable (Hz)	Stress Allowable (psi)	Frequency Avoid (Hz)
1	During	20.1	1.86	0 - 15	< 1	15-25
2	During	74.59	0.1736	25 - 70	< 1	70 -80
3	Before	165	4.6	80 -155	<1	155-180
3	During	291.2	61.96	180 - 255	< 1	255-295
4	After	320	43	295 - 310	< 4	310 - 350

Table 28 Frequencies to Avoid, FPA 2" Diameter, SS, 36" Long

Mode	Mode Location	Peak Frequency (Hz)	Peak Stress (psi)	Frequency Allowable (Hz)	Stress Allowable (psi)	Frequency Avoid (Hz)
1	During	19.88	7.101	0-15	<1	15-30
1	After	65	3.7447	30 -60	<1	60-75
2	During	73.62	0.18682	75 - 155	<1	155-180
3	Before	165	4.6036	180 - 255	<1	255-335
3	During	288.03	4.4681	335-350	<3	N/A
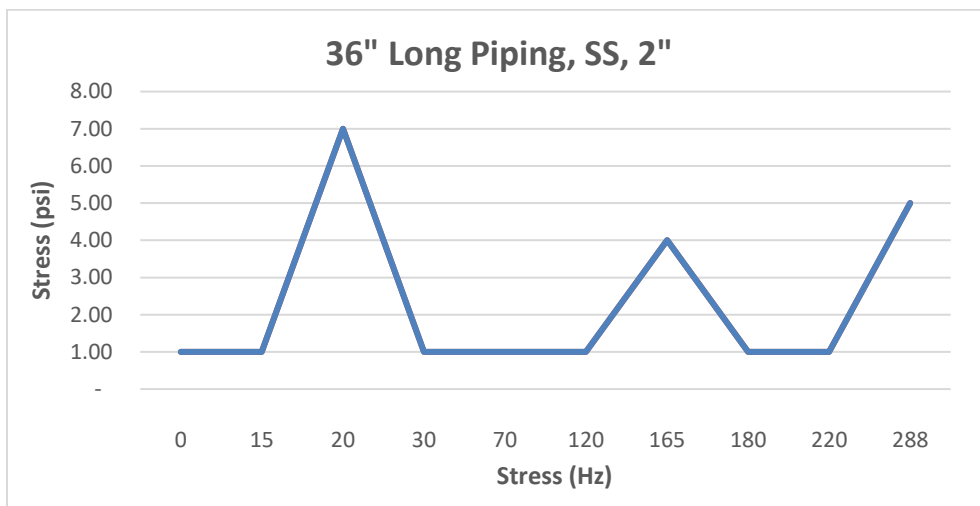
Figure 57 Stress vs. Frequency of FPA 2" Diameter, SS, 36" Long

Table 29 Frequencies to Avoid, FPA 2" Diameter, CS, 48" Long

				48" Long Piping, CS, 2"		
Mode	Mode Location	Peak Frequency (Hz)	Peak Stress (psi)	Frequency Allowable (Hz)	Stress Allowable (psi)	Frequency Avoid (Hz)
1	During	21.91	0.354	0 - 15	< 1	15 -25
2	During	83.6	0.13	25 - 75	< 1	75 -85
	After	140	5.11	85 - 130	< 1	130 -155
3	Before	140	5.11	155 - 180	< 1	180-200
	During	191.22	32.33	200 - 210	< 2	210 - 220
4	During	212.6	1.06	220-235	< 2	235 - 265
	After	250	20.4	265 - 320	< 2	320 -350

Table 30 Frequencies to Avoid, FPA 2" Diameter, SS, 48" Long

				48" Long Piping, SS, 2"		
Mode	Mode Location	Peak Frequency (Hz)	Peak Stress (psi)	Frequency Allowable (Hz)	Stress Allowable (psi)	Frequency Avoid (Hz)
1	During	22	3.82	0 - 20	< 1	20 - 30
2	During	82	0.13	30 - 75	< 1	75 - 85
	After	140	15.72	85 - 130	< 1	135 - 150
3	During	189	54.77	150 - 180	< 1	180 - 260
4	During	210	1	260 - 315	< 2	315 - 350
	After	245	31	N/A	N/A	N/A
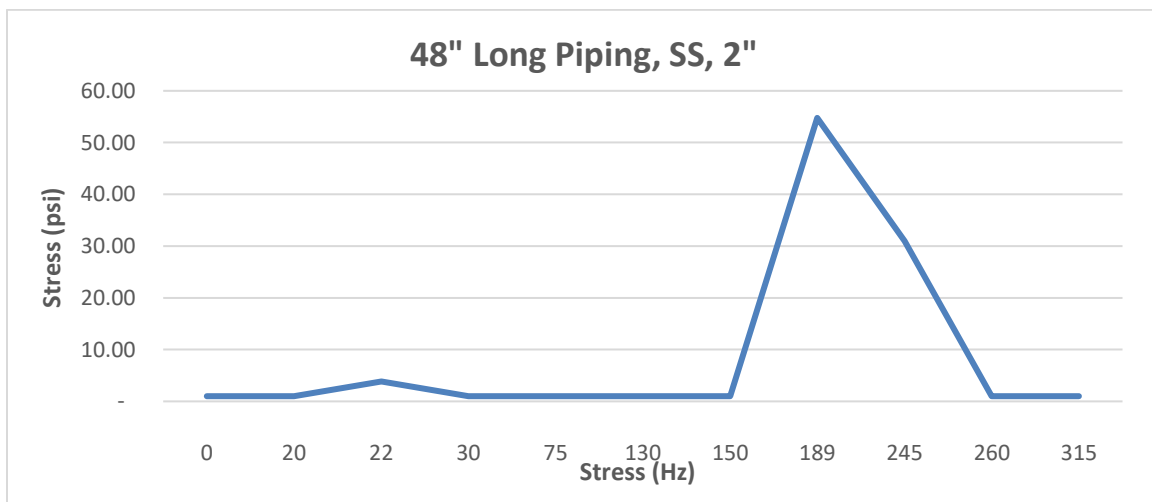
Figure 58 Stress vs. Frequency of FPA 2" Diameter, SS, 48" Long
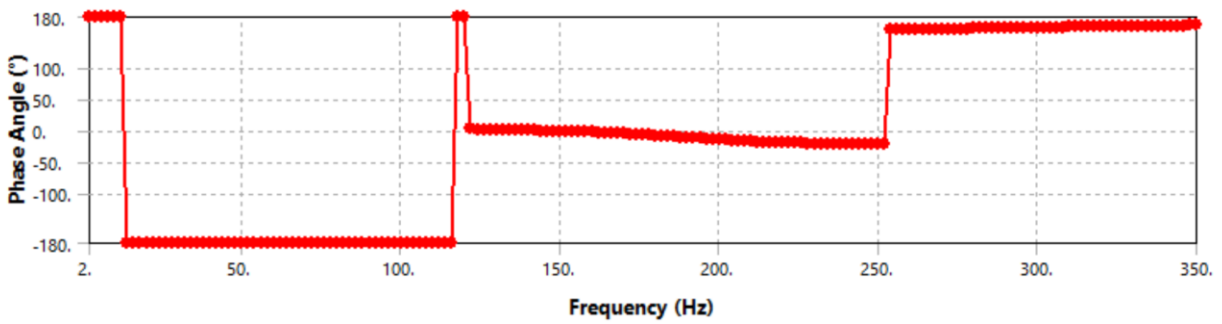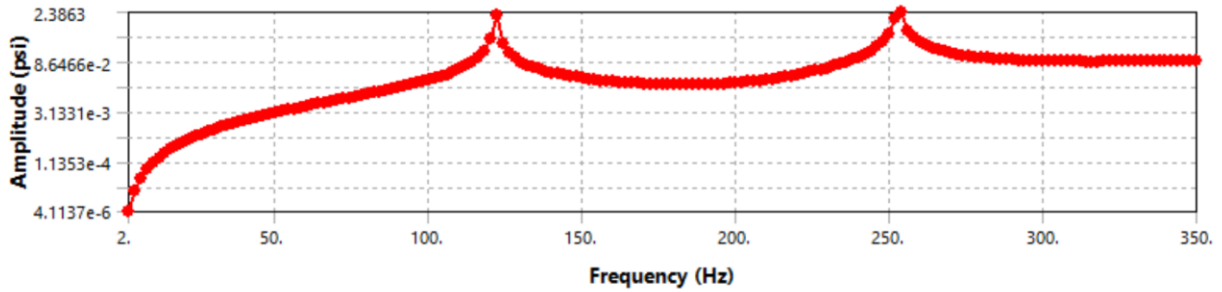
Figure 59 Phase Angle and Amplitude of FPA, CS, 2" Diameter, 12" Long
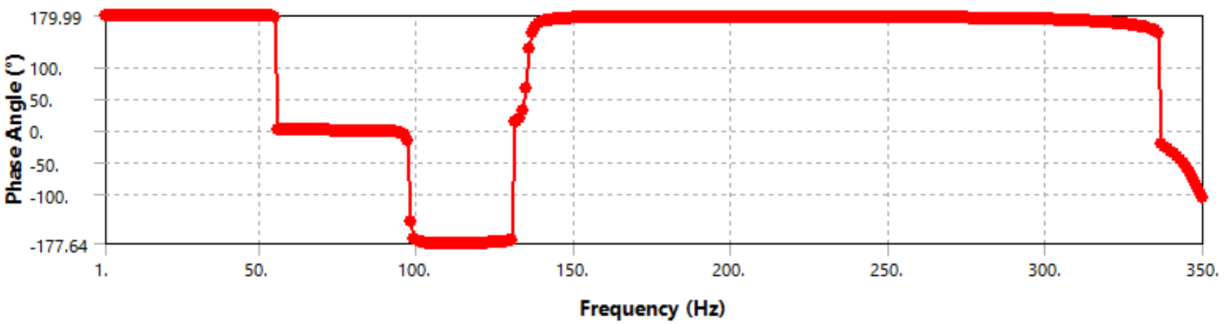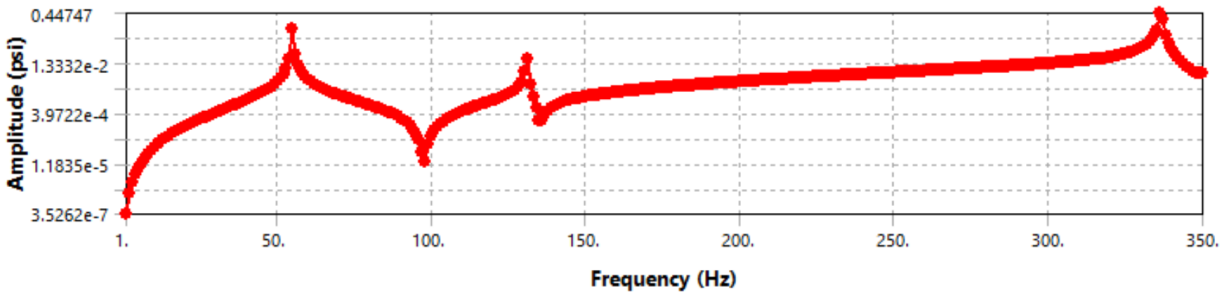
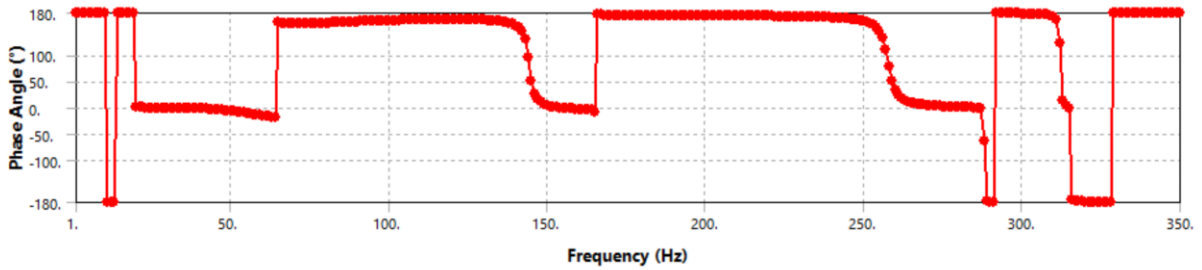**Figure 60 Phase Angle and Amplitude of FPA, CS, 2" Diameter, 24" Long**
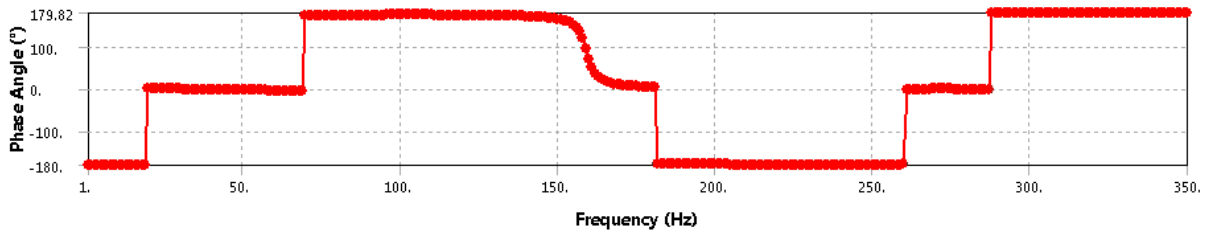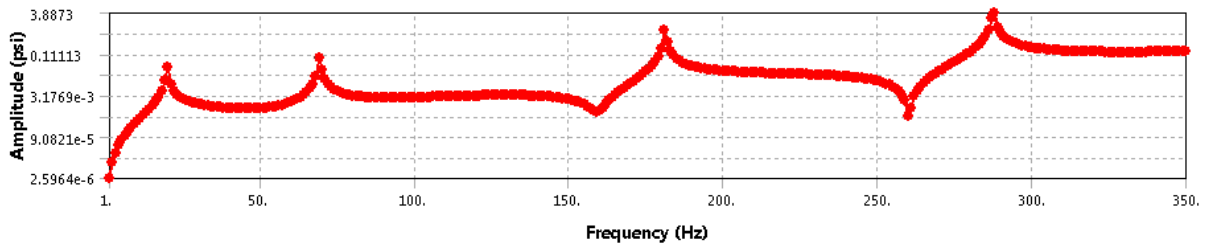
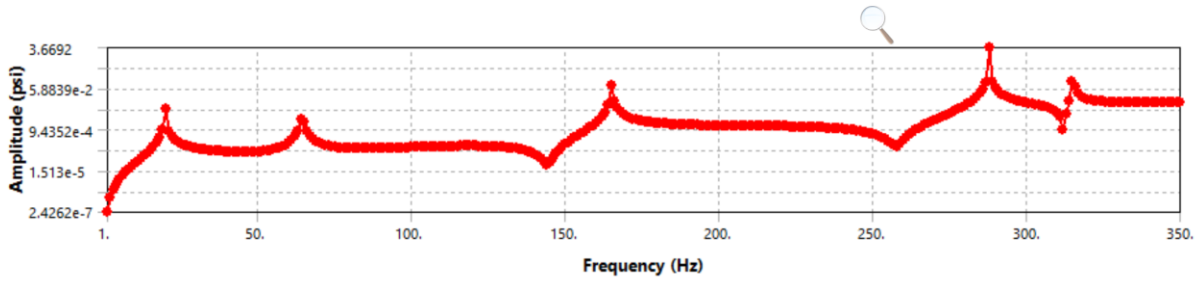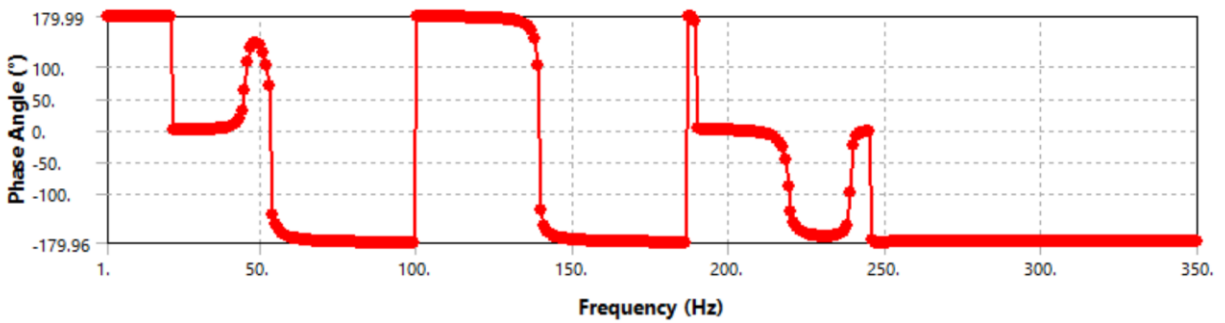**Figure 61 Phase Angle and Amplitude of FPA, CS, 2" Diameter, 36" Long**
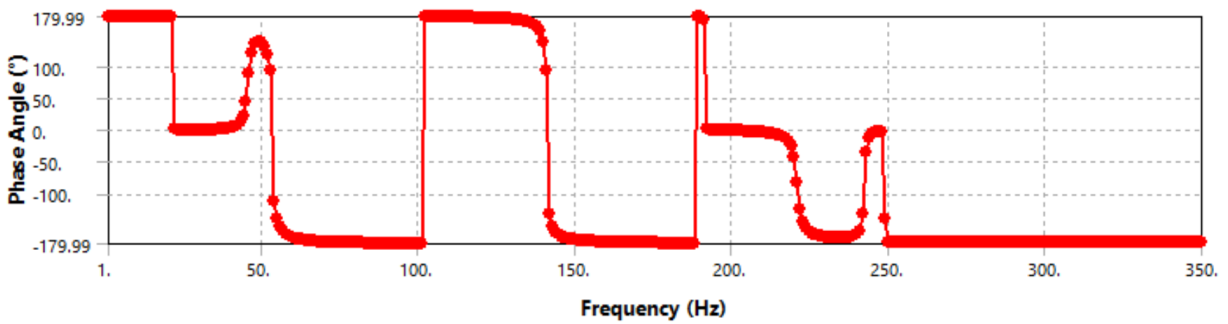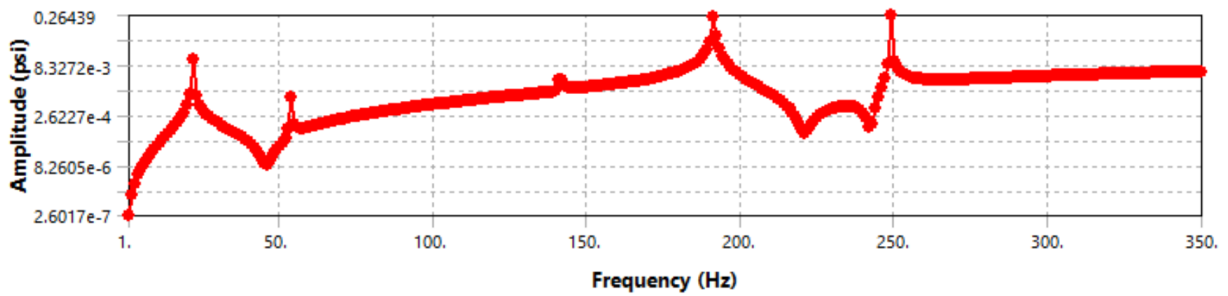
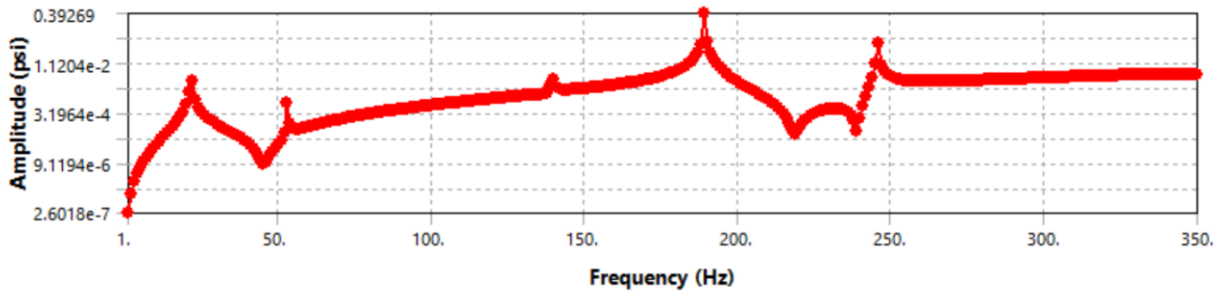**Figure 62 Phase Angle and Amplitude of FPA, CS, 2" Diameter, 48" Long**
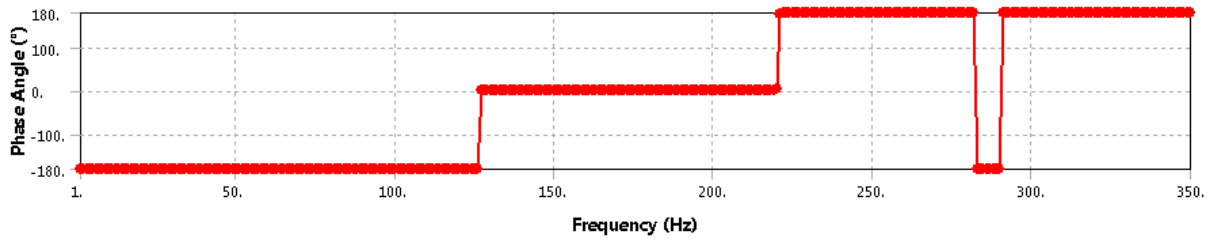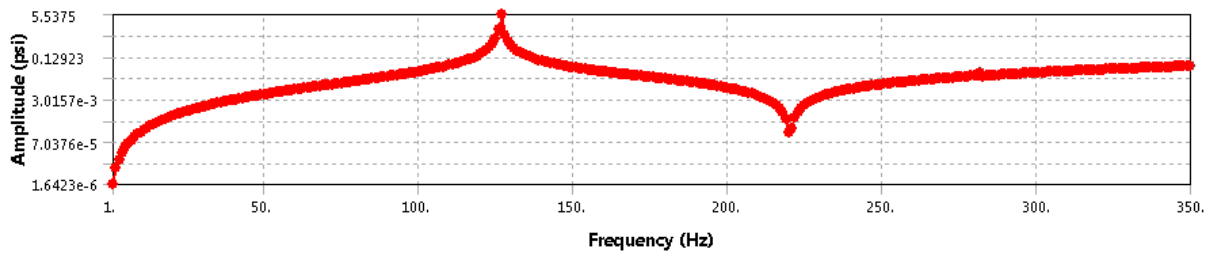
Figure 63 Phase Angle and Amplitude of FPA, SS, 2" Diameter, 12" Long
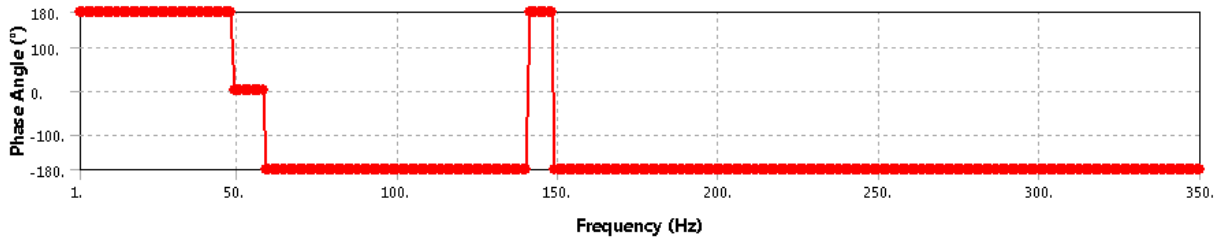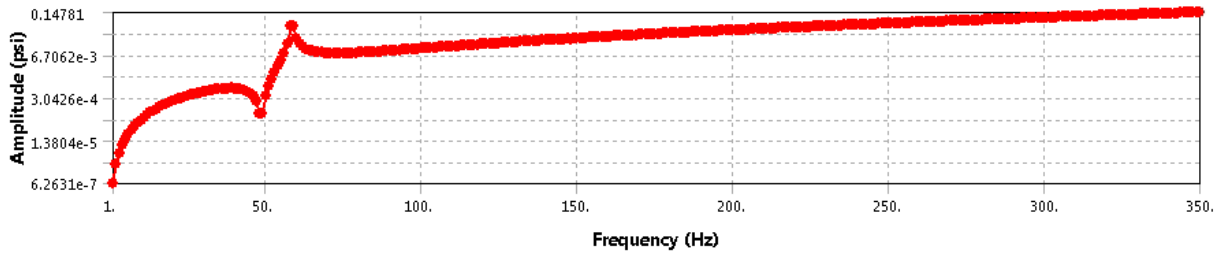
Figure 64 Phase Angle and Amplitude of FPA, SS, 2" Diameter, 24" Long

Figure 65 Phase Angle and Amplitude of FPA, SS, 2" Diameter, 36" Long

Figure 66 Phase Angle and Amplitude of FPA, SS, 2" Diameter, 48" Long

Changing the Frequency

If it is not possible to add additional supports due to the orientation of the piping, or if the previous does not adequately change the frequencies that the assembly is experiencing, it is recommended to install an additional mass to the piping. This can be accomplished by installing a metal wear pad, with a brass or aluminum material of construction via a U-bolt, Figure 67. It is very important to select the correct material of construction, or else wear and damage to the piping will occur which could result in a leak. A 2" diameter, 24" long, CS flanged piping assembly was modeled with a wear pad connected to the piping assembly, approximately in the middle of the 24" length. The results of the frequency of the assembly with and without the wear pad were compared.
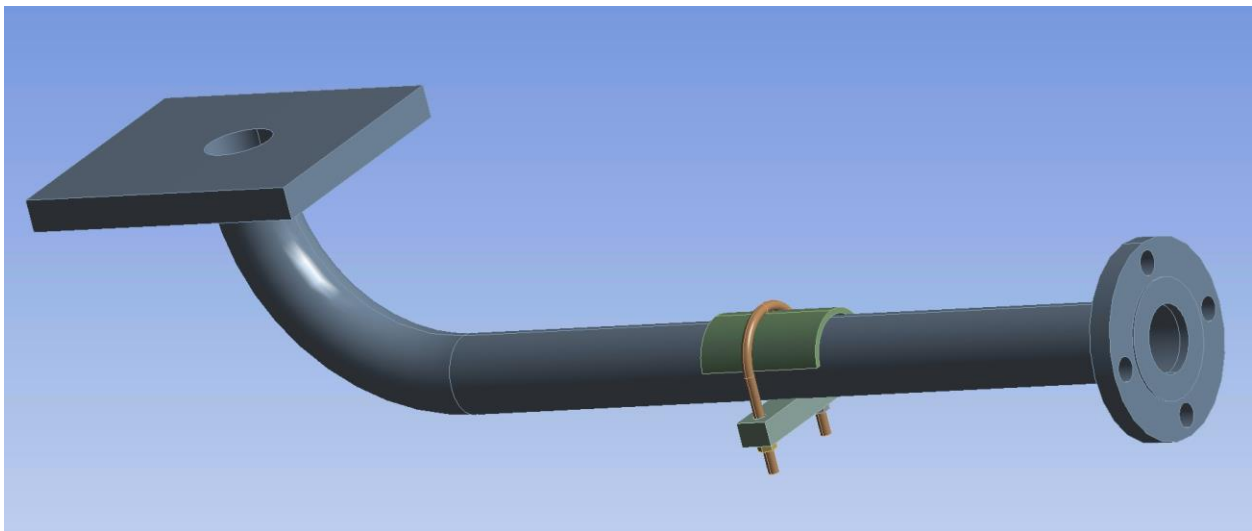
Figure 67 FPA, 2 Inch Diameter, CS, 24 Inches Long, with Wear Pad

The mass installed on the piping model was 0.736 lbs and it changed the peak frequency from 55 and 132 Hz to 59 and 145 Hz. Increasing the mass of the piping, shifted the peak frequencies to the right on the plot. Therefore if the goal is to completely avoid the peak frequencies, add enough mass that it increases the peak frequencies above the startup and

running frequencies of the turbomachinery. Comparing the frequencies in Figure 68, it is distinctly seen that the original piping assembly has three peaks of increased amplitude. With the wear pad installed on the piping, the last two peaks are no longer observed and the first peak has moved slightly to a larger frequency. The addition of a mass to the piping assembly clearly reduces the number of peak stress amplitudes that the assembly experiences.
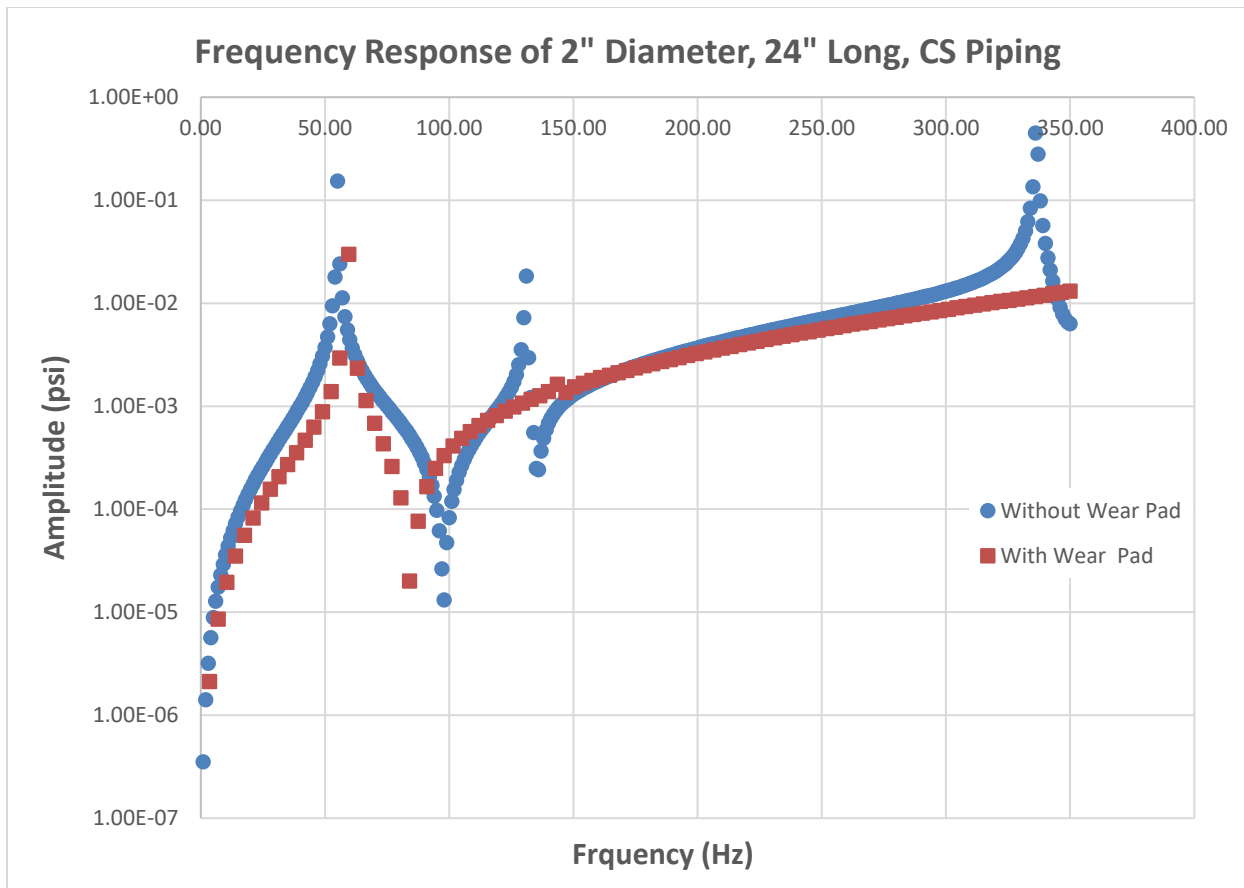
Figure 68 Frquency Response of FPA, CS, 2" Diameter, 24" Long

CHAPTER FOUR: SOCKET WELD CONNECTIONS

The socket weld piping assemblies were analyzed in the same manner as the flanged piping assemblies. The mode shapes, stresses, and unacceptable frequencies of the piping assemblies were collected. In Figure 69 is a crude drawing of a compressor body and the approximate locations where the socket weld piping connections are attached.
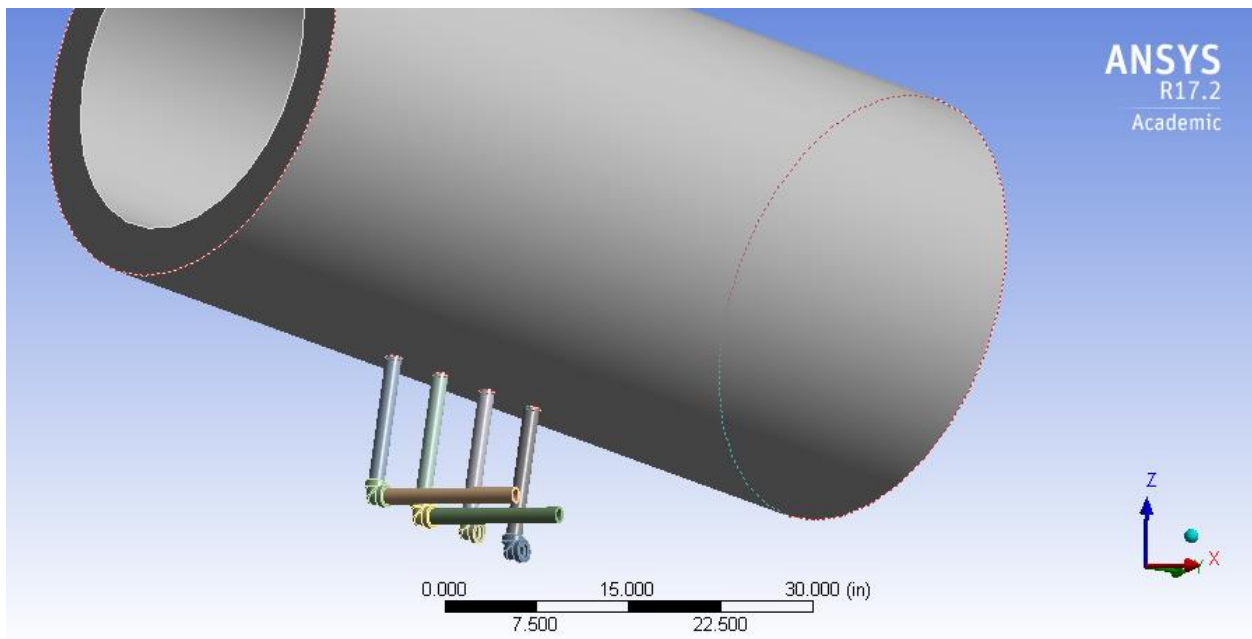
Figure 69 Compressor Body with the Socket Weld Piping Assembly

Mode Shapes

1" Diameter Piping

Evaluating the comparison of the mode shapes of between the carbon steel and stainless steel, as with the FPA, the modes are within 5% of each other, Table 33. This verifies that the technician will not have to worry about the material of construction when setting up the pipe to avoid its natural frequency.

Table 31 Mode Shapes of the SWPA, CS, 1" Diameter Piping

	Frequency and Displacement at Pipe Length							
	12"		24"		36"		48"	
Mode	HZ	in	HZ	in	HZ	in	HZ	in
1	48.51	3.56	19.44	3.49	15.14	3.47	14.83	3.45
2	414.97	18.18	249.15	13.21	156.44	12.44	100.04	11.29
3	802.69	6.58	404.34	15.96	205.85	13.46	119.99	11.74
4	1145.30	9.39	476.82	15.13	316.20	14.74	241.80	10.96
5	1295.20	19.918	838.08	6.51	547.86	12.79	324.90	11.17
6	1306.6	19.097	1007.5	14.76	574.86	12.145	368.87	13.38

Table 32 Mode Shapes of the SWPA, SS, 1" Diameter Piping

	Frequency and Displacement at Pipe Length							
	12"		24"		36"		48"	
Mode	HZ	in	HZ	in	HZ	in	HZ	in
1	46.37	3.59	19.23	3.5188	14.99	3.49	14.67	3.01
2	400.54	18.92	246.30	13.30	154.78	12.52	98.87	9.84
3	832.76	6.70	399.91	16.07	203.98	13.55	118.66	10.24
4	1181.70	14.18	471.36	15.23	314.07	14.84	239.03	9.55
5	1261.40	20.215	828.07	6.56	550.17	12.87	321.29	9.74
6	1309.9	16.103	997.54	14.862	577.87	12.221	382.44	11.66

Table 33 % Difference of the SWPA, CS vs SS, 1" Diameter Piping

	% Difference Between Mode Shapes							
	12"		24"		36"		48"	
Mode	HZ	in	HZ	in	HZ	in	HZ	in
1	4.415	0.777	1.080	0.818	0.991	0.573	1.079	12.754
2	3.477	3.895	1.144	0.662	1.061	0.639	1.170	12.843
3	3.611	1.791	1.096	0.654	0.908	0.664	1.108	12.777
4	3.080	33.779	1.145	0.670	0.674	0.674	1.146	12.865
5	2.610	1.469	1.194	0.820	0.420	0.622	1.111	12.802
6	0.252	15.678	0.989	0.686	0.521	0.622	3.548	12.855

Note that the displacement of the 12" and 48" piping are not within a few percentage of each other, unlike that observed in the FPA's. This is not critical for the technician who will only be looking to avoid the natural frequency of the piping all together, the displacement that occurs will not be prevalent. The frequency, on the other hand, is within a few percentages.

The mode shape deformations for the socket weld piping assemblies are much different than the flanged piping assemblies. The first mode, the piping deformation is minimal, after the 2nd mode the piping is deformed to the point where it is flattened. This is observed throughout almost all the piping lengths, but as the piping length increases, the deformation decreases, Figure 70 and Figure 71. The first mode experiences the most dramatic deformation where the assembly is construed in a mangled manner during for the fourth through sixth mode. The displacement of the 12" piping is about twice as large at 19" vs. 11". The unscaled figures can be observed in Appendix C.
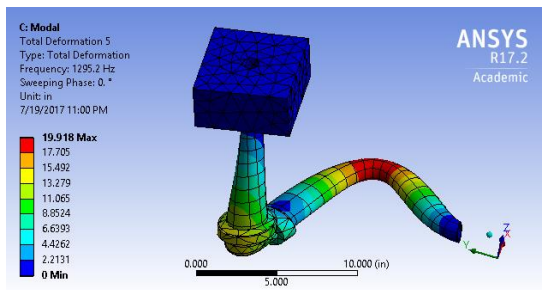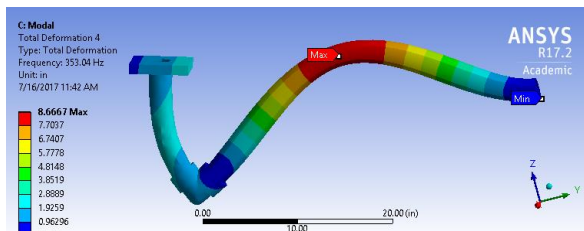

Figure 70 The 5th Mode for SWPA, 1 Inch Diameter, CS, 12 Inches Long
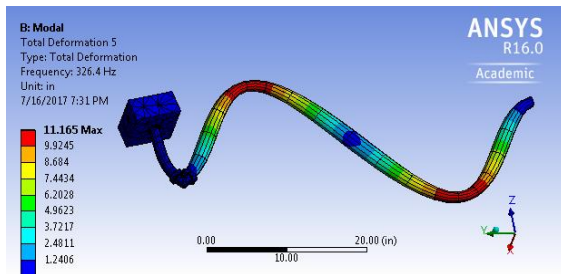
Figure 71 The 5th Mode for SWPA, 1 Inch Diameter, CS, 48 Inches Long

The comparisons between the displacements of the SS vs CS, Figure 72and Figure 73, show that they are similar in shape and displacement. The displacement of the SS is 3.51 inches and of the carbon steel is 3.48 inches. Notice that the maximum displacement occurs at the compressor. When comparing all the modes, the maximum displacement does not always occur

at the compressor connection, see Figure 74, where the maximum displacement occurs at the piping.
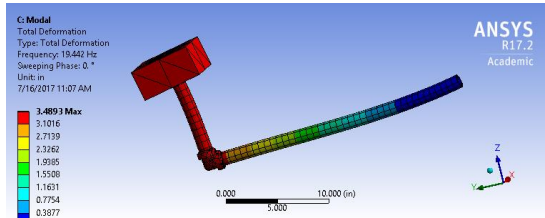
Figure 72 The 1st Mode for SWPA, 1 Inch Diameter, CS, 24 Inches Long
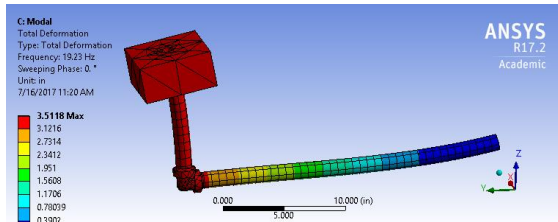
Figure 73 The 1st Mode for SWPA, 1 Inch Diameter, SS, 24 Inches Long
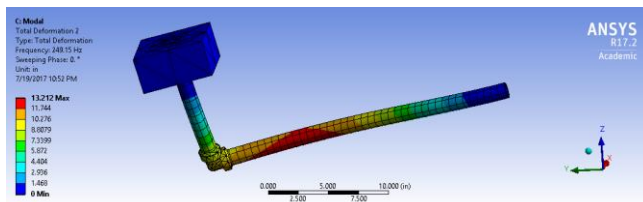
Figure 74 The 2nd Mode for SWPA, 1 Inch Diameter, CS, 24 Inches Long

2" Diameter Piping

The 2 inch piping material comparison was similar to the previous but with all the frequencies within 6% instead of 5%. Unlike the 1" piping only six of the displacement values are not with 3% of each other. Comparing the 2" SWPA to the 2" FPA, there was only one displacement that had a difference greater than 3%.

Table 34 Mode Shapes of the SWPA, CS, 2" Diameter Piping

	Frequency and Displacement at Pipe Length							
	12"		24"		36"		48"	
Mode	HZ	in	HZ	in	HZ	in	HZ	in
1	119.28	3.65	73.01	4.69	41.65	4.51	26.95	4.29
2	238.90	8.27	123.83	8.36	75.93	7.82	55.36	6.21
3	594.58	6.06	655.72	9.80	340.64	8.39	210.16	7.35
4	652.73	7.42	661.45	9.27	353.04	8.67	214.20	7.61
5	1717.00	9.526	973.32	9.61	796.36	6.93	538.45	7.35
6	1732.5	11.771	975.65	9.5678	837.66	7.5659	574.03	7.22

Table 35 Mode Shapes of the SWPA, SS, 2" Diameter Piping

	Frequency and Displacement at Pipe Length							
	12"		24"		36"		48"	
Mode	HZ	in	HZ	in	HZ	in	HZ	in
1	117.97	3.67	71.66	4.74	40.68	4.90	26.65	4.32
2	236.04	8.33	118.87	8.49	74.78	7.64	54.63	7.04
3	588.07	6.10	637.79	9.86	336.16	8.45	207.62	7.40
4	645.27	7.47	648.30	9.35	348.07	8.70	211.79	7.66
5	1697.60	9.5955	954.28	7.65	779.73	6.98	532.10	7.40
6	1711.9	11.854	959.01	7.1779	8.24.4	7.5458	540.79	7.27

Table 36 % Difference of the SWPA, CS vs SS, 2" Diameter Piping

	% Difference Between Displacements and Mode							
	12"		24"		36"		48"	
Mode	HZ	in	HZ	in	HZ	in	HZ	in
1	1.098	0.638	1.844	1.054	2.339	7.855	1.117	0.639
2	1.197	0.699	4.005	1.591	1.512	-2.275	1.315	11.716
3	1.095	0.699	2.734	0.668	1.315	0.656	1.209	0.646
4	1.143	0.664	1.988	0.843	1.408	0.348	1.125	0.645
5	1.130	0.724	1.956	20.380	2.088	0.705	1.179	0.658
6	1.189	0.700	1.706	24.979	1.583	-0.266	5.791	0.656

The deformation of the 2 inch piping, as in the FPA, are less misconfigured, especially

when reaching the 36" and 48" piping lengths. There is a very noticeable difference when

comparing the 12 lengths, where the deformation of the piping looks plausible unlike the 1 inch

piping where it is flat and bent, Figure 75 and Figure 76. The 24 inch piping, at the compressor

flange is experiencing a lot of movement of the piping at the flange, in a noticeable difference than the other lengths of piping.
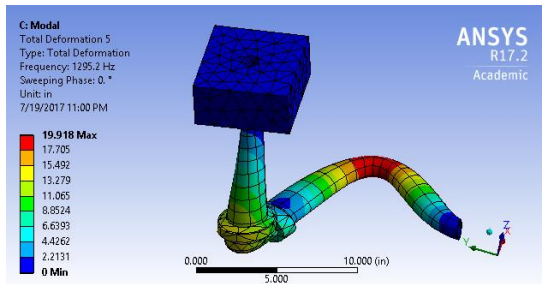
Figure 75 The 5th Mode for SWPA, 1 Inch Diameter, CS, 12 Inches Long
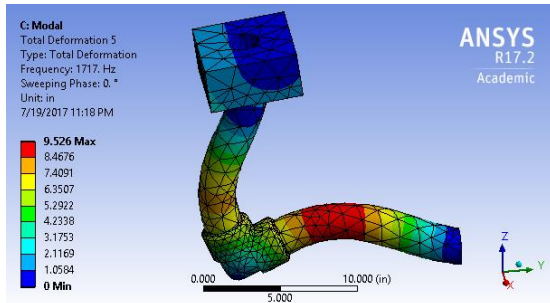
Figure 76 The 5th Mode for SWPA, 2 Inch Diameter, CS, 12 Inches Long

The stainless steel piping experiences almost the same piping configurations as the carbon steel. The models are less deformed than the 1 inch diameters and only the last three modes of the 12 inch length are conformed into very abnormal shapes. Overall the 2" stainless steel piping exhibits the same characteristics as that of the carbon steel, Figure 77 and Figure 78.

Figure 77 The 4th Mode for SWPA, 2 Inch Diameter, CS, 36 Inches Long
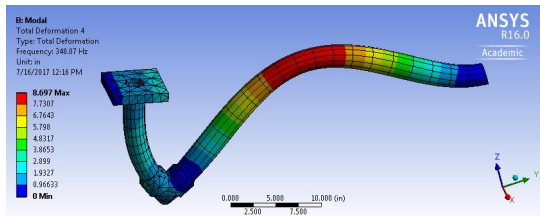
Figure 78 The 4th Mode for SWPA, 2 Inch Diameter, SS, 36 Inches Long

<u>Acceptable Vibration Range</u>

For the SWPA the frequencies were evaluated to identify any outlier spikes in stress other than at the mode shapes. Throughout the tables it is seen that the stress is far below the endurance limit of the materials, therefore additional FEA analysis would be necessary to apply the correct forcing at the compressor body of the piping assembly to obtain the correct frequency ranges to avoid. The acceptable frequency range reported in the tables was below 1 psi. It was noticed that at the modes shapes, the stress experienced is not always above 1 psi, therefore in the table, it is automatically assumed that the allowable frequencies must be 5 – 10 Hz away from the mode shape frequencies.

<u>1" Diameter Piping</u>

Comparing the frequencies to avoid, it is noted that between 10 -25 Hz, 90 – 135 Hz, and 265 – 290 Hz, almost all the lengths of piping need to avoid these frequencies. These frequencies should be especially noted by the technician when performing an analysis of the piping assemblies. The 12" supported piping is the pipping length that is outside the ranges listed above, therefore it would be recommended to support the piping every 12 inches since the frequencies listed above are prevalent to most of the other piping lengths.

Table 37 Frequencies to Avoid, SWPA 1" Diameter, CS, 12" Long

		12" Long Piping, CS, 1"				
Mode	Mode Location	Peak Frequency (Hz)	Peak Stress (psi)	Frequency Allowable (Hz)	Stress Allowable (psi)	Frequency Avoid (Hz)
1	During	29.638	0.22946	0 - 35	< 1	35 - 60
	After	50	5.883	60 - 100	< 1	N/A
2	During	105.65	0.47386	110 -350	N/A	100 - 110

Table 38 Frequencies to Avoid, SWPA 1" Diameter, SS, 12" Long

		12" Long Piping, SS, 1"				
Mode	Mode Location	Peak Frequency (Hz)	Peak Stress (psi)	Frequency Allowable (Hz)	Stress Allowable (psi)	Frequency Avoid (Hz)
1	During	46.37	4.539	0 - 40	< 1	45 -50
2	During	400.54	N/A	55 - 350	N/A	N/A

Table 39 Frequencies to Avoid, SWPA 1" Diameter, CS, 24" Long

		24" Long Piping, CS, 1"				
Mode	Mode Location	Peak Frequency (Hz)	Peak Stress (psi)	Frequency Allowable (Hz)	Stress Allowable (psi)	Frequency Avoid (Hz)
1	During	19.442	3.4915	0-15	<1	15 - 20
2	During	249.15	0.29948	25 - 240	<1	240 -255
	After	280	5.0986	255 - 265	< 1	265 - 290
3	During	404.34	N/A	295 >	< 1	N/A

Table 40 Frequencies to Avoid, SWPA 1" Diameter, SS, 24" Long

		24" Long Piping, SS, 1"				
Mode	Mode Location	Peak Frequency (Hz)	Peak Stress (psi)	Frequency Allowable (Hz)	Stress Allowable (psi)	Frequency Avoid (Hz)
1	During	21.18	3.4945	0-15	<1	15- 25
	After	132	4.6878	25 - 130	<1	130 - 135
2	During	249.15	0.30637	135 - 240	< 1	270 - 290
	After	273	8.5384	290 -135	< 1	N/A

Comparing the frequencies to avoid across the same pipe length but different material, it is seen that most of the frequencies correspond. It is recommended for the 24" and 48" piping

that the technician pay attention to the material of construction due to all the frequencies to avoid

being listed on both the carbon steel and stainless steel charts.

Table 41 Frequencies to Avoid, SWPA 1" Diameter, CS, 36" Long

		36" Long Piping, CS, 1"				
Mode	Mode Location	Peak Frequency (Hz)	Peak Stress (psi)	Frequency Allowable (Hz)	Stress Allowable (psi)	Frequency Avoid (Hz)
1	During	15.14	0.7249	0 - 10	< 1	10 - 20
2	During	156.44	0.159	20 -150	< 1	150 - 160
3	During	205.85	0.38095	160 - 200	< 1	200 - 210
4	During	316.2	0.29227	210 - 300 320 -350	< 1	300 - 320

Table 42 Frequencies to Avoid, SWPA 1" Diameter, SS, 36" Long

		36" Long Piping, SS, 1"				
Mode	Mode Location	Peak Frequency (Hz)	Peak Stress (psi)	Frequency Allowable (Hz)	Stress Allowable (psi)	Frequency Avoid (Hz)
1	During	14.99	11.872	0 - 10	< 1	10 - 20
2	During	154.78	0.15638	20 - 150	<1	150 - 160
3	During	203.98	0.37826	160 - 195	<1	195 - 205
4	During	314.07	0.28762	205 - 305 320 - 350	<1	305 - 320

Table 43 Frequencies to Avoid, SWPA 1" Diameter, CS, 48" Long

		48" Long Piping, CS, 1"				
Mode	Mode Location	Peak Frequency (Hz)	Peak Stress (psi)	Frequency Allowable (Hz)	Stress Allowable (psi)	Frequency Avoid (Hz)
1	During	14.83	5.8722	0 -10	< 1	10 - 20
2	During	100.04	0.067985	20 -90	<1	90 - 110
3	During	119.19	2.0259	N/A	< 1	115 - 125
4	Before	120	26.934	125 - 185	< 1	185-195
	Before	190	6.8933	195 - 235	< 1	235 - 245
	During	241.8	0.24153	245 - 265	< 1	265-280
5	Before	270	2.0458	280 - 315	< 1	315 - 330
	During	324.9	5.8248	N/A	N/A	N/A

Table 44 Frequencies to Avoid, SWPA 1" Diameter, SS, 48" Long

Mode	Mode Location	Peak Frequency (Hz)	Peak Stress (psi)	Frequency Allowable (Hz)	Stress Allowable (psi)	Frequency Avoid (Hz)
1	During	14.668	2.6909	0-10	<1	10 - 20
2	During	98.866	0.064879	20 - 90	<1	90 - 105
3	During	118.66	8.8656	105 -110	< 1	110 - 125
4	During	239.03	0.2381	125 - 230	< 1	230 - 290
4	After	270	8.2169	290 - 315	< 1	315 - 330
5	During	321.29	4.3866	330 - 350	< 1	N/A

Table title "48" Long Piping, SS, 1"" spans the full header.
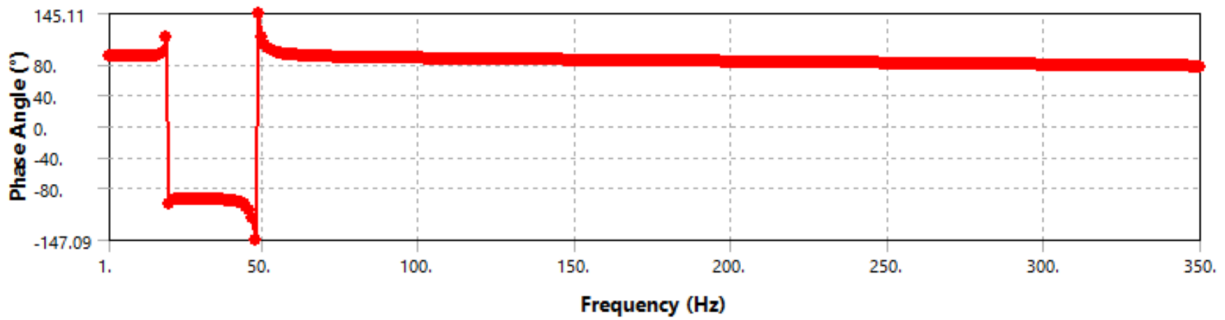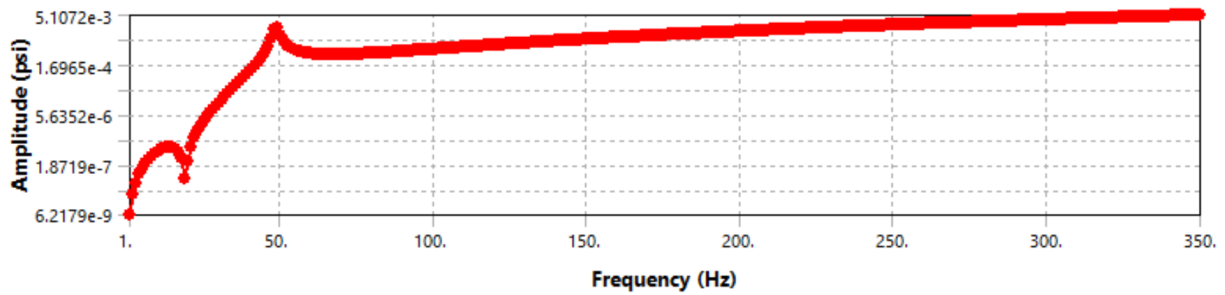
Figure 79 Phase Angle and Amplitude of SWPA, CS, 1" Diameter, 12" Long
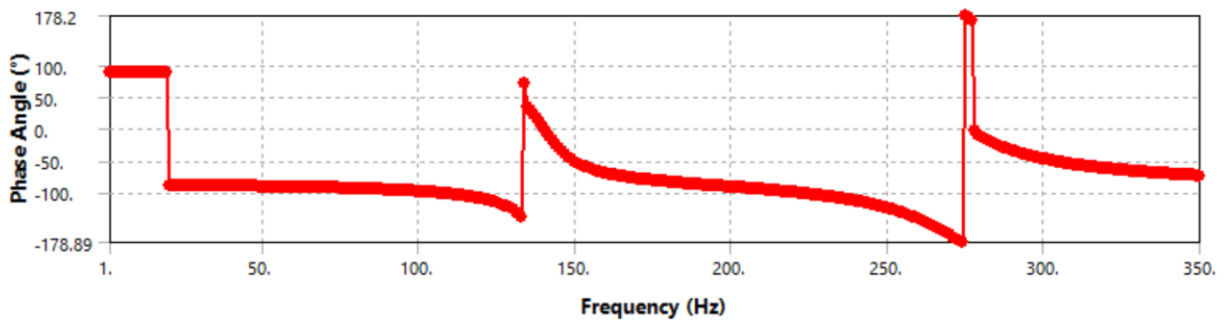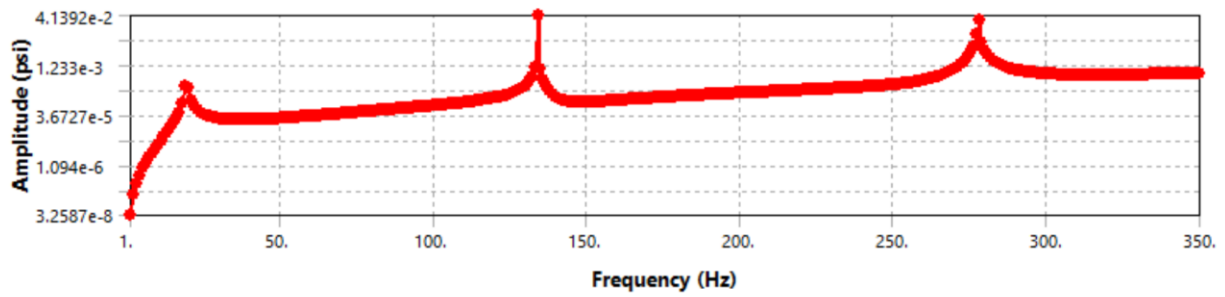
Figure 80 Phase Angle and Amplitude of SWPA, CS, 1" Diameter, 24" Long
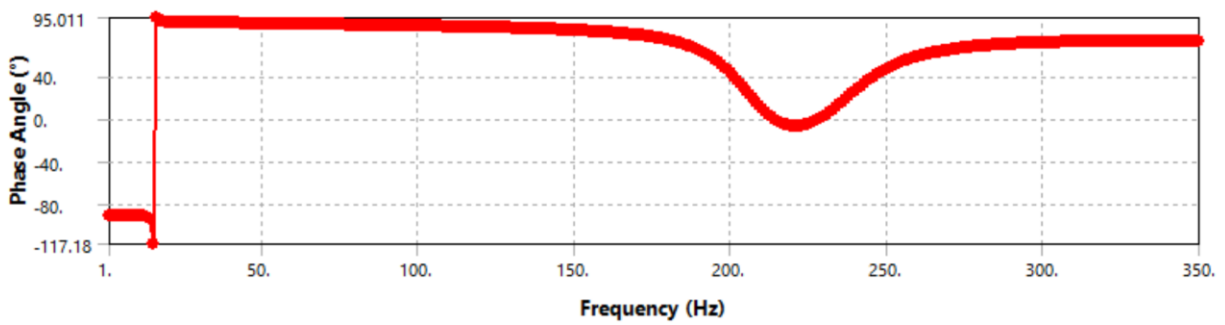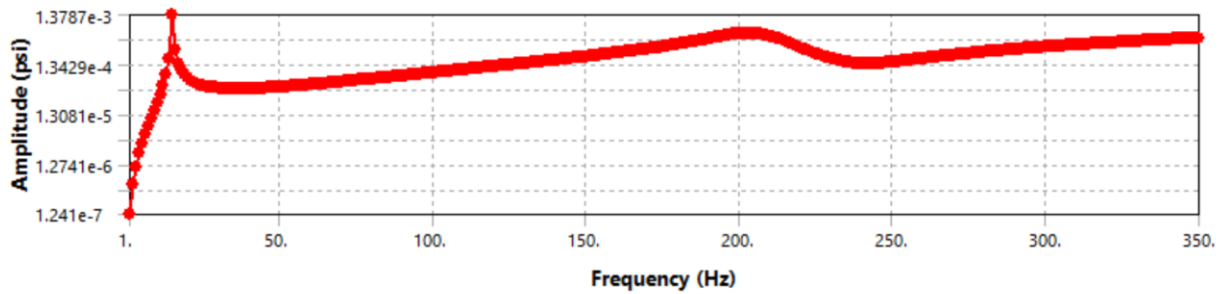
Figure 81 Phase Angle and Amplitude of SWPA, CS, 1" Diameter, 36" Long
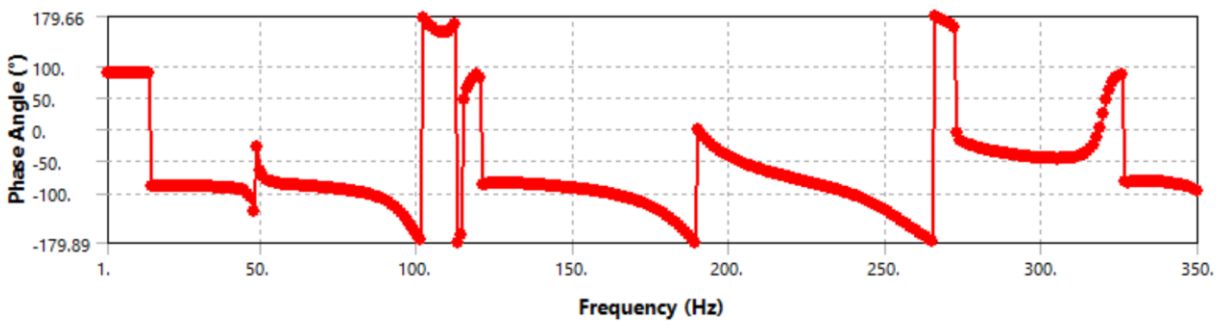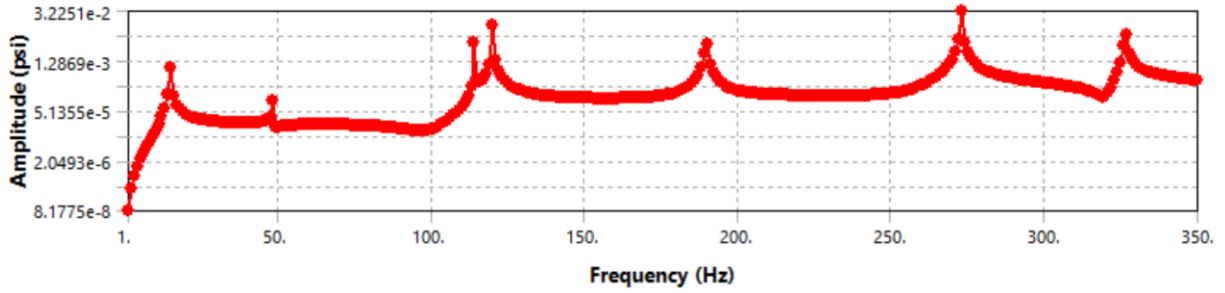
Figure 82 Phase Angle and Amplitude of SWPA, CS, 1" Diameter, 48" Long
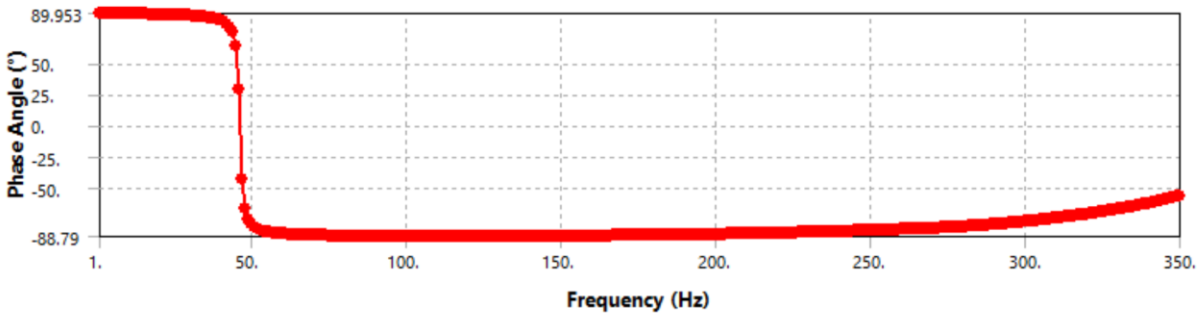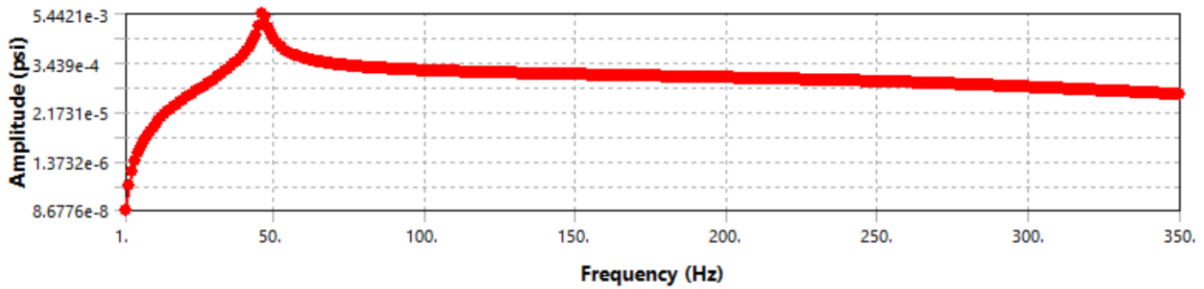
Figure 83 Phase Angle and Amplitude of SWPA, SS, 1" Diameter, 12" Long
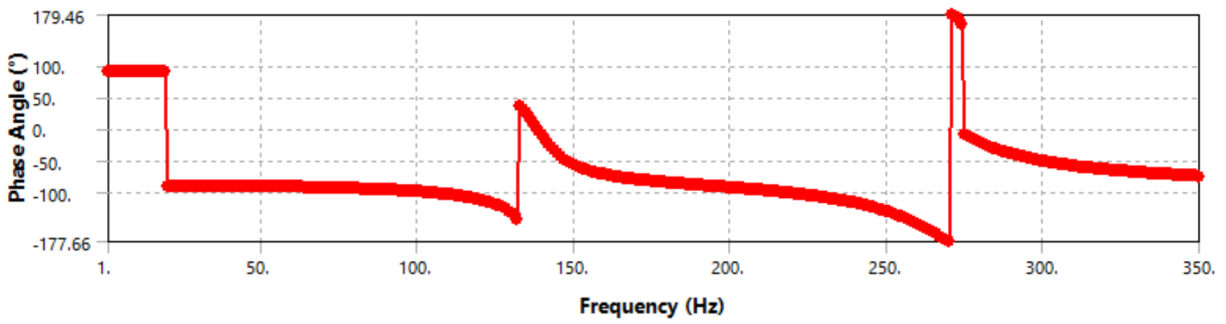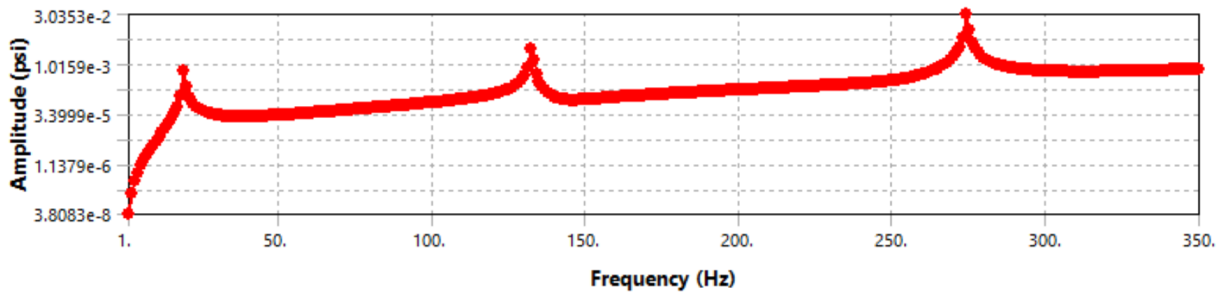
Figure 84 Phase Angle and Amplitude of SWPA, SS, 1" Diameter, 24" Long
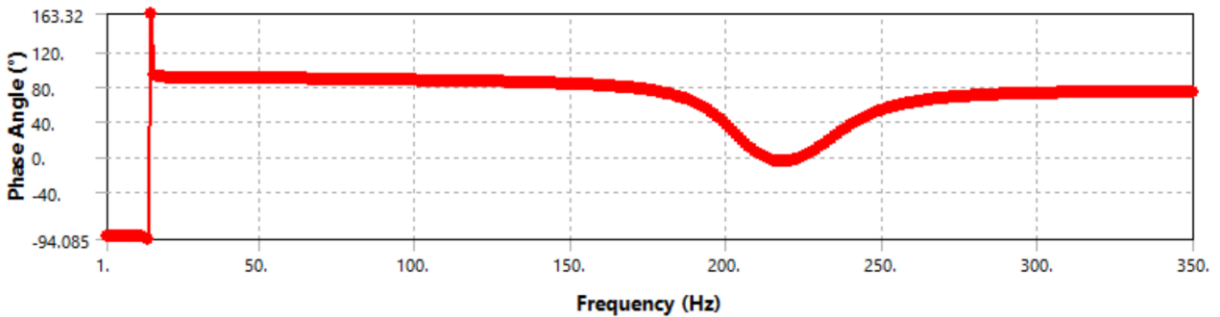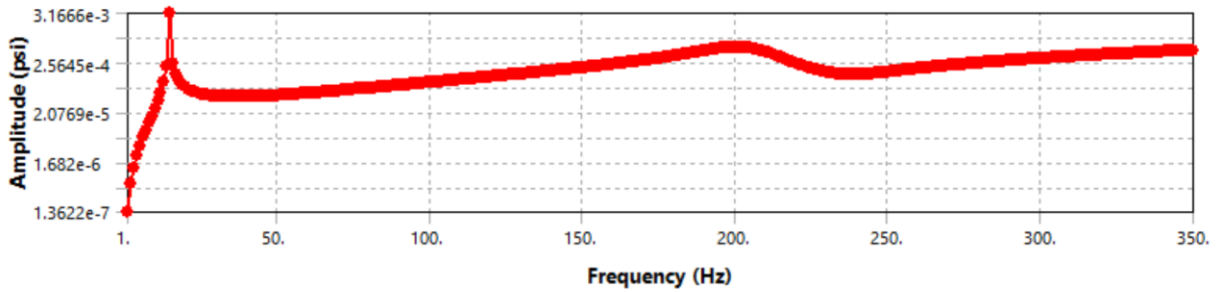
Figure 85 Phase Angle and Amplitude of SWPA, SS, 1" Diameter, 36" Long
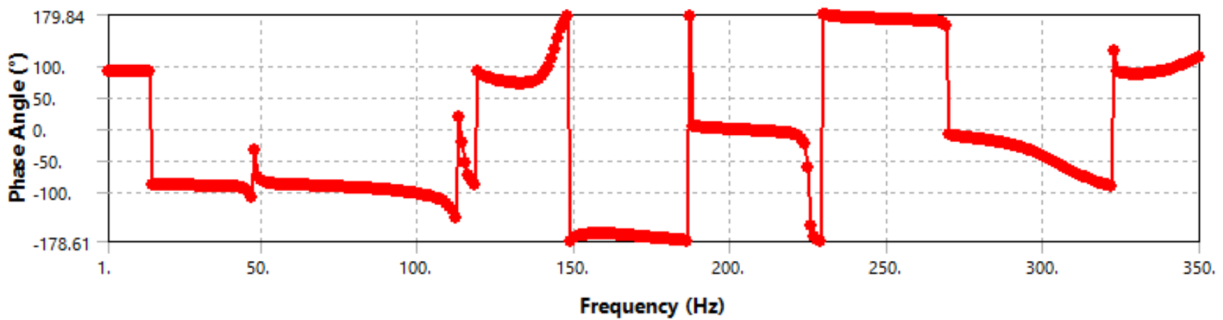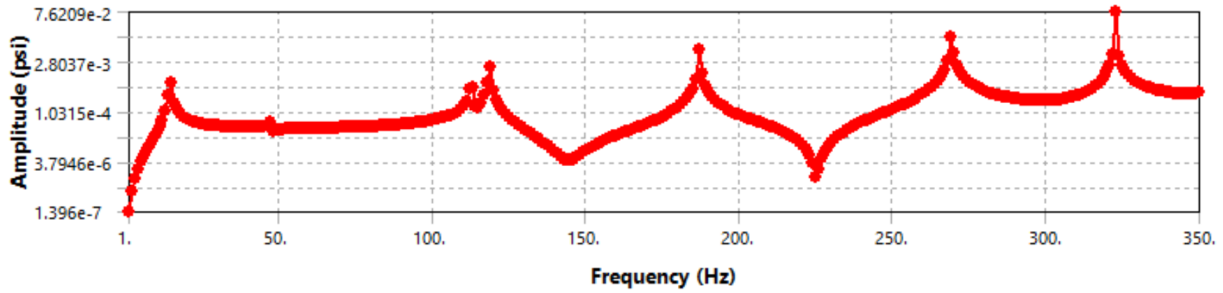
Figure 86 Phase Angle and Amplitude of SWPA, SS, 1" Diameter, 48" Long

2" Diameter Piping

There is only one frequency range, between 50 – 80 Hz, at which a few lengths of piping all have listed as unacceptable. This may relay that as the piping diameter increases, the correspondence between avoidable frequencies decreases. This would also indicate that changing the location of the supports, to move the system out of an unacceptable range, a wider selection of supports changes that can be incorporated. Most of the frequencies, when comparing between the materials of construction, correspond. There is not any length that all the unacceptable frequencies correspond for both materials; therefore the technician will have to have both material tables when evaluating the piping assemblies.

Table 45 Frequencies to Avoid, SWPA 2" Diameter, CS, 12" Long

for title 12" Long Piping, CS, 2"						
Mode	Mode Location	Peak Frequency (Hz)	Peak Stress (psi)	Frequency Allowable (Hz)	Stress Allowable (psi)	Frequency Avoid (Hz)
1	During	119.28	36.258	0- 120	< 1	120 - 130
2	During	238.9	0.33565	130 - 350	< 1	N/A

Table 46 Frequencies to Avoid, SWPA 2" Diameter, SS, 12" Long

12" Long Piping, SS, 2"						
Mode	Mode Location	Peak Frequency (Hz)	Peak Stress (psi)	Frequency Allowable (Hz)	Stress Allowable (psi)	Frequency Avoid (Hz)
1	During	117.94	135.71	0 -105	< 1	110 - 125
2	During	236.04	0.32779	130 - 350	< 1	N/A

Table 47 Frequencies to Avoid, SWPA 2" Diameter, CS, 24" Long

24" Long Piping, CS, 2"						
Mode	Mode Location	Peak Frequency (Hz)	Peak Stress (psi)	Frequency Allowable (Hz)	Stress Allowable (psi)	Frequency Avoid (Hz)
1	During	73.006	820	0 - 65	< 1	65 - 80
2	During	123.83	0.45473	80 - 115	< 1	115 - 125
	After	350	3.5	125 - 315	< 1	320 - 350

Table 48 Frequencies to Avoid, SWPA 2" Diameter, SS, 24" Long

24" Long Piping, SS, 1"						
Mode	Mode Location	Peak Frequency (Hz)	Peak Stress (psi)	Frequency Allowable (Hz)	Stress Allowable (psi)	Frequency Avoid (Hz)
1	During	21.18	3.4945	0-15	<1	15- 25
	After	132	4.6878	25 - 130	<1	130 - 135
2	During	249.15	0.30637	135 - 240	< 1	270 - 290
	After	273	8.5384	290 -135	< 1	N/A

Table 49 Frequencies to Avoid, SWPA 2" Diameter, CS, 36" Long

Mode	Mode Location	Peak Frequency (Hz)	Peak Stress (psi)	Frequency Allowable (Hz)	Stress Allowable (psi)	Frequency Avoid (Hz)
		36" Long Piping, CS, 2"				
1	During	41.65	3.7457	0 - 40	< 1	40 - 45
1	After	65	1.3224	45 - 60	< 1	60 - 70
2	During	75.93	0.12609	70 - 190	< 1	190 - 200
2	After	195	2.8423	205 - 335	< 1	335 >
3	During	340.64	1.443	N/A	N/A	N/A

Table 50 Frequencies to Avoid, SWPA 2" Diameter, SS, 36" Long

Mode	Mode Location	Peak Frequency (Hz)	Peak Stress (psi)	Frequency Allowable (Hz)	Stress Allowable (psi)	Frequency Avoid (Hz)
		36" Long Piping, SS, 2"				
1	During	40.68	1.6586	0 - 35	< 1	35 -45
2	During	74.78	0.038318	45 - 70	< 1	70 -80
2	After	147	0.13041	80 - 140	< 1	140 - 155
3	During	336.16	1.2542	155 - 330	< 1	330 - 350
4	During	348.07	234.17	N/A	N/A	N/A

Table 51 Frequencies to Avoid, SWPA 2" Diameter, CS, 48" Long

Mode	Mode Location	Peak Frequency (Hz)	Peak Stress (psi)	Frequency Allowable (Hz)	Stress Allowable (psi)	Frequency Avoid (Hz)
		48" Long Piping, CS, 2"				
1	During	26.95	8.8311	0 - 20	< 1	20 -30
2	During	55.36	0.047739	30 - 50	< 1	50 - 70
2	After	65	0.043683	70 -200	< 1	200 -230
3	During	210.16	2.0708	N/A	< 1	N/A
4	During	214.2	44.131	230 - 350	< 1	N/A

Table 52 Frequencies to Avoid, SWPA 2" Diameter, SS, 48" Long

Mode	Mode Location	Peak Frequency (Hz)	Peak Stress (psi)	Frequency Allowable (Hz)	Stress Allowable (psi)	Frequency Avoid (Hz)
1	During	27	1.24	0 - 25	< 1	25- 30
2	During	55	0.05	30 - 50	< 1	50 - 60
	After	64	0.05	N/A	< 1	60 - 70
3	Before	150	0.12	70 - 145	< 1	145 - 155
	During	208	2.22	155 - 200	< 1	200 - 225
4	During	212	2.22	225 - 350	< 1	N/A
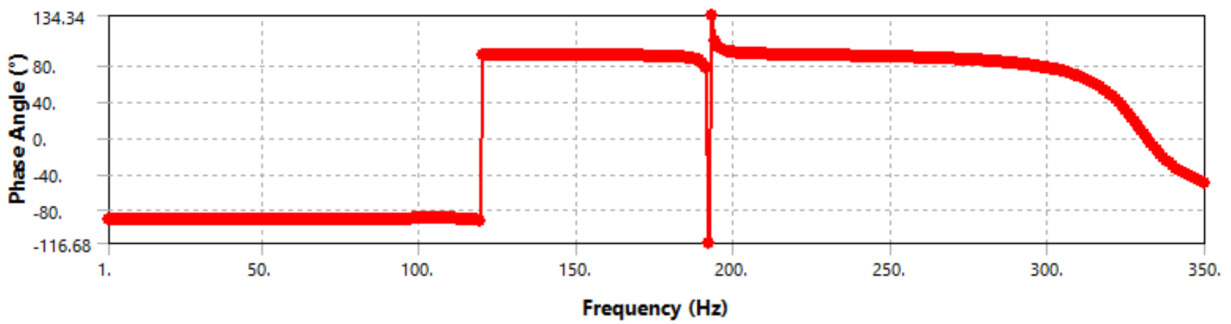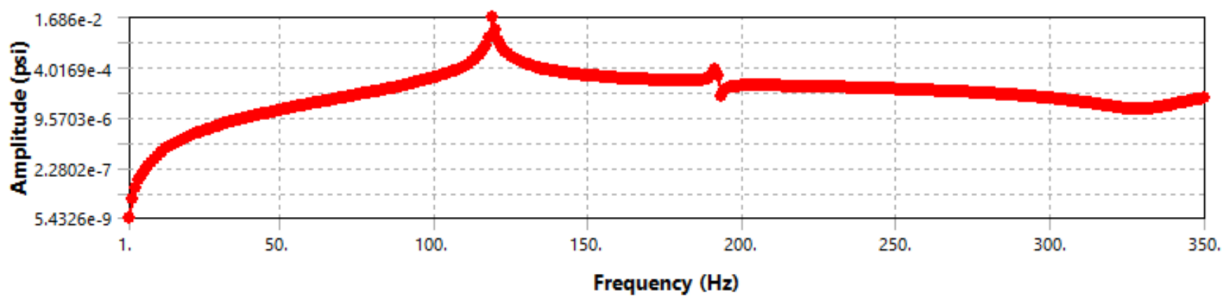
Figure 87 Phase Angle and Amplitude of SWPA, CS, 2" Diameter, 12" Long
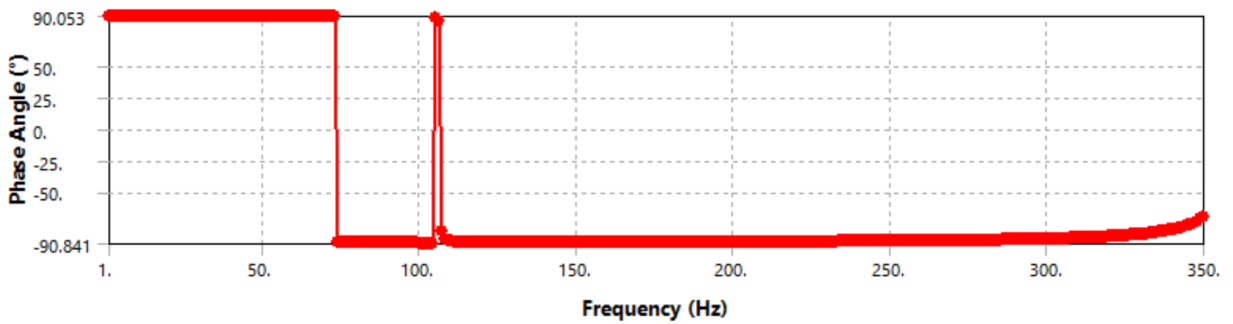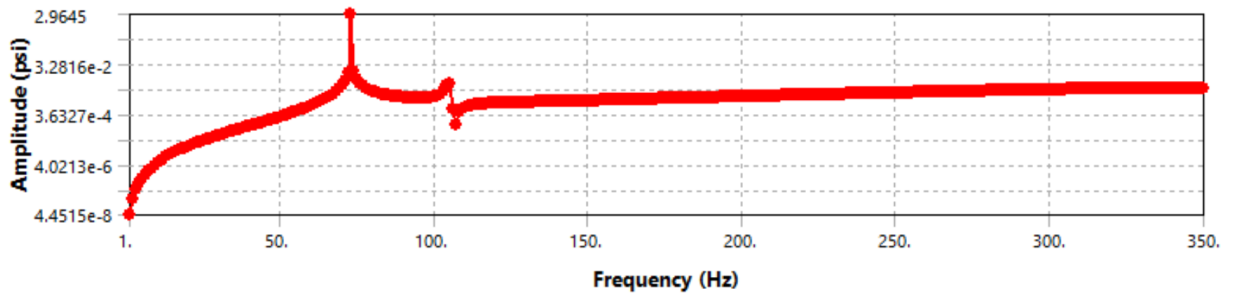
Figure 88 Phase Angle and Amplitude of SWPA, CS, 2" Diameter, 24" Long
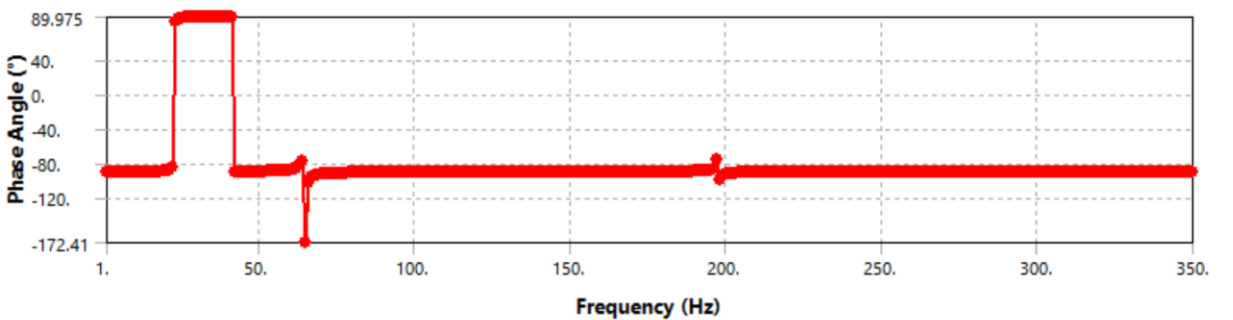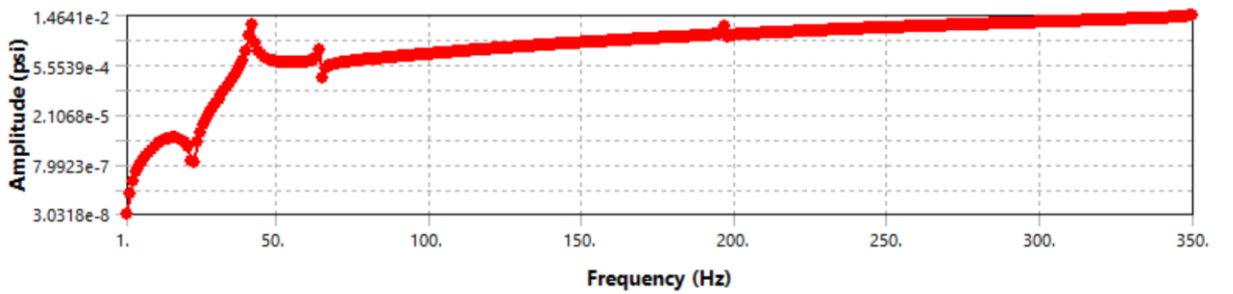
Figure 89 Phase Angle and Amplitude of SWPA, CS, 2" Diameter, 36" Long
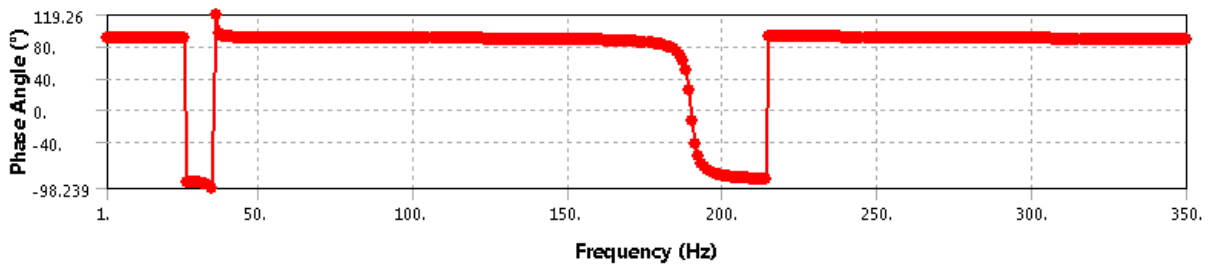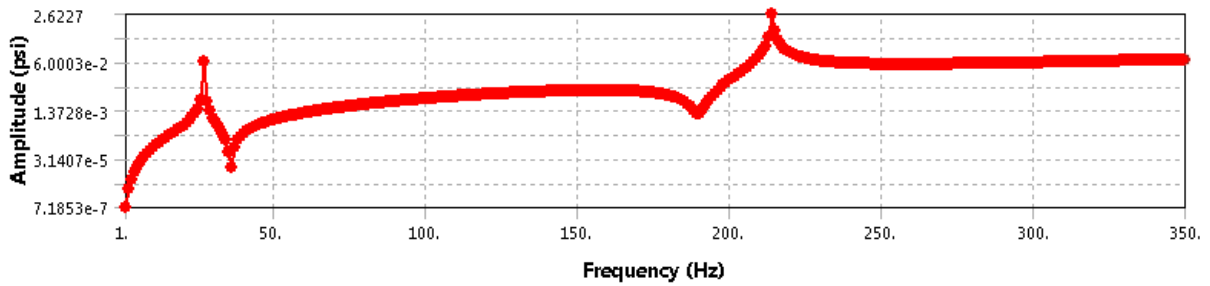
Figure 90 Phase Angle and Amplitude of SWPA, CS, 2" Diameter, 48" Long
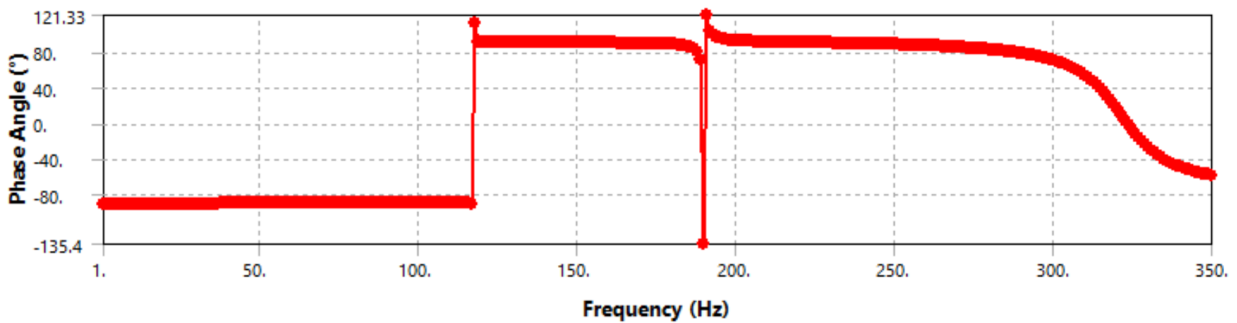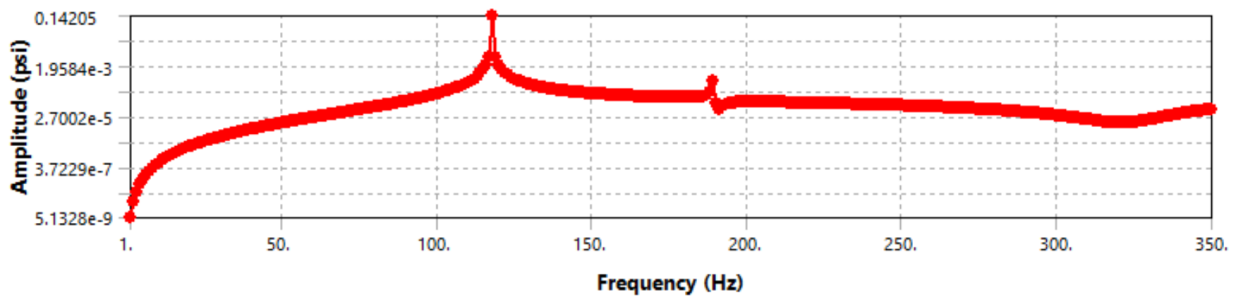
Figure 91 Phase Angle and Amplitude of SWPA, SS, 2" Diameter, 12" Long
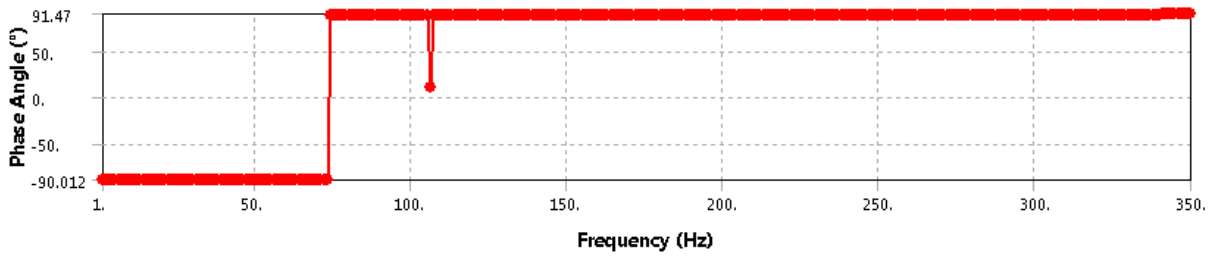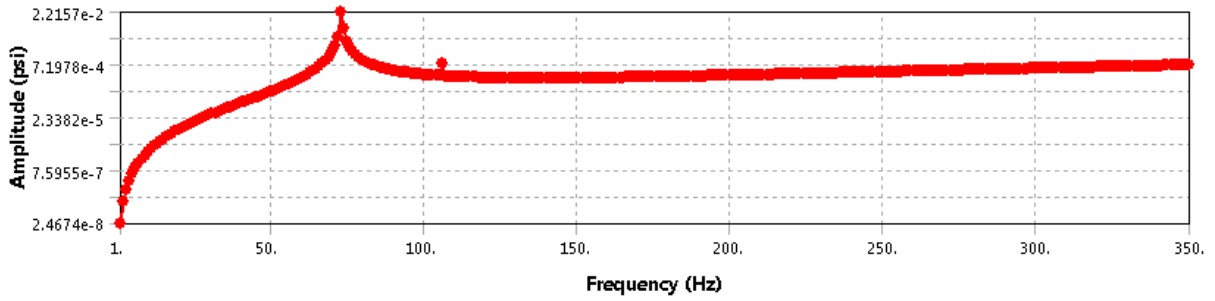
Figure 92 Phase Angle and Amplitude of SWPA, SS, 2" Diameter, 24" Long
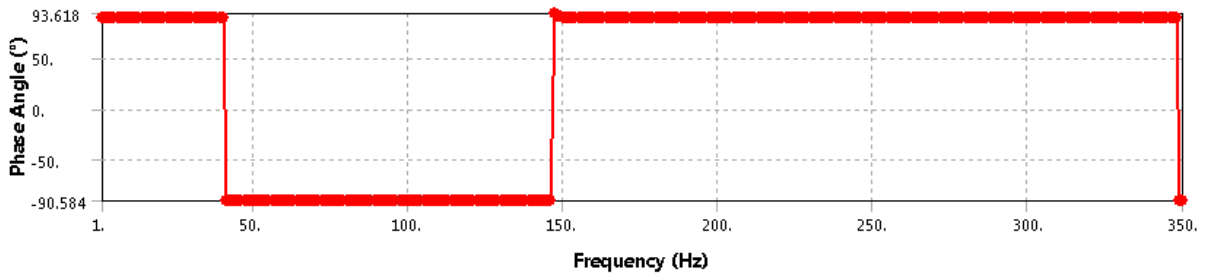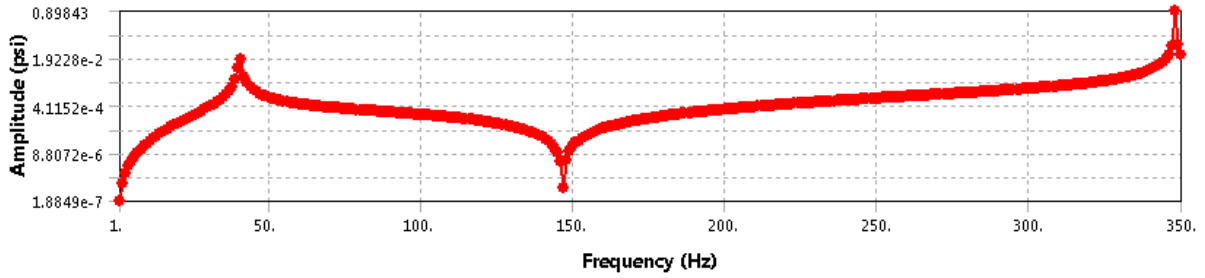
Figure 93 Phase Angle and Amplitude of SWPA, SS, 2" Diameter, 36" Long
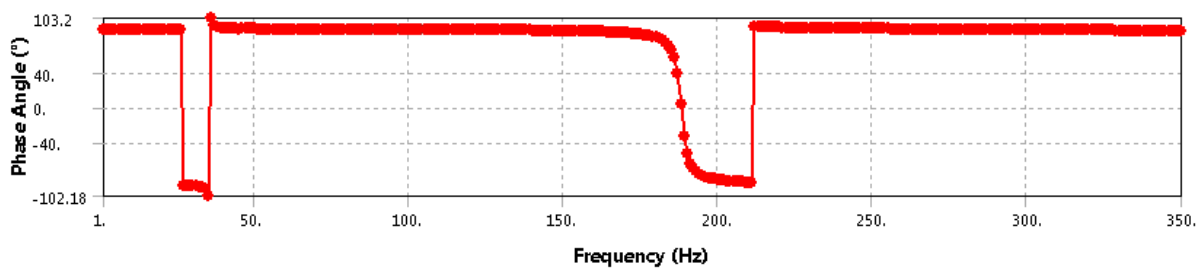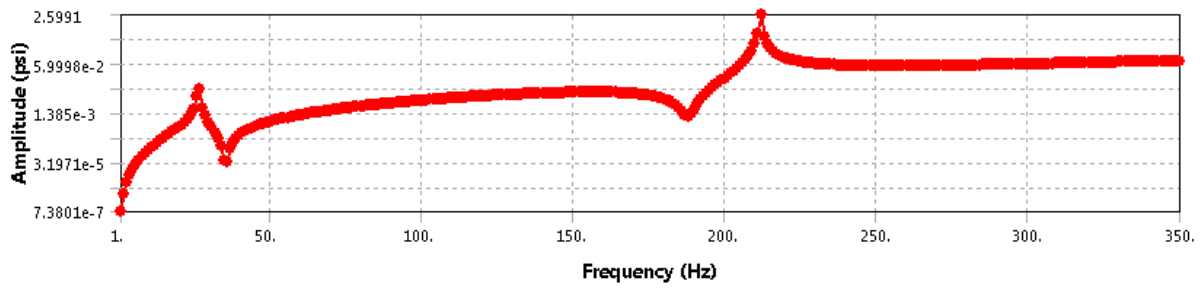
Figure 94 Phase Angle and Amplitude of SWPA, SS, 2" Diameter, 48" Long

CHAPTER FIVE: CONCLUSION & FUTURE WORK

It is especially important in industry to prevent welds from failing on turbomachinery applications. When a small pipe weld fails, it will cause a shutdown of the equipment, resulting in thousands to millions of dollars. To avoid this, understanding how to prevent the welds from failing during operation is very important. This includes correct installation by properly welding the connections per ASME standards, ensuring the piping is correctly supported, and then proactively replacing piping during a planned shutdown that are expected to fail.

The modes shapes and the stress at the welds were studied for two different piping assemblies, flange and socket weld. When comparing the modes shapes of the FPA, it was discovered that no matter the material of construction, the mode shapes were very similar, within 4% of each other to be exact. This can make the work of the technician in the field simpler when studying the piping assemblies of 24" - 36" piping lengths for vibrating near a mode, where material of construction per use of table is of no consequence. The SWPA also was similar to the FPA with respect to the mode shapes, where the piping with the same length but different material of construction was within 5% of each other. For both assemblies, although the mode shapes corresponded, it was noted that the displacement were not within a small percentage. The technician is only concerned where the mode shapes are located on the frequency spectrum, in order to avoid excessive displacements and stresses.

The intent of this study was to determine what the acceptable frequency ranges for small bore piping. This was done by looking at the frequencies to determine when the stress was above an acceptable level. The acceptable stress is below the material endurance limit, which for carbon steel is 27 ksi and stainless steel 37 ksi. The experimental method chosen did not result in

the high stress loads that would cause failure gathered from the model were in the psi range instead of the ksi range. It would be recommended to perform analysis of the problem in a different manner, such as the proposed full compressor analysis which would complete an FEA of compressor housing and bearing, as described at the end of chapter 2. Therefore the results reported on the unacceptable frequencies prove to be nil in this study. Due to the model being linear, the stress levels reaching above the endurance limit may very well be within the unacceptable ranges specified. Most likely, the actual unacceptable ranges may be fewer and have a larger spread compared to the results in this study. The acceptable level has been chosen by comparing the frequencies between the mode shapes, and choosing a value that was extremely below any stress peaks. In conclusion, additional FEA analysis needs to be completed to achieve the correct stresses that the piping will experience throughout the 0 – 350 Hz frequency range.

APPENDIX A: UNBALANCE CALCULATIONS

Mathcad Code calculating the allowable unbalance of a rotor per RPM

$m := 1000 \text{lb} = 453.592 \, \text{kg}$ mass of rotor

$G := 2.5 \dfrac{\text{mm}}{\text{s}}$ G number per ISO 1940

$U :=$ for $i \in 1, 2 .. 10$

        $U_i \leftarrow \dfrac{9.54 \cdot G \cdot m}{i \cdot 2000}(s)$

        U

$U =$

	0
0	0
1	0.469
2	0.235
3	0.156
4	0.117
5	0.094
6	0.078
7	0.067
8	0.059
9	0.052
10	0.047

$\cdot \text{in} \cdot \text{lb}$

APPENDIX B: FORCE TRANSMITTED CALCULATIONS

Calculating the Force Transmitted to the Compressor Base

$R_s := 2.5 in$ Compressor Shaft Radius

Dampening Constant Calculations

Dampening of the Bearing Oil (c1)

$\nu := 11 \cdot 10^{-6} \cdot \dfrac{m^2}{s} = 0.000011 \dfrac{m^2}{s}$ *Kinematic viscisity of the oil, R&O 100*

$\rho_{oil} := .8777 \cdot \dfrac{kg}{m^3}$ Density of the oil, R&O 100

$\mu := \nu \cdot \rho_{oil} = 0.0000096547 \cdot \dfrac{N \cdot s}{m^2}$ *Dynamic viscisity of the oil, R&O 100*

$l_1 := 6 in$ *length of the bearing*

$d := 0.0015 \cdot 2 \cdot R_s = 0.008 \cdot in$ *Radial* Clearance between bearing and shaft

$x := 2$ *number of bearings*

$$c_1 := x \cdot \dfrac{\pi \cdot \mu \cdot R_s \cdot l_1}{d} = 0.0030816433 \dfrac{s}{m} \cdot N$$

Calculating the Spring Constant the Bearing (k2a and k2b) and Housing (k3)

$$\rho_{Tin} := 7850 \frac{kg}{m^3}$$ Density of Tin

$$\rho_{CS} := 7310 \frac{kg}{m^3}$$ Density of Carbon Steel

$$E_{Tin} := 4.16 \times 10^{10} \ Pa$$ Elasticity of Tin

$$E_{CS} := 2.02 \times 10^{11} \ Pa$$ Elasticity of Carbon Steel

$$L_2 := 6in$$ Length of the bearing

$$r_1 := R_s + d = 2.5075 \cdot in$$ Inner Radius of the Bearing

$$r_2 := r_1 + .5in = 3.0075 \cdot in$$ Outer Radius of the Bearing

$$r_3 := r_2 + 3.5in = 6.5075 \cdot in$$ Outer Radius of the Bearing Housing

$$t_2 := .015in$$ Thickness of Babbett Material

$$r_{1b} := r_1 + t_2 = 2.5225 \cdot in$$

$$V_{Tin} := \frac{\pi}{2} \cdot r_1^2 \cdot t_2 = 0.1481470539 \cdot in^3$$ Volume of Babbett Material

$$m_{Tin} := \rho_{Tin} \cdot V_{Tin} = 0.0190574077 \cdot kg$$ Mass of the Tin Layer on the Bearing

$$I_{Tin} := \frac{\pi}{2} \cdot \left(r_{1b}^4 - r_1^4 \right) = 1.4993014387 \cdot in^4$$ Moment of Inertia of Thin Tin Layer

$$I_{Brg} := \frac{\pi}{2} \cdot \left(r_2^4 - r_1^4 \right) = 66.4127644222 \cdot in^4$$ Moment of Inertia of the Bearing

$$I_{BrgHousing} := \frac{\pi}{2} \cdot \left(r_3^4 - r_2^4 \right) = 2688.4218053992 \cdot in^4$$ Moment of Intertia of the Bearing Housing

$$x := 2$$ Number of Bearings

$$k_{2a} := x \frac{3 \cdot E_{Tin} \cdot I_{Tin}}{L_2^{\,3}} = 44006163.116767295 \cdot \frac{N}{m}$$

spring constant of the Tin

$$k_{2b} := x \frac{3 \cdot E_{CS} \cdot I_{Brg}}{L_2^{\,3}} = 9465294769.3700256 \cdot \frac{N}{m}$$

Spring Constant of the carbon steel of the bearing

$$k_3 := x \frac{3 \cdot E_{CS} \cdot I_{BrgHousing}}{L_2^{\,3}} = 383159849976.16602 \cdot \frac{N}{m}$$

Spring Constant of the Bearing Housing

Calculating the Spring Constant the Compressor (k4)

$L_4 := 4ft$ Half the length of the compressor

$r_{4a} := 5.5in$ Inner Radius of the Compressor Housing

$r_{4b} := 20in$ Outer Radius of the Compressor Housing

$$I_{Comp} := \frac{\pi}{2} \cdot \left(r_{4b}^{\,4} - r_{4a}^{\,4} \right)$$

Moment Inertia of the Compressor Housing

$x := 2$ Number of Compressor Housings

$$k_4 := x \frac{3 \cdot E_{CS} \cdot I_{Comp}}{L_4^{\,3}} = 69560318685.270096 \cdot \frac{N}{m}$$

Spring Constant of the Compressor Housing

Calculating the Spring Costant of the Concrete (k5)

$$E_{con} := 210 \times 10^9 Pa = 298690209.44951081 \frac{m}{s^2} \cdot \frac{lb}{in^2}$$

Elasticity of the Concrete

$$A_5 := 8in \cdot 12in = 96 \cdot in^2$$ Cross-Sectional Area of the Concrete Pad for the one foot

$$L_5 := 6in = 0.1524\,m$$ Thickness of the Concrete Foot

$x := 4$ Number of concrete Pads

87

$$k_5 := x \frac{A_5 \cdot E_{con}}{L_5} = 341376000000 \cdot \frac{N}{m}$$

Spring Constant of the concrete base for one Compressor Foot

Dampening Constant Calculations (Continued)

Dampening of the Concrete Base (c5)

$$\rho_{con} := 2400 \frac{kg}{m^3}$$

Density of Concrete

$$V_5 := A_5 \cdot L_5 = 576 \cdot in^3$$

Volume of the concrete base

$$m_5 := \rho_{con} \cdot V_5 = 22.6534772736$$ *Mass of the concrete base*

Typical Dampening Ratio of Concrete

$$\xi := 0.055$$

$$c_5 := \xi \cdot 2 \cdot \sqrt{k_5 \cdot m_5} = 305897.9843653843 \cdot \frac{N \cdot s}{m}$$

Dampening Coefficient of the Concrete Base for one foot

$$x := 4 \qquad \text{number of concrete support pads}$$

$$c_5 := x \cdot 51.169 \frac{N \cdot s}{m} = 204.676 \frac{kg}{s}$$

Total Dampening and Spring Constants

$$\frac{1}{K_{eq}} := \frac{1}{k_{2a}} + \frac{1}{k_{2b}} + \frac{1}{k_3} + \frac{1}{k_4} + \frac{1}{k_5} \blacksquare \qquad \text{Total Spring Constant Equation}$$

$$\frac{1}{C_{eq}} := \frac{1}{c_1} + \frac{1}{c_5} \blacksquare \qquad \text{Total Dampening Constant Equation}$$

$$K_{eq} := \frac{1}{\left(\dfrac{1}{k_{2a}} + \dfrac{1}{k_{2b}} + \dfrac{1}{k_3} + \dfrac{1}{k_4} + \dfrac{1}{k_5}\right)} = 43764338.706686854 \frac{kg}{s^2}$$

$$C_{eq} := \frac{1}{\left(\dfrac{1}{c_1} + \dfrac{1}{c_5}\right)} = 0.0030815969 \frac{kg}{s}$$

Equation of Motion

$$M\left(\frac{d^2}{dt^2}x\right) + \left(C_{eq}\right)\cdot\left(\frac{d}{dt}x\right) + \left(K_{eq}\right)\cdot(x) := F_R\cdot sin(\omega\cdot t) \blacksquare$$

Masses

$m_d := 250lb$ *Mass of Disk*

$m_s := 250lb$ *Mass of Shaft*

$r_d := 6in$ *Radius of Disk*

$M := m_d\cdot3 + m_s = 453.59237\,kg$ *Rotor Assembly Weight*

$M = 1000\cdot lb$

Eccentricity

$$U := e \cdot M$$

Unbalance

$$U := .040 in \cdot lb$$

$$e_s := \frac{U}{M} = 0.00004 \cdot in$$

Unbalance. The max allowable U at 20,000 rpm for a 1000 lb rotor is .047"

eccentricity

$$U := r_e \cdot m_e$$

Unbalance

$$r_e := 5.5 in$$

Distance from center or rotor to center of gravity of unbalance

$$m_e := \frac{U}{r_e} = 0.007273 \cdot lb$$

Unbalance Mass

Force of Rotor to the Compressor

$$F_R := U \cdot \omega^2$$

Equation of Motion Amplitude

$$X := \frac{F_R}{\sqrt{\left(K_{eq} - M \cdot \omega^2\right)^2 + \left(C_{eq} \cdot \omega\right)^2}} \quad => \quad X := \frac{F_R}{\sqrt{(A)^2 + (B)^2}} \quad => \quad X := \frac{F_R}{Xd}$$

Amplitude of Vibration at the Base

$$\phi := atan\left(\frac{C_{eq} \cdot \omega}{K_{eq} - M \cdot \omega^2}\right) \quad => \quad \phi := atan\left(\frac{B}{A}\right)$$

Phase Angle

$ORIGIN := 1$

$$\omega := \begin{vmatrix} for\ i \in 1,2..10 \\ \quad \omega_i \leftarrow 2000 \cdot i \cdot \dfrac{rad}{s} \\ \omega \end{vmatrix}$$

$$A := \begin{vmatrix} for\ i \in 1,2..10 \\ \quad A_i \leftarrow K_{eq} - M \cdot \left(\omega_i\right)^2 \\ A \end{vmatrix}$$

	1
1	$-6.971 \cdot 10^{10}$
2	$-2.84 \cdot 10^{11}$
3	$-6.412 \cdot 10^{11}$
4	$-1.141 \cdot 10^{12}$
5	$-1.784 \cdot 10^{12}$
6	$-2.57 \cdot 10^{12}$
7	$-3.498 \cdot 10^{12}$
8	$-4.57 \cdot 10^{12}$
9	$-5.784 \cdot 10^{12}$
10	$-7.141 \cdot 10^{12}$

$A = \ldots\ Pa \cdot in$

	1
1	2000
2	4000
3	6000
4	8000
5	10000
6	12000
7	14000
8	16000
9	18000
10	20000

$\omega = \ldots\ \dfrac{1}{s}$

$$B := \begin{vmatrix} for\ i \in 1,2..10 \\ \quad B_i \leftarrow C_{eq} \cdot \omega_i \\ B \end{vmatrix}$$

	1
1	$6.163 \cdot 10^{0}$
2	$1.233 \cdot 10^{1}$
3	$1.849 \cdot 10^{1}$
4	$2.465 \cdot 10^{1}$
5	$3.082 \cdot 10^{1}$
6	$3.698 \cdot 10^{1}$
7	$4.314 \cdot 10^{1}$
8	$4.931 \cdot 10^{1}$
9	$5.547 \cdot 10^{1}$
10	$6.163 \cdot 10^{1}$

$B = \ldots\ \dfrac{kg}{s^{2 \times 10^{0}}}$

$$F_R := \begin{vmatrix} for\ i \in 1,2..10 \\ \quad F_{R_i} \leftarrow U \cdot \left(\omega_i\right)^2 \\ F_R \end{vmatrix}$$

	1
1	$1.843 \cdot 10^{3}$
2	$7.374 \cdot 10^{3}$
3	$1.659 \cdot 10^{4}$
4	$2.949 \cdot 10^{4}$
5	$4.608 \cdot 10^{4}$
6	$6.636 \cdot 10^{4}$
7	$9.033 \cdot 10^{4}$
8	$1.18 \cdot 10^{5}$
9	$1.493 \cdot 10^{5}$
10	$1.843 \cdot 10^{5}$

$F_R = \ldots\ N$

$$Xd := \sqrt{(A)^2 + (B)^2}$$

	1
1	$1.771 \cdot 10^{9}$
2	$7.214 \cdot 10^{9}$
3	$1.629 \cdot 10^{10}$
4	$2.899 \cdot 10^{10}$
5	$4.532 \cdot 10^{10}$
6	$6.527 \cdot 10^{10}$
7	$8.886 \cdot 10^{10}$
8	$1.161 \cdot 10^{11}$
9	$1.469 \cdot 10^{11}$
10	$1.814 \cdot 10^{11}$

$Xd = \ldots\ \dfrac{kg}{s^{2 \times 10^{0}}}$

	1
1	$4.099 \cdot 10^{-5}$
2	$4.024 \cdot 10^{-5}$
3	$4.011 \cdot 10^{-5}$
4	$4.006 \cdot 10^{-5}$
5	$4.004 \cdot 10^{-5}$
6	$4.003 \cdot 10^{-5}$
7	$4.002 \cdot 10^{-5}$
8	$4.002 \cdot 10^{-5}$
9	$4.001 \cdot 10^{-5}$
10	$4.001 \cdot 10^{-5}$

$$X := \frac{F_R}{Xd} = \quad \cdot in$$

Amplitude

$$\phi := atan\left(\frac{B}{A}\right) =$$

Phase

	1
1	$-3.481 \cdot 10^{-9}$
2	$-1.709 \cdot 10^{-9}$
3	$-1.135 \cdot 10^{-9}$
4	$-8.505 \cdot 10^{-10}$
5	$-6.8 \cdot 10^{-10}$
6	$-5.665 \cdot 10^{-10}$
7	$-4.855 \cdot 10^{-10}$
8	$-4.248 \cdot 10^{-10}$
9	$-3.775 \cdot 10^{-10}$
10	$-3.398 \cdot 10^{-10}$

Force Transmitted to Concrete Base

$$F_T := F_R \cdot \left[\sqrt{\frac{K_{eq}^2 + \left(C_{eq} \cdot \omega\right)^2}{\left(K_{eq} - M \cdot \omega^2\right)^2 + \left(C_{eq} \cdot \omega\right)^2}}\right]^{\blacksquare} \quad => \quad F_T := F_R \cdot \left[\sqrt{\frac{K_{eq}^2 + (B)^2}{(A)^2 + (B)^2}}\right]^{\blacksquare}$$

Force Transmitted to Base

$$=> \quad F_T := F_R \cdot \left(\sqrt{\frac{XN}{XD}}\right)^{\blacksquare} \quad => \quad F_T := F_R \cdot (XT)^{\blacksquare}$$

$$XN := K_{eq}^2 + (B)^2$$

$$XD := (A)^2 + (B)^2$$

$$XD = \quad \frac{kg^{2 \times 10^0}}{s^{4 \times 10^0}}$$

	1
1	$3.135 \cdot 10^{18}$
2	$5.204 \cdot 10^{19}$
3	$2.652 \cdot 10^{20}$
4	$8.402 \cdot 10^{20}$
5	$2.053 \cdot 10^{21}$
6	$4.261 \cdot 10^{21}$
7	$7.896 \cdot 10^{21}$
8	$1.347 \cdot 10^{22}$
9	$2.159 \cdot 10^{22}$
10	$3.29 \cdot 10^{22}$

$$XN = \quad \frac{kg^{2 \times 10^0}}{s^{4 \times 10^0}}$$

	1
1	$1.915 \cdot 10^{15}$
2	$1.915 \cdot 10^{15}$
3	$1.915 \cdot 10^{15}$
4	$1.915 \cdot 10^{15}$
5	$1.915 \cdot 10^{15}$
6	$1.915 \cdot 10^{15}$
7	$1.915 \cdot 10^{15}$
8	$1.915 \cdot 10^{15}$
9	$1.915 \cdot 10^{15}$
10	$1.915 \cdot 10^{15}$

$$XT := \sqrt{\frac{XN}{XD}}$$

$$F_T := F_R \cdot (XT)^{\blacksquare}$$

$$F_T := \begin{vmatrix} for \ i \in 1, 2 .. 10 \\ \quad F_{T_i} \leftarrow F_{R_i} \cdot \left(XT_i\right) \\ F_T \end{vmatrix}$$

$$F_T = \begin{array}{|c|c|} \hline & 1 \\ \hline 1 & 10.243 \\ \hline 2 & 10.057 \\ \hline 3 & 10.023 \\ \hline 4 & 10.011 \\ \hline 5 & 10.006 \\ \hline 6 & 10.003 \\ \hline 7 & 10.001 \\ \hline 8 & 10 \\ \hline 9 & 9.999 \\ \hline 10 & 9.998 \\ \hline \end{array} \ \cdot lbf$$

$$XT = \begin{array}{|c|c|} \hline & 1 \\ \hline 1 & 2.472 \cdot 10^{-2} \\ \hline 2 & 6.067 \cdot 10^{-3} \\ \hline 3 & 2.687 \cdot 10^{-3} \\ \hline 4 & 1.51 \cdot 10^{-3} \\ \hline 5 & 9.658 \cdot 10^{-4} \\ \hline 6 & 6.705 \cdot 10^{-4} \\ \hline 7 & 4.925 \cdot 10^{-4} \\ \hline 8 & 3.77 \cdot 10^{-4} \\ \hline 9 & 2.979 \cdot 10^{-4} \\ \hline 10 & 2.413 \cdot 10^{-4} \\ \hline \end{array}$$

Unbalance (U) Transmitted to Concrete Base

$$U_T := \begin{vmatrix} for \ i \in 1, 2 .. 10 \\ \quad U_{T_i} \leftarrow \dfrac{F_{T_i}}{\left(\omega_i\right)^2} \\ U_T \end{vmatrix}$$

$$U_T = \begin{array}{|c|c|} \hline & 1 \\ \hline 1 & 1.139 \cdot 10^{-5} \\ \hline 2 & 2.796 \cdot 10^{-6} \\ \hline 3 & 1.238 \cdot 10^{-6} \\ \hline 4 & 6.958 \cdot 10^{-7} \\ \hline 5 & 4.451 \cdot 10^{-7} \\ \hline 6 & 3.09 \cdot 10^{-7} \\ \hline 7 & 2.27 \cdot 10^{-7} \\ \hline 8 & 1.738 \cdot 10^{-7} \\ \hline 9 & 1.373 \cdot 10^{-7} \\ \hline 10 & 1.112 \cdot 10^{-7} \\ \hline \end{array} \ kg \cdot m$$

$$U := r_e \cdot m_e^{\blacksquare}$$

$$m_{eT} := \begin{vmatrix} for \ i \in 1, 2 .. 10 \\ \quad m_{eT_i} \leftarrow \dfrac{U_{T_i}}{r_e} \\ m_{eT} \end{vmatrix}$$

$$m_{eT} = \begin{array}{|c|c|} \hline & 1 \\ \hline 1 & 0.0001797611970405 \\ \hline 2 & 0.0000441223644518 \\ \hline 3 & 0.0000195440672907 \\ \hline 4 & 0.0000109806279509 \\ \hline 5 & 0.0000070237841733 \\ \hline 6 & 0.0000048761889519 \\ \hline 7 & 0.0000035818690209 \\ \hline 8 & 0.0000027420519505 \\ \hline 9 & 0.0000021663881391 \\ \hline 10 & 0.0000017546750835 \\ \hline \end{array} \ \cdot lb$$

APPENDIX C: MODE SHAPES
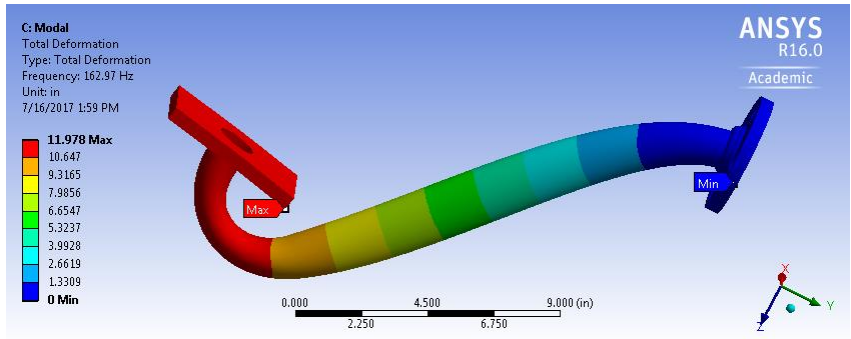
Figure 95 The 1st Mode for FPA, 1 Inch Diameter, CS, 12 Inches Long
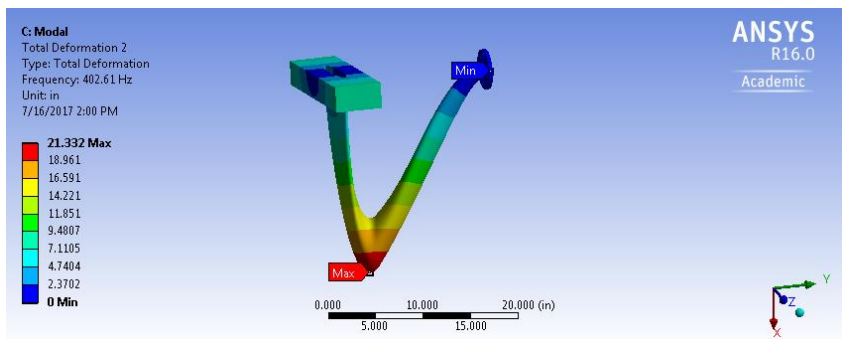
Figure 96 The 2nd Mode for FPA, 1 Inch Diameter, CS, 12 Inches Long
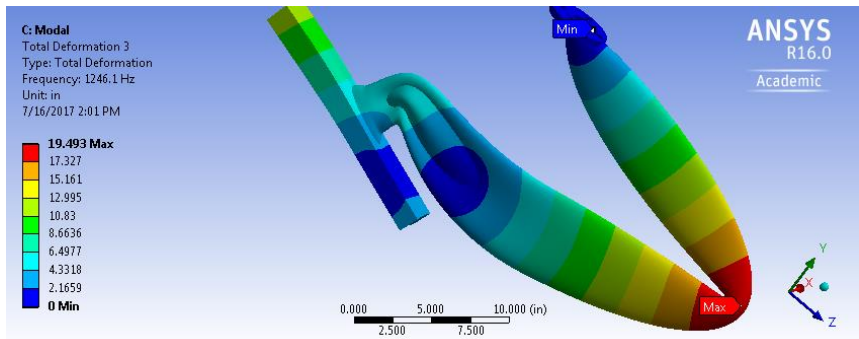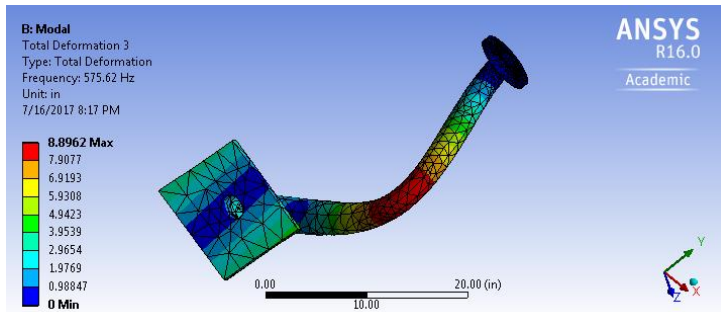

**Figure 97 The 3rd Mode for FPA, 1 Inch Diameter, CS, 12 Inches Long**
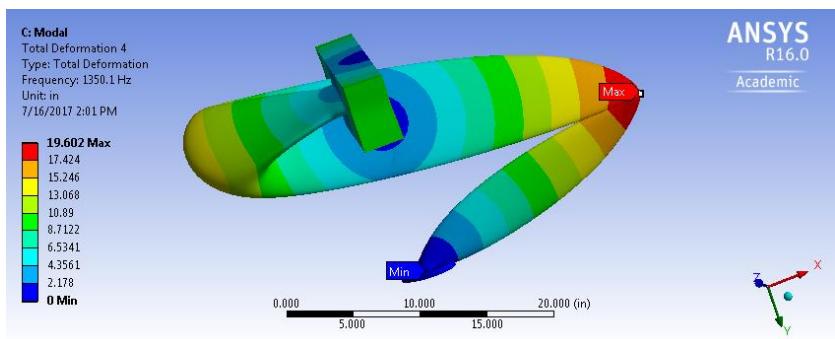
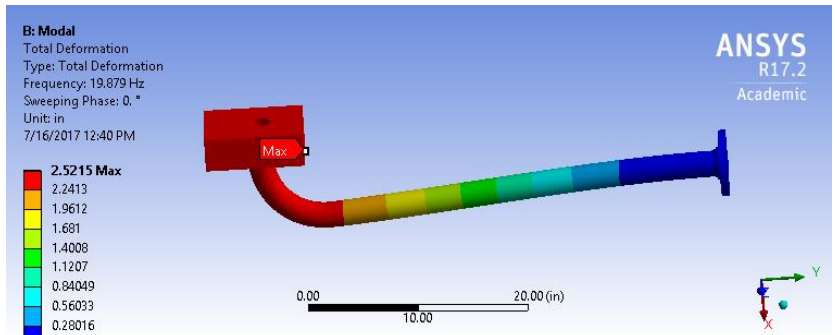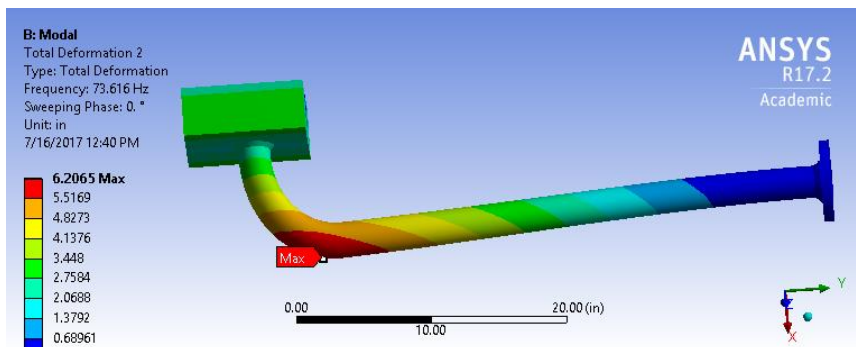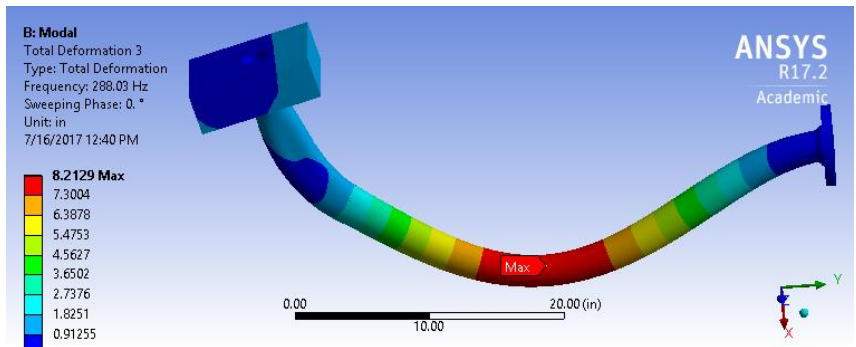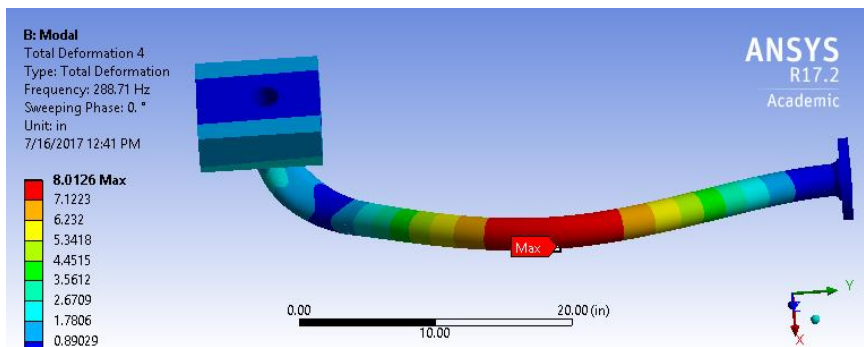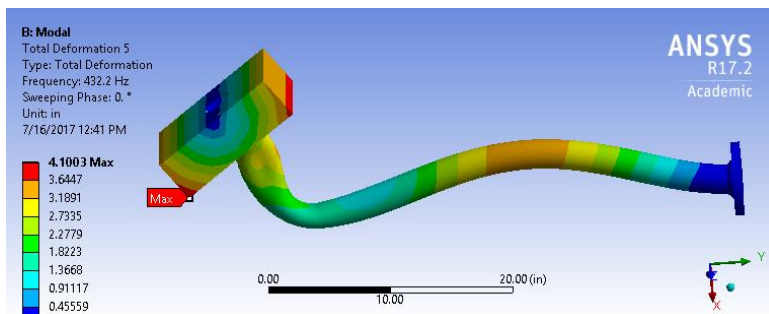**Figure 98 The 4th Mode for FPA, 1 Inch Diameter, CS, 12 Inches Long**

95
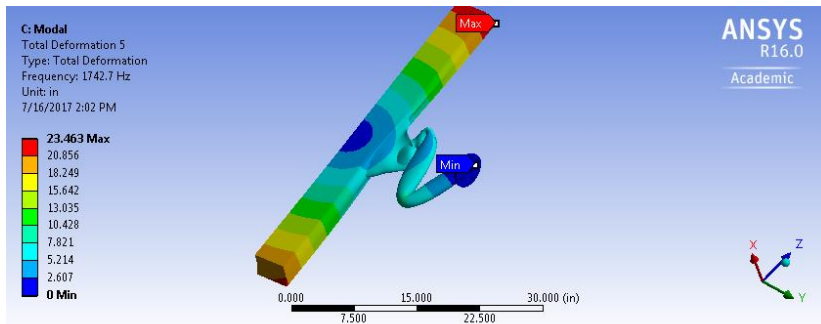
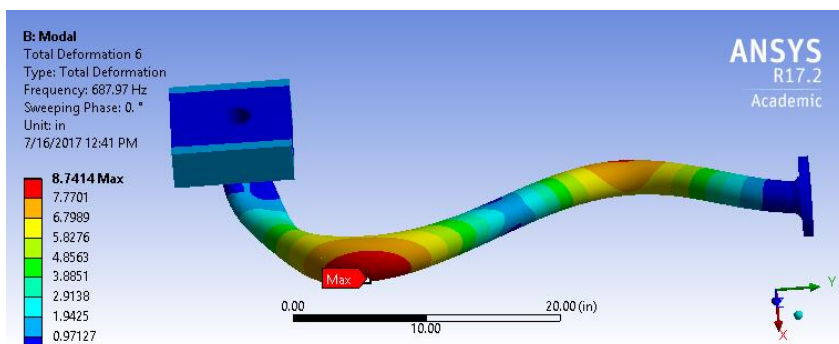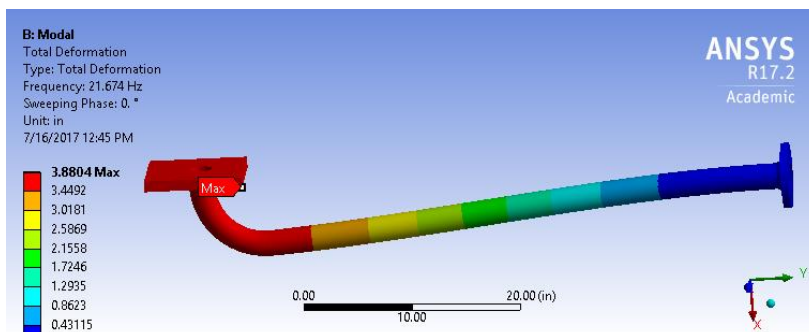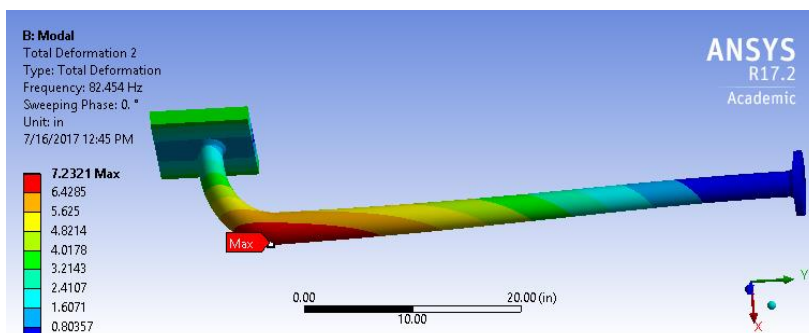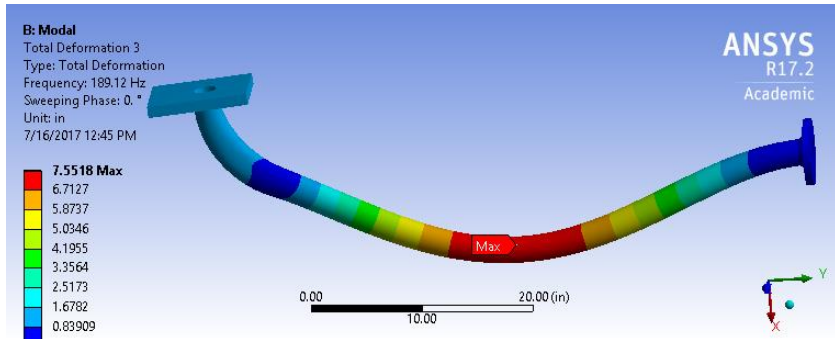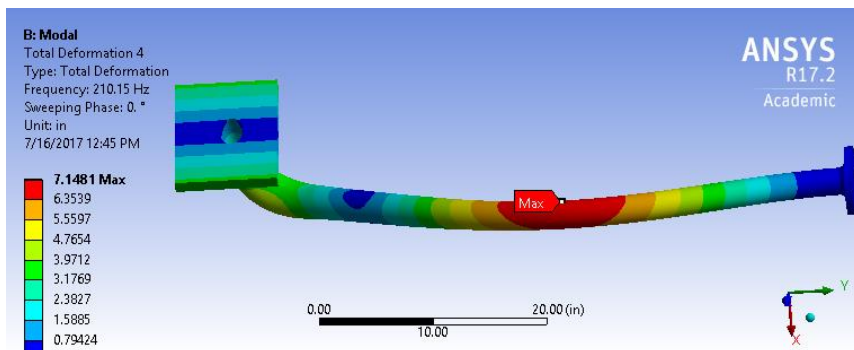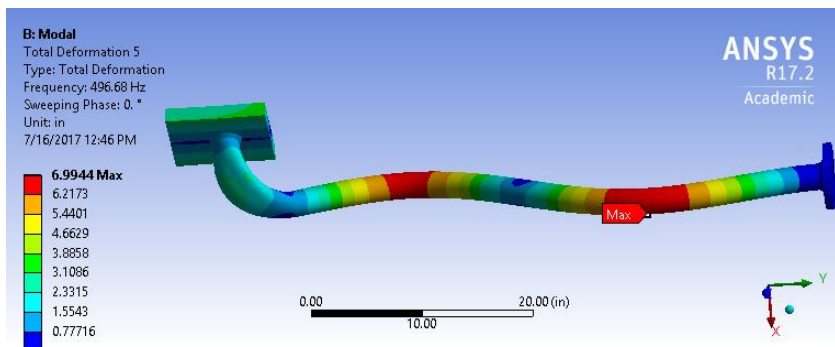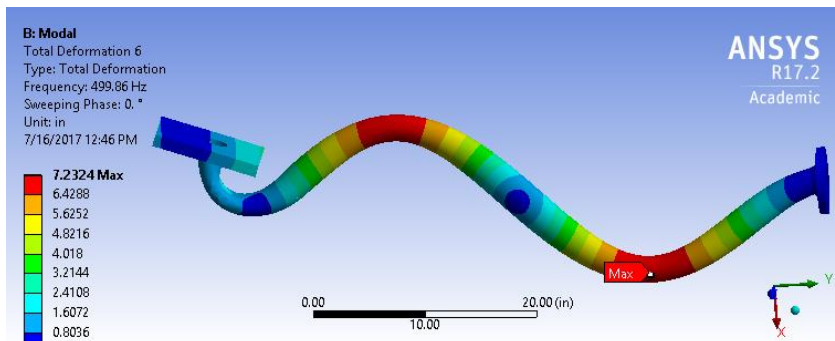**Figure 99 The 5th Mode for FPA, 1 Inch Diameter, CS, 12 Inches Long**
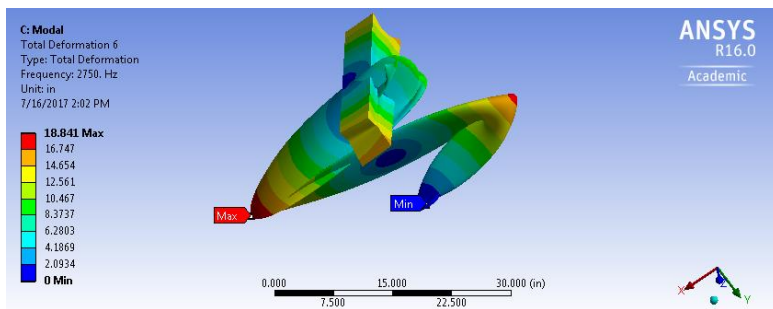
Figure 100 The 6th Mode for FPA, 1 Inch Diameter, CS, 12 Inches Long
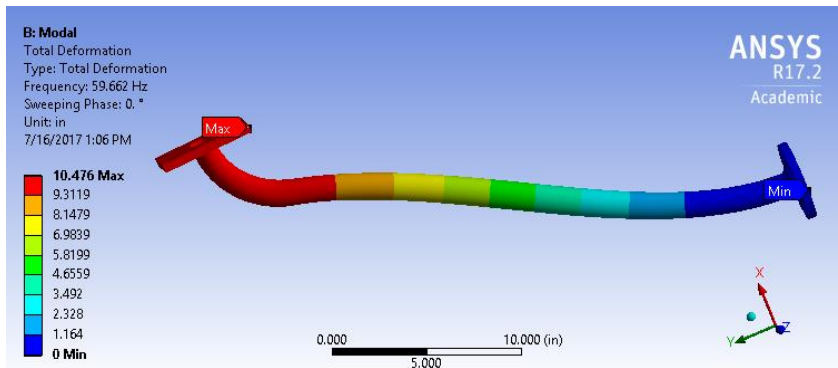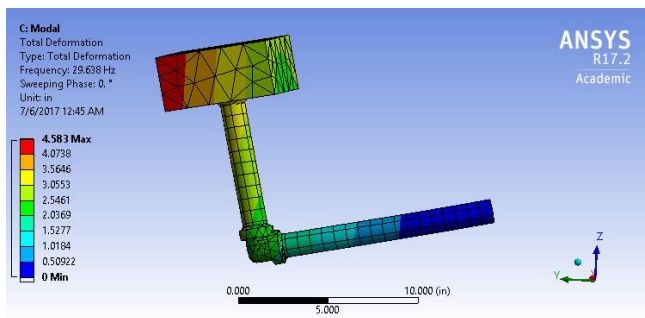

Figure 101 The 1st Mode for FPA, 1 Inch Diameter, CS, 24 Inches Long
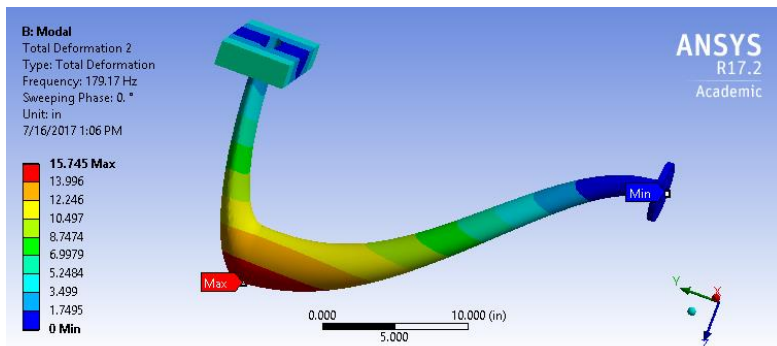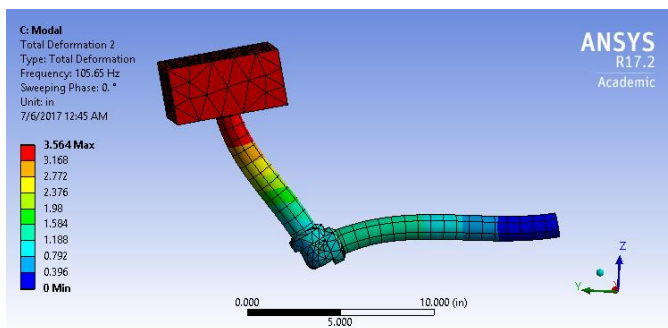

Figure 102 The 2nd Mode for FPA, 1 Inch Diameter, CS, 24 Inches Long
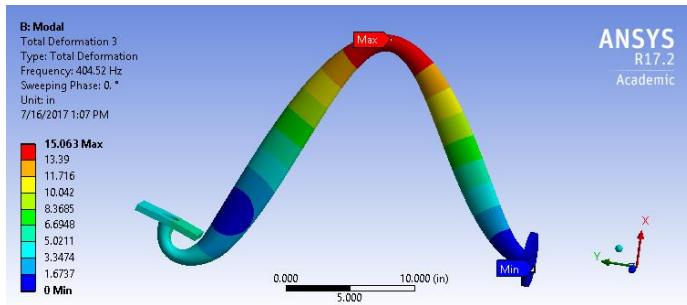
Figure 103 The 3rd Mode for FPA, 1 Inch Diameter, CS, 24 Inches Long
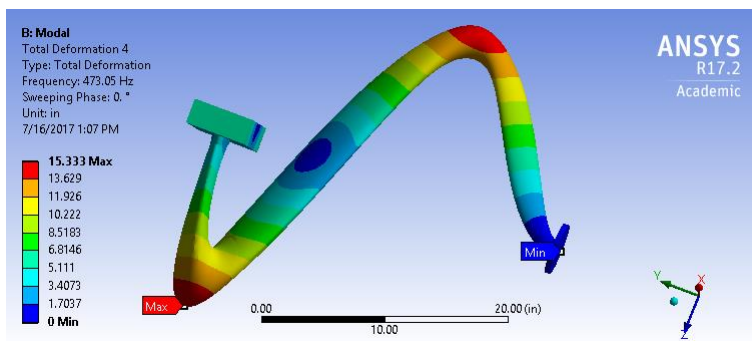
Figure 104 The 4th Mode for FPA, 1 Inch Diameter, CS, 24 Inches Long
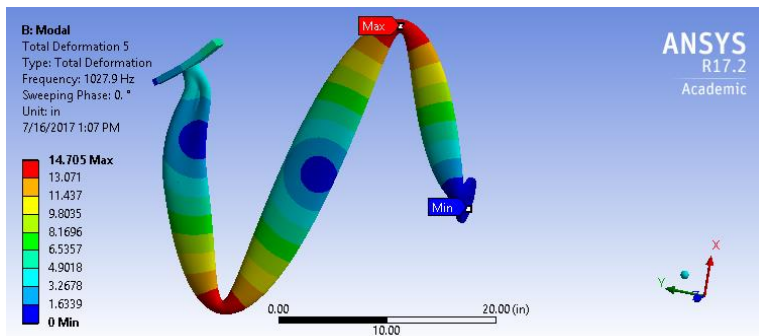
Figure 105 The 5th Mode for FPA, 1 Inch Diameter, CS, 24 Inches Long
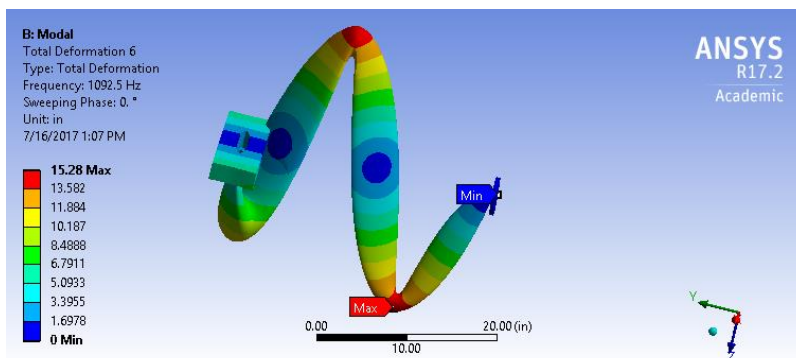
Figure 106 The 6th Mode for FPA, 1 Inch Diameter, CS, 24 Inches Long
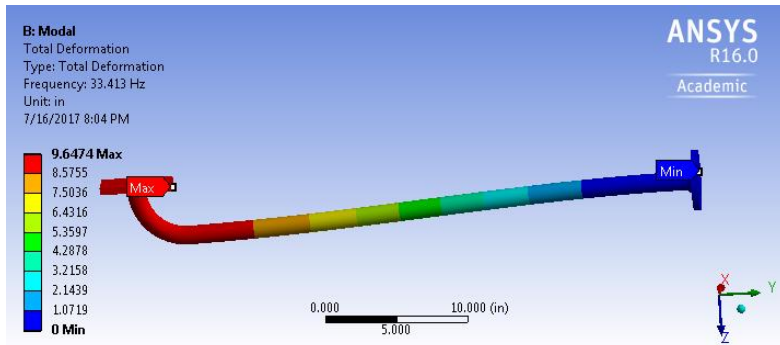
Figure 107 The 1st Mode for FPA, 1 Inch Diameter, CS, 36 Inches Long
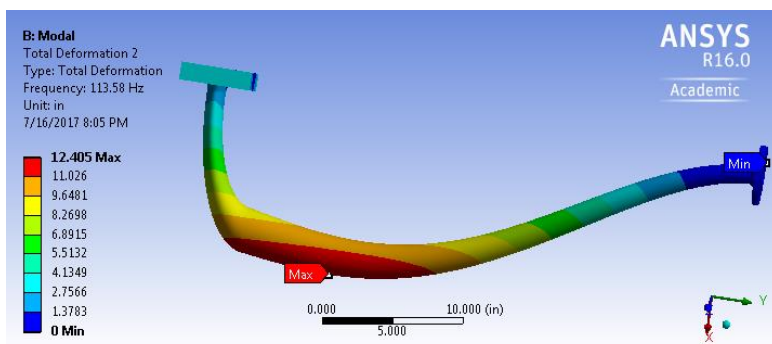
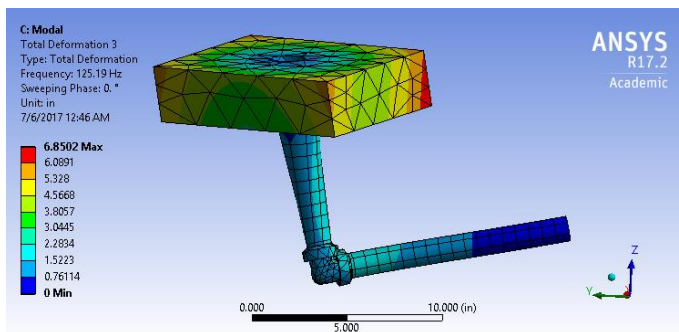**Figure 108 The 2nd Mode for FPA, 1 Inch Diameter, CS, 36 Inches Long**
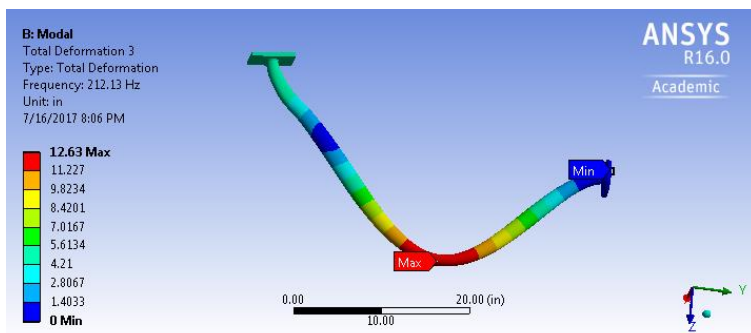
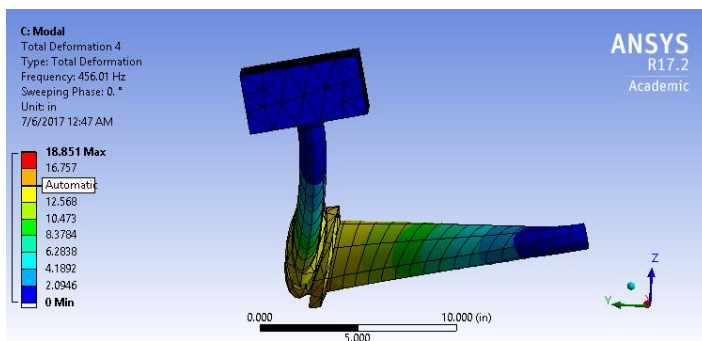**Figure 109 The 3rd Mode for FPA, 1 Inch Diameter, CS, 36 Inches Long**
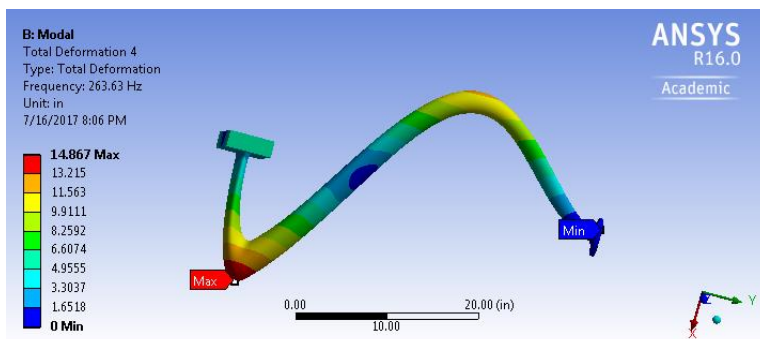
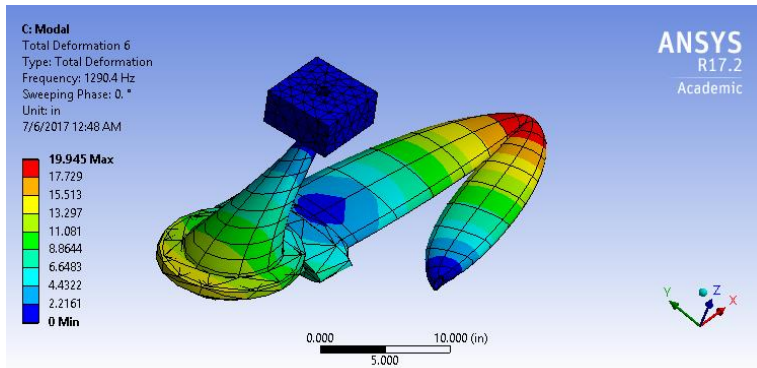**Figure 110 The 4th Mode for FPA, 1 Inch Diameter, CS, 36 Inches Long**
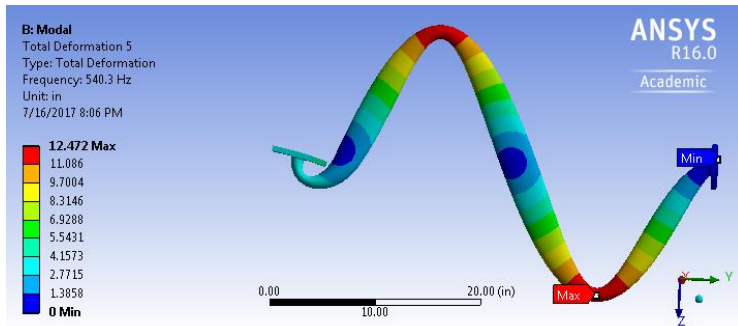
Figure 111 The 5th Mode for FPA, 1 Inch Diameter, CS, 36 Inches Long
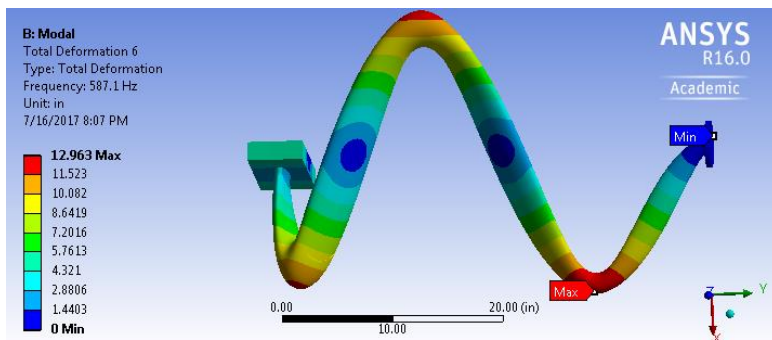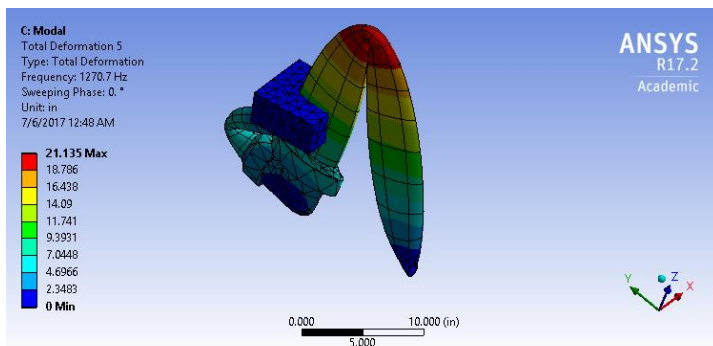

Figure 112 The 6th Mode for FPA, 1 Inch Diameter, CS, 36 Inches Long
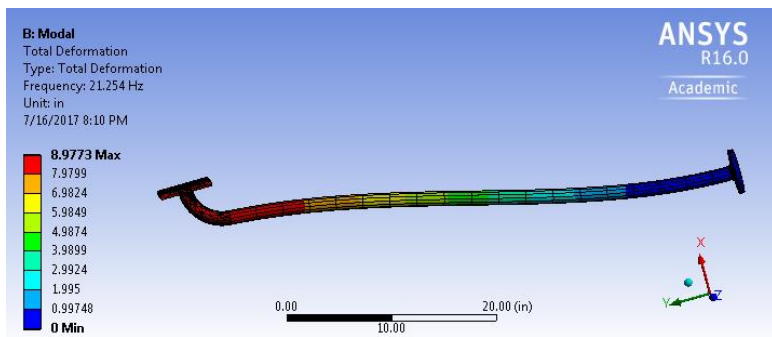
Figure 113 The 1st Mode for FPA, 1 Inch Diameter, CS, 48 Inches Long
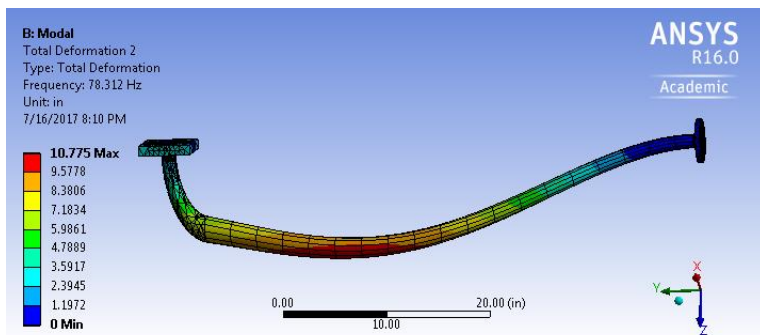
Figure 114 The 2nd Mode for FPA, 1 Inch Diameter, CS, 48 Inches Long

99
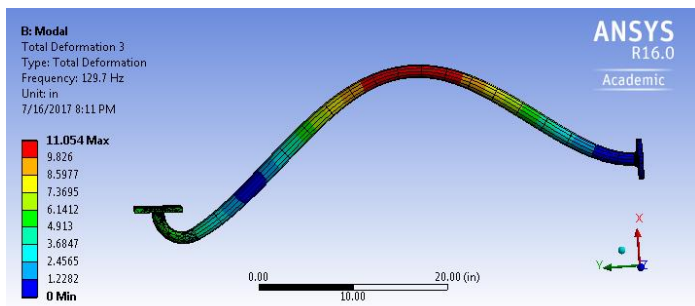
Figure 115 The 3rd Mode for FPA, 1 Inch Diameter, CS, 48 Inches Long
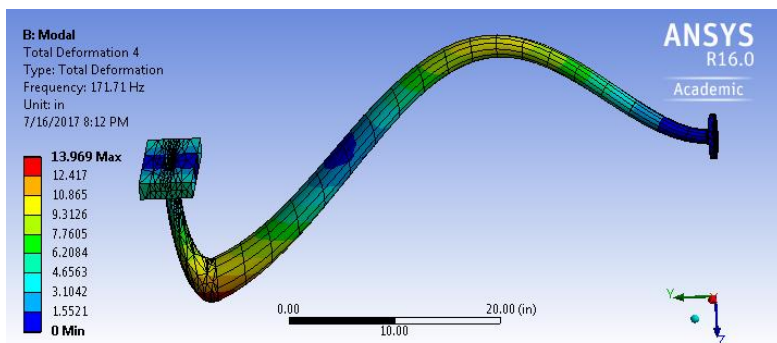
Figure 116 The 4th Mode for FPA, 1 Inch Diameter, CS, 48 Inches Long
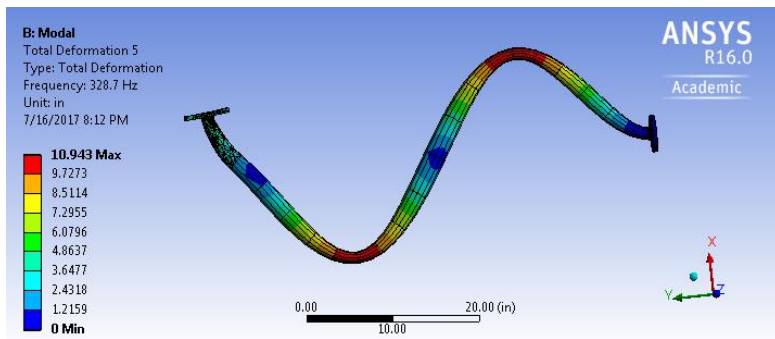
Figure 117 The 5th Mode for FPA, 1 Inch Diameter, CS, 48 Inches Long
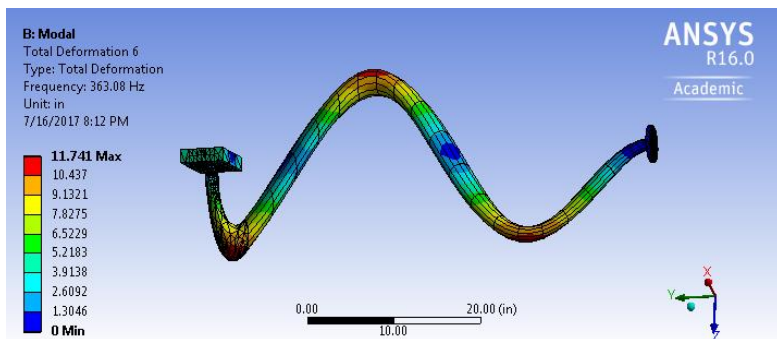
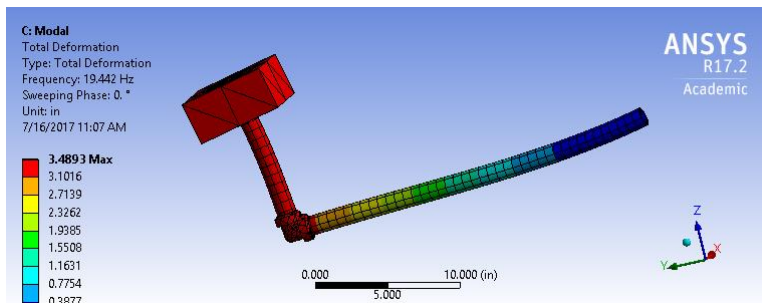**Figure 118 The 6th Mode for FPA, 1 Inch Diameter, CS, 48 Inches Long**

100
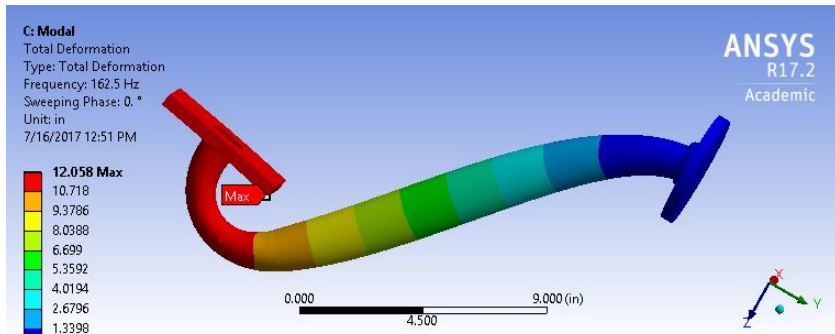
Figure 119 The 1st Mode for FPA, 1 Inch Diameter, SS, 12 Inches Long
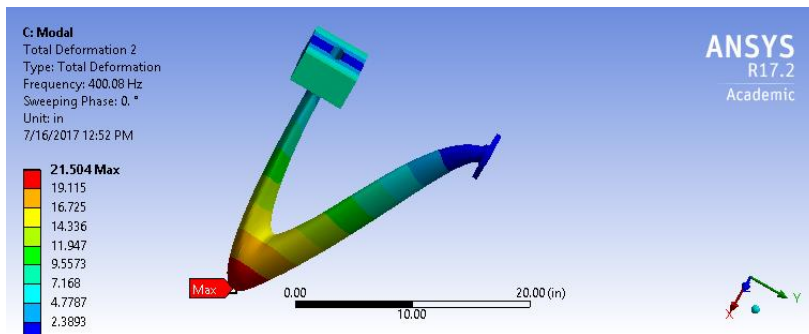
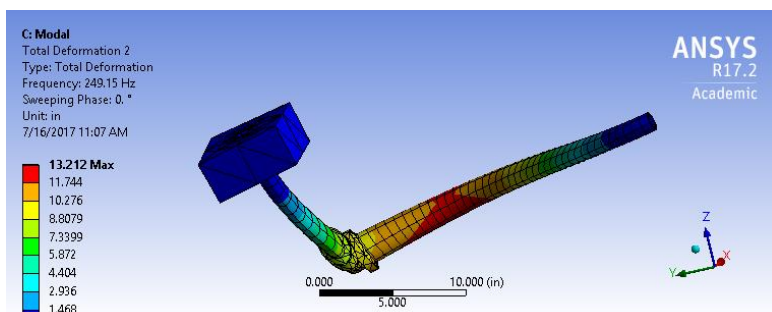
**Figure 120 The 2nd Mode for FPA, 1 Inch Diameter, SS, 12 Inches Long**
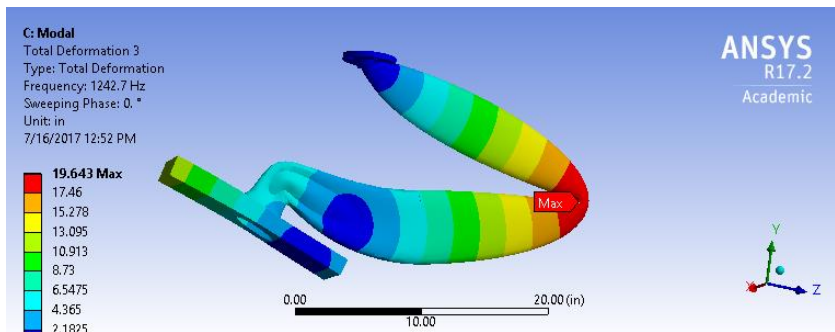
**Figure 121 The 3rd Mode for FPA, 1 Inch Diameter, SS, 12 Inches Long**
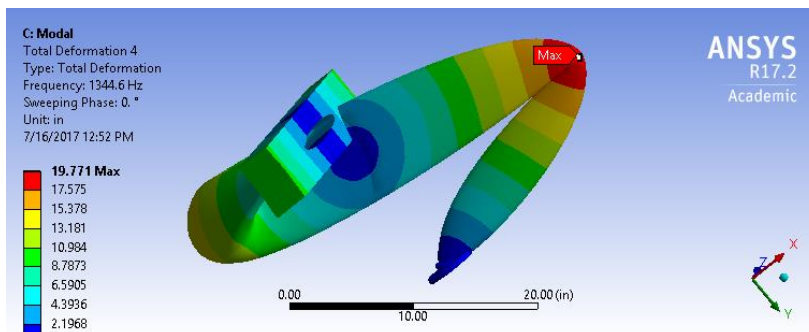
**Figure 122 The 4th Mode for FPA, 1 Inch Diameter, SS, 12 Inches Long**

101
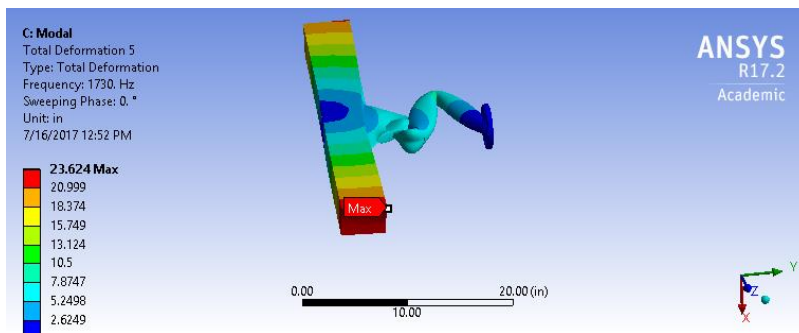
Figure 123 The 5th Mode for FPA, 1 Inch Diameter, SS, 12 Inches Long
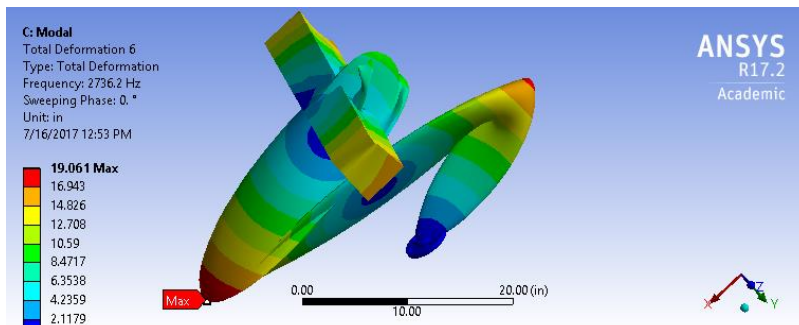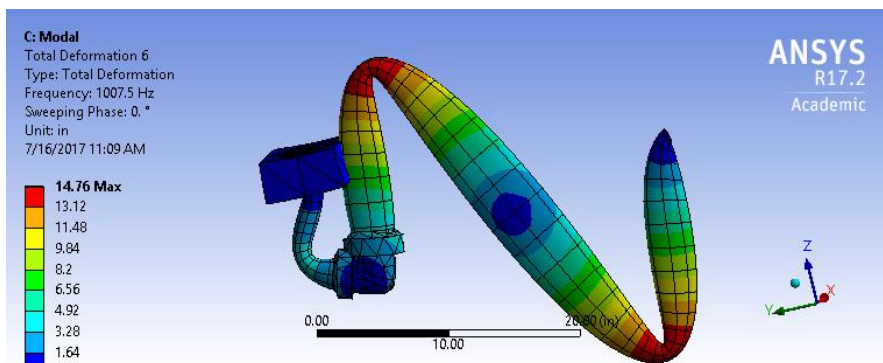

Figure 124 The 6th Mode for FPA, 1 Inch Diameter, SS, 12 Inches Long
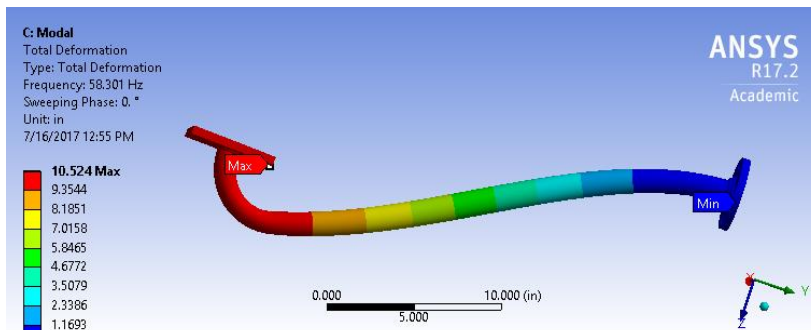
Figure 125 The 1st Mode for FPA, 1 Inch Diameter, SS, 24 Inches Long
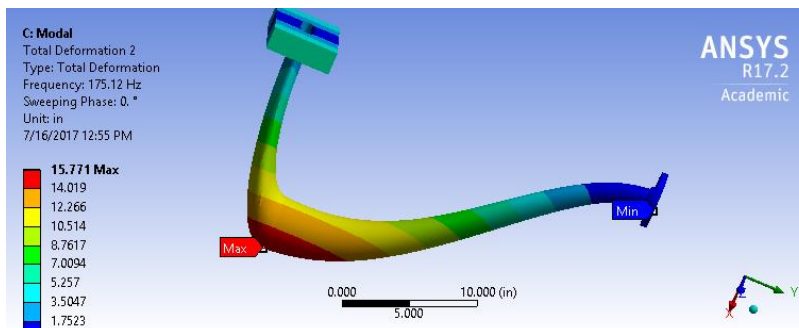
Figure 126 The 2nd Mode for FPA, 1 Inch Diameter, SS, 24 Inches Long

102
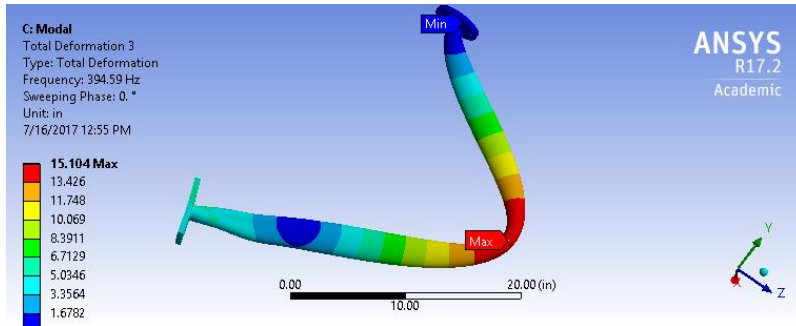
Figure 127 The 3rd Mode for FPA, 1 Inch Diameter, SS, 24 Inches Long
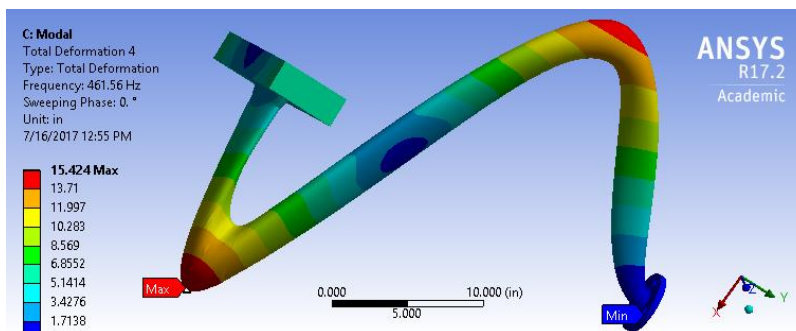
Figure 128 The 4th Mode for FPA, 1 Inch Diameter, SS, 24 Inches Long
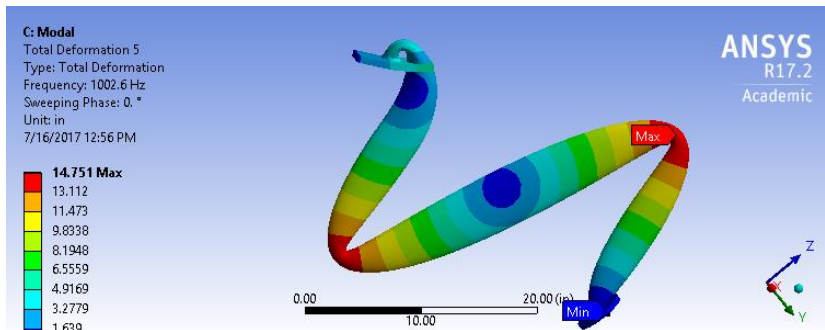
Figure 129 The 5th Mode for FPA, 1 Inch Diameter, SS, 24 Inches Long
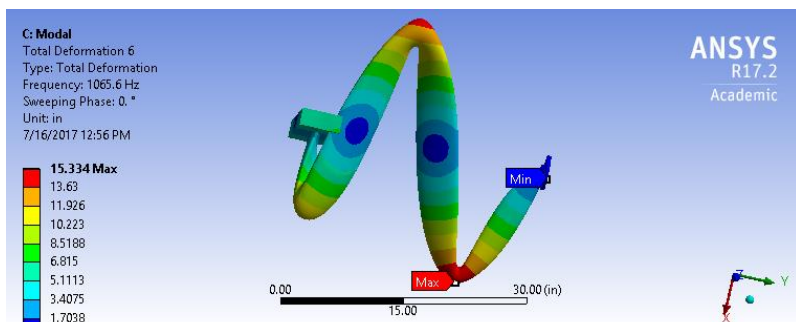
**Figure 130 The 6th Mode for FPA, 1 Inch Diameter, SS, 24 Inches Long**

103
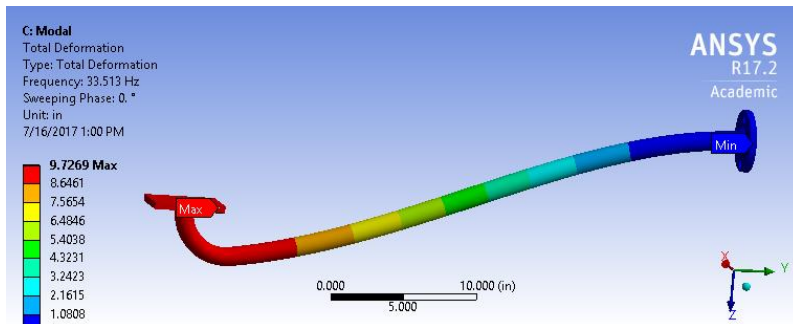
Figure 131 The 1st Mode for FPA, 1 Inch Diameter, SS, 36 Inches Long
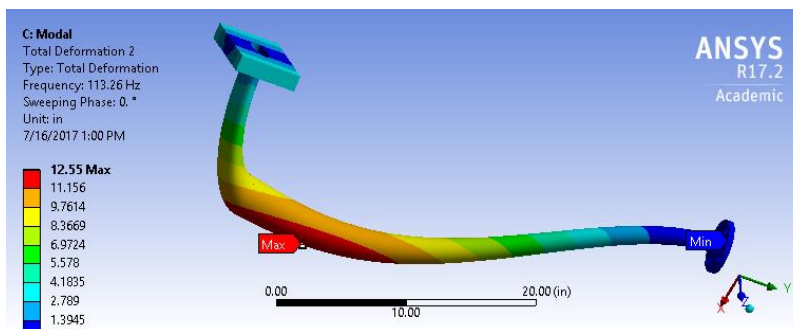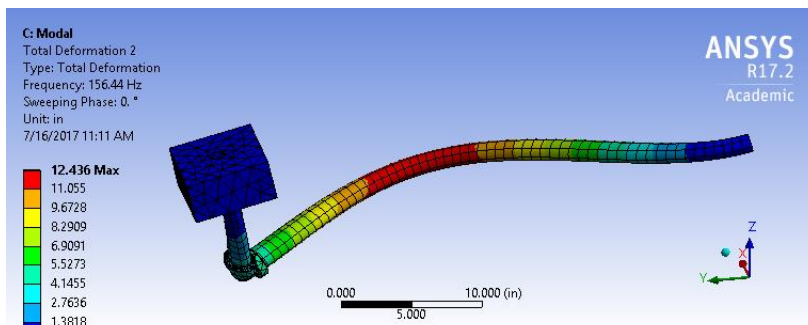

**Figure 132 The 2nd Mode for FPA, 1 Inch Diameter, SS, 36 Inches Long**
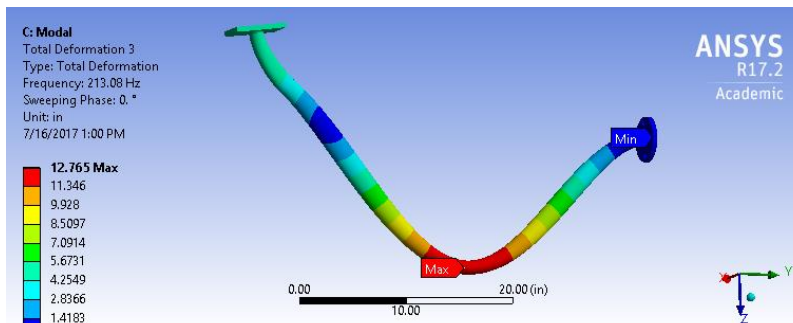
**Figure 133 The 3rd Mode for FPA, 1 Inch Diameter, SS, 36 Inches Long**
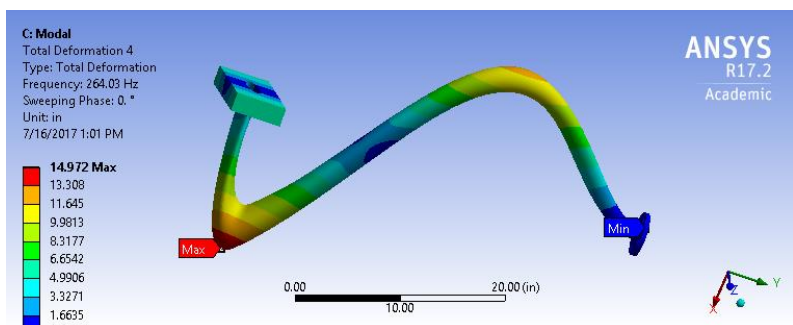
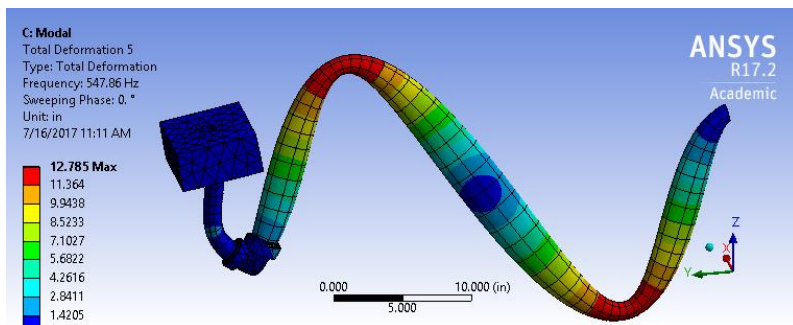**Figure 134 The 4th Mode for FPA, 1 Inch Diameter, SS, 36 Inches Long**
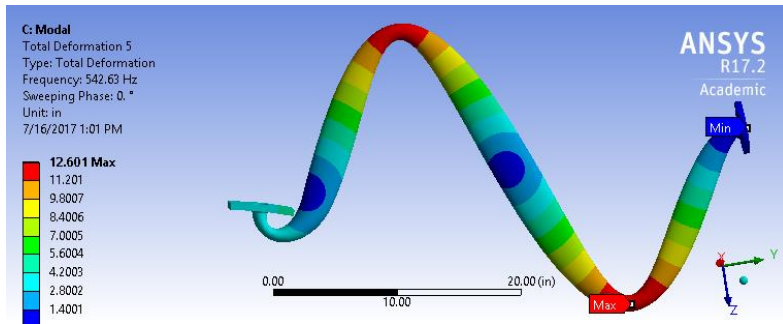
Figure 135 The 5th Mode for FPA, 1 Inch Diameter, SS, 36 Inches Long
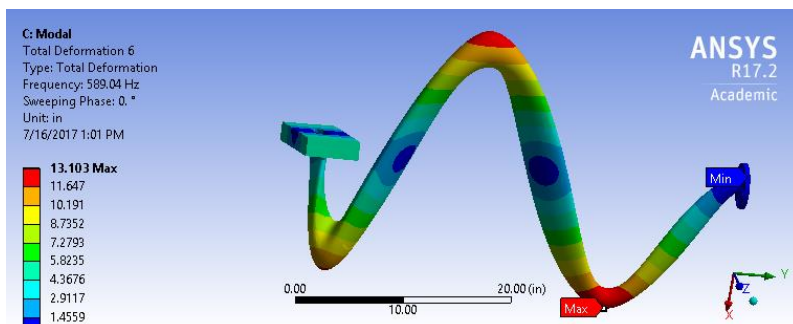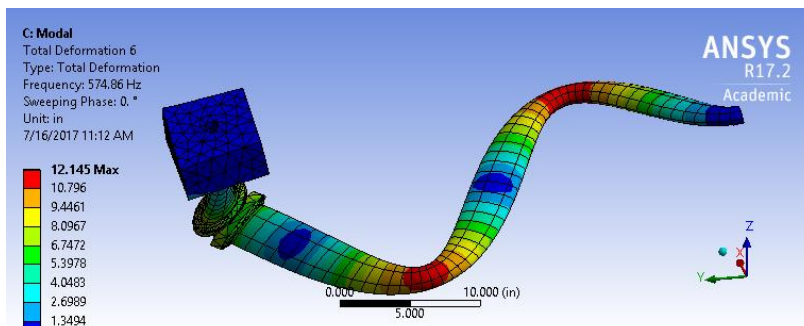

Figure 136 The 6th Mode for FPA, 1 Inch Diameter, SS, 36 Inches Long
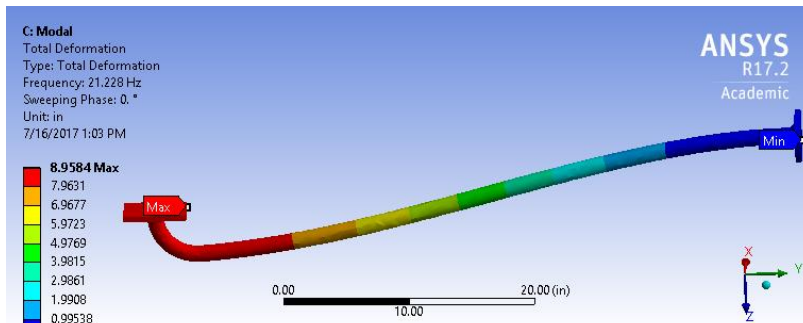
Figure 137 The 1st Mode for FPA, 1 Inch Diameter, SS, 48 Inches Long
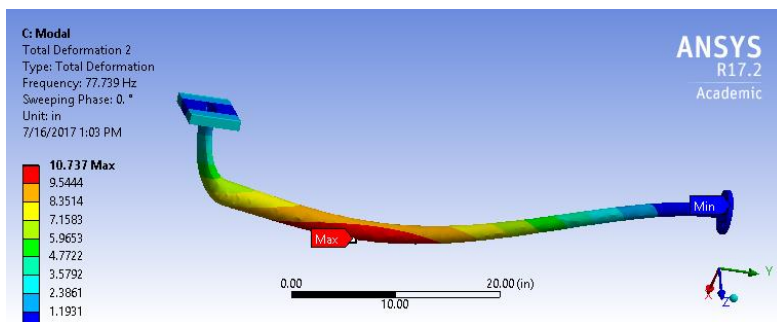
Figure 138 The 2nd Mode for FPA, 1 Inch Diameter, SS, 48 Inches Long
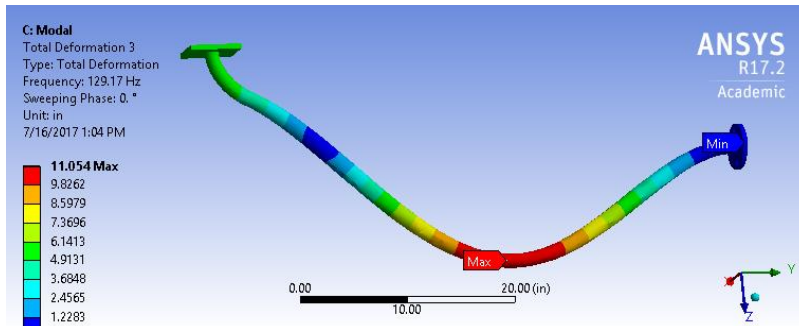
Figure 139 The 3rd Mode for FPA, 1 Inch Diameter, SS, 48 Inches Long
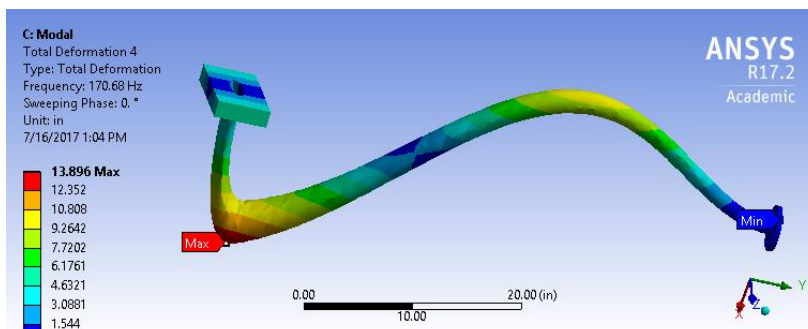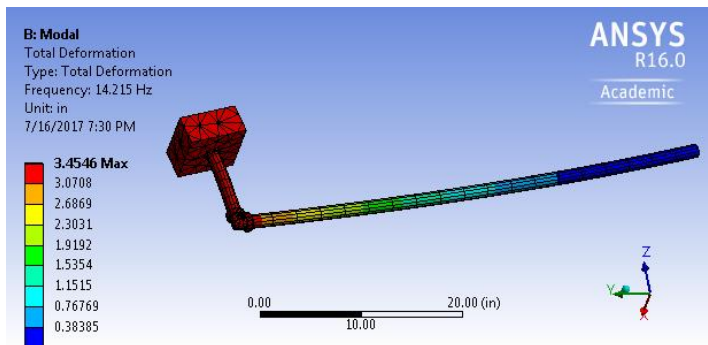

Figure 140 The 4th Mode for FPA, 1 Inch Diameter, SS, 48 Inches Long
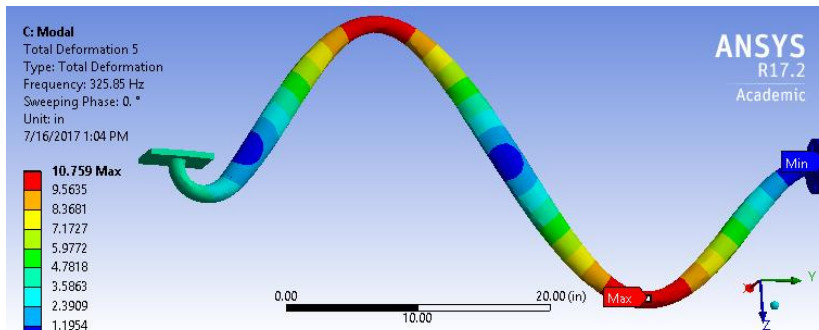
Figure 141 The 5th Mode for FPA, 1 Inch Diameter, SS, 48 Inches Long
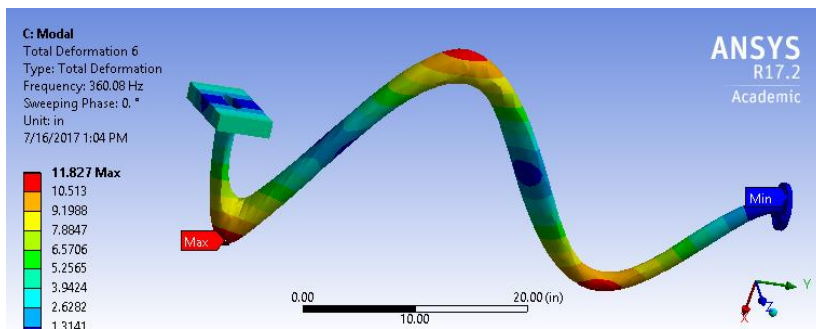
Figure 142 The 6th Mode for FPA, 1 Inch Diameter, SS, 48 Inches Long

106
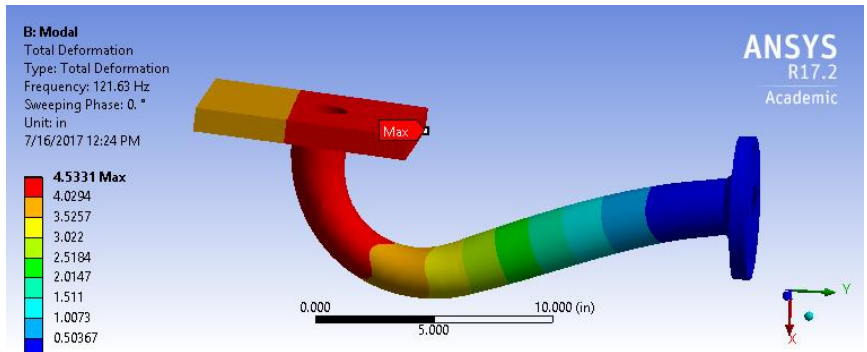
Figure 143 The 1st Mode for FPA, 2 Inch Diameter, CS, 12 Inches Long
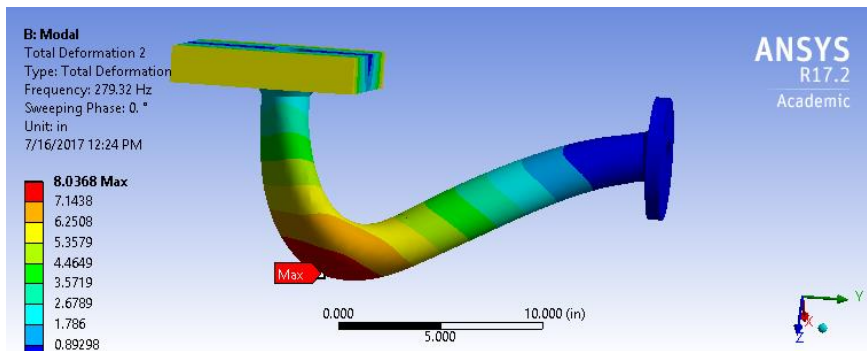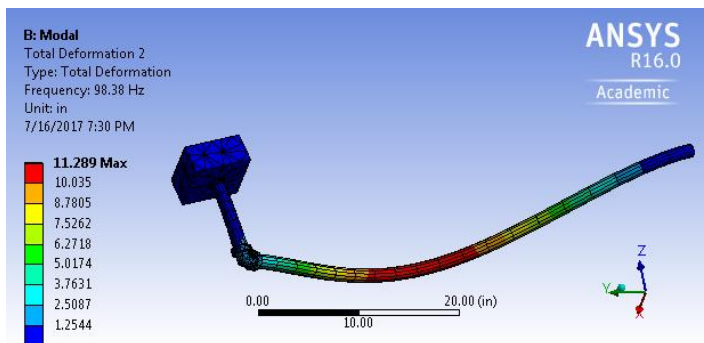

Figure 144 The 2nd Mode for FPA, 2 Inch Diameter, CS, 12 Inches Long
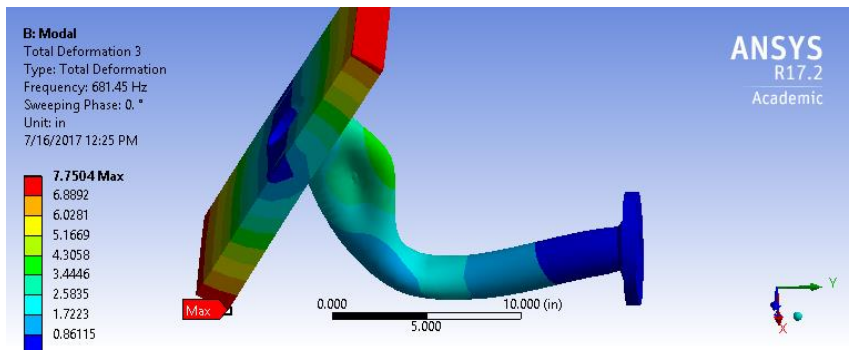
**Figure 145 The 3rd Mode for FPA, 2 Inch Diameter, CS, 12 Inches Long**
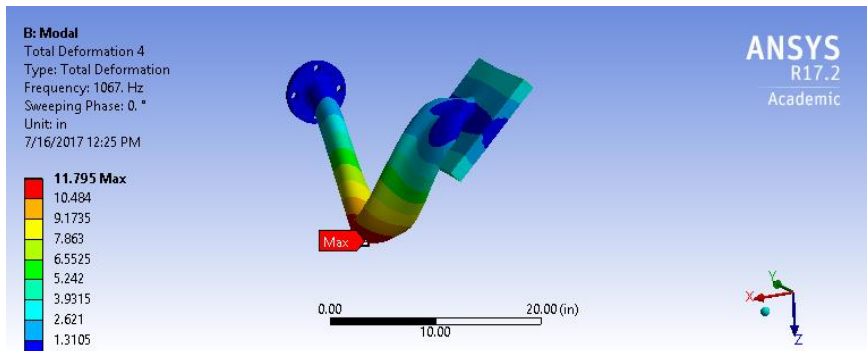
Figure 146 The 4th Mode for FPA, 2 Inch Diameter, CS, 12 Inches Long

107
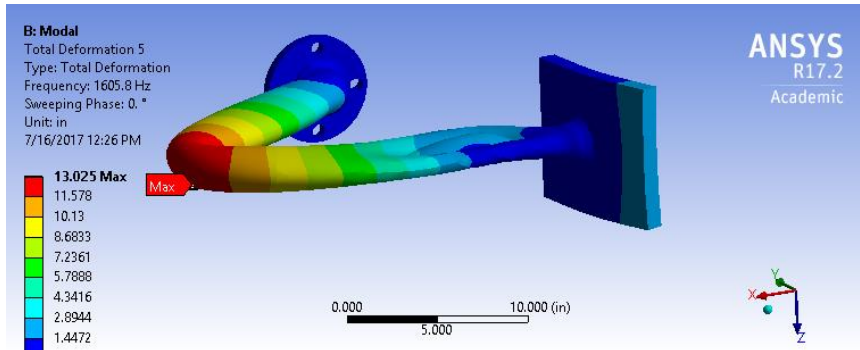
Figure 147 The 5th Mode for FPA, 2 Inch Diameter, CS, 12 Inches Long
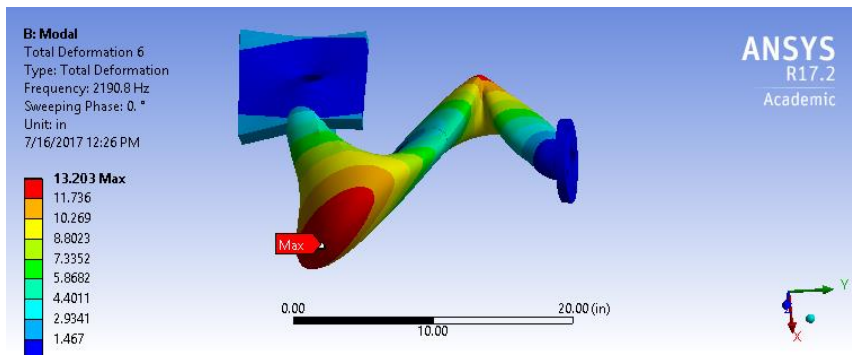
Figure 148 The 6th Mode for FPA, 2 Inch Diameter, CS, 12 Inches Long
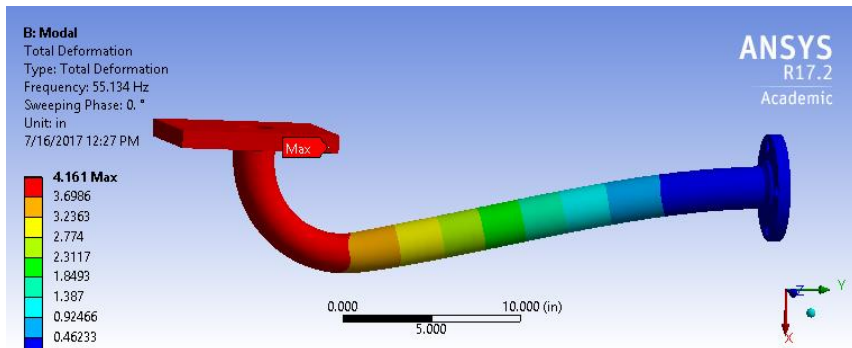
Figure 149 The 1st Mode for FPA, 2 Inch Diameter, CS, 24 Inches Long
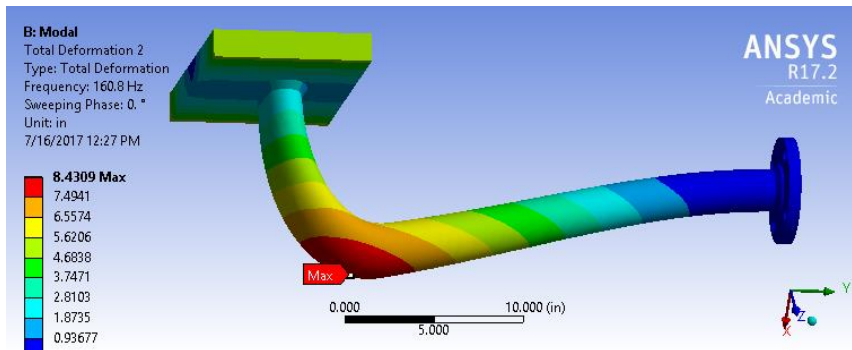
Figure 150 The 2nd Mode for FPA, 2 Inch Diameter, CS, 24 Inches Long
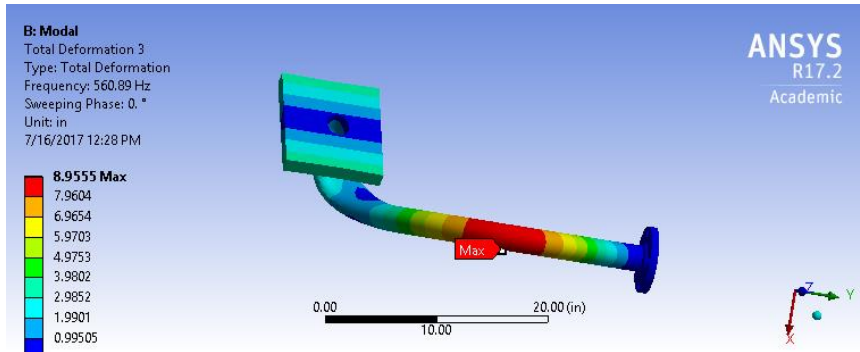
Figure 151 The 3rd Mode for FPA, 2 Inch Diameter, CS, 24 Inches Long
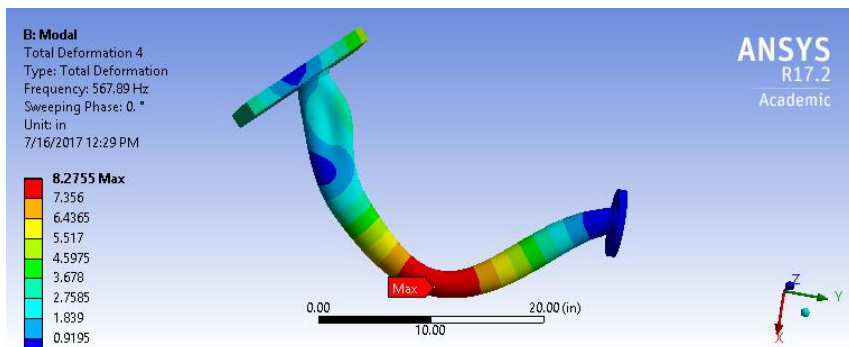
**Figure 152 The 4th Mode for FPA, 2 Inch Diameter, CS, 24 Inches Long**
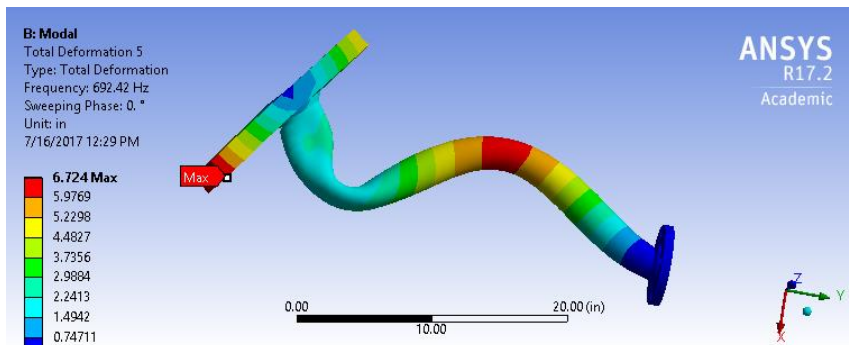
**Figure 153 The 5th Mode for FPA, 2 Inch Diameter, CS, 24 Inches Long**
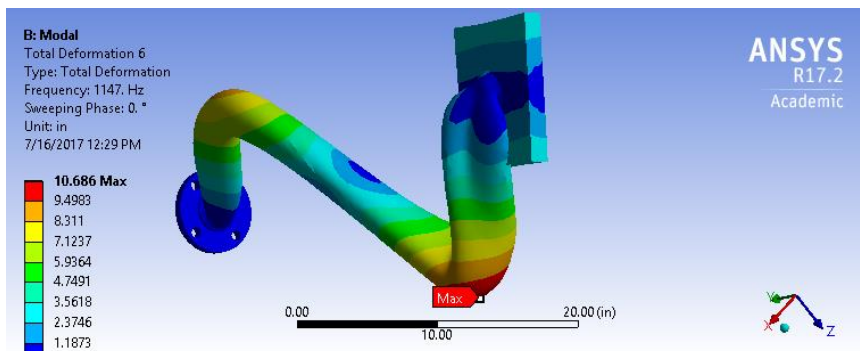
**Figure 154 The 6th Mode for FPA, 2 Inch Diameter, CS, 24 Inches Long**

109
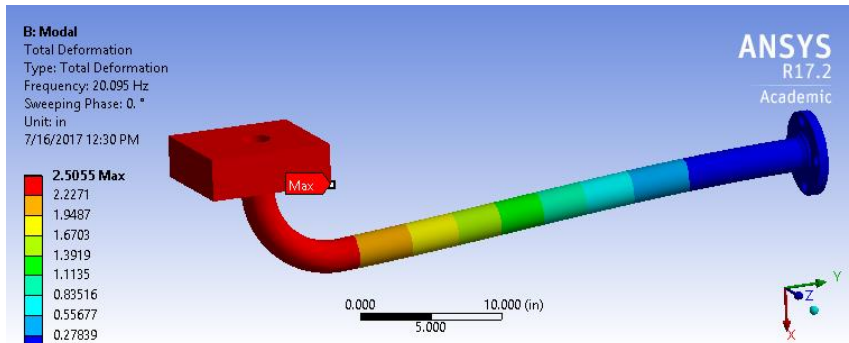
Figure 155 The 1st Mode for FPA, 2 Inch Diameter, CS, 36 Inches Long
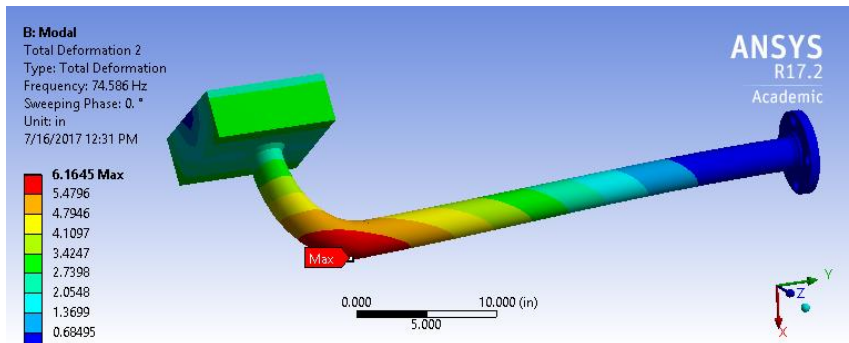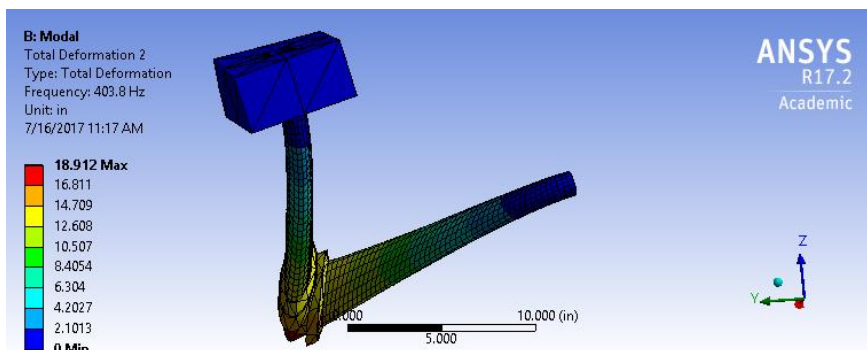

**Figure 156 The 2nd Mode for FPA, 2 Inch Diameter, CS, 36 Inches Long**
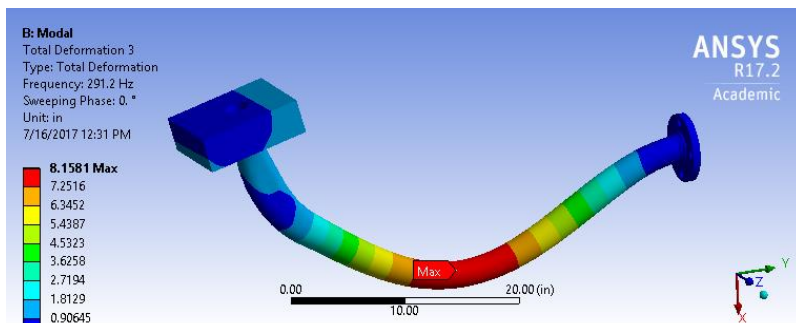
Figure 157 The 3rd Mode for FPA, 2 Inch Diameter, CS, 36 Inches Long
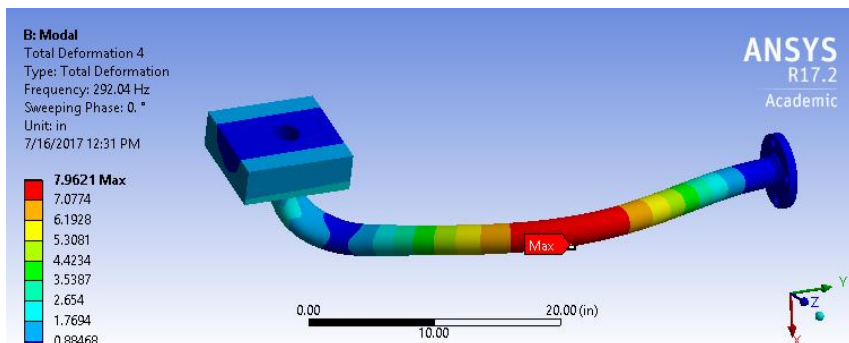
Figure 158 The 4th Mode for FPA, 2 Inch Diameter, CS, 36 Inches Long

110
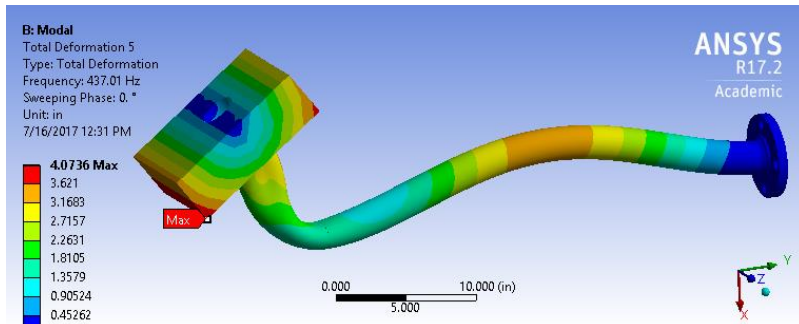
Figure 159 The 5th Mode for FPA, 2 Inch Diameter, CS, 36 Inches Long
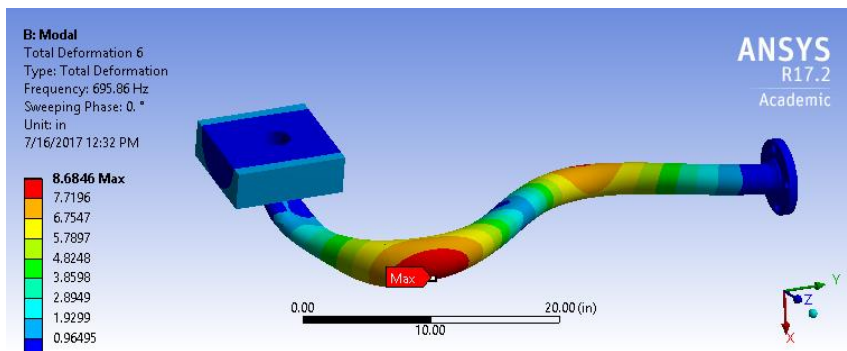
Figure 160 The 6th Mode for FPA, 2 Inch Diameter, CS, 36 Inches Long
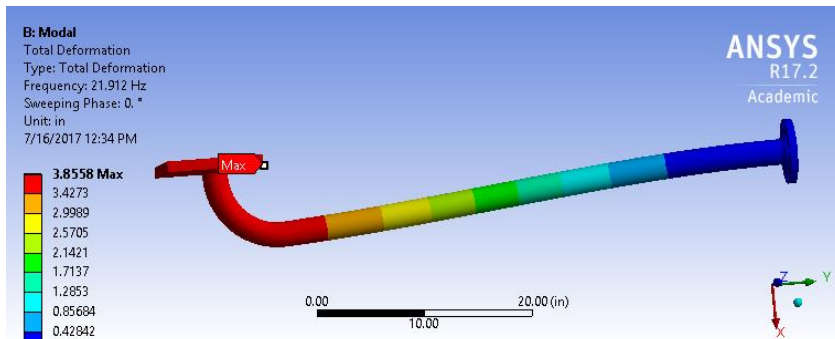
Figure 161 The 1st Mode for FPA, 2 Inch Diameter, CS, 48 Inches Long
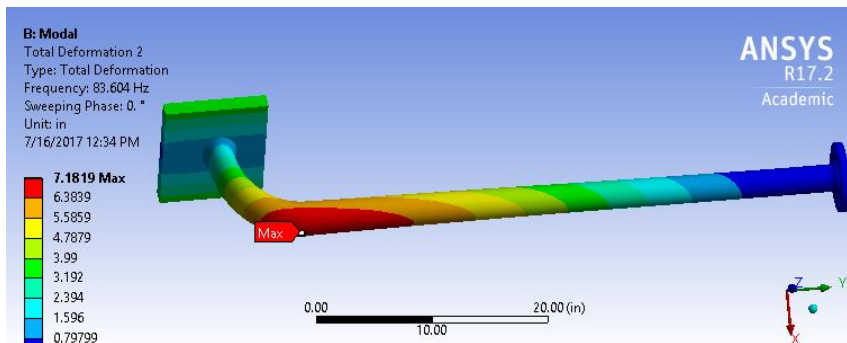
Figure 162 The 2nd Mode for FPA, 2 Inch Diameter, CS, 48 Inches Long
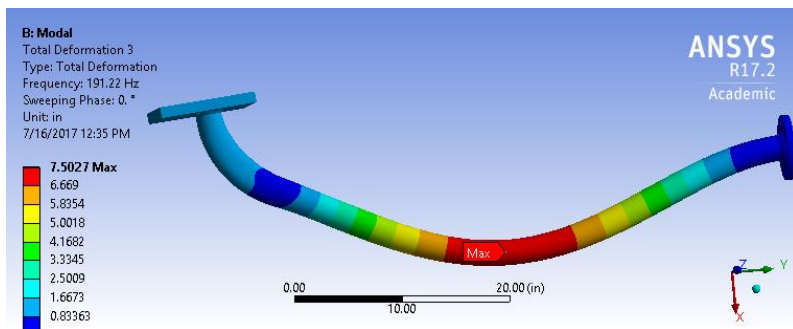
**Figure 163 The 3rd Mode for FPA, 2 Inch Diameter, CS, 48 Inches Long**
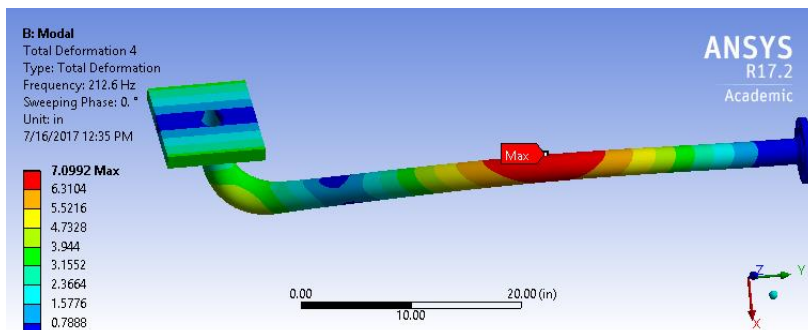
Figure 164 The 4th Mode for FPA, 2 Inch Diameter, CS, 48 Inches Long
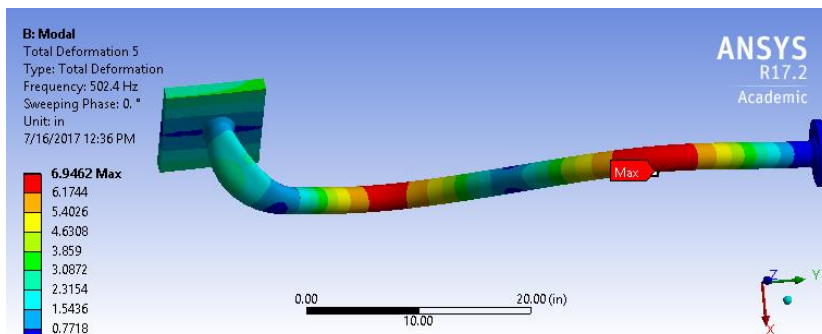
**Figure 165 The 5th Mode for FPA, 2 Inch Diameter, CS, 48 Inches Long**
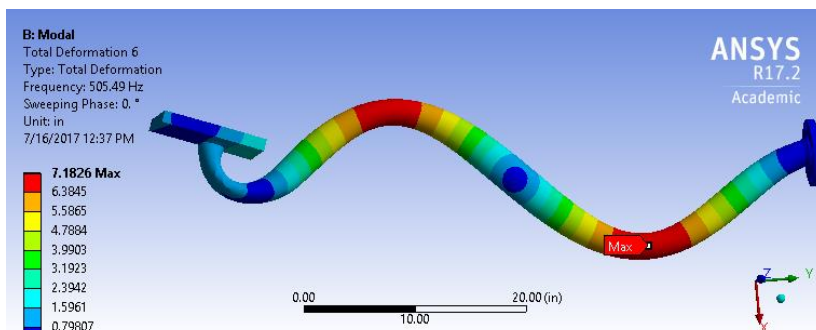
**Figure 166 The 6th Mode for FPA, 2 Inch Diameter, CS, 48 Inches Long**
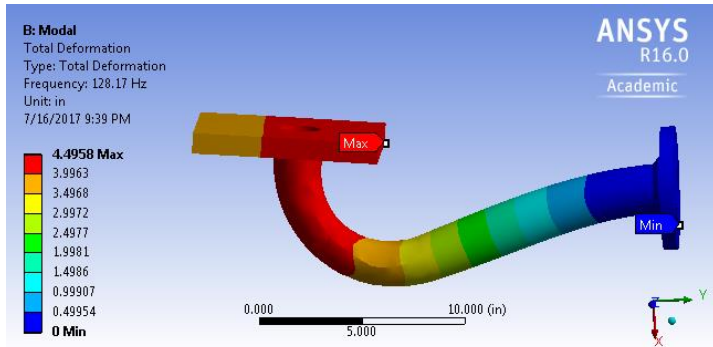
Figure 167 The 1st Mode for FPA, 2 Inch Diameter, SS, 12 Inches Long
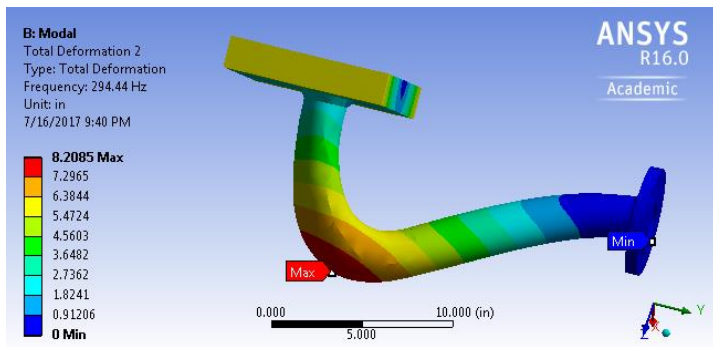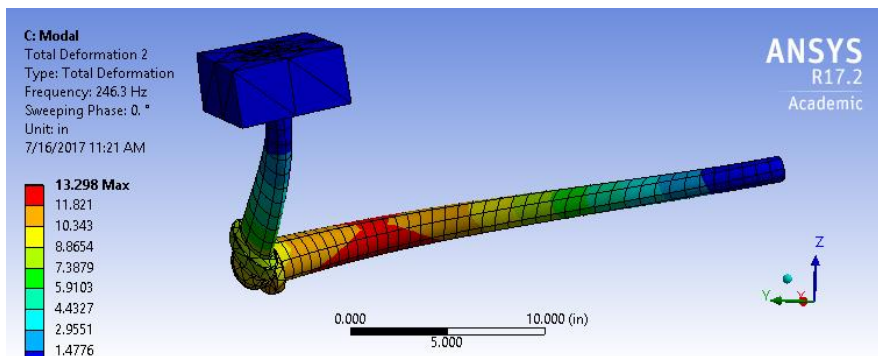

**Figure 168 The 2nd Mode for FPA, 2 Inch Diameter, SS, 12 Inches Long**
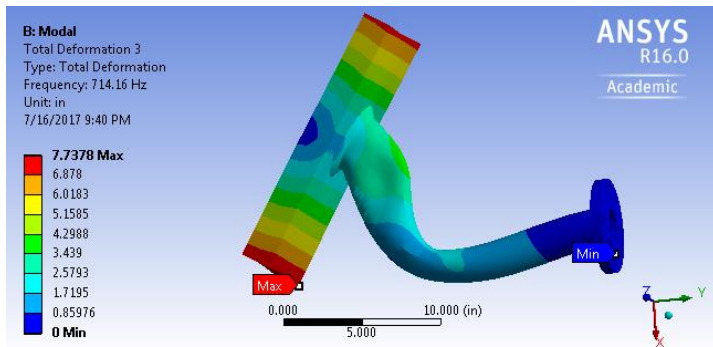
Figure 169 The 3rd Mode for FPA, 2 Inch Diameter, SS, 12 Inches Long
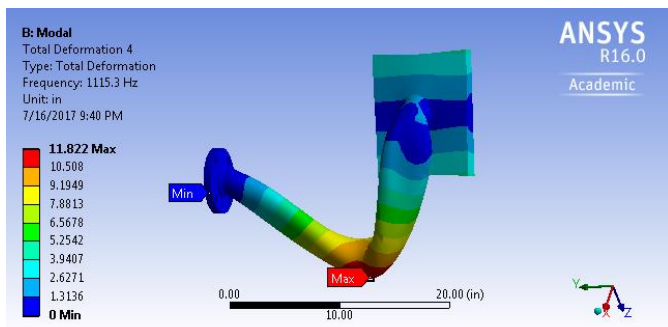
Figure 170 The 4th Mode for FPA, 2 Inch Diameter, SS, 12 Inches Long

113
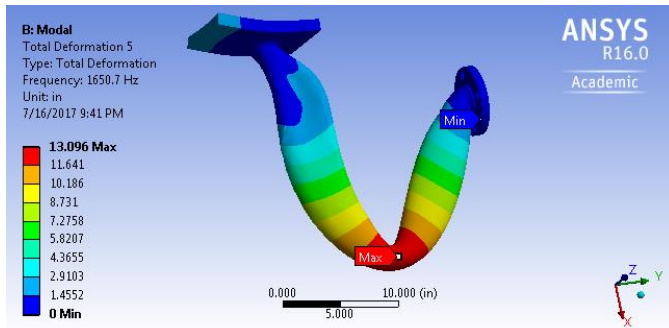
Figure 171 The 5th Mode for FPA, 2 Inch Diameter, SS, 12 Inches Long
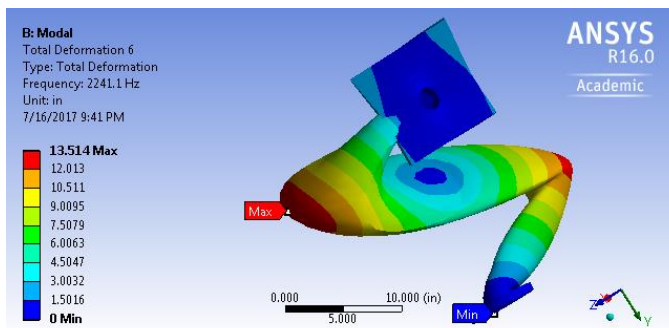
Figure 172 The 6th Mode for FPA, 2 Inch Diameter, SS, 12 Inches Long
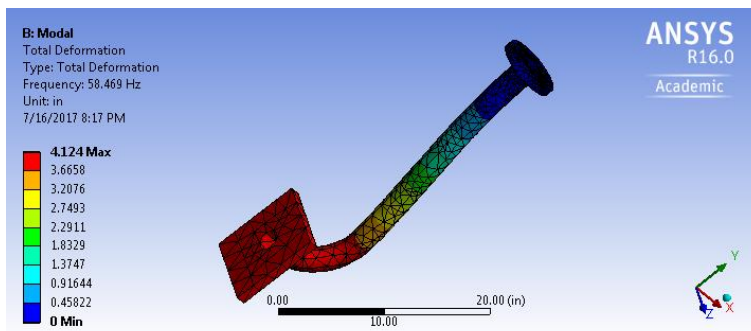
Figure 173 The 1st Mode for FPA, 2 Inch Diameter, SS, 24 Inches Long
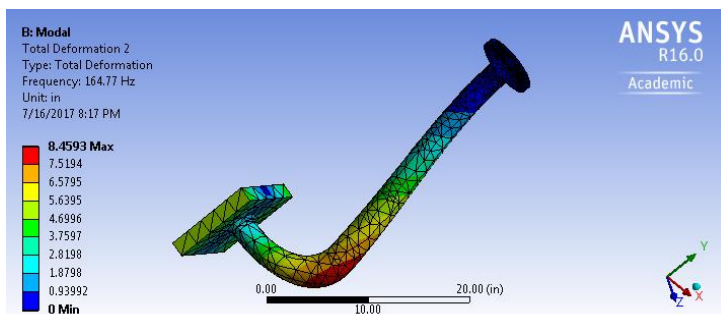
Figure 174 The 2nd Mode for FPA, 2 Inch Diameter, SS, 24 Inches Long

114

Figure 175 The 3rd Mode for FPA, 2 Inch Diameter, SS, 24 Inches Long
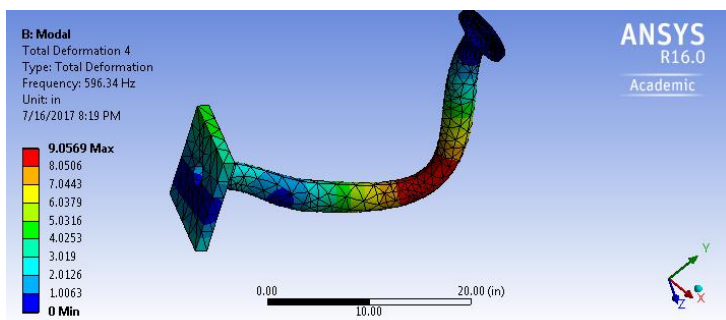
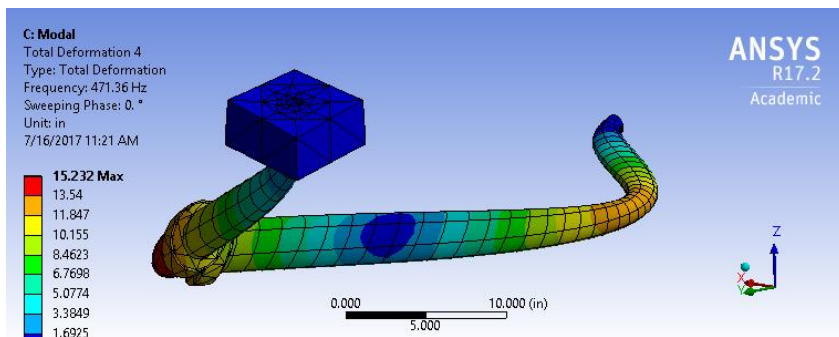

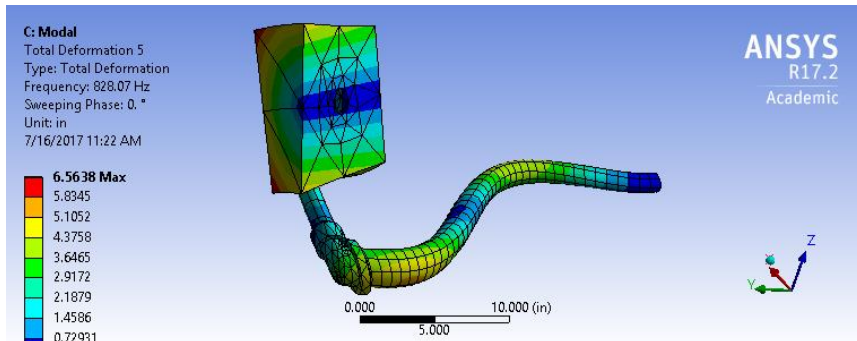**Figure 176 The 4th Mode for FPA, 2 Inch Diameter, SS, 24 Inches Long**
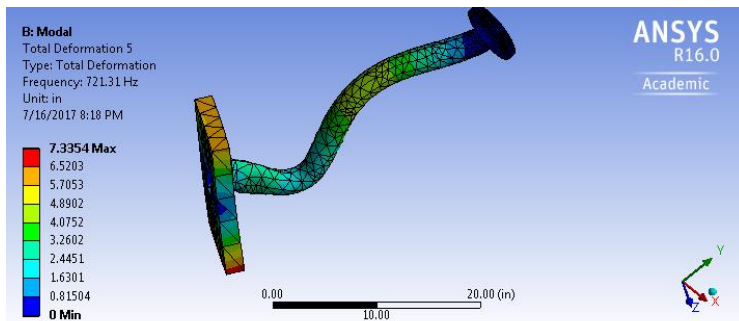
**Figure 177 The 5th Mode for FPA, 2 Inch Diameter, SS, 24 Inches Long**
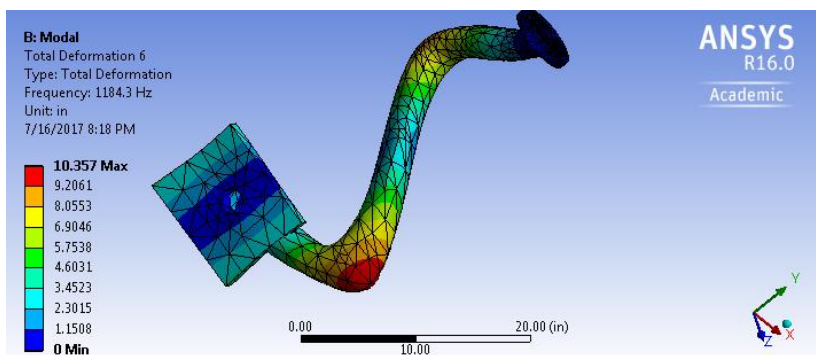
**Figure 178 The 6th Mode for FPA, 2 Inch Diameter, SS, 24 Inches Long**

115

Figure 179 The 1st Mode for FPA, 2 Inch Diameter, SS, 36 Inches Long
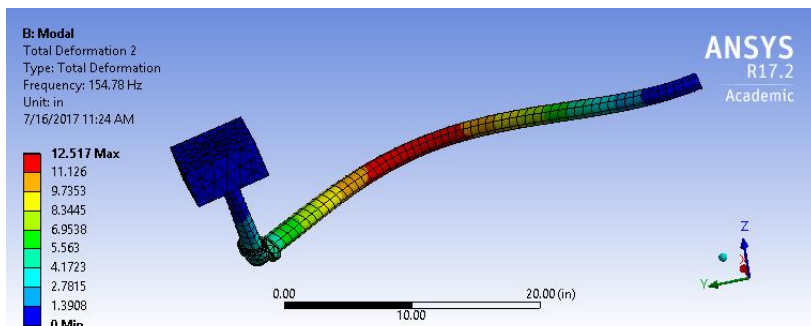

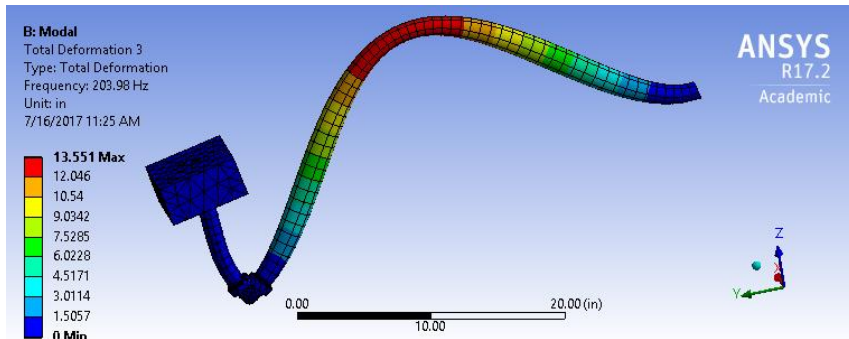**Figure 180 The 2nd Mode for FPA, 2 Inch Diameter, SS, 36 Inches Long**

**Figure 181 The 3rd Mode for FPA, 2 Inch Diameter, SS, 36 Inches Long**

Figure 182 The 4th Mode for FPA, 2 Inch Diameter, SS, 36 Inches Long
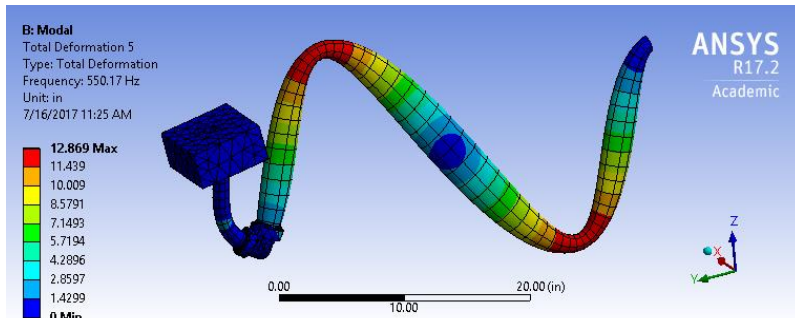
116

Figure 183 The 5th Mode for FPA, 2 Inch Diameter, SS, 36 Inches Long

Figure 184 The 6th Mode for FPA, 2 Inch Diameter, SS, 36 Inches Long

Figure 185 The 1st Mode for FPA, 2 Inch Diameter, SS, 48 Inches Long

Figure 186 The 2nd Mode for FPA, 2 Inch Diameter, SS, 48 Inches Long

117

Figure 187 The 3rd Mode for FPA, 2 Inch Diameter, SS, 48 Inches Long

Figure 188 The 4th Mode for FPA, 2 Inch Diameter, SS, 48 Inches Long

Figure 189 The 5th Mode for FPA, 2 Inch Diameter, SS, 48 Inches Long
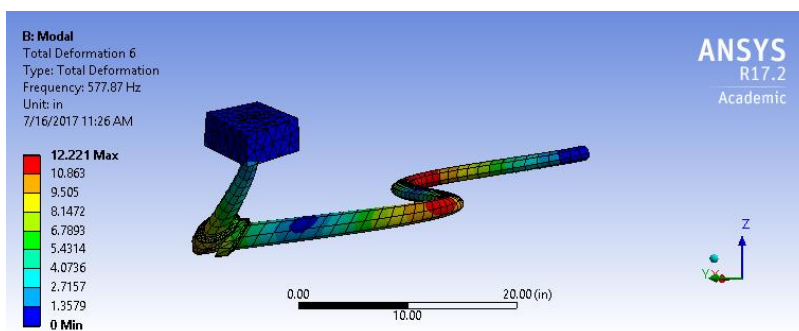

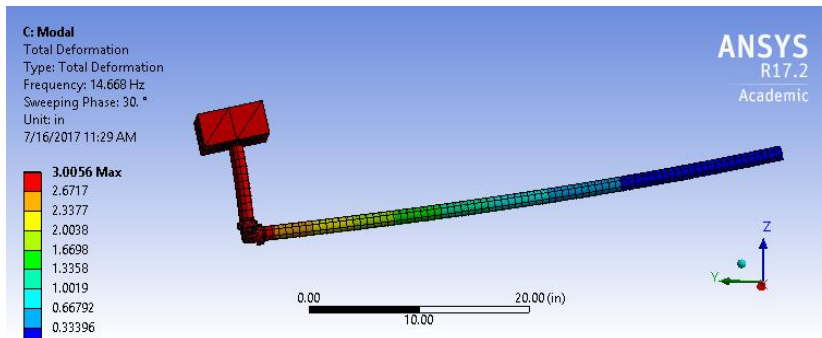**Figure 190 The 6th Mode for FPA, 2 Inch Diameter, SS, 48 Inches Long**

Figure 191 The 1st Mode for SWPA, 1 Inch Diameter, CS, 12 Inches Long

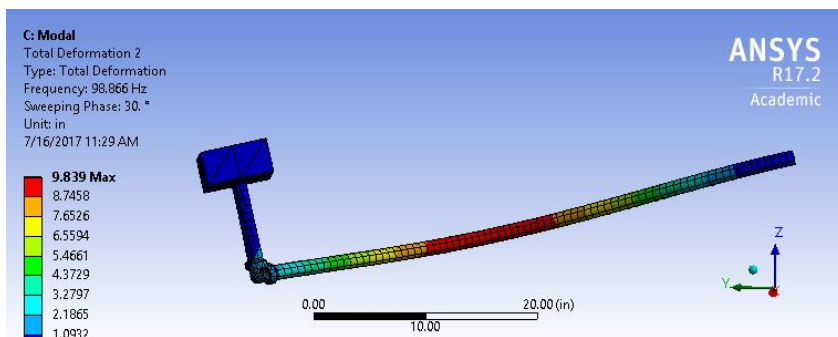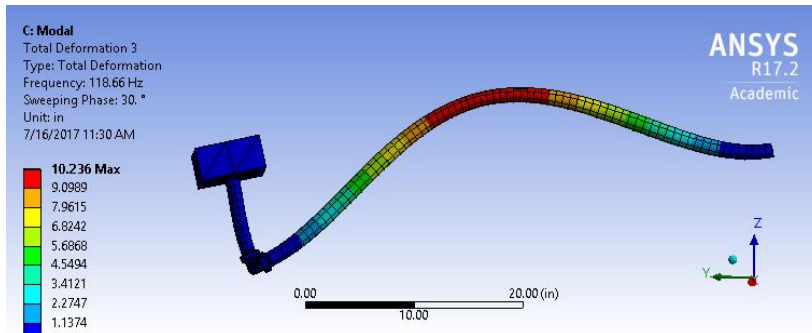**Figure 192 The 2nd Mode for SWPA, 1 Inch Diameter, CS, 12 Inches Long**

Figure 193 The 3rd Mode for SWPA, 1 Inch Diameter, CS, 12 Inches Long

Figure 194 The 4th Mode for SWPA, 1 Inch Diameter, CS, 12 Inches Long

Figure 195 The 5th Mode for SWPA, 1 Inch Diameter, CS, 12 Inches Long

Figure 196 The 6th Mode for SWPA, 1 Inch Diameter, CS, 12 Inches Long

Figure 197 The 1st Mode for SWPA, 1 Inch Diameter, CS, 24 Inches Long

Figure 198 The 2nd Mode for SWPA, 1 Inch Diameter, CS, 24 Inches Long

120
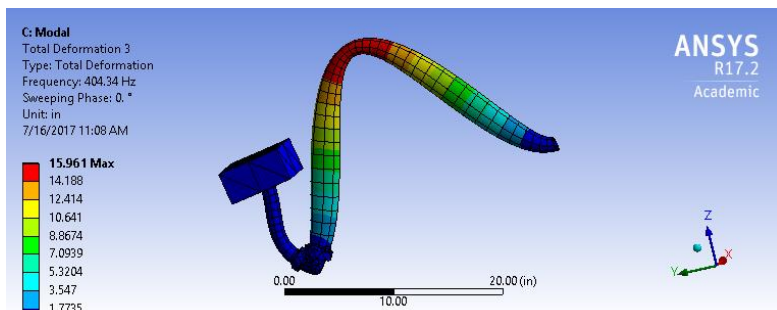
Figure 199 The 3rd Mode for SWPA, 1 Inch Diameter, CS, 24 Inches Long
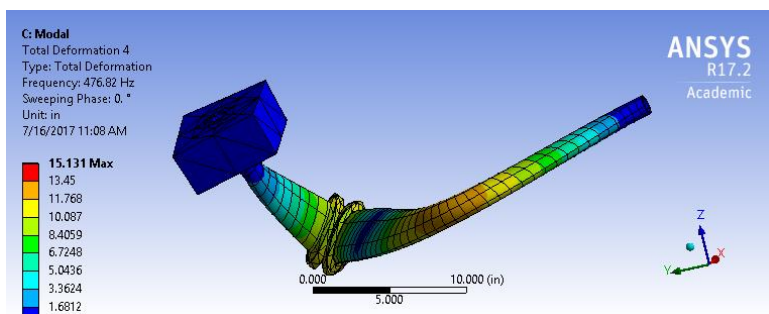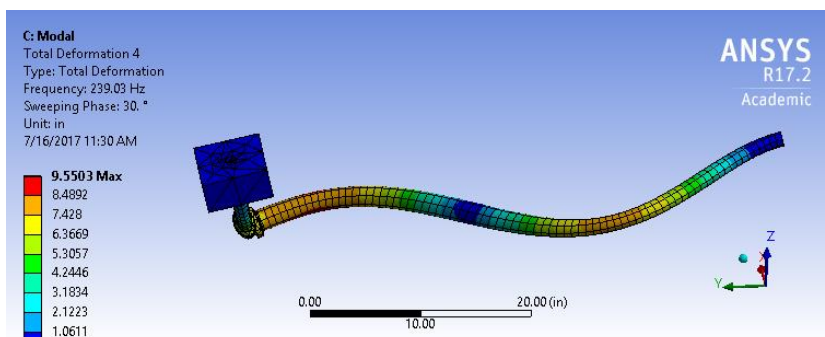

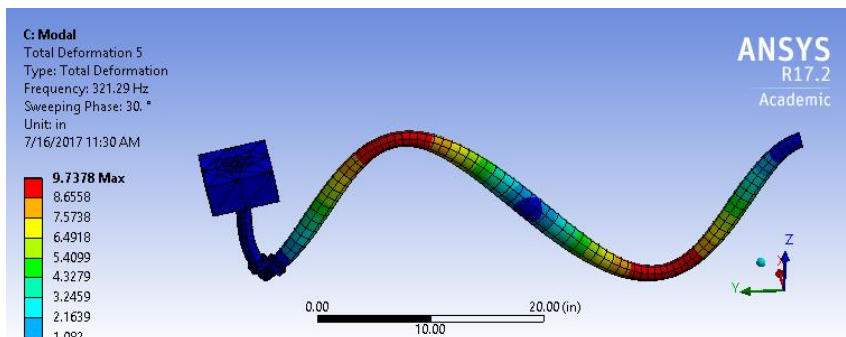**Figure 200 The 4th Mode for SWPA, 1 Inch Diameter, CS, 24 Inches Long**
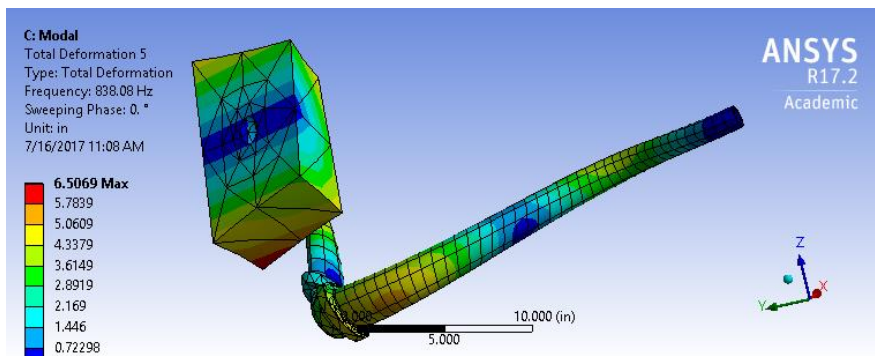
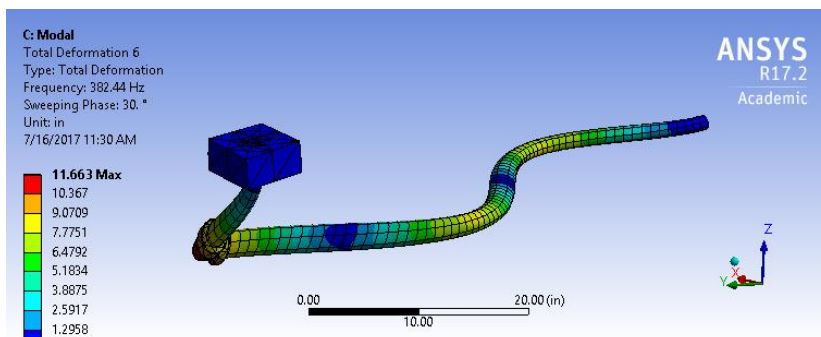**Figure 201 The 5th Mode for SWPA, 1 Inch Diameter, CS, 24 Inches Long**

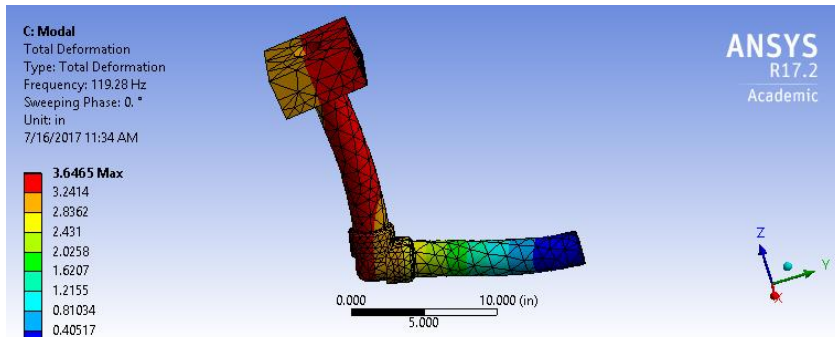**Figure 202 The 6th Mode for SWPA, 1 Inch Diameter, CS, 24 Inches Long**

121
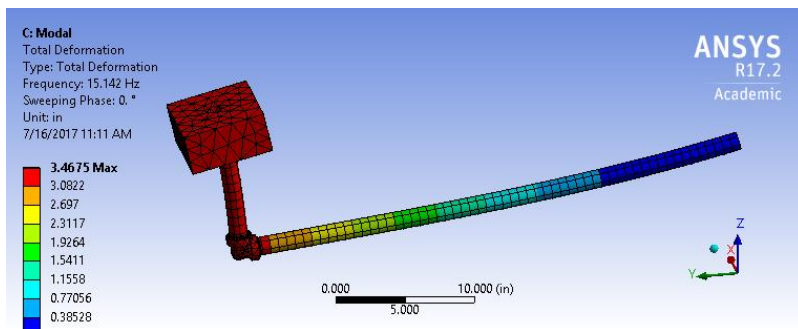
Figure 203 The 1st Mode for SWPA, 1 Inch Diameter, CS, 36 Inches Long

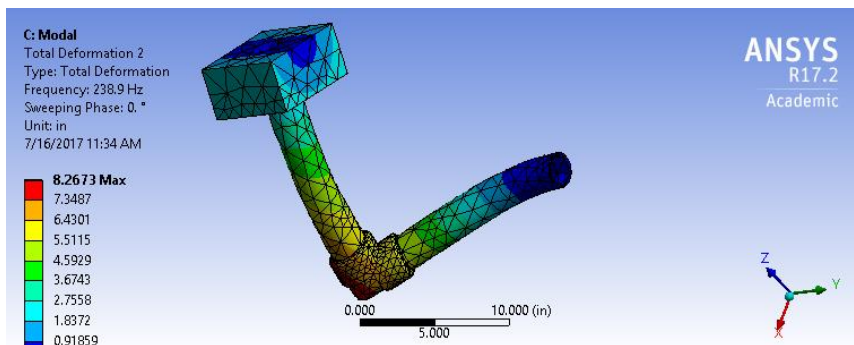**Figure 204 The 2nd Mode for SWPA, 1 Inch Diameter, CS, 36 Inches Long**
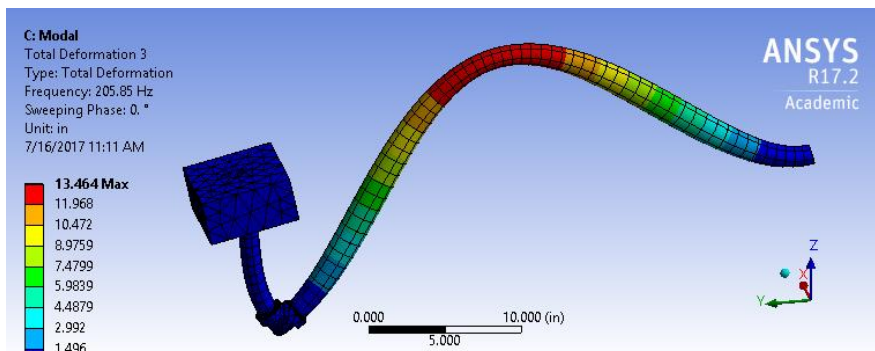
Figure 205 The 3rd Mode for SWPA, 1 Inch Diameter, CS, 36 Inches Long
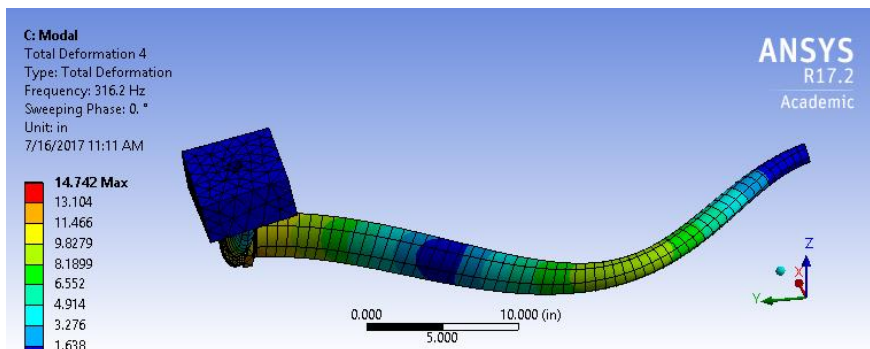
Figure 206 The 4th Mode for SWPA, 1 Inch Diameter, CS, 36 Inches Long

122

Figure 207 The 5th Mode for SWPA, 1 Inch Diameter, CS, 36 Inches Long

Figure 208 The 6th Mode for SWPA, 1 Inch Diameter, CS, 36 Inches Long

Figure 209 The 1st Mode for SWPA, 1 Inch Diameter, CS, 48 Inches Long

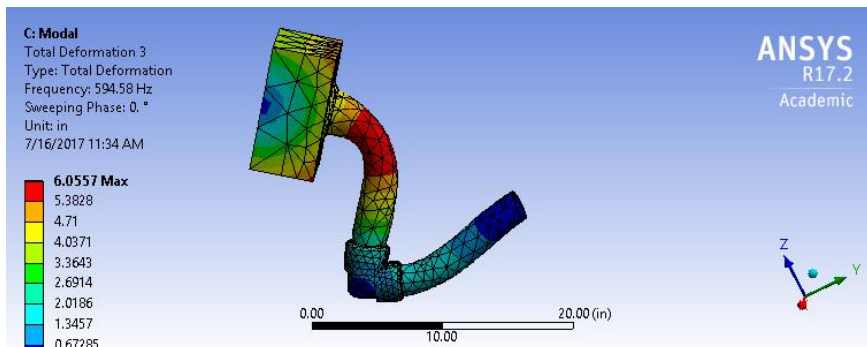**Figure 210 The 2nd Mode for SWPA, 1 Inch Diameter, CS, 48 Inches Long**
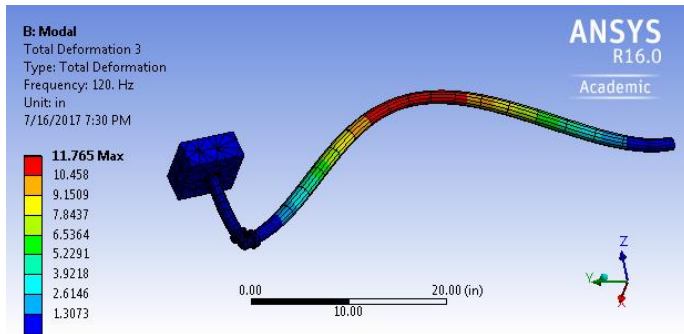
Figure 211 The 3rd Mode for SWPA, 1 Inch Diameter, CS, 48 Inches Long
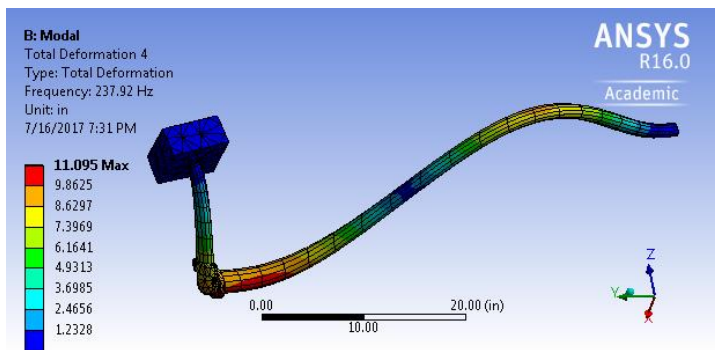
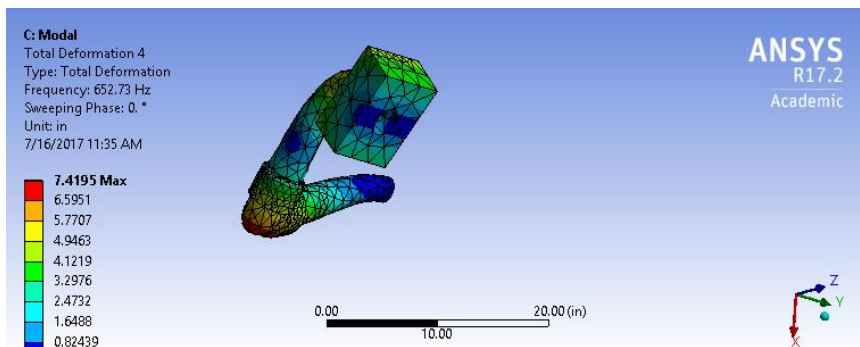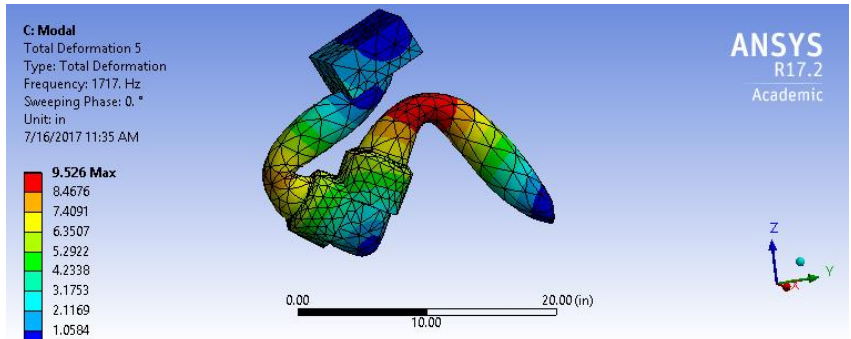**Figure 212 The 4th Mode for SWPA, 1 Inch Diameter, CS, 48 Inches Long**
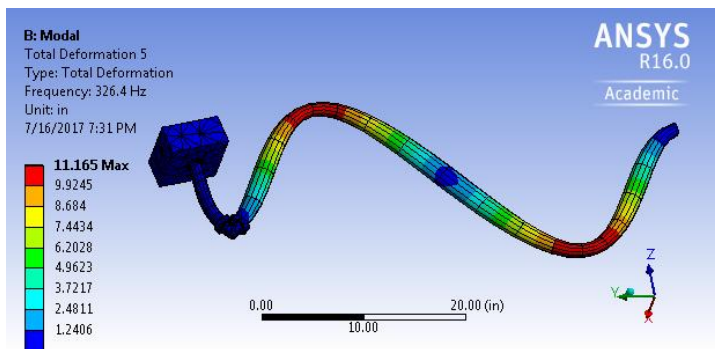
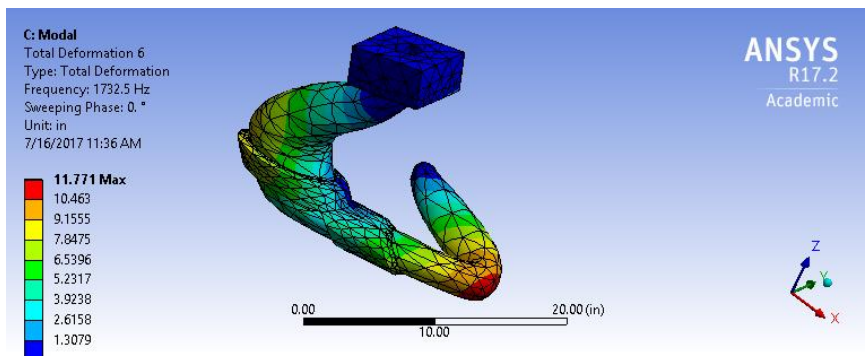**Figure 213 The 5th Mode for SWPA, 1 Inch Diameter, CS, 48 Inches Long**
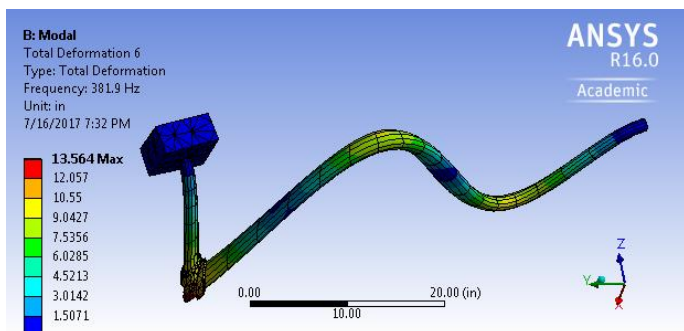
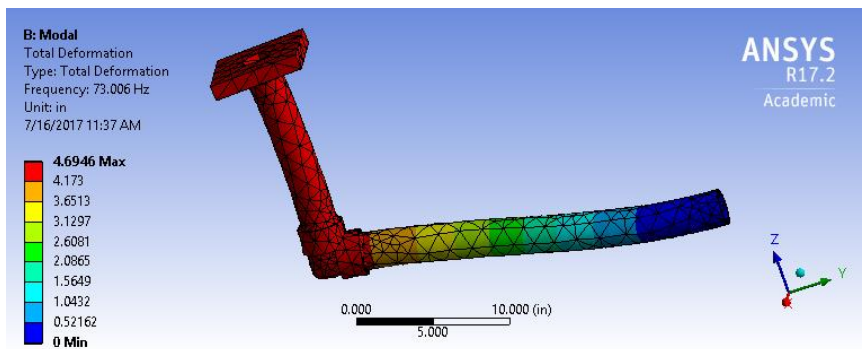**Figure 214 The 6th Mode for SWPA, 1 Inch Diameter, CS, 48 Inches Long**

124
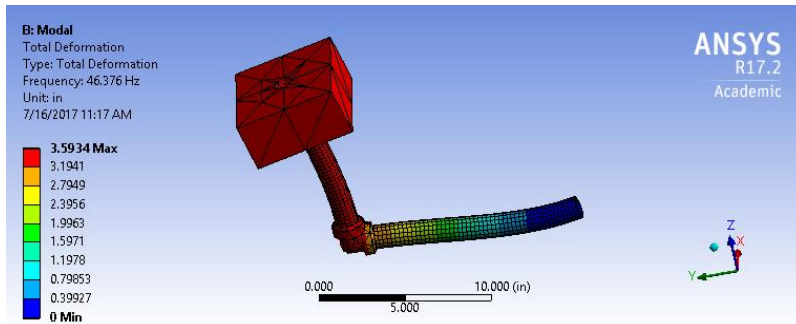
Figure 215 The 1st Mode for SWPA, 1 Inch Diameter, SS, 12 Inches Long

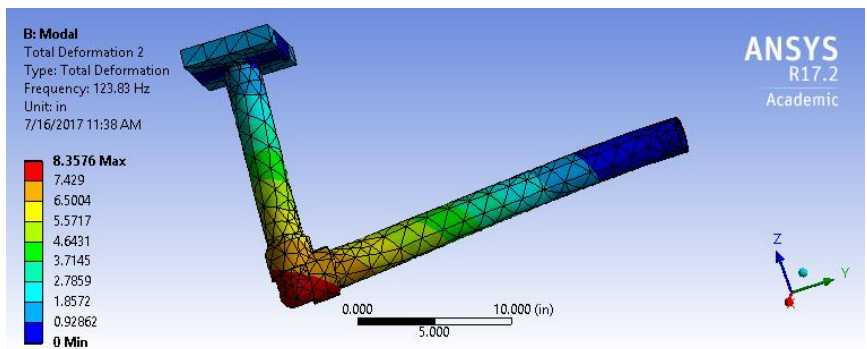**Figure 216 The 2nd Mode for SWPA, 1 Inch Diameter, SS, 12 Inches Long**
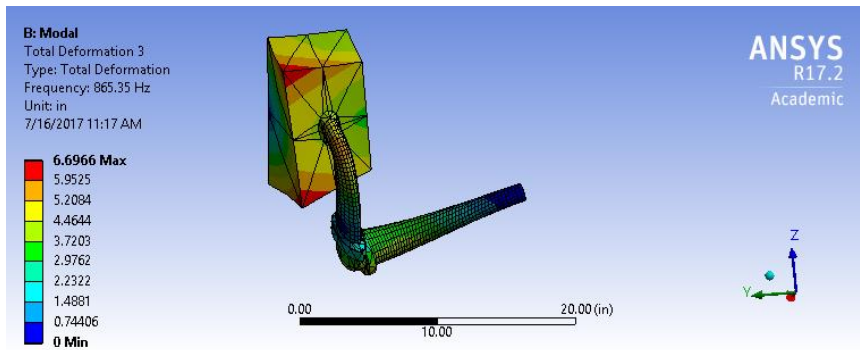
Figure 217 The 3rd Mode for SWPA, 1 Inch Diameter, SS, 12 Inches Long
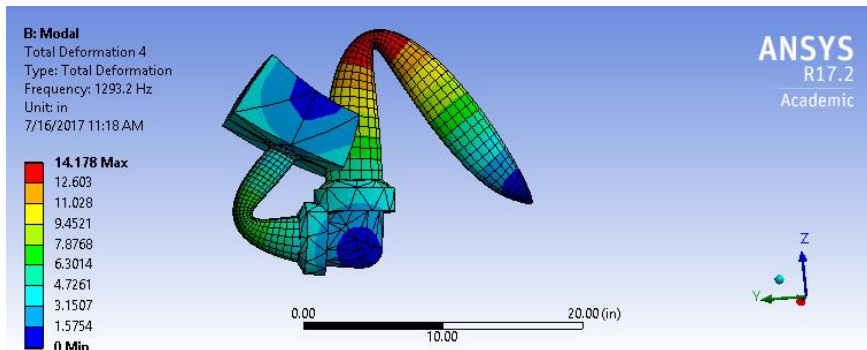
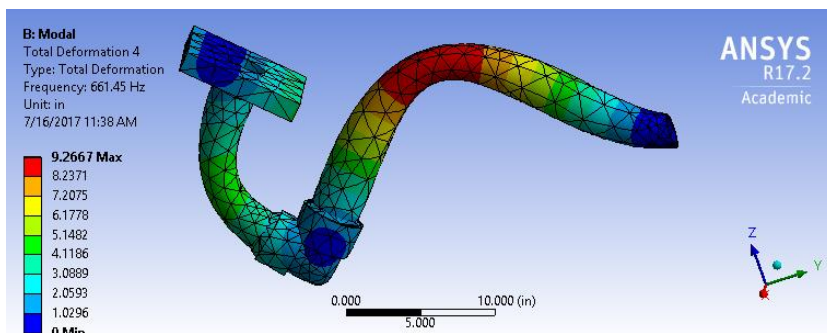**Figure 218 The 4th Mode for SWPA, 1 Inch Diameter, SS, 12 Inches Long**
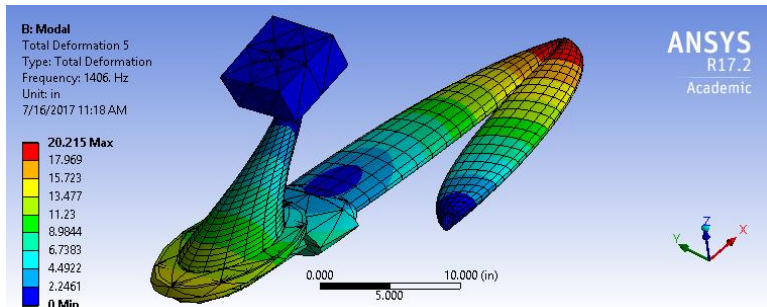
Figure 219 The 5th Mode for SWPA, 1 Inch Diameter, SS, 12 Inches Long
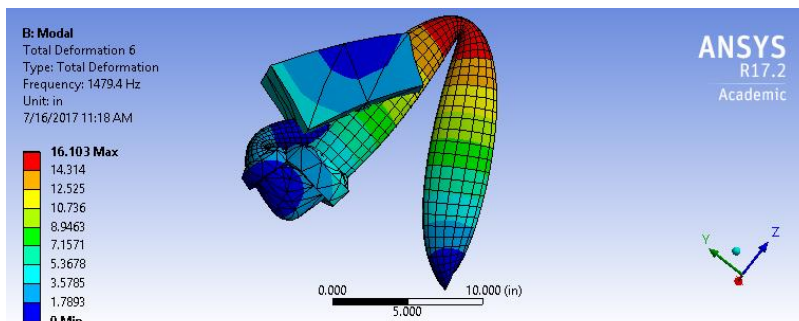
Figure 220 The 6th Mode for SWPA, 1 Inch Diameter, SS, 12 Inches Long
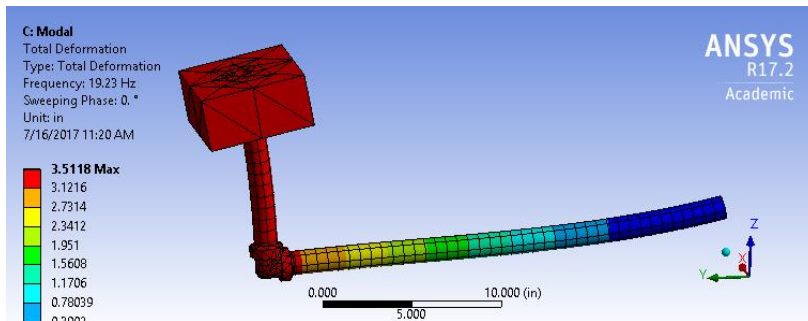
Figure 221 The 1st Mode for SWPA, 1 Inch Diameter, SS, 24 Inches Long

Figure 222 The 2nd Mode for SWPA, 1 Inch Diameter, SS, 24 Inches Long
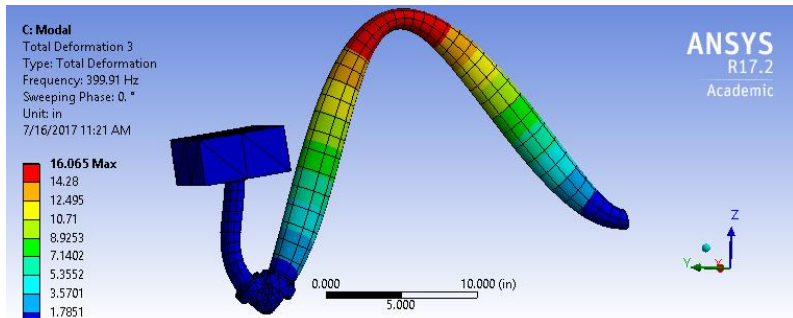
Figure 223 The 3rd Mode for SWPA, 1 Inch Diameter, SS, 24 Inches Long

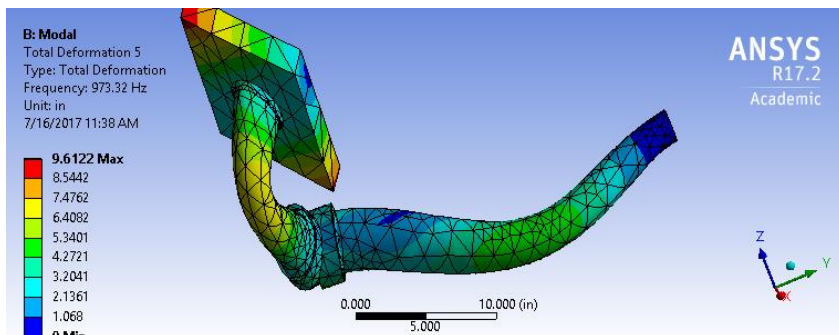**Figure 224 The 4th Mode for SWPA, 1 Inch Diameter, SS, 24 Inches Long**

Figure 225 The 5th Mode for SWPA, 1 Inch Diameter, SS, 24 Inches Long
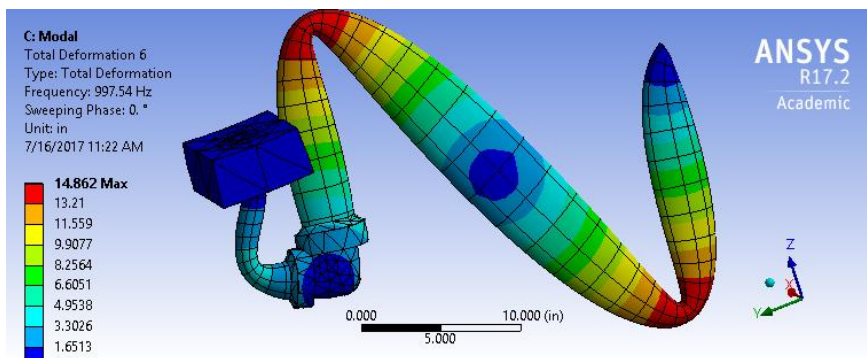
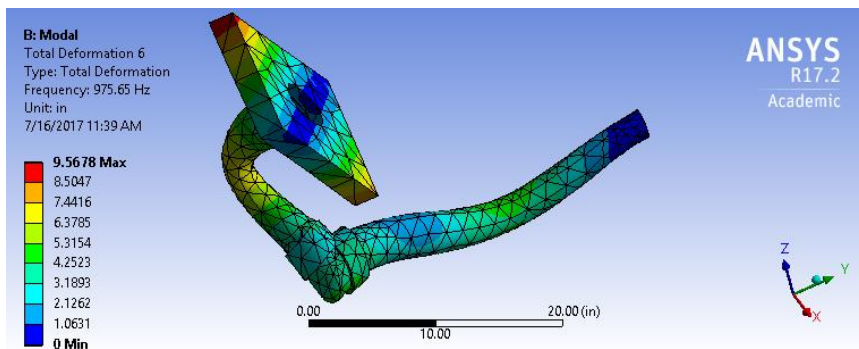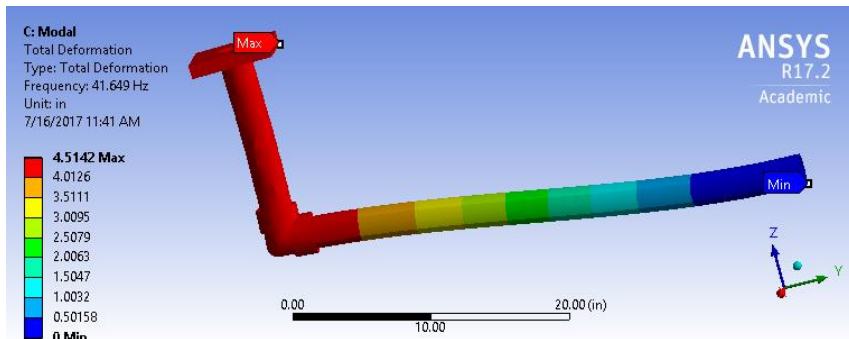**Figure 226 The 6th Mode for SWPA, 1 Inch Diameter, SS, 24 Inches Long**
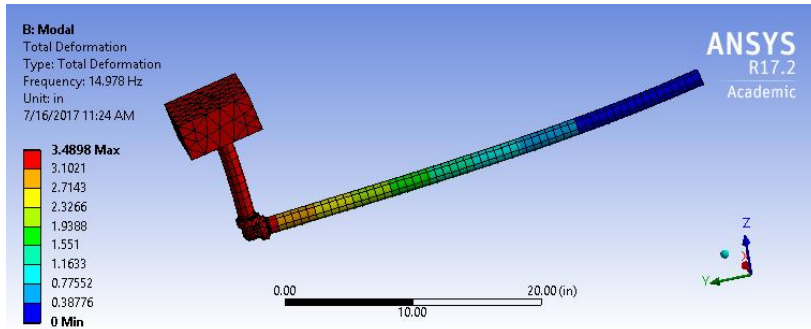
Figure 227 The 1st Mode for SWPA, 1 Inch Diameter, SS, 36 Inches Long

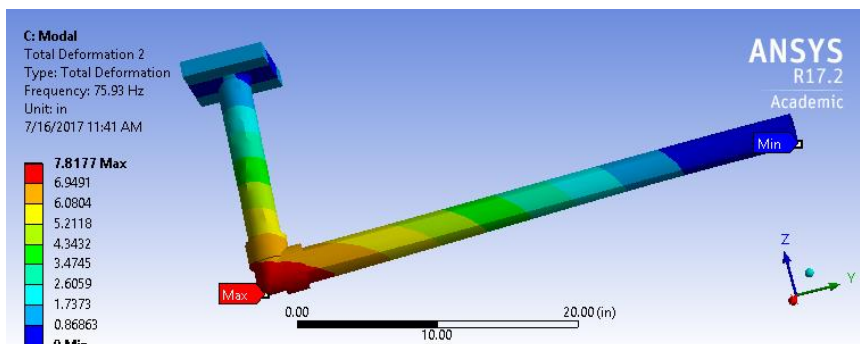**Figure 228 The 2nd Mode for SWPA, 1 Inch Diameter, SS, 36 Inches Long**

Figure 229 The 3rd Mode for SWPA, 1 Inch Diameter, SS, 36 Inches Long
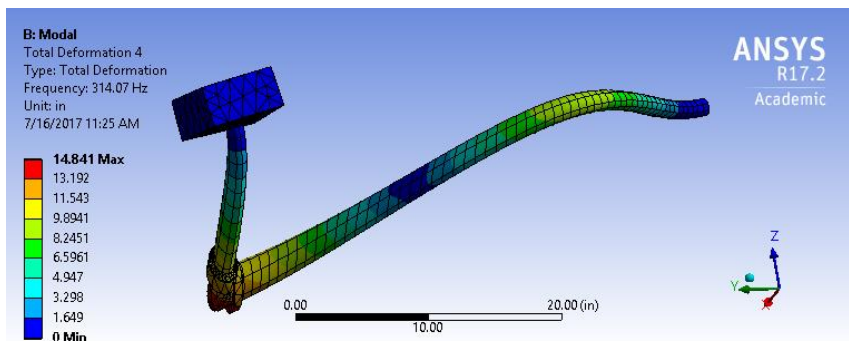
Figure 230 The 4th Mode for SWPA, 1 Inch Diameter, SS, 36 Inches Long

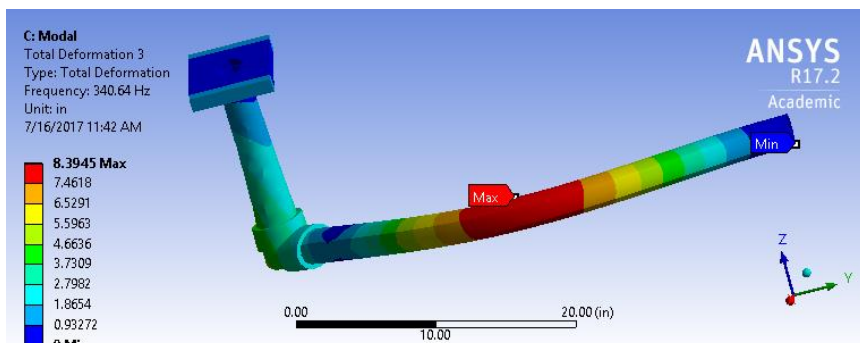**Figure 231 The 5th Mode for SWPA, 1 Inch Diameter, SS, 36 Inches Long**

Figure 232 The 6th Mode for SWPA, 1 Inch Diameter, SS, 36 Inches Long

Figure 233 The 1st Mode for SWPA, 1 Inch Diameter, SS, 48 Inches Long

Figure 234 The 2nd Mode for SWPA, 1 Inch Diameter, SS, 48 Inches Long

129

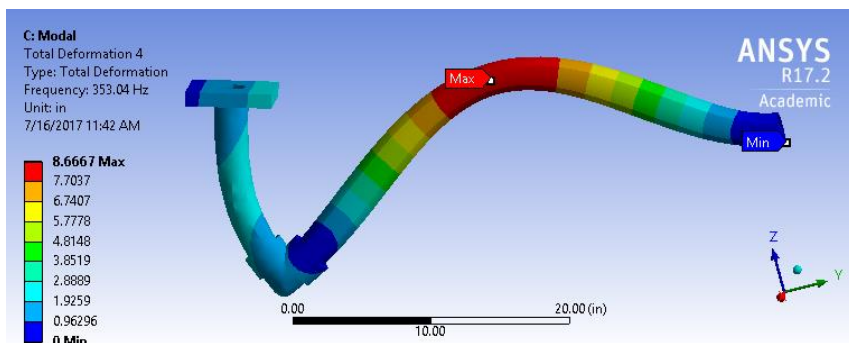**Figure 235 The 3rd Mode for SWPA, 1 Inch Diameter, SS, 48 Inches Long**

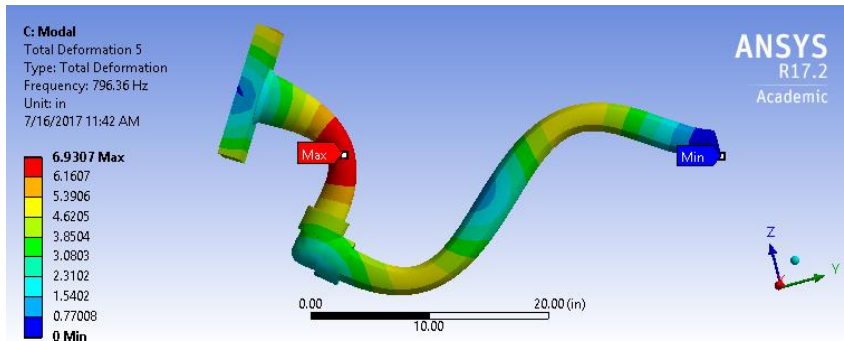**Figure 236 The 4th Mode for SWPA, 1 Inch Diameter, SS, 48 Inches Long**

Figure 237 The 5th Mode for SWPA, 1 Inch Diameter, SS, 48 Inches Long
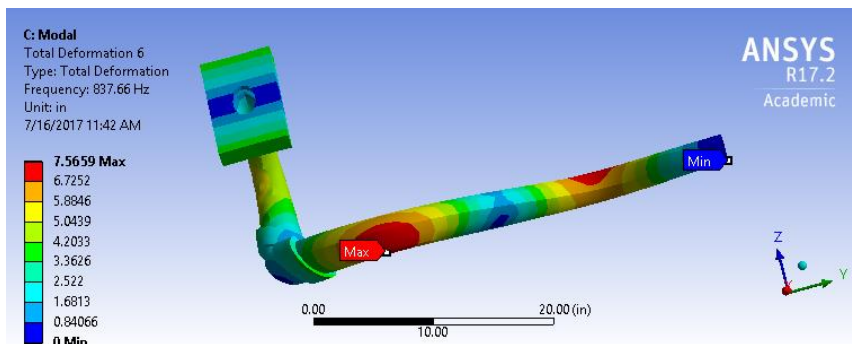

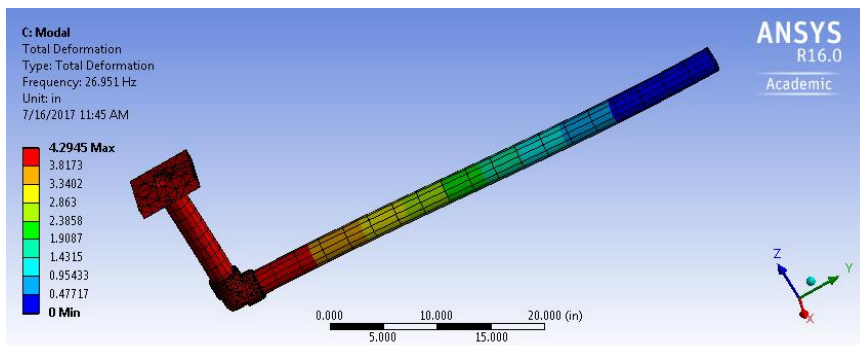**Figure 238 The 6th Mode for SWPA, 1 Inch Diameter, SS, 48 Inches Long**

Figure 239 The 1st Mode for SWPA, 2 Inch Diameter, CS, 12 Inches Long

Figure 240 The 2nd Mode for SWPA, 2 Inch Diameter, CS, 12 Inches Long

Figure 241 The 3rd Mode for SWPA, 2 Inch Diameter, CS, 12 Inches Long

Figure 242 The 4th Mode for SWPA, 2 Inch Diameter, CS, 12 Inches Long

131

Figure 243 The 5th Mode for SWPA, 2 Inch Diameter, CS, 12 Inches Long

Figure 244 The 6th Mode for SWPA, 2 Inch Diameter, CS, 12 Inches Long

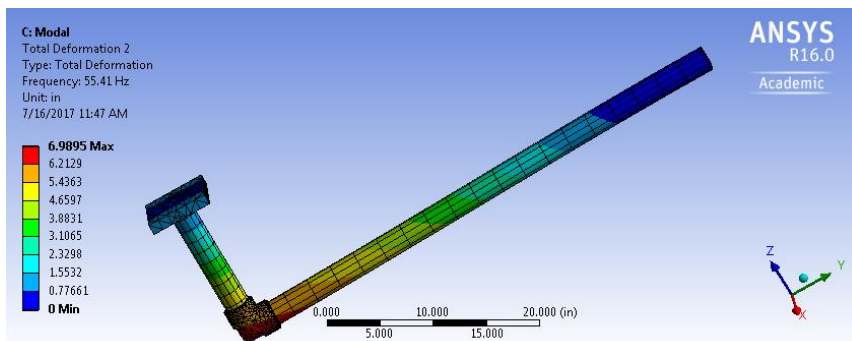**Figure 245 The 1st Mode for SWPA, 2 Inch Diameter, CS, 24 Inches Long**

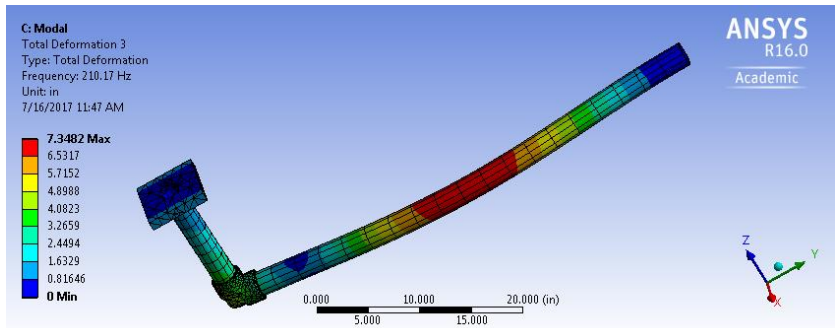**Figure 246 The 2nd Mode for SWPA, 2 Inch Diameter, CS, 24 Inches Long**
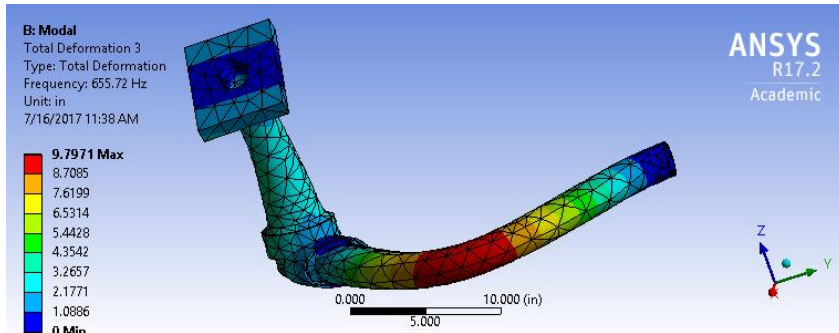
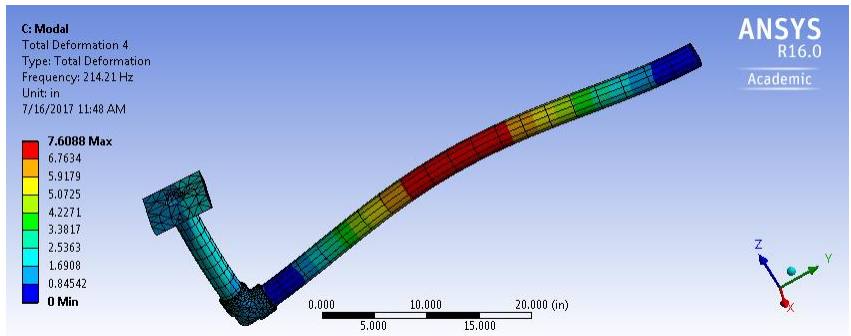**Figure 247 The 3rd Mode for SWPA, 2 Inch Diameter, CS, 24 Inches Long**

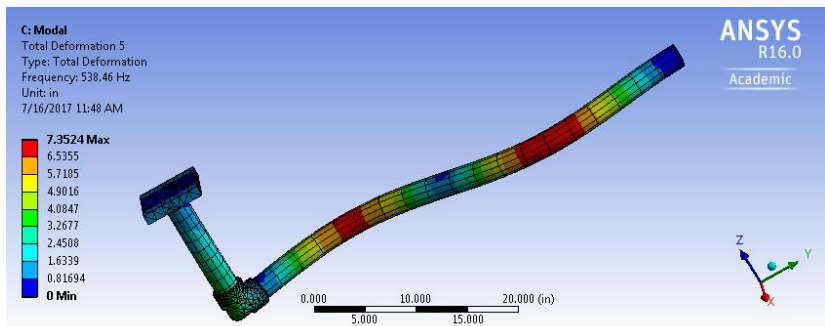**Figure 248 The 4th Mode for SWPA, 2 Inch Diameter, CS, 24 Inches Long**

Figure 249 The 5th Mode for SWPA, 2 Inch Diameter, CS, 24 Inches Long

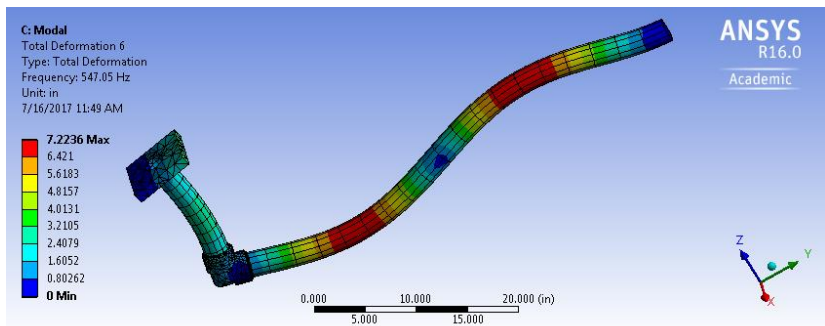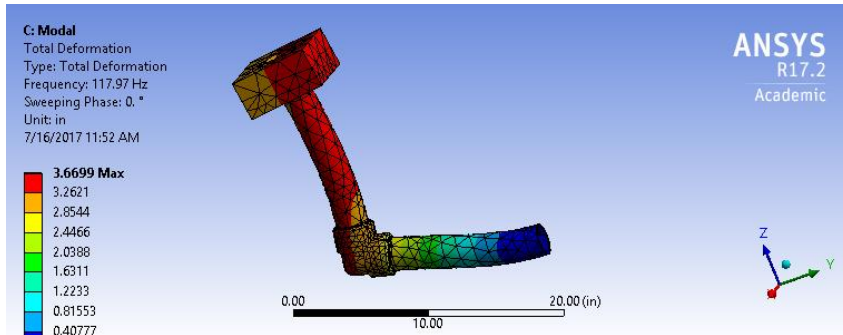**Figure 250 The 6th Mode for SWPA, 2 Inch Diameter, CS, 24 Inches Long**

Figure 251 The 1st Mode for SWPA, 2 Inch Diameter, CS, 36 Inches Long

Figure 252 The 2nd Mode for SWPA, 2 Inch Diameter, CS, 36 Inches Long

Figure 253 The 3rd Mode for SWPA, 2 Inch Diameter, CS, 36 Inches Long

Figure 254 The 4th Mode for SWPA, 2 Inch Diameter, CS, 36 Inches Long

134

Figure 255 The 5th Mode for SWPA, 2 Inch Diameter, CS, 36 Inches Long

Figure 256 The 6th Mode for SWPA, 2 Inch Diameter, CS, 36 Inches Long

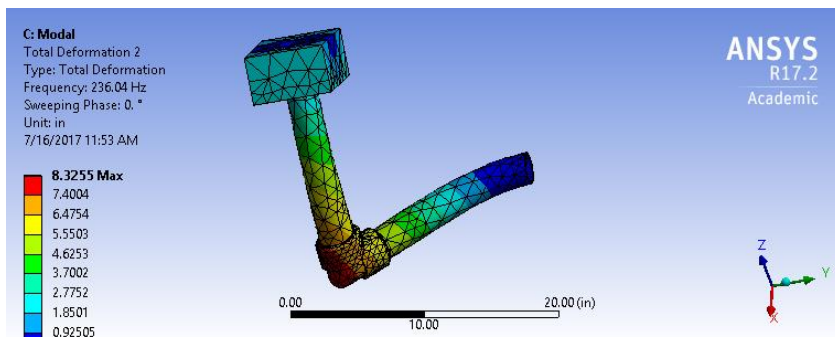**Figure 257 The 1st Mode for SWPA, 2 Inch Diameter, CS, 48 Inches Long**

Figure 258 The 2nd Mode for SWPA, 2 Inch Diameter, CS, 48 Inches Long

135

Figure 259 The 3rd Mode for SWPA, 2 Inch Diameter, CS, 48 Inches Long

Figure 260 The 4th Mode for SWPA, 2 Inch Diameter, CS, 48 Inches Long

Figure 261 The 5th Mode for SWPA, 2 Inch Diameter, CS, 48 Inches Long

Figure 262 The 6th Mode for SWPA, 2 Inch Diameter, CS, 48 Inches Long

136

Figure 263 The 1st Mode for SWPA, 2 Inch Diameter, SS, 12 Inches Long

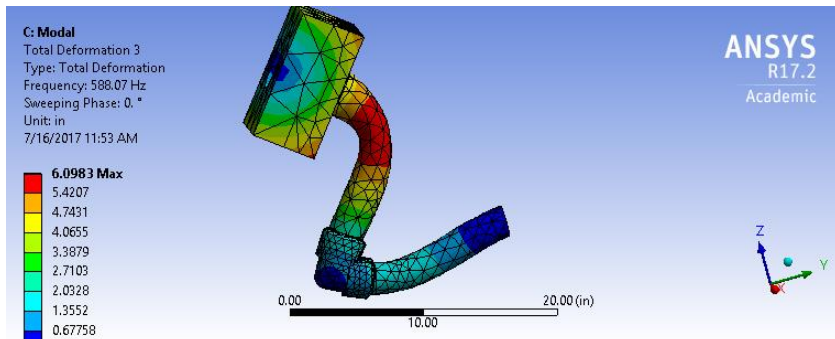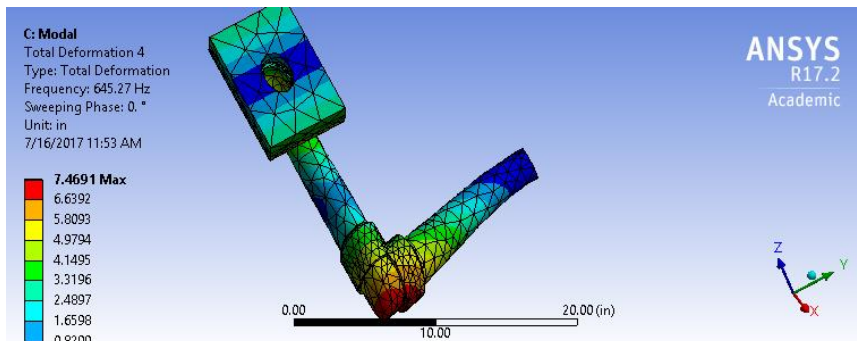**Figure 264 The 2nd Mode for SWPA, 2 Inch Diameter, SS, 12 Inches Long**

Figure 265 The 3rd Mode for SWPA, 2 Inch Diameter, SS, 12 Inches Long

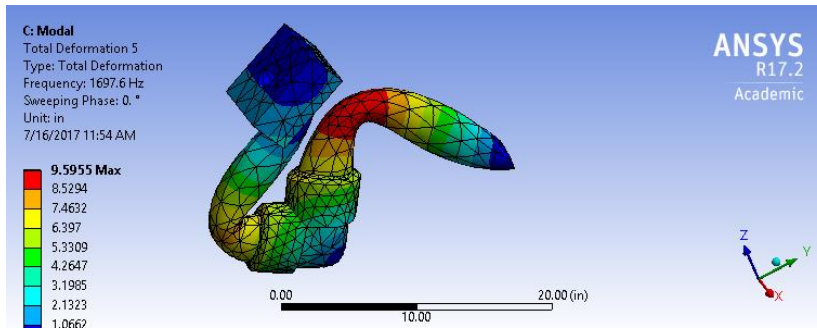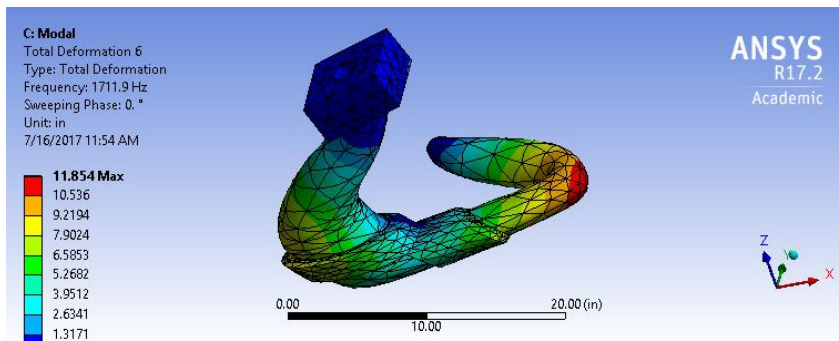**Figure 266 The 4th Mode for SWPA, 2 Inch Diameter, SS, 12 Inches Long**

137

Figure 267 The 5th Mode for SWPA, 2 Inch Diameter, SS, 12 Inches Long

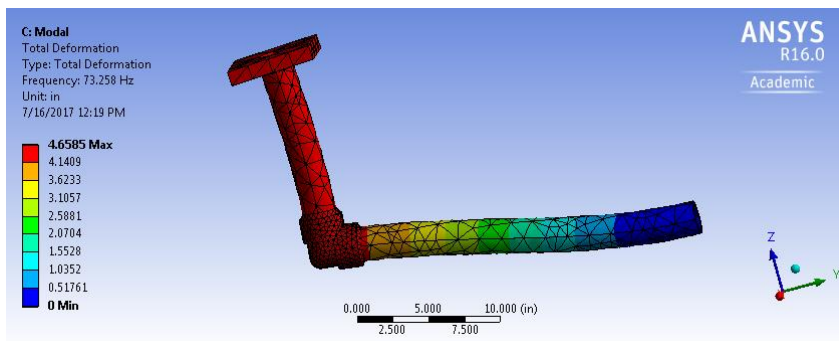**Figure 268 The 6th Mode for SWPA, 2 Inch Diameter, SS, 12 Inches Long**

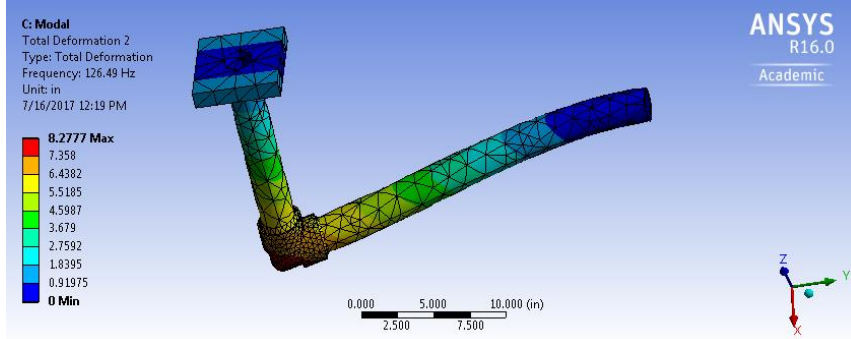**Figure 269 The 1st Mode for SWPA, 2 Inch Diameter, SS, 24 Inches Long**

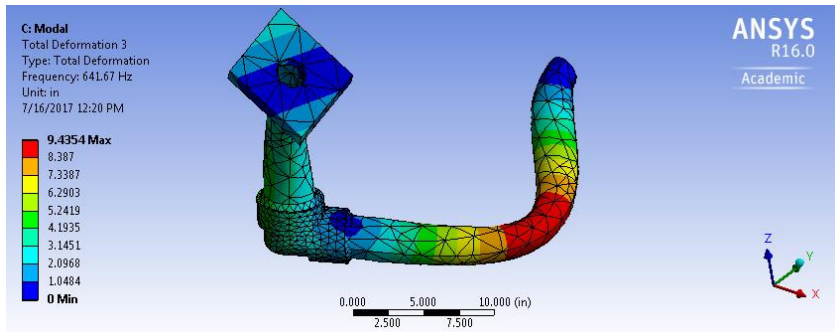**Figure 270 The 2nd Mode for SWPA, 2 Inch Diameter, SS, 24 Inches Long**

138

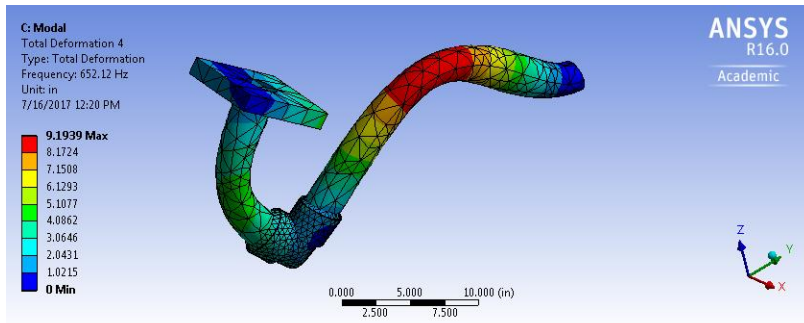**Figure 271 The 3rd Mode for SWPA, 2 Inch Diameter, SS, 24 Inches Long**

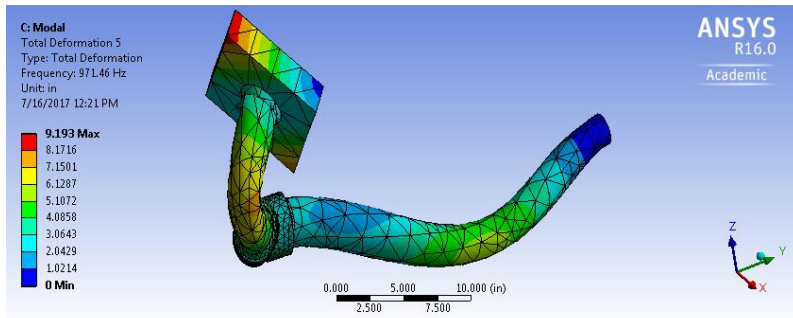**Figure 272 The 4th Mode for SWPA, 2 Inch Diameter, SS, 24 Inches Long**

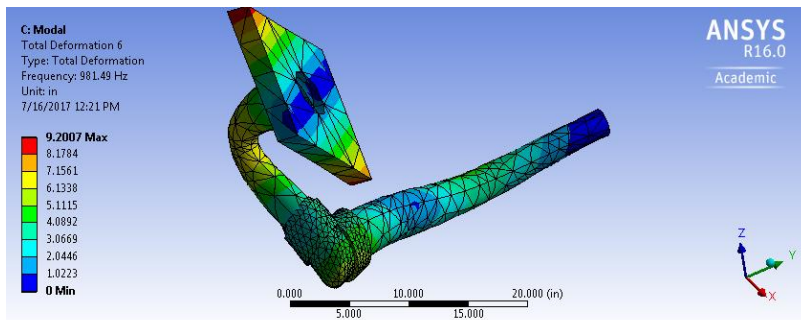**Figure 273 The 5th Mode for SWPA, 2 Inch Diameter, SS, 24 Inches Long**

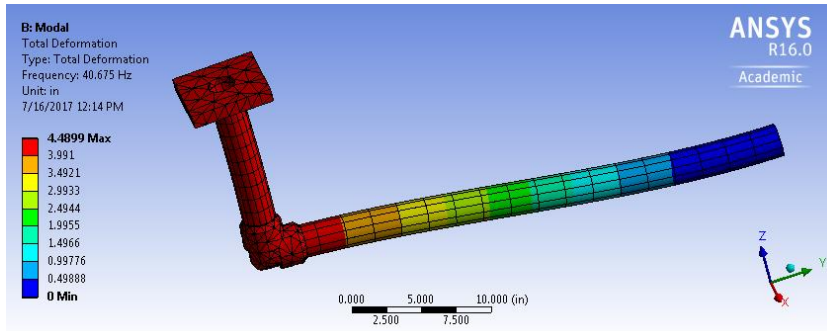**Figure 274 The 6th Mode for SWPA, 2 Inch Diameter, SS, 24 Inches Long**

Figure 275 The 1st Mode for SWPA, 2 Inch Diameter, SS, 36 Inches Long

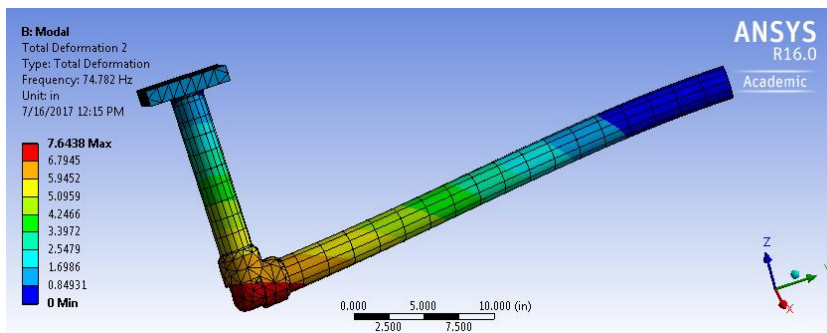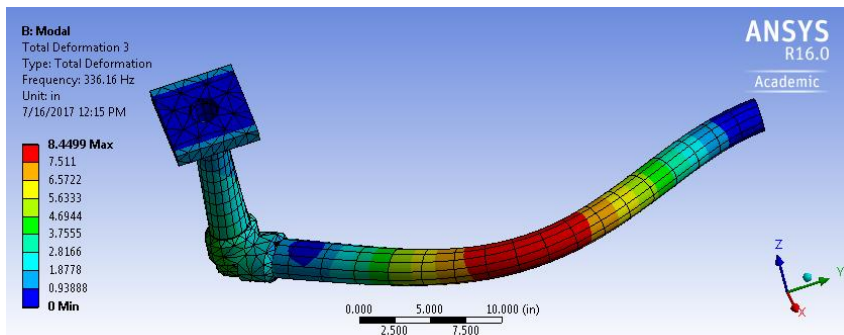**Figure 276 The 2nd Mode for SWPA, 2 Inch Diameter, SS, 36 Inches Long**

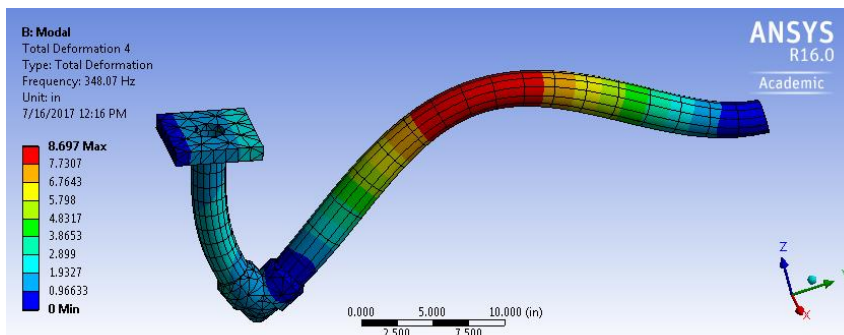**Figure 277 The 3rd Mode for SWPA, 2 Inch Diameter, SS, 36 Inches Long**

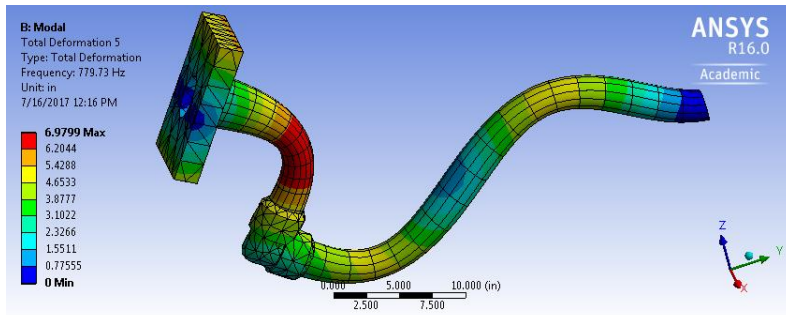**Figure 278 The 4th Mode for SWPA, 2 Inch Diameter, SS, 36 Inches Long**

140

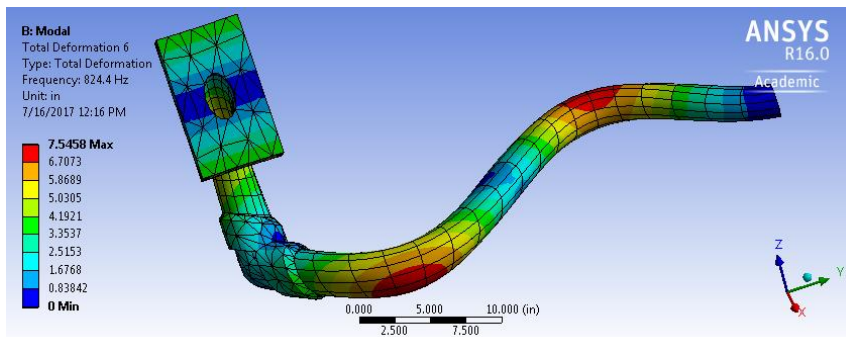**Figure 279 The 5th Mode for SWPA, 2 Inch Diameter, SS, 36 Inches Long**

Figure 280 The 6th Mode for SWPA, 2 Inch Diameter, SS, 36 Inches Long

Figure 281 The 1st Mode for SWPA, 2 Inch Diameter, SS, 48 Inches Long

Figure 282 The 2nd Mode for SWPA, 2 Inch Diameter, SS, 48 Inches Long

Figure 283 The 3rd Mode for SWPA, 2 Inch Diameter, SS, 48 Inches Long

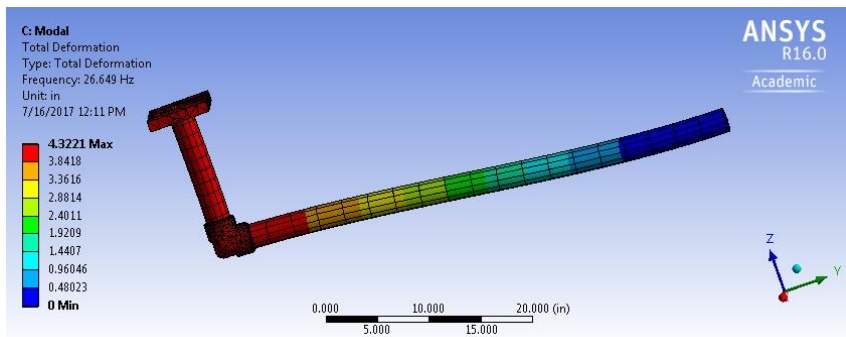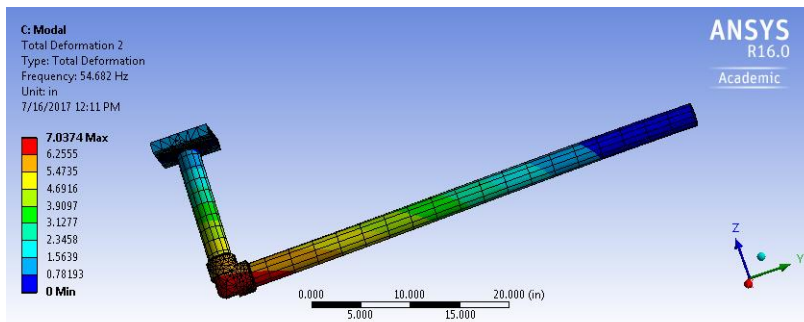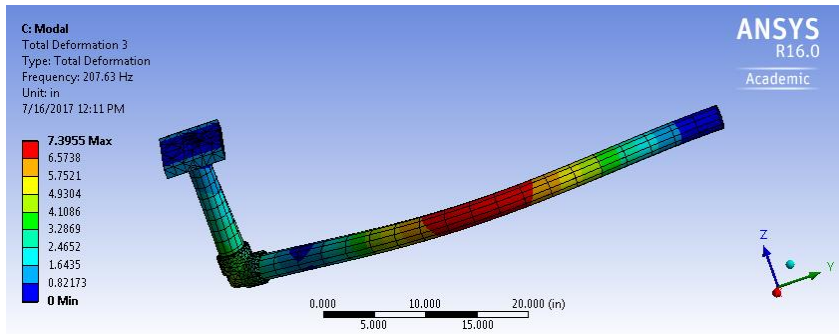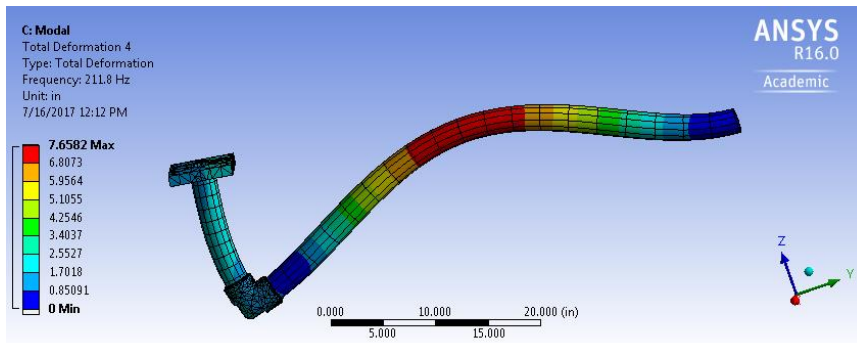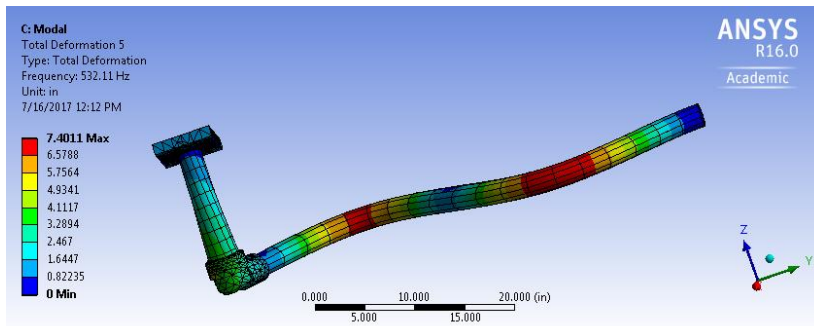**Figure 284 The 4th Mode for SWPA, 2 Inch Diameter, SS, 48 Inches Long**

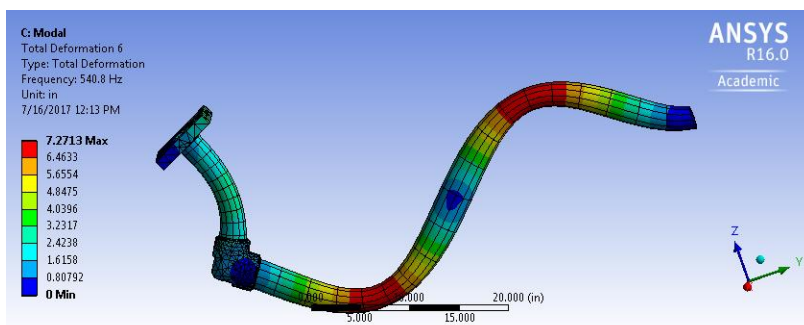**Figure 285 The 5th Mode for SWPA, 2 Inch Diameter, SS, 48 Inches Long**

Figure 286 The 6th Mode for SWPA, 2 Inch Diameter, SS, 48 Inches Long

LIST OF REFERENCES

Hamblin, M. (2003). Fatigue of Cantilevered Pipe Fittings Subjected to Vibration. *Fatigue Fracture Engineering Material Structure, 26*, 695-707.

Fei, X., Zhao-Xi, W., Lei, L., Wen-Xin, T., Ming-Xiang, G., Peng, L., & Guo-Gang, S. (2010). Experimental and Numerical Evaluation of the Vibration Fatigue of Small Bore Pipe in PWR. *Advanced Materials Research, 97*, 848-851.

Xiu, J., Jing, H., Han, Y., Zhao, L., & Xu, L. (2013). Effect of Groove on Socket Welds Under the Condition of Vibration Fatigue. *Journal of Nuclear Materials, 433*, 10-16.

Yoon, B., Kim, Y., & Lee, J. (2013). Steam Generator Small Bore Piping Socket Weld Inspection Using the Phased Array Ultrasonic Technique. *Journal of Nuclear Science and Technology, 51*, 231-239.

Xiu, J., Jing, H., Han, Y., Zhao, L., & Xu, L., (2012). Effects Of Radial Gap And Penetration Depth on Vibration Fatigue Behaviour of 304L Stainless Steel Piping With Socket Weld, *Materials Science and Technology, 28:7*, 850-856.

Choi, Y., Choi, S., (2007). Socket Weld Integrity in Nuclear Piping Under Fatigue Loading Condition, Nuclear Engineering and Design, 237, 213–218.

Zeng, L., Luo, C., & Jansson, L., (2015). More on Mixed Mode Cracking and Integrity Assessment of a Dissimilar Metal Weld for Ageing Nuclear Power Piping, *Procedia Engineering 130,* 930 – 947.

Rao, S. (2011) *Mechanical Vibrations.* Hoboken, NJ: Pearson Education, Inc, 1-291.

Volokhovskaya, O., Barmina, O., (2016). Effect of Residual Bending and Residual Eccentricicty of a Turbine Rotor on Its Transient Vibrational Amplitues, *Jouurnal of Machinery Manufacture and Reliability, 45,* 113-121.

Goroshko, A., Royzman, V., Ostasevicius, V., (2017). Balancing of Turbomachine Rotors by Increasing the Eccentricity Identification Accuracy, *Mechanika, 22,* 206-2011.

Cao, L., Wang, J., Li, P., Hu, F., Li, Y., (2017). Numerical Analysis on Steam Exciting Force Caused by Rotor Eccentricity, *Shock and Vibration, 2017,* 1-9.

(2003). Mechanical Vibration Balance Quality Requirements for Rotors In A Constant (Rigid) State, *Internationl Standard ISO 1940, 2,* 1-36.

Norfield, D. (2006). *Practical Balancing of Rotating Machinery*, Oxford: 1-19.Elsevier Science.

Leader, M., Understanding Journal Bearings, Applied Machinery Dynamics.

Sing, C., Love, P., Davis, P., (2014). Experimental study on condition assessment of reinforced concrete structure using a dynamics response approach; *Structural Survey, 2,* 89-101.

Consuegra, F., Irfanoglu, A., (2012).Variation of Small Amplitude Vibration Dynamic Properties with Displacement in Reinforced Concrete Structures, *Experimental Mechanics, 52,* 817-828.

Zhang, J., Liu, X., Mang, H., (2015). Multiscale Modeling of the Effect of The Interfacial Transition Zone on The Modulus of Elasticity of Fiber-Reinforced Fine Concrete, *Computational Mechanics, 55,* 37-55.

Hibbler, R., (2011). *Mechanics of Materials*. Upper Saddle River, NJ: Pearson Education, Inc, 108-109.